

DISS. ETH NO. 16182

**BIOPHYSICAL STUDIES ON THE INTERACTION OF  
CELL-PENETRATING PEPTIDES WITH MODEL MEMBRANES**

A dissertation submitted to the  
SWISS FEDERAL INSTITUTE OF TECHNOLOGY ZURICH

for the degree of  
Doctor of Natural Sciences

presented by

**Michael Edgar Herbig**  
Pharmacist, University of Würzburg  
born 11.11.1975  
Citizen of Germany

accepted on the recommendation of  
Prof. Dr. H. P. Merkle, examiner  
Prof. Dr. A. G. Beck-Sickinger, co-examiner  
PD Dr. O. Zerbe, co-examiner

**2005**



*Meinen Eltern,  
meinen Großmüttern  
und dem Andenken meiner Großväter*



**CONTENTS**

<b>ABBREVIATIONS</b>	III
<b>INTRODUCTION</b>	
Background and purpose	1
Abstract	5
Zusammenfassung	9
<b>CHAPTER I</b>	15
Reviewing biophysical and cell biological methodologies for cell penetrating peptide (CPP) research	
1. Introduction	17
2. Bilayer models to study CPP-lipid membrane interactions	21
3. Biophysical methods to investigate CPP-model membrane interactions	27
4. Cellular models to assess CPP translocation	40
5. Consistency and transferability of biophysical and cell biological studies	60
6. Conclusions	62
<b>CHAPTER II</b>	87
Bilayer interaction and localization of cell penetrating peptides with model membranes: a comparative study of a human calcitonin (hCT) derived peptide with pVEC and pAntp(43-58)	
<b>CHAPTER III</b>	129
Membrane surface associated helices promote lipid interactions and cellular uptake of human calcitonin-derived cell penetrating peptides	
<b>CHAPTER IV</b>	165
The cell penetrating peptides pVEC and W2-pVEC induce transformation of gel phase domains in phospholipid bilayers without affecting their integrity	
<b>GENERAL DISCUSSION AND CONCLUSION</b>	203
<b>CURRICULUM VITAE</b>	209
<b>PUBLICATIONS AND PRESENTATIONS</b>	210
<b>ACKNOWLEDGEMENTS</b>	213



<b>Abbreviation or notation</b>	<b>Definition</b>
AFM	atomic force microscopy
ANS	anilino naphthalene sulfonate
Antp	Antennapedia
ATP	adenosine triphosphate
Br-PC	1-palmitoyl-2-stearoyl-dibromo-sn-glycero-3-phosphocholine
calcein-AM	calcein-acetoxy methyl ester
CD	circular dichroism
CF	carboxyfluorescein
CHO	Chinese hamster ovary cell line
CLSM	confocal laser scanning microscopy
CPP	cell penetrating peptide
CS	chondroitin sulphate
DHPC	dihexanoyl phosphatidylcholine
DLS	dynamic light scattering
DNA	deoxyribonucleic acid
DMEM	Dulbecco's modified Eagles medium
DMPC	dimyristoyl phosphatidylcholine
DMPG	dimyristoyl phosphatidylglycerol
DOG	2-deoxy-D-glucose
DOPC	1,2-dioleoyl-phosphatidylcholine
DOPG	1,2-dioleoyl-phosphatidylglycerol
DPC	dodecyl phosphocholine
DPH	1,6-diphenyl-1,3,5-hexatriene
EDTA	ethylenediamine tetraacetic acid
EEA1	early endosomal antigen 1
EthD-1	ethidium homodimer-1

FACS	fluorescence associated cell sorting
$\Delta G_{\text{oct}}$	whole residue free energy of transfer from water to octanol
$\Delta G_{\text{wif}}$	whole residue free energy of transfer from water to POPC interface
GAG	glycosaminoglycan
GFP	green fluorescent protein
GUV	giant unilamellar vesicles
HBSS	Hank's balanced salt solution buffer
hCT	human calcitonin
HeLa	human cervix epithelial adenocarcinoma cell line
HEPES	4-(2-hydroxyethyl)-1-piperazineethanesulfonic acid
HPLC	high performance liquid chromatography
HS	heparan sulphate
HPSG	heparan sulphate proteoglycans
$^3J(H^N, H^\alpha)$	vicinal spin-spin coupling constants between the backbone amide proton and $\alpha$ proton
K <sub>sv</sub>	Stern-Volmer constant
LDH	lactate dehydrogenase
LUV	large unilamellar vesicles
MAP	model amphipathic peptide
MALDI-TOF	matrix assisted laser desorption/ionization-time of flight
M $\beta$ CD	methyl- $\beta$ -cyclodextrin
MDCK	Madin-Darby canine kidney cell line
MLV	multilamellar vesicles
MTS	3-(4,5-dimethylthiazol-2-yl)-5-(3-carboxymethoxyphenyl)-2-(4-sulfophenyl)-2H-tetrazolium
MTT	3-(4,5-dimethylthiazol-2-yl)-2,5-diphenyl tetrazolium bromid
NADH	nicotinamide adenine dinucleotide

NBD	7-nitro-2,1,3-benzoxadiazol-4-yl
NBD-PE	N-(7-nitrobenzofurazan-4-yl)-1,2-dipalmitoyl-sn-glycero-3-phosphoethanolamine
NLS	nuclear localization sequence
NMR	nuclear magnetic resonance
NOE	nuclear Overhauser effect
NOESY	nuclear Overhauser effect NMR spectroscopy
ON	oligonucleotide(s)
pAntp	Antennapedia homeodomain-derived CPP
PBS	phosphate buffered saline
PC	phophatidylcholine
PG	phosphatidylglycerol
PI	propidium iodide
PMS	phenozine methosulfate
PNA	peptide nucleic acids
POPC	1-palmitoyl-2-oleoyl-phosphatidylcholine
POPG	1-palmitoyl-2-oleoyl-phosphatidylglycerol
PS	phosphatidylserine
pVEC	vascular endothelial cadherin-derived CPP
RET	resonance energy transfer
RP-HPLC	reversed phase HPLC
SDS	sodium docecytl sulfate
SM	sphingomyelin
SPB	supported phospholipid bilayers
SUV	small unilamellar vesicles
Tat	trans-activating transduction
TFA	trifluoroacetic acid
T <sub>m</sub>	phase transition temperature
TMA-DPH	trimethylammonium-1,6-diphenyl-1,3,5-hexatriene

TOCSY	total correlation NMR spectroscopy
XTT	sodium 3-[1-[(phenylamino)-carbonyl]-3,4-tetrazolium]-bis(4-methoxy-6-nitro)benzene-sulfonic acid hydrate

## BACKGROUND AND PURPOSE

Biopolymers, such as peptides, proteins, oligonucleotides or plasmid DNA, offer great potential for the treatment of human diseases. However, they often suffer from poor cellular uptake and membrane permeation, owing to the hydrophobicity and charge selectivity of the plasma membrane, as well as the tight-junctional and enzymatic barrier functions of epithelial and endothelial membranes. Therefore, the capacity of biopolymers to reach their cellular or tissular target sites is largely compromised. The discovery of several peptides with the ability to rapidly translocate the plasma membrane and the potential to even reach the nuclear region of mammalian cells has opened new expectations in biomedical research. Such peptide sequences, referred to as cell penetrating peptides (CPP), which are usually shorter than 30 amino acids, are often derived from naturally occurring proteins, but comprise also synthetic model peptides and designed peptides with domains of different origin (1). CPP have been demonstrated to enter a large number of cell types (2) and to function as vectors for various macromolecular cargoes such as proteins, DNA oligomers, and peptide-nucleic acids (PNA), or particles like liposomes and magnetic nanoparticles (3-6). Prominent examples of protein derived CPP are the Tat peptides (7), penetratin (8), and pVEC (9), whereas polyarginins (10) represent synthetic model peptides, and transportan (11) a designed chimeric peptide. Although the exact mechanisms of the cellular translocation of CPP are as yet not fully understood, several similarities in translocation have been reported. Early studies reported that translocation was neither significantly inhibited by low temperature, depletion of the ATP pool, nor by various inhibitors of endocytosis. Translocation was therefore concluded to result form a direct, physical transfer through the lipid bilayer. More recently, however, experimental shortcomings in early studies have been discovered and the mechanisms of translocation have been re-evaluated. Meanwhile a majority of studies suggests the involvement of endocytic processes.

In addition to cell biological studies, a second branch in current CPP research deals with biophysical investigations of the interactions of CPP with membrane models of various lipid compositions. Such studies are mainly focused on the first step of CPP uptake: the initial adherence to the surface of the membrane leading to an enrichment in the phospholipid bilayer, which may subsequently trigger endocytic uptake. Common biophysical methodologies for such studies are, e.g., liposome leakage, liposome partitioning, fluorescence quenching, the study of lipid microviscosity, and NMR, CD, or IR based spectroscopy of the interactions of CPP with lipid mono- and bilayers. Although quite distant from the actual cell biology of CPP translocation, the flavor of such methodologies lies in the clear definition of the experimental setup and the possibility to obtain data on a molecular level.

Previous studies in our laboratory demonstrated that human calcitonin (hCT) and its N-terminal fragment hCT(9-32) were internalized in vitro by bovine nasal mucosa (12). Ensuing studies by Tréhin et al. identified the fragment hCT(9-32) as the so far most efficient hCT derived CPP and found strong evidence for the involvement of endocytic uptake processes (13). Whereas successful uptake into different cell lines and the lack of toxicity could be demonstrated for hCT(9-32), no relevant permeation of the CPP through epithelial models could be found (14). The aim of the present PhD study is now to investigate fundamental principles of CPP interactions with model membranes in order to obtain a more detailed understanding of the first step in the uptake process.

For this purpose, we applied a broad range of methodological approaches, with particular emphasis on liposome-buffer partitioning experiments to assess the affinities of CPP towards lipid membranes, and Trp quenching studies to obtain localization profiles in bilayers. In these cases – and generally, wherever technically feasible, large unilamellar vesicles (LUV) were preferred as membrane models. Their lipid composition was varied in order to provide LUV of different charge and charge density. We investigated both hCT derived

peptides, having a rather mild cationic character, and recognized CPP of strongly cationic nature, namely penetratin and pVEC.

Furthermore, we used NMR to investigate the effects of systematic amino acid modifications of hCT(9-32) derived CPP on their affinity to the lipid membrane. The results were correlated with their *in vitro* uptake efficiency. Finally, we performed an AFM study on supported phospholipid membranes, in which we demonstrated for the first time a non-detrimental transformation of these bilayers by CPP.

## REFERENCES:

1. Zorko, M. and U. Langel, *Cell-penetrating peptides: mechanism and kinetics of cargo delivery*. Adv Drug Deliv Rev, (2005). **57**(4): p. 529-45.
2. Schwarze, S.R., K.A. Hruska, and S.F. Dowdy, *Protein transduction: unrestricted delivery into all cells?* Trends Cell Biol, (2000). **10**(7): p. 290-295.
3. Gupta, B., T.S. Levchenko, and V.P. Torchilin, *Intracellular delivery of large molecules and small particles by cell-penetrating proteins and peptides*. Adv Drug Deliv Rev, (2005). **57**(4): p. 637-51.
4. Bogoyevitch, M.A., T.S. Kendrick, D.C. Ng, and R.K. Barr, *Taking the cell by stealth or storm? Protein transduction domains (PTDs) as versatile vectors for delivery*. DNA Cell Biol, (2002). **21**(12): p. 879-94.
5. Fisher, L., U. Soomets, V. Cortes Toro, L. Chilton, Y. Jiang, U. Langel, and K. Iverfeldt, *Cellular delivery of a double-stranded oligonucleotide NFκB decoy by hybridization to complementary PNA linked to a cell-penetrating peptide*. Gene Ther, (2004). **11**(16): p. 1264-72.
6. Snyder, E.L. and S.F. Dowdy, *Cell penetrating peptides in drug delivery*. Pharm Res, (2004). **21**(3): p. 389-393.
7. Vives, E., P. Brodin, and B. Lebleu, *A truncated HIV-1 Tat protein basic domain rapidly translocates through the plasma membrane and*

- accumulates in the cell nucleus.* J Biol Chem, (1997). **272**(25): p. 16010-16017.
8. Derossi, D., G. Chassaing, and A. Prochiantz, *Trojan peptides: the penetratin system for intracellular delivery.* Trends Cell Biol, (1998). **8**(2): p. 84-87.
  9. Elmquist, A., M. Lindgren, T. Bartfai, and U. Langel, *VE-cadherin-derived cell-penetrating peptide, pVEC, with carrier functions.* Exp Cell Res, (2001). **269**(2): p. 237-244.
  10. Futaki, S., T. Suzuki, W. Ohashi, T. Yagami, S. Tanaka, K. Ueda, and Y. Sugiura, *Arginine-rich peptides. An abundant source of membrane-permeable peptides having potential as carriers for intracellular protein delivery.* J Biol Chem, (2001). **276**(8): p. 5836-5840.
  11. Pooga, M., M. Hallbrink, M. Zorko, and U. Langel, *Cell penetration by transportan.* Faseb J, (1998). **12**(1): p. 67-77.
  12. Schmidt, M.C., B. Rothen-Rutishauser, B. Rist, A. Beck-Sickinger, H. Wunderli-Allenspach, W. Rubas, W. Sadee, and H.P. Merkle, *Translocation of human calcitonin in respiratory nasal epithelium is associated with self-assembly in lipid membrane.* Biochemistry, (1998). **37**(47): p. 16582-16590.
  13. Trehin, R., U. Krauss, R. Muff, M. Meinecke, A.G. Beck-Sickinger, and H.P. Merkle, *Cellular internalization of human calcitonin derived peptides in MDCK monolayers: a comparative study with Tat(47-57) and penetratin(43-58).* Pharm Res, (2004). **21**(1): p. 33-42.
  14. Trehin, R., U. Krauss, A.G. Beck-Sickinger, H.P. Merkle, and H.M. Nielsen, *Cellular uptake but low permeation of human calcitonin-derived cell penetrating peptides and Tat(47-57) through well-differentiated epithelial models.* Pharm Res, (2004). **21**(7): p. 1248-1256.

**ABSTRACT**

The ability of cell penetrating peptides (CPP) to translocate a therapeutic cargo, particularly peptide, protein and nucleic acid biopharmaceuticals, across the plasma membrane of mammalian cells renders them of broad interest in cell biology, biotechnology and drug delivery. This thesis is primarily concerned with studies involving human calcitonin (hCT) derived CPP and CPP from the pVEC family, which derives from the murine vascular endothelium cadherin. The major focus will be on fundamental biophysical aspects of interactions between CPP and lipid membrane models, such as membrane affinity and localization, also featuring related effects of systematic amino acid substitutions on CPP function, and the transformation of lipid bilayers as induced by selected CPP.

In the *first chapter* we review some of the most commonly used biophysical and cell biological methodologies in CPP research in order to critically assess their potentials and limitations. In the past ten years, a large number of cell biological studies on the efficiency of uptake, the mechanisms of translocation, and toxicological effects of CPP have been performed. Similarly, the fundamental principles of CPP-membrane interactions with membrane models were investigated in several biophysical studies. However, both avenues of research suffered to some extent from misinterpretations of data as well as frequent premature extrapolations, whereas reasonable efforts to combine both approaches within one study have been undertaken only sporadically. Owing to that fact, the literature is sometimes contradictory, particularly with regards on CPP uptake mechanisms and the efficiency of uptake into meaningful cellular models. Therefore, we provided a critical evaluation of the potentials and limitations of biophysical methodologies, such as fluorescence and nuclear magnetic resonance (NMR) spectroscopy, circular dichroism (CD), atomic force microscopy (AFM), and partitioning and also included a characterization of the most important membrane models. In the same way, we describe important cell biological methodologies, in particular confocal laser scanning microscopy

(CLSM) and fluorescence associated cell sorting (FACS), in combination with various techniques to distinguish between translocated and non-translocated CPP. Moreover, we discuss the diverse methodologies to follow the pathways of CPP translocation and their routes of intracellular trafficking.

In previous studies in our group, hCT(9-32) has been identified as the most efficient CPP among C-terminal fragments of hCT. Also we demonstrated its translocation into various epithelial models. Furthermore, analogous to several recent studies with other peptides, strong evidence for the involvement of endocytic processes in the translocation of CPP has been brought up. However, as yet the exact mechanisms of translocation are still under investigation. In the *second chapter* of this thesis, we investigated the interactions of CPP with phospholipid bilayers as the first step of translocation. For this purpose, we employed four independent techniques: (i) liposome buffer equilibrium dialysis, (ii) Trp fluorescence quenching, (iii) fluorescence polarization, and (iv) determination of  $\zeta$ -potentials. Using unilamellar vesicles (LUV) of different phospholipid composition, we compared weakly cationic human calcitonin (hCT) derived peptides with oligocationic CPP such as pVEC and penetratin (pAntp). The apparent partition coefficients ( $D$ ) of hCT derived peptides in neutral POPC LUV were dependent on the amino acid composition and secondary structure; partitioning into negatively charged POPC/POPG (80:20) LUV was increased and mainly governed by electrostatic interactions. For hCT(9-32) and its derivatives,  $D$  values boosted from about 100-200 in POPC to about 1000 to 1500 when negatively charged lipids were present. The localisation of the CPP as analysed by Trp fluorescence quenching were dependent on the charge density of the LUV. In POPC/POPG (80:20) hCT derived CPP were located on the bilayer surface, whereas pVEC and pAntp resided deeper in the membrane. In POPG LUV an increase in fluorescence polarization was observed for pVEC and pAntp but not for hCT derived peptides. Generally, we found strong peptide-phospholipid interactions, especially when negatively charged lipids were present.

The *third chapter* is focussed on an in-depth investigation of the localization of hCT(9-32) in model membranes, and the effects of systematic amino acid substitutions. To gain insight into the molecular orientation of hCT(9-32) when interacting with lipid membrane models, and to learn more about its mode of action, various biophysical techniques from liposome partitioning to high-resolution 2D NMR spectroscopy were utilized. Moreover, to establish the role of individual residues for the topology of its association with the lipid membrane, two mutants of hCT(9-32), namely W30-hCT(9-32) and A23-hCT(9-32), were also investigated. Whereas unstructured in aqueous solution, hCT(9-32) adopted two short  $\alpha$ -helical stretches when bound to dodecylphosphocholine (DPC) micelles, extending from Thr10 to Asn17 and from Gln24 to Val29. A23-hCT(9-32), in which the helix-breaking Pro23 was replaced by Ala, displayed a continuous  $\alpha$ -helix spanning from residue 12 to 26. Probing with the spin-label 5-doxylstearate revealed that association with DPC micelles was such that the  $\alpha$ -helix engaged in a *parallel* orientation to the micelle surface. Moreover, the Gly to Trp exchange in W30-hCT(9-32) resulted in a more stable anchoring of the C-terminal segment close to the interface, as reflected by a twofold increase in the partition coefficient in liposomes. Interestingly, tighter binding to model membranes was associated with an increase in the *in vitro* uptake in HeLa cells. Liposome leakage studies excluded pore formation, and the punctuated fluorescence pattern of internalized peptide indicated vesicular localization and, in conclusion, strongly suggested an endocytic pathway of translocation.

In the *forth chapter*, we investigated the pVEC and W2-pVEC, an Ile to Trp modification of the former. pVEC has been shown to translocate efficiently the plasma membrane of different mammalian cell lines by a receptor-independent mechanism without exhibiting cellular toxicity. To gain insight into the interaction of CPP with biomembranes, we studied their interaction on phase separated supported phospholipid bilayers (SPB) by atomic force microscopy (AFM), which is capable to achieve lateral resolutions of 0.5 nm and vertical resolutions of 0.1 nm under close to physiological conditions. W2-pVEC

induced a transformation of dipalmitoyl phosphatidylcholine (DPPC) domains from a gel phase state via an intermediate state with fractal-like structures into essentially flat bilayers. With pVEC the transformation followed a similar pathway but was slower. Employing fluorescence polarisation, we revealed the capability of the investigated peptides to enhance the fluidity of DPPC domains as the underlying mechanism of transformation. Due to their tighter packing, resulting from stronger intra- and intermolecular hydrogen bonds in the head group region, sphingomyelin (SM) domains were not transformed. By combination, AFM observations, dynamic light scattering studies, and liposome leakage experiments indicated that bilayer integrity was not compromised by the peptides. Transformation of gel phase domains in SPB by CPP represents a novel aspect in the discussion on uptake mechanisms of CPP.

In conclusion, we found that the localization of the investigated CPP was generally found either on the surface or at the interface of phospholipid bilayers, rather than in the hydrophobic core. The moderately cationic hCT derived CPP, which represent a CPP family of its own, showed a more superficial localization in neutral and slightly negatively charged bilayers, yet sufficient to trigger endocytic uptake into cells. Furthermore, we demonstrated that an enhanced interfacial anchoring over the entire CPP sequence resulted in increased cellular uptake. The discovery of the capability of pVEC derived CPP to transform gel phase domains in SPB without affecting their integrity reveals a novel aspect to be considered for the cellular uptake of CPP.

## ZUSAMMENFASSUNG

Zellpenetrierende Peptide (cell penetrating peptides, CPP) sind auf Grund ihrer Fähigkeit, therapeutisch relevante Moleküle wie Peptide, Proteine und DNA-Therapeutika durch die Plasmamembran von Säugerzellen zu befördern, von vielfältigem Interesse in der Zellbiologie, der Biotechnologie und im Bereich Drug Delivery. Die vorliegende Arbeit setzt sich schwerpunktmässig mit CPP auseinander, die entweder vom humanen Calcitonin (hCT) abgeleitet sind oder zur pVEC-Familie gehören, welches sich vom Cadherin des Gefäßendothels der Maus herleitet. Der Fokus der Arbeit liegt im Bereich grundlegender biophysikalischer Aspekte der Interaktionen zwischen CPP und verschiedenen Modellen für Lipidmembranen, insbesondere zu ihrer Membranaffinität und -lokalisierung. Weiterhin wird untersucht, wie sich systematische Variationen der Aminosäurensquenz auf die Effektivität der CPP auswirken und wie bestimmte CPP Transformationen von Lipiddoppelschichten induzieren.

Im *ersten Kapitel* geben wir einen Überblick über einige wichtige biophysikalische und zellbiologische Methoden in der CPP Forschung, verbunden mit einer kritischen Einschätzung ihrer Potentiale wie auch ihrer Limitationen. Im zurückliegenden Jahrzehnt wurden die Effizienz der CPP Aufnahme in Zellen, der Mechanismus ihrer Translokation und toxikologische Aspekte in einer Vielzahl von zellbiologischen Studien untersucht. Ebenso wurde eine Reihe von biophysikalischen Studien an Membranmodellen durchgeführt, um grundlegende Aspekte der CPP-Membran-Interaktionen genauer zu verstehen. Es stellte sich jedoch heraus, dass es in beiden Bereichen teilweise zu Missinterpretationen der Daten und voreiligen Extrapolationen kam, wohingegen eine sinnvoll erscheinende Kombination biophysikalischer und zellbiologischer Ansätze innerhalb einer Studie nur sehr selten unternommen wurde. Dies führte dazu, dass die publizierte Literatur an manchen Stellen, besonders hinsichtlich der Aufnahmemechanismen und der

Effizienz der CPP Aufnahme in bedeutsame Zellmodelle, widersprüchlich ist. Aus diesem Grund unternahmen wir eine kritische Untersuchung von häufig angewandten biophysikalischen Methodiken, wie Fluoreszenz- und Kernresonanzspektroskopie (NMR), Zirkulardichroismus (CD), Rasterkraftmikroskopie (AFM) und Verteilungsstudien hinsichtlich ihrer Möglichkeiten und Einschränkungen in der CPP-Forschung vor. Des Weiteren beschrieben wir wichtige physikalische und chemische Eigenschaften der verwendeten Membranmodelle. In gleicher Weise wurden gebräuchliche zellbiologische Methoden, insbesondere die konfokale Laser Scanning Mikroskopie (CLSM) und fluorescence associated cell sorting (FACS) in Zusammenhang mit unterschiedlichen Techniken zur Unterscheidung von aufgenommenen und nicht aufgenommenen Peptid beschrieben. Weiterhin wurden mehrere Methoden zur Aufklärung des Aufnahmemechanismus und der anschliessenden intrazellulären Transportwege beschrieben. Schliesslich wurde noch die gegenseitige Übertragbarkeit von biophysikalischen und zellbiologischen Ergebnissen untersucht.

In früheren Studien in unserem Arbeitskreis konnten wir hCT(9-32) als das effizienteste CPP der C-terminalen hCT Fragmente identifizieren und seine Aufnahme in verschiedene epitheliale Zellkulturmodelle demonstrieren. In Übereinstimmung mit mehreren anderen neuen Studien wurden überzeugende Indizien für die Beteiligung endozytotischer Prozesse am Aufnahmemechanismus der CPP gefunden; der exakte Translokations-mechanismus der Peptide ist dennoch noch immer nicht vollständig aufgeklärt. Im *zweiten Kapitel* dieser Arbeit untersuchten wir deshalb die Interaktionen von CPP mit Phospholipid-Bilayern, was den ersten Schritt im Translokationsprozess darstellt. Zu diesem Zweck verwendeten wir vier von einander unabhängige Techniken, nämlich (i) die Bestimmung von Verteilungskoeffizienten durch Liposomen-Puffer-Gleichgewichtsdialyse, (ii) Trp-Fluoreszenzquenching, (iii) Fluoreszenzpolarisation und (iv) die Bestimmung von  $\zeta$ -Potentialen und verglichen die Wechselwirkung von den moderat kationischen hCT-Derivaten

auf der einen Seite und den stark kationischen Peptiden pVEC und Penetratin (pAntp) auf der anderen Seite mit unilamellaren Liposomen (large unilamellar vesicles, LUV) unterschiedlicher Phospholipidzusammensetzung. Die scheinbaren Verteilungskoeffizienten (D) der hCT-Derivate in neutralen POPC LUV waren in erster Linie von der Aminosäurezusammensetzung und der Sekundärstruktur der Peptide abhängig, wohingegen die Verteilung in negativ geladenen POPC/POPG (80:20) LUV generell höher war und von elektrostatischen Wechselwirkungen dominiert wurde. Für hCT(9-32) und dessen Derivate stiegen die D-Werte von etwa 100-200 mit neutralem POPC auf 1000-1500 in Gegenwart von negativ geladenen Lipiden an. Die mittels Trp Fluoreszenzquenching bestimmte Lokalisation der CPP in Lipid-Doppelschichten war von der Dichte negativer Ladungen in den LUV abhängig. In POPC/POPG (80:20) Vesikeln waren die hCT-Derivate auf der Oberfläche der Bilayer lokalisiert, wobei sich pVEC und pAntp tiefer in der Membran befanden, als die hCT-Derivate. Ein Anstieg der Fluoreszenzpolarisation in POPG LUV als Indiz einer Veränderung der Mikroviskosität der Bilayer wurde lediglich für pVEC und pAntp, nicht aber für die hCT-Derivate beobachtet. Die beobachteten Peptid-Lipid-Interaktionen waren generell stark ausgeprägt, insbesondere dann, wenn negativ geladenes Lipid in den Membranen vorhanden war.

Das *dritte Kapitel* beschäftigt sich mit einer eingehenden Untersuchung der genaueren Lokalisation von CPP in Membranmodellen und analysiert die Effekte systematischer Aminosäuresubstitutionen in der Sequenz von hCT(9-32). Um einen Einblick in die molekulare Orientierung von hCT(9-32) in der Interaktion mit Lipidmembranen zu gewinnen und mehr über seine Aktionsweise herauszufinden, wurde verschiedene Techniken von Liposomen-Puffer-Verteilung bis zu hochauflösender zweidimensionaler NMR Spektroskopie eingesetzt. Darüberhinaus wurden zur Untersuchung der Bedeutung einzelner Aminosäurereste für die Topologie der Assoziation mit Lipidmembranen zwei Modifikationen von hCT(9-32), nämlich W30-hCT(9-32) und A23-hCT(9-32), untersucht. hCT(9-32) ist in wässriger Lösung

unstrukturiert, nimmt aber in Dodecylphosphatidylcholin (DPC) Mizellen eine Struktur mit zwei kurzen  $\alpha$ -helikalen Segmenten von Thr10 bis Asn17 und von Gln24 bis Val29 an. A23-hCT(9-32), in welchem das helixbrechende Pro23 durch ein Ala ersetzt wurde, zeigt erwartungsgemäss eine kontinuierliche  $\alpha$ -Helix von Aminosäure 12 bis 26. Eine Untersuchung in mit dem Spin-Label 5-Doxylstearinsäure markierten DPC Mizellen zeigte, dass das Peptid *parallel* zu Mizelloberfläche orientiert war. Der Austausch von Gly gegen Trp in der Modifikation W30-hCT(9-32) führte zu einer noch stabileren Verankerung des C-terminalen Segments im Interface der Mizelle; diese verbesserte Interaktion spiegelte sich auch in einer Verdopplung des Verteilungskoeffizienten in Liposomen wider. Bemerkenswerterweise ging die stärkere Bindung an Modellmembranen mit einem Anstieg der *in vitro* Aufnahme in HeLa Zellen einher. Eine von den Peptiden induzierte Porenbildung, die zytotoxische Effekte mit sich bringen würde, konnte mittels eines Liposomen-Leakage-Essays ausgeschlossen werden; ebenso konnte in einem MTT-Assay gezeigt werden, dass die Viabilität der Zellen selbst bei Peptidkonzentrationen von 100  $\mu$ M nicht beeinträchtigt war. Das punktartige Verteilungsmuster der internalisierten Peptide zeigt eine vesikuläre Lokalisation der CPP an und stellt folglich ein starkes Indiz für einen endozytotischen Aufnahmeweg dar.

Im *vierten Kapitel* untersuchten wir die Interaktionen von pVEC und W2-pVEC, einer Modifikation des ersten, in der Ile durch Trp ersetzt ist. Es ist bekannt, dass pVEC effizient und mittels eines Rezeptor-unabhängigen Mechanismus durch Plasmamembranen verschiedener Säugetierzellen transloziert, ohne dabei zelltoxische Effekte zu verursachen. Um nun die Wechselwirkung dieser CPP mit Biomembranen genauer zu verstehen, untersuchten wir deren Interaktionen mit phasenseparierten unterstützten Phospholipiddoppelschichten (supported phospholipid bilayers, SPB) mittels Rasterkraftmikroskopie (atomic force microscopy, AFM). Mittels dieser Technik lassen sich in Puffer unter annähernd physiologischen Bedingungen laterale Auflösungen von 0.5 nm und vertikale von 0.1 nm zu erzielen. Auf diese Weise konnten wir zeigen, dass W2-pVEC eine Transformation der Dipalmitoylphosphatidylcholin (DOPC) Domänen

vom Gelphasenzustand via eines Übergangszustandes mit fraktal-ähnlichen Strukturen hin zu nahezu komplett flachen Bilayern induziert. Die von pVEC induzierte Transformation folgte einem sehr ähnlichen Ablauf, vollzog sich aber etwas langsamer. Mittels Fluoreszenzpolarisationsstudien konnten wir demonstrieren, dass die untersuchten Peptide in der Lage sind, die Fluidität der DPPC Domänen zu erhöhen und somit den dem Transformationsprozess zugrunde liegenden Mechanismus aufzeigen. Sphingomyelin (SM) Domänen wurden aufgrund ihrer dichteren Packung, die aus den im Vergleich zu DPPC stärkeren inter- und intrmolekularen Wasserstoffbrückenbindungen resultiert, von den CPP nicht transformiert. Sowohl die AFM Beobachtungen, also auch Lichtstreustudien und Liposomen-Leakage Assays zeigten, dass die untersuchten Peptide die Integrität der Bilayer nicht beeinträchtigten. Mit der Beoachtung und Charakterisierung solcher Transformationen von Gelphasendomänen in Bilayern konnten wir einen neuartigen Aspekt in der Diskussion von CPP Aufnahmemechanismen aufzeigen.

Zusammenfassend lässt sich sagen, dass alle untersuchten CPP generell auf der Oberfläche oder im Interface, nicht aber im hydrophoben Kern der Membranen lokalisiert sind. Die nur mässig kationischen hCT-Peptide lassen sich zu einer eigenen, von den stark kationischen CCP unterscheidbaren, Familie zusammenfassen und zeigten eine stärker oberflächliche Lokalisation in neutralen oder nur leicht negativ geladenden Bilayern, die aber dennoch ausreicht, um eine endozytotische Aufnahme in Zellen auszulösen. Weiterhin konnten wir zeigen, dass eine verstärkte Verankerung der Peptide im Interface der Membranen zu einer erhöhten Aufnahme in Zellen führt. Schliesslich stellt die Beobachtung, dass die Peptide der pVEC-Familie in der Lage sind, Gelphasendomänen in SPB zu transformieren, ohne deren Integrität zu beeinträchtigen, neuartigen Aspekt in Zusammenhang mit der zellulären Aufnahme von CCP dar.



# CHAPTER I

Reviewing biophysical and cell biological methodologies for  
cell penetrating peptide (CPP) research

*Michael E. Herbig, Kathrin M. Weller, and Hans P. Merkle*

Drug Formulation & Delivery Group, Department of Chemistry and Applied  
BioSciences, Swiss Federal Institute of Technology Zurich (ETH Zurich),  
Wolfgang-Pauli-Strasse 10, CH-8093 Zurich, Switzerland

## ABSTRACT

Cell penetrating peptides (CPP) with the ability to translocate the plasma membranes of mammalian cells give rise to the intracellular delivery of problematic therapeutic cargoes, such as peptide, protein, and nucleic acid biopharmaceuticals, and even drug delivery vectors like liposomes and nanoparticles. Therefore CPP have been the subject of intensive research for more than a decade. Over this period of time numerous novel peptide sequences with CPP function have been introduced and tested in various cell culture models, and even *in vivo*. Biophysical studies in membrane models to investigate fundamental principles of CPP-lipid membrane interactions as well as cell biological studies focusing on the efficiency of uptake, mechanisms of translocation, and toxicity issues have been performed. However, both lines of research suffered from misinterpretations as well as premature extrapolations. Efforts to combine both approaches have been sporadic. Owing to that fact, the CPP literature to date suffers from a number of contradictions, particularly with regard to the translocation mechanisms of CPP and their uptake efficiency in meaningful cell culture models. In this review, we provide a critical evaluation of the potentials and limitations of selected biophysical methodologies, such as fluorescence spectroscopy, circular dichroism (CD) and nuclear magnetic resonance (NMR) spectroscopy, atomic force microscopy (AFM), and non-spectroscopic methods, including a characterization of the most important bilayer membrane models. In the same way, we describe important cell biological methodologies, in particular confocal laser scanning microscopy (CLSM) and fluorescence associated cell sorting (FACS), in combination with various techniques to distinguish between translocated and non-translocated CPP. Moreover, we discuss the diverse methodologies to follow the pathways of CPP translocation and their routes of intracellular trafficking.

## 1. INTRODUCTION

More than a decade ago the discovery of cell penetrating peptides (CPP), i.e. peptides endowed with an innate capability to translocate the plasma membrane of mammalian cells, has created a new horizon in biomedical research (1, 2). Particularly in vitro and so far less in vivo, CPP have been shown to carry substantial cargoes like peptides (3, 4), proteins (5), plasmid DNA (6), oligonucleotides (7), peptide nucleic acids (PNA) (8, 9), and even nanoparticles (10) and liposomes (11), across the plasma membrane into cellular compartments. Several hundred original articles have been published in this area and a variety of new CPP sequences - mostly from protein origin - have been discovered (1, 2), modified (5, 7), or even rationally designed (12, 13). A representative set of CPP and their respective origins is presented in Table I.

A major focus in CPP research was put on the elucidation of the translocation mechanism. In earlier literature, passive, temperature-independent processes insensitive to endocytosis inhibitors were the preferred mechanism to explain the cellular uptake of CPP (1, 2, 14). Recently, convincing evidence for energy independent mechanisms has been revisited and resulted in increasing support for endocytic translocation to occur with many CPP (15-17). This general shift of paradigms from the idea of a direct physical transfer of CPP into cells towards concepts involving endocytic uptake was also reflected by the fact that several research groups revised their own findings within a few years (2, 15, 18). This demonstrates that CPP research was not immune against misinterpretation of data and premature extrapolations. We are therefore convinced that a thorough and critical evaluation of the potentials and limitations of the employed methodologies - as provided in the present review - will help to assess the significance of CPP related findings.

There are currently two main avenues to analyze the principles of CPP function. First comes the study of the interactions of CPP with lipid bilayer and monolayer models of various lipid compositions. Typically, analysis of physical interactions of CPP with various bilayer models under various conditions

happened to play a major role. The range of biophysical methodologies available in this field is diverse, e.g. spectroscopic approaches such as CD, fluorescence quenching, fluorescence polarisation, and NMR, and - equally important - non-spectroscopic approaches. A simple but efficient tool is the assessment of apparent partition coefficients in liposomal dispersions of suitable lipids. More sophisticated approaches are AFM on phase separated supported bilayers and calorimetry. Obviously, lipid-peptide interactions may be analyzed by classical monolayer models (19), e.g. Langmuir-Blotgett films. Because both monolayer analysis and calorimetry of CPP have been previously reviewed in some detail (19, 20), we abstain here from including these fields in our review. Monolayer studies represent a specialized methodology to follow the insertion of solutes into a monolayer by measuring its surface pressure by means of a Langmuir balance. The assets of this technique are its standardized set-up and the ease in varying the lipid composition. Its limitation lies in the fact that the information obtained is averaged over an area that is very large relative to the size of a lipid or peptide molecule. Moreover, the monolayer technique may be insensitive to interactions different from an actual insertion of a solute into the monolayer, e.g., an association with the head groups of the lipids or an aggregation process. In fact, it has been shown that the absence of an increase in surface pressure does not necessarily indicate that a peptide would not interact with a monolayer (21). By calorimetry, heat signals, that are associated with every chemical or physical reaction, may be used to investigate interactions between membrane lipids and CPP. High sensitivity titration calorimetry would allow the determination of a complete set of thermodynamic parameters, in particular binding constants and reaction enthalpies.

The second branch in current CPP research is represented by translocation studies with suitable cell culture models. Their primary objectives are to identify the cellular translocation potential of CPP, and to study their pertinent pathways

---

*Table I. Name, amino acid sequence, origin and representative studies of reviewed CPP.*

CPP	Sequence	Origin	Biological studies	Biophysical studies
hCT(9-32)	LGTYTQDFNKFHTFPQTAIGVGAP-amide	human calcitonin	[16, 23, 106]	[88, 89, 107, 209]
hCT(9-32)-br	LGTYTQDFNKFHTFPQTAIGVGAP-amide   AFGVGPDEVKRKKP-amide	human calcitonin NLS of SV-40 large T antigen	[16, 146]	
KLA1	KLALKLALKAWKAALKLAA-amide	amphiphatic model peptide	[164]	
MAP	KLALKLALKAWKAALKLAA-amide	amphiphatic model peptide	[3, 148]	
MPG	GALFLGFLGAAGSTMGAWSQPKSKRKV-Cya	fusion peptide of HIV-1 gp41 and the NLS of SV40 large T-antigen	[6, 7]	[96]
pAmp*	RQIKIWFQNRRMKWKK	third helix of the DNA binding domain of Antennapedia, a Drosophila transcription factor	[1, 3, 26, 27, 137, 139, 148, 167]	[26, 27, 40-42, 47, 56, 58, 66-69, 71, 77, 79, 89, 103, 139, 208]
Pep-1	KETWWETWWTEWSQPKKKRKV-Cya	hydrophobic tryptophane-rich motif fused to the NLS of SV-40 large T antigen connected by a spacer	[5]	[44, 96]
pVEC	LLJILRRRIRKQAHAAHSK-amide	murine vascular endothelial cadherin	[161]	[89]
SAP	VRLPPPVRLLPPPVRLLPPP	modified maize zein sequence	[16]	
SynB3	RRLSYSRRRF	protegrin 1, an antimicrobial peptide	[66]	[66]
Tat(49-57)*	RKKRQRQRR	human immunodeficiency virus 1	[2, 3, 10, 17, 18, 22, 24, 25, 136-138, 143, 145, 147, 159, 167, 173, 177, 206]	[70, 57, 56, 24, 70, 173]
Transportan	GWTLNSAGYLLGKINLKALAALAKISII-amide	neuropeptide galanin coupled to the wasp venom peptide mastoparan via Lys	[3]	[42, 47, 67, 95]
TP10	AGYLLGKINLKALAALAKKII-amide	modification of Transportan	[184]	
VP22	DAATATGRRSAASRPTERPRAPARSASRPRRPVD	herpes simplex virus	[162, 165]	

\*minimal sequence required for uptake; frequently sequences elongated at their C- or N-terminus were used.

and routes across the plasma membrane and in the course of intracellular trafficking, and the thereby involved biological mechanisms. Commonly, either adherent or suspended, proliferation state cell cultures have been used for this purpose. Such models have distinct limitations as their cellular complexity may be quite distant from that of organized tissues, which typically consist of fully differentiated cells. In fact, when in the proliferation state, cell cultures fall short to mimic, e.g., epithelial barriers. Fully differentiated cell cultures were used in only a few cases, e.g. in the form of confluent epithelial cell cultures as models for epithelial barriers (22-25). In the present work, we will review both types of cellular models, mainly with respect to the capacities of translocation, translocation mechanisms, cell viability and membrane integrity.

In detail, after reviewing the various cellular models, we cover critically the diverse methodologies to monitor translocation by spectroscopic approaches. The most frequent methodologies for the qualitative analysis of translocation are fluorescence microscopy and confocal laser scanning microscopy (CLSM) combined with various markers or inhibitors of cellular trafficking pathways. Quantitative analysis is typically accomplished by fluorescence associated cell sorting (FACS) analysis. We further review specifically the various methodologies to distinguish between translocated and non-translocated CPP which have been a source of experimental artefacts and misinterpretation in the past. This can be achieved by sophisticated protocols that either digest, camouflage, or derivatize surface bound CPP. In the same context we evaluate methods to monitor cellular viability and toxicity as exerted by CPP by determination of the metabolic activity and cell membrane integrity through the use of cell membrane impermeable or permeable markers, respectively. Finally, we present principal approaches how to pinpoint the various mechanisms of translocation by reviewing methods using low temperature, endocytosis inhibitors and, on the molecular level, endocytosis markers. Further, methodologies to identify the influence of lipid rafts and the extracellular matrix will be explained.

Although rather distant from cell biology, the peculiarity of biophysical methodologies lies in the clear definition of the experimental setup, sometimes at the expense of direct cell biological relevance. Nevertheless, when considered in conjunction with the biological context, the physicochemical analysis of CPP/lipid membrane interactions remains an indispensable tool. Unfortunately, the two avenues of research, biophysical and cell biological studies, have so far rarely been connected within one study with only few exceptions (26, 27). Such a combination of different approaches, however, might be helpful to develop more realistic and significant ideas regarding uptake mechanism and therapeutic potentials of CPP.

## 2. LIPID BILAYER MODELS TO STUDY CPP-LIPID MEMBRANE INTERACTIONS

Bilayer models have an important and successful history in the biophysical assessment of the interactions of bioactive molecules with the lipid membrane (28-31). In the following section, we will review a series of well-established classical and more recent models such as (i) micellar and (ii) liposomal dispersions. We will also include more recent bilayer models such as (iii) the so-called bicelles and (iv) giant vesicles. Their use is typically in the form of nanoparticulate or microparticulate aqueous dispersions forming scaffolds for interactions with CPP whose nature and intensity may be studied with spectroscopical and non-spectroscopical methodologies. Furthermore, we demonstrate the use of (v) bilayers on solid supports, denoted supported bilayers. We will discuss both their assets and drawbacks, mention typical examples and evaluate critically their suitability for different methodological approaches in CPP research.

## 2.1 Lipid bilayer models – aqueous dispersions

*Micelles:* Aqueous dispersions of micelles composed of detergents such as sodium docecy1 sulfate (SDS) or dodecyl phosphocholine (DPC) represent a quite simplified but often reasonable model for biological membranes. Their biological relevance to mimic the plasma membrane of mammalian cells is limited, but preparation is rapid and straightforward, in most cases simply by dispersing a given amount of a suitable lipid or lipid mixture in a buffer. Being thermodynamically stable, micelles show good physical stability. DPC and SDS micelles have diameters of about 3 to 5 nm (32, 33), which is close to the thickness of phospholipid bilayers, ranging from 3.7 to 5.3 nm, dependent on the type of lipid and its physical state (34-36). DPC and SDS micelles were found to consist of about 60 (37) or 70 molecules (32), respectively. Owing to their small size and high surface curvature, as schematically represented in Fig. 1A, package of the lipids is rather loose and characterised by low lipid packing densities corresponding to 10 mN/m only (38), while biological membranes have typical packing densities of about 35 mN/m (19). Obviously, charge and molecular structure of the interface of DPC micelles and particularly of SDS micelles differ markedly from membrane phospholipids. In contrast to the anionic SDS, the zwitterionic DPC is a non-denaturing detergent and should therefore be preferred, eventually doped with a small fraction of SDS to create a negatively charged surface.

Based on their typical drawbacks such as low lipid packing density and unphysiological lipid composition of micelles, their use as lipid bilayer models for CPP studies is necessarily restricted to methodologies where the usage of liposomal systems is prohibited or technically problematic, namely for NMR (39-45), and occasionally for CD studies (45-47), respectively. It needs to be added that for <sup>1</sup>H NMR studies fully deuterated detergents must be employed.

*Bicelles.* In order to overcome the typical limitations of micelles, e.g., their low lipid packing density, Vold et al. (48) were the first to introduce the so-called

bicelle model as a scaffold to study the interaction of polypeptides with the lipid bilayer by means of liquid-state NMR. Bicelles (Fig. 1B) are disc-shaped, mixed micelles composed of bilayered long-chain phospholipids such as dimyristoyl phosphatidylcholine (DMPC) surrounded by a rim of short-chain detergents such as dihexanoyl phosphatidylcholine (DHPC). The ratio of DMPC to DHPC is denoted as  $q$  and is the determinate factor for the diameter of the bicelles. Bicelles may be doped with up to 25% phosphatidylserine (PS) or phosphatidylglycerol (PG), making them negatively charged with otherwise very similar biophysical properties (49). In terms of lipid packing density, conformation and dynamics, the DMPC-containing bilayer of a bicelle closely resembles the liquid crystalline state DMPC bilayer in liposomes (50). Employing bicellar model systems generally assumes an interaction of the investigated solutes with the tightly packed DMPC bilayer domain; nevertheless, preferential interaction of solutes with the looser packed DHPC rim cannot be excluded. To our knowledge, this complication has not yet been systematically investigated. Furthermore, due to the necessity to use fully deuterated lipid components for  $^1\text{H}$  NMR studies, experiments with bicelles are rather expensive. In CPP research, the bicelles are mainly used for NMR positioning studies. Further properties and applications of bicelles were reviewed by Sanders and Prosser (51).

*Small and large unilamellar liposomes.* Due to their superior resemblance to biological membranes as compared to micelles and bicelles, unilamellar liposome model systems have been the preferred lipid scaffolds for biophysical studies with CPP involving fluorescence quenching and polarization, CD, calorimetric and partitioning studies. Typically, either small unilamellar vesicles (SUV) in the diameter range of 25 to 35 nm (52, 53) or large unilamellar vesicles (LUV) with diameters of 100 to 200 nm (52) have been employed. Usually SUV are prepared by sonication. As illustrated in Fig. 1C, SUV of 30 nm diameter have a high surface curvature, resulting in loose packing of the phospholipids with packing densities of about 23 mN/m only (54). At this

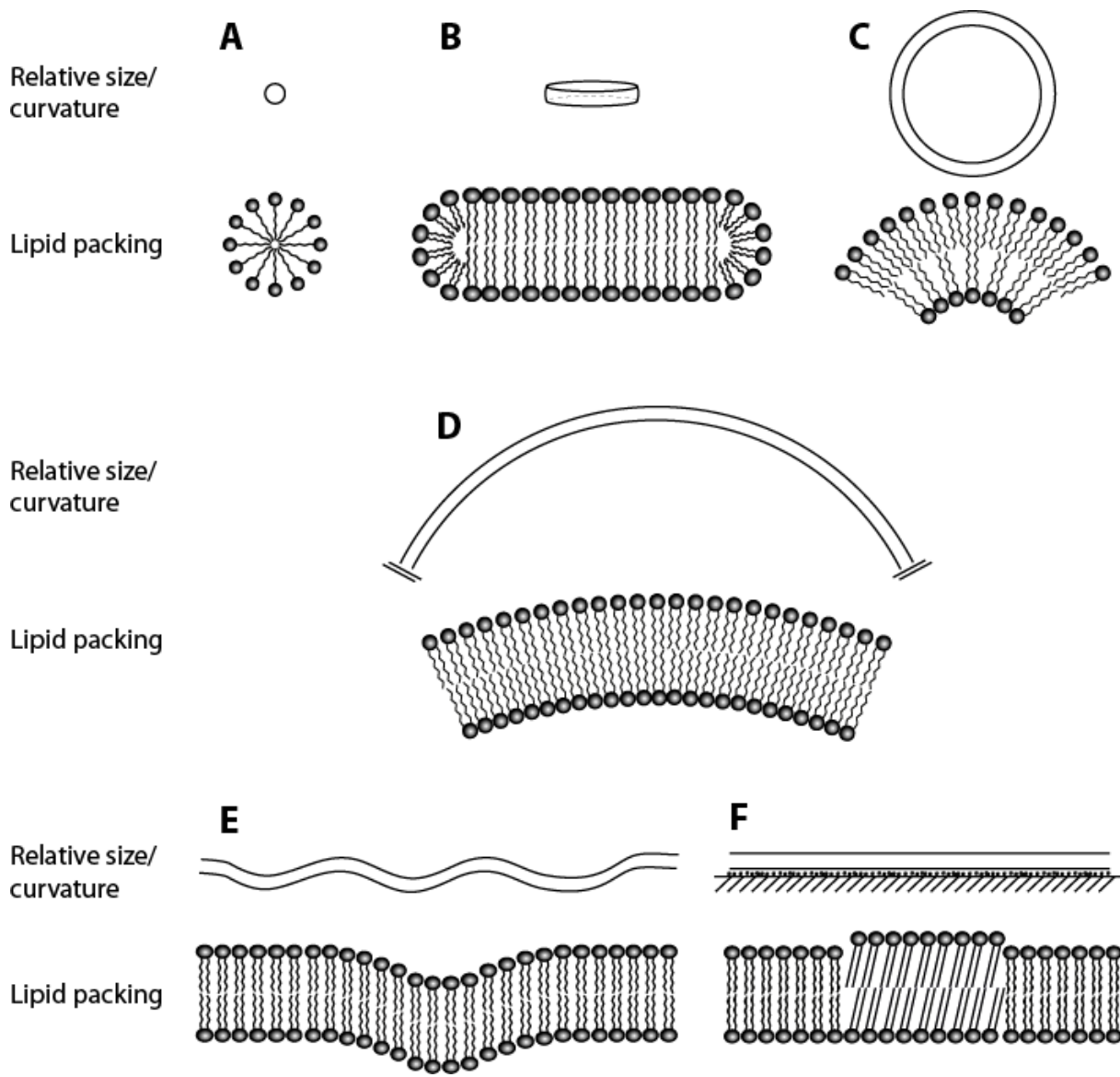


Fig. 1. Relative size, curvature and schematic representation of lipid packing for selected lipid bilayer models. (A) micelles, (B) bicelles, (C) SUV, (D) LUV, (E) GUV, (F) SPB.

reduced surface pressure, insertion of solutes is more likely as compared to larger liposomes. In fact, anomalously enhanced peptide binding to SUV has been reported in literature (55). SUV are frequently used models in CPP research, especially for fluorescence quenching studies (47, 56, 57) and CD (26, 58, 59)

LUV are generally prepared by repetitive extrusion, resulting in unilamellar vesicles of narrow size distribution (60). The diameter of thus produced

liposomes is determined by the respective pore size of the extrusion membrane (usually 100 or 200 nm). Fig. 1D shows a schematic representation of a 100 nm LUV. Its surface curvature is quite small and leads to a minor decrease in lipid packing density only. In fact, LUV of 100 nm have a lipid packing density of about 32 mN/m (54, 61) which is very close to the packing density of 35 mN/m typical for biological membranes (19). Together with the manifold opportunities to modify their lipid composition, this renders LUV a particularly suitable model for biomembranes.

In this context we now give a brief overview about the types of lipids that are commonly used to prepare liposomes for biophysical studies with CPP: In most of the recent studies chemically defined synthetic lipids are preferred over natural lipids from tissue extracts such as egg or soybean lecithin. Although lecithins reflect the composition of many biological membranes more closely, natural fluctuations in composition, different extraction protocols, and the presence of lysophospholipids (62) imply possible drawbacks of these natural products. Because of the detergent like character of lysophospholipids they may compromise the stability of bilayers (52).

Phosphatidylcholine (PC) represents the principal constituent of mammalian cell membranes (63). Hence, in biophysical studies on CPP function, 1-palmitoyl-2-oleoyl-phosphatidylcholine (POPC) or 1,2-dioleoyl-phosphatidylcholine (DOPC) have been the most frequently used neutral phospholipids (26, 44, 45, 56-59, 63-70). The corresponding phosphatidylglycerols (PG), 1-palmitoyl-2-oleoyl-phosphatidylglycerol (POPG) or 1,2-dioleoyl-phosphatidylglycerol (DOPG), have been employed as negatively charged bilayer constituents (26, 44, 45, 47, 56-59, 63-71). Occasionally, 1,2-dimyristoyl-phosphatidylcholine (DMPC) was also used instead of DOPC (47, 64), and phosphoethanolamines (PE) instead of PG (72, 73). At room and physiological temperatures all of the above mentioned lipids are found in the liquid crystalline state (74). If natural lipids are employed, usually egg PC (24, 27, 39, 75-77) or soybean PC (78, 79) were chosen as zwitterionic lipids and brain phosphatidylserine (PS) as negatively charged lipid component (27, 39, 77). In a few studies, 5 to 33% of

cholesterol was added to the phospholipids to mimic the composition of biological membranes more closely (24, 75-77).

*Giant unilamellar vesicles.* Giant unilamellar vesicles (GUV) are characterized by diameters above 10 µm, i.e. two orders of magnitude larger than LUV. GUV can be prepared either by electroformation (80) or via SUV by a dehydration/rehydration procedure as described by Karlson et al. (81). The main asset of GUV is their ready visualization by light and fluorescence microscopy, which provides an opportunity for direct observation of association or translocation processes of fluorophore labeled peptides into or through the GUV bilayer (56, 57, 79). Owing to their large size, the bilayer of GUV can be considered as flat, and their lipid packing density is comparable to cellular membranes. However, as illustrated in Fig. 1E, especially when responding to physical triggers like increased temperature or small osmotic gradients, GUV tend to have undulated surfaces with bulges and valleys entailing a dynamic behaviour (82, 83). In fact, GUV have been demonstrated to feature increased permeabilities for a number of solutes in comparison to LUV or SUV (82). Therefore, under certain conditions, GUV cannot be excluded to show extraordinary bilayer properties different from other bilayer models and from a cellular perspective. Hence, not by all means represent GUV a bilayer model that can closest mimic biological lipid membranes.

## 2.2 *Lipid bilayers on solid supports*

*Supported phospholipid bilayers (SPB).* Supported phospholipid bilayers (SPB), either homogeneous or phase separated, represent a novel and attractive bilayer model to study CPP-lipid interactions. SPB are single lipid bilayers which may be adsorbed on freshly cleaved, atomically flat mica discs. SPB are prepared by adsorption and fusion of unilamellar vesicles onto a mica surface at temperatures well above the phase transition of the employed lipids (84). A thin layer of water

was found to be adsorbed between the mica surface and the bilayer (85, 86), as shown in Fig. 1F. To investigate whether solutes interact preferentially with lipids in the liquid crystalline or gel phase state, phase separated SPB may be prepared (Fig. 1F). This added complexity contributes significantly to its physiological relevance. Changes in the topology of phase separated SPB after incubation with CPP may be analyzed, e.g., by atomic force microscopy (AFM) in a time resolved manner. Gel phase lipid domains protrude by about 0.8 to 1.1 nm out of the liquid crystalline phase (86-88). CPP-lipid interactions have been shown to lead to a time dependent flattening of this topology caused by a transition from the gel to the liquid crystalline phase (89) (Chapter 2). Overall, SPB allow visualization of CPP bilayer interactions at close to physiological conditions at high resolution, namely 0.5 – 1 nm in lateral and 0.1 – 0.2 nm in vertical direction (90).

### 3. BIOPHYSICAL METHODOLOGIES FOR CPP-LIPID MEMBRANE INTERACTIONS

The typical CPP function of certain peptide sequences has initially been discovered in cell biological experiments. In an effort to achieve a more fundamental understanding of the translocation process, however, interactions of CPP with lipid bilayer and monolayer models of various lipid compositions have been investigated. For this purpose, a broad range of biophysical methodologies is available. In the following we will describe some important spectroscopic techniques, such as NMR, CD, and fluorescence quenching and polarization, as well as non-spectroscopic approaches like the assessment of apparent partition coefficients by means of equilibrium dialysis and, in addition, AFM studies on phase separated SPB.

### 3.1 Spectroscopic approaches

*Circular dichroism (CD).* CD spectroscopy is an established tool to investigate the secondary structure of CPP in the absence or presence of a lipid bilayer scaffold such as SUV or LUV (27, 57, 58, 67-69, 71, 77). Because of stronger signals in this region, CD spectra of peptides are usually recorded in the far-UV (250-180 nm) but not in the near-UV region (300-250 nm). This precludes the use of various common buffers, like HEPES and acetate buffer. CD spectroscopy measures the differential absorption of right- and left-polarized light which depends on the wavelength of light and is only observed for asymmetric molecules. CD spectra of peptides result from asymmetrical elements in the backbone and from contributions of aromatic amino acids in the side chains (91). Since the chiroptical properties of various conformations are additive, the observed mean residue ellipticities of peptide spectra represent a net result as the weighted sum of all contributions of different secondary structures over the entire molecule. Clearly, such secondary structure calculations depend largely on the methods and models chosen and especially on the applied set of reference spectra (92-94). In contrast, secondary structure calculations derived from NMR allow full molecular resolution. Despite the mentioned limitations and constraints, CD allows a quick estimation of secondary structures, and is well suited to follow changes in secondary structures dependent on peptide concentration, pH, buffer, and on the nature and composition of the lipid.

The secondary structure of penetratin has been investigated in a number of studies under various conditions. As a general trend penetratin turned out to be mainly unstructured in buffer (occasionally with a significant  $\beta$ -sheet contribution) and was shown to become  $\alpha$ -helical in SDS micelles and neutral PC liposomes, whereas negatively charged liposomes induced  $\beta$ -sheet formation. In more detail, penetratin was found mainly unstructured in water or buffer (39, 40, 57, 67). In SDS micelles  $\alpha$ -helical contributions of 37% (39), 40% (45), and 50% (47) were typical. In neutral bicelles a moderate  $\alpha$ -helicity

has been reported, which increased when negatively charged lipid was present (40). Like SDS micelles, also neutral liposomes or liposomes with small to moderate fractions of negatively charged lipids primarily induce  $\alpha$ -helix formation. An  $\alpha$ -helical contribution of 39% was found in POPC/POPG (70:30) SUV (45); similar to that,  $\alpha$ -helicity in the range of 26% to 67% was found in SUV and LUV of comparable composition, provided that the liposome dispersion was not aggregated (27, 57, 58, 67-69, 71, 77). In liposomes entirely composed of negatively charged lipids, however,  $\beta$ -sheet contributions of 45% to 66% were found (47, 58, 67, 71). Interestingly, the secondary structure of penetratin is also dependent on the peptide/lipid-ratio (P/L); it has been shown that at low P/L  $\alpha$ -helical conformations and at high P/L  $\beta$ -sheets, respectively, are favoured (27, 58). Persson et al. (69) demonstrated that the  $\alpha$ -helix to  $\beta$ -sheet transition occurred during vesicle aggregation, and a subsequent transformation back to an  $\alpha$ -helical conformation took place during the spontaneous disaggregation. Sequence modifications of penetratin with one or two Trp replaced by Phe showed higher propensities for  $\beta$ -sheet structures and lower ones for  $\alpha$ -helices (67). In general, the secondary structure of penetratin appears to be highly dependent on various key factors, like type and charge of lipid, concentration, and peptide to lipid ratio.

In contrast to penetratin, the secondary structure of transportan was found to be less variable and independent of lipid charge density. Transportan displayed about 30%  $\alpha$ -helicity in water and 50% to 60% in membrane model systems like SDS micelles (42), DPC micelles (95), and LUV composed of POPC/POPG (70:30), or pure POPG (67). As shown by NMR, mainly the mastoparan part contributes to the  $\alpha$ -helical structure (42). Tat(47-57), however, showed random coil conformation in buffer and remained unstructured in POPC/POPG (75:25) SUV (70), as well as in DOPC/DOPG/DSPE-PEG (60/35/5) LUV (57).

The N-terminal fragment of the mouse prion protein, PrP(1-28), displayed random coil conformation in pure water, whereas increasing peptide concentration, temperature or addition of salt increased  $\beta$ -sheet contributions. In neutral POPC SUV  $\alpha$ -helix and in negatively charged POPG SUV  $\beta$ -sheet

structure were predominant (59). Similarly, the N-terminal fragment of the bovine prion protein, bPrP<sub>p</sub>(1-30), featuring CPP properties, showed mainly random coil and  $\beta$ -sheet conformation in water as well as in buffer, but 62% to 66%  $\alpha$ -helical in neutral bicelles, whereas fairly high  $\beta$ -sheet contributions were found in partially negatively charged bicelles (43).

Pep-1, a synthetic CPP consisting of a hydrophobic Trp-rich motif and a hydrophilic cationic nuclear localization sequence (NLS) was poorly structured at concentrations below 0.3 mg/mL, but  $\alpha$ -helical at concentrations above 3 mg/mL and in SDS micelles (44). The similarly designed peptide MPG, occasionally also referred to as [P $\beta$ ], however, showed a different conformational status: Whereas the peptide displayed a random coil conformation in water, there were indications for a transition to  $\beta$ -sheet in SDS micelles under certain conditions (96).

*Nuclear magnetic resonance (NMR) spectroscopy.* Solution-state NMR is a particularly powerful tool to study how CPP interact with bilayer models. Suitable bilayer scaffolds for interaction are micelles and bicelles, whereas liposomal dispersion would lead to unwanted signal broadening. Its main application in CPP research is the determination of the secondary structures of the peptides and their positioning relative to the micelle or bicelle surface. Whereas CD allows a quick, cheap, and relatively simple first estimation of the peptides' secondary structures, NMR studies afford specialized expertise, may be time-consuming and expensive, and need relatively high amounts of peptides. Their major asset, though, lies in the significance and precision of the obtained results owing to the fact that NMR experiments provide distinct information for every single amino acid, whereas CD provides a net structural information for the peptide as a whole. In general, secondary structures can be immediately derived from interresidual nuclear Overhauser effects (NOEs) in the spectra.

Studies on the positioning of CPP relative to micelle or bicelle surfaces may be performed by means of paramagnetic spin labels, which contain unpaired electrons and selectively broaden resonances in their vicinity. Several spin labels

are at hand. For instance,  $Mn^{2+}$  ions form a suitable spin label to probe for residues exposed to the water phase, with some effects on the head groups of the lipid. Whereas 5-doxylstearic acid broadens signals in the interface region of a micelle (97), 12-doxylstearic acid is expected to broaden signals originating from the interior of a micelle. Nevertheless, because both spin labels are rather far-reaching, i.e. in the range of 11 - 12 Å (98, 99), 5- and 12-doxylstearic acid have been found to broaden similar resonances of membrane associated peptides (100). Methodological and practical aspects, as well as membrane model systems for NMR studies on membrane associated peptides and proteins have been recently reviewed in more detail by Bader et al. (50) and Damberg et al. (101).

An early NMR study on the secondary structure and localisation of penetratin in micelles has been performed by Berlose et al. (39):  $^1H$ -NMR spectroscopy of penetratin, i.e. pAntp(43-58), in SDS micelles revealed an  $\alpha$ -helix from amino acid 44 to 55 with a local deformation in the 48 to 50 region allowing its adaptation to the micelle surface. As expected, its analogue [Pro50]pAntp(43-58) showed a shorter  $\alpha$ -helix from amino acid 43 to 51. Surprisingly, however, the helical domain was longer than expected because Pro is a well known and strong  $\alpha$ -helix breaker, and usually interrupts a helix 2 to 3 residues backwards from its position towards the N-terminus. Later Drin et al. (45) and Lindberg and Graslund (41) confirmed an  $\alpha$ -helical conformation of penetratin in SDS micelles with an unstructured N- and C-terminus. In contrast to the latter study which was based on paramagnetic broadening experiments employing the spin labels  $Mn^{2+}$ , 5- and 12-doxylstearic acid, Lindberg and Graslund proposed a positioning perpendicular to the micelle surface with the C-terminus buried inside the micelle and the N-terminus near the surface. A NMR study in partially negatively charged bicelles (DMPG:DMPC = 0.1) revealed, again in agreement with previous studies, an  $\alpha$ -helix from residues 48 to 56. For a modified penetratin, penetratin(W48F,W56F), i.e. with two Trp replaced by Phe, a similar secondary structure was found. However, the bicellar positioning of the two peptides was slightly different: Whereas wild-type penetratin was located in the

bicelle interface, the N-terminal part of penetratin(W48F,W56F) was inserted more deeply into the bicelle (40). Interestingly, owing to the Trp to Phe exchange, the translocation efficiency of penetratin(W48F,W56F) was essentially lost (102). In SDS micelles both peptides revealed quite similar secondary structures. Nevertheless, positioning of the peptides could not be determined without ambiguity. Again, 5-doxyl stearic acid caused the most pronounced interference, indicating - at least partially - an interfacial positioning (40).

Andersson et al. (103) used  $^{15}\text{N}$  spin relaxation and translational diffusion experiments to demonstrate that penetratin binds strongly to different membrane models. However for negatively charged membrane mimicking models, binding was even higher, and so was restriction in motional flexibility.

Upon interaction with SDS micelles, transportan, a chimeric peptide constructed from galanin and mastoparan, was found to be  $\alpha$ -helical in the mastoparan part and mainly unstructured in the galanin domain. Based on spin-label experiments the mastoparan segment inserts into the micelle whereas the galanin part resides in the interface (42). Mastoparan, a pore forming peptide from the wasp venom, has been demonstrated to form a transmembrane  $\alpha$ -helix perpendicular to a bicelle surface (104). In a more recent study in neutral bicelles the mastoparan part was observed to adopt a well-defined  $\alpha$ -helix, whereas the galanin part displayed a weaker tendency to form an  $\alpha$ -helix. The whole peptide was found to be positioned in parallel to the membrane-water interface (95).

Pep-1, an amphiphilic CPP was previously reported to bind protein cargoes via hydrophobic interactions with its tryptophane rich N-terminus (5). Deshayes et al. detected an  $\alpha$ -helical conformation for the hydrophobic, Trp-rich motif of Pep-1, both in water and in SDS micelles, whereas the cationic C-terminal nuclear localization sequence (NLS) turned out to be unstructured. In SDS micelles the helix was slightly extended towards the N-terminus and showed some indications of a  $3_{10}$  helix (44).

Further, Pep-1 turned out to form an  $\alpha$ -helix in its hydrophobic part, but its hydrophilic part remained unstructured also in the presence of DPC/SDS

micelles. Pep-1 and two C-terminal modifications displayed an orientation parallel to the micelle surface. Membrane affinity of the C-terminus increased in the order free carboxy group, amidated C-terminus and cysteamine ending. Remarkably, better C-terminal anchoring corresponded with enhanced translocation (K. Weller, unpublished data).

The human calcitonin (hCT) derived CPP hCT(9-32), previously introduced by our group (105, 106) was found to display two short  $\alpha$ -helical stretches, interrupted by the Pro in position 23. The N-terminal section of the peptide showed a flat orientation in the interface of zwitterionic DPC micelles, with the C-terminal part extending into the water phase. Replacement of Pro23 by Ala resulted in a continuous, moderately amphipathic  $\alpha$ -helix with an enhanced interaction with the interface of the micelle. When Gly30 was replaced by a Trp, the flat anchorage of the peptide in the interface of the micelles was even tighter, also comprising the C-terminal section. Intriguingly, an enhanced interaction with DPC micelles, as analysed by NMR, corresponded well with a more efficient in vitro uptake in HeLa cells (Chapter 3).

For further examples for related NMR studies we now refer to prion protein derived peptides. For an N-terminal sequence (residues 1-30) of the bovine prion protein, bPrP<sup>c</sup>, featuring a similar CPP-like function like a segment of the mouse prion protein (residues 1-28) (59), Biverstahl et al. (43) found an  $\alpha$ -helical domain in the mid section of the peptide (residues 8-21). In contrast to other CPP, which were found to be positioned in the interface parallel to the bilayer surface, Biverstahl et al. found indications for a transmembrane positioning of bPrP<sup>c</sup>. Their observation may be explained by the peptide's hydrophobic  $\alpha$ -helix in the mid section together with cationic Lys residues at both the N- and C-termini, but may be linked to its enhanced propensity for cytotoxicity (43).

Solid-state NMR studies in CPP research are scarce. An interesting example though is a study on the interaction of hCT(9-32) with multilamellar vesicles (107).

*Trp fluorescence quenching studies.* Trp fluorescence quenching studies are well suited to obtain information about the positioning of CPP within lipid bilayers. For that purpose, membrane anchored as well as aqueous phase quenchers are used to quench the intrinsic Trp fluorescence of suitable peptides located in close proximity to the quenching probe in- or outside the bilayer. Quenching studies provide information about the depth of CPP penetration into membrane models, and the mode and intensity of this interaction, depending on surface charge, lipid composition and surrounding medium, and may contribute to the understanding of the translocation process. The quenching efficiency ( $F_0/F$ ) can be calculated by dividing the Trp fluorescence intensity of the peptide/liposome solution alone ( $F_0$ ) by the fluorescence intensity of the peptide/liposome solution in the presence of different concentrations of quenching probes ( $F$ ). Quenching constants  $K_{SV}$  for different molar concentrations of the quenchers,  $[Q]$ , can be determined by linear regression using the Stern–Volmer equation for a dynamic process:

$$\frac{F_0}{F} = 1 + K_{SV} [Q] \quad (1)$$

There are different types of quenchers, which may be used in such studies: In N-(7-nitrobenzofuran-4-yl)-1,2-dipalmitoyl-sn-glycero-3-phosphoethanolamine (NBD-PE), the NBD group is covalently attached to the head group of a phosphatidylethanolamine molecule. Therefore, it acts as a probe for the polar head groups on the level of the phosphate groups in lipid bilayers (108-110). 5-doxylo stearic acid represents a probe for the deeper interface region, whereas 12-doxylo stearic acid is a quencher for the deep hydrophobic core of a bilayer (101). Alternatively, brominated 1-palmitoyl-2-stearoyl-sn-glycero-3-phosphocholines (Br-PC), which resemble the natural membrane lipids more closely, may be used as membrane anchored quenchers. For the 1-palmitoyl-2-stearoyl-dibromo-sn-glycero-3-phosphocholine (Br-PC) derivatives 6,7-, 8,9-, and 11,12-Br-PC average bromine distances from the bilayer centre of 10.8 Å, 8.3 Å, and 6.3 Å, respectively, have been determined (108, 111). The radius of quenching for

brominated probes is 8 - 9 Å (112), whereas spin-labeled probes quench over a range of 11 - 12 Å (98, 99). Therefore, it is necessary to employ several quenchers located at different depths in the bilayer in order to convincingly determine the positioning of the peptides.

In addition to membrane anchored quenchers the neutral hydrophilic quencher acrylamide is used to determine the exposure of Trp containing CPP in LUV or SUV dispersions. Acrylamide is unable to penetrate into the hydrophobic core of the membrane and, therefore, non-polar fluorophores embedded in the bilayer cannot be quenched (113). Generally, unilamellar liposomes (LUV or SUV) of varying charge density are employed, often using synthetic PC and PG (47, 57, 67, 69), but occasionally also natural lipids like egg PC and brain PS (27, 77). Magzoub et al. (47) demonstrated that penetratin as well as pIsl, a related homeodomain peptide, are largely exposed to the aqueous phase in the presence of neutral DMPC SUV as indicated by pronounced acrylamide quenching. In the presence of negatively charged DMPG SUV, quenching was largely reduced, indicating a stronger binding and/or deeper penetration into the bilayer. An increased affinity of penetratin towards liposomes consisting of 20% or more negatively charged lipids was later confirmed by Christiaens et al. (77). For transportan, however, no differences between the two lipids were found. An ensuing study employing the membrane anchored quenchers 5- and 12-doxylstearic acid revealed for both pure POPG and POPC/POPG (70:30) LUV, that penetratin and transportan were preferentially positioned in the bilayer interface as shown by strong 5-doxylstearic acid quenching, but minimal 12-doxylstearic acid effects. In POPC/POPG (70:30) both quenchers exhibited weaker effects on transportan as compared to penetratin (67). In agreement with that, a much stronger quenching of penetratin fluorescence was found for the shallower quencher 6,7-Br-PC than for 11,12-BrPC in PC/PS (70:30) LUV (27). In another study employing a total of four different quenchers we demonstrated that penetratin as well as W2-pVEC, a Trp containing modification of the highly cationic pVEC, were located in the deeper interface of both POPC/POPG (80:20) and pure POPG LUV. Interestingly, two Trp containing derivatives of

the only slightly cationic hCT(9-32) demonstrated distinctly different positioning data: In POPC/POPG (80:20) LUV the two CPP were found to be superficially located, in pure POPG, however, insertion was deeper than the cationic peptides (89) (Chapter 2).

The findings of Persson et al. (56) and Thoren et al. (57), which describe the strongest effects for the deepest quenchers in POPC/POPG (60:40) SUV, suggest an almost identical positioning of 9.6 Å to 10.3 Å from the bilayer center for penetratin, two of its modifications, two Tat modifications, a Trp containing polyarginin (R<sub>7</sub>W), and as controls Ac-18A-NH<sub>2</sub>, a non-translocating, α-helical peptide, and Trp octyl ester. The two latter studies were at least partially in discrepancy to the former, which have found an interfacial positioning of penetratin and other cationic peptides. Interfacial positioning of penetratin and other cationic peptides has also been determined in several NMR studies (see above). So far, the reasons behind these inconsistencies are elusive.

*Fluorescence polarization.* The polarization of the membrane-bound fluorophore 1,6-diphenyl-1,3,5-hexatriene (DPH) is a commonly used tool to estimate the internal microviscosity of bilayer membranes. By this means, effects of CPP on membrane order and fluidity may be detected. An increase in DPH polarization implies an increase in microviscosity and, therefore, restricted mobility of the acyl chains of the lipid molecules. DPH is non-fluorescent in aqueous dispersion, but partitions readily into lipid membranes with a lipid–water partition coefficient K<sub>p</sub> of 1.3 x 10<sup>6</sup>, accompanied by strong fluorescence enhancement (114). Previously, the positioning of DPH was found to be close to the centre of the lipid bilayer, whereas trimethylammonium-1,6-diphenyl-1,3,5-hexatriene (TMA-DPH), was concluded to anchor on the surface (115, 116), obviously by interaction with the TMA substituent. Steady-state fluorescence polarization *P* can be determined according to the following equation (117):

$$P = \frac{I_{VV} - G I_{VH}}{I_{VV} + G I_{VH}} \quad (2)$$

where  $I_{VV}$  is the emission intensity of vertically polarized light parallel to the plane of excitation and  $I_{VH}$  is the emission intensity of horizontally polarized light perpendicular to the plane of excitation. The instrumental factor  $G$  ( $G = I_{HV}/I_{HH}$ ) is determined by measuring the polarized components of the probe's fluorescence with horizontally polarized excitation.

Magzoub et al. (67) investigated the polarization effects of transportan and penetratin on SUV of various charge density. It was shown that in SUV, composed of either neutral POPC or negatively charged POPC/POPG (70:30), penetratin and two of its modifications led to no or only a minimal increase in polarization. Transportan, on the other hand, exhibited a significant, concentration-dependent effect, indicating a rigidification of the lipid membranes, probably due to its mastoparan part, which is well known for its insertion into the hydrophobic core of the membrane, also explaining its significant cellular toxicity. In pure POPG, however, penetratin induced a strong increase in polarization, indicating significant membrane perturbation, whereas the effects of transportan were independent of charge density. Interestingly, diminishing the electrostatic effects by adding salt (150 mM KF) resulted in a decrease in DPH polarization. In a study on pVEC, a short and highly cationic CPP similar to penetratin, we observed a comparable behavior, featuring a considerable decrease in membrane fluidity for pure POPG LUV, but no effects on neutral or mixed LUV. In contrast, hCT(9-32) and other human calcitonin-derived CPP exhibited no effects on any of the LUV, indicating that their interaction with the bilayer was restricted to the interface (89) (Chapter 2).

Nagy et al. (118) investigated the effects of membrane penetrating, cationic peptide conjugates, consisting of the linear epitope peptide derived from VP3 capsid protein of Hepatitis A virus and polylysine based polypeptides, on the fluidity of POPC/POPG (95:5) LUV. The conjugated peptides increased the polarization of the membrane surface bound Na anilino naphthalene sulfonate (ANS) indicating a rigidification of the bilayer on the level of the outer polar heads. A significant decrease in membrane fluidity on the level of the

hydrophobic core of the bilayer was only observed at temperatures above phase transition, where a deep integration of the peptides occurs more likely.

### 3.2 Non-spectroscopic approaches

*Liposome-buffer partitioning.* Liposome-buffer partitioning by equilibrium dialysis has been introduced to investigate drug partitioning in lipid systems which resemble biological membranes more closely than bulk solvents such as octanol (119). For this purpose, the partitioning of solutes between buffer and a LUV dispersion at a known lipid concentration is determined at equilibrium. In contrast to titration calorimetry, by which exact binding constants can be obtained, liposome-buffer partitioning provides apparent partition coefficients ( $D$ ), which may be calculated according to:

$$D = \frac{C_{P(b)}}{C_{P(f)} \cdot C_L} \quad (3)$$

where  $C_{P(b)}$  is the concentration of peptide bound to liposomes,  $C_{P(f)}$  the concentration of free peptide, and  $C_L$  is the concentration of lipid molecules.  $C_{P(b)}$  is calculated by subtracting the peptide concentration in the buffer compartment from the peptide concentration in the liposome compartment (28).

The main advantage of this method is its simplicity in combination with the possibility to determine an *overall affinity* of CPP towards model membranes, including actual insertion into the bilayer, superficial association and aggregation phenomena. In a comparative study of various hCT derived CPP, we demonstrated that the interaction of these peptides with neutral LUV is dominated by the hydrophobicity and secondary structure of the peptides, whereas the interaction with negatively charged LUV is controlled by electrostatic forces and, hence, by the peptides' positive charge density (89) (Chapter 2). Most impressively, partition coefficients could be correlated with

both membrane positioning as assessed by NMR spectroscopy and in vitro uptake studies in HeLa cells (Chapter 3).

*Atomic force microscopy (AFM).* After the introduction of the atomic force microscope by Binnig et al. in 1986 (120), AFM of supported phospholipid bilayers (SPB) has become an essential tool in the analysis of membrane models, particularly for the study of the interactions of drugs, peptides and proteins with lipid bilayers (121). The major assets of AFM are (i) the capacity to probe the surface structure of SPB in real time and under conditions close to physiological, (ii) the flexibility in modifying SPB composition and structure, and (iii) the opportunity to visualize physical properties directly and at very high spatial resolution. In aqueous buffers structure topologies may be acquired with a lateral resolution of 0.5 – 1 nm and a vertical resolution of 0.1 – 0.2 nm (90).

So far, mainly distribution and aggregation phenomena, and the effects of physiological proteins on SPB membrane restructuring have been characterized by AFM (122-126). Further, successful visualization was reported for the formation of striated domains in DPPC bilayers induced by transmembrane peptides (127, 128), and the dissolution process of DOPC bilayers induced by the pore-forming melittin (129). Despite the potential of AFM to contribute substantially to a better understanding of CPP action on lipid membranes, as yet only two AFM studies featuring CPP effects on SPB have been published. In one study, a human calcitonin derived CPP, hCT(9-32), alone or coupled to enhanced green fluorescent protein (eGFP) as cargo, has been found to aggregate in the DOPC fluid phase of DOPC/DPPC phase separated SPB in the absence of cholesterol, and in the DPPC liquid ordered phase, when cholesterol was present. It could be demonstrated that hCT(9-32) played the decisive role for the positioning of the peptide-cargo complex in the bilayer (88).

In another time-lapse AFM study under conditions close to physiological, we demonstrated for the first time a CPP-induced time- and concentration-dependent transformation process of the gel phase DPPC domains, without compromising the bilayer integrity. Both investigated CPP, pVEC and W2-

pVEC, were able to transform the DPPC gel phase domains, which initially protruded by 1 nm from the DOPC phase, via an intermediate state of fractal appearance into a physical state that was indistinguishable from the liquid-crystalline DOPC phase. By fluorescence polarization we confirmed the hypothesis that the effects may be caused by the two peptides' capabilities to increase the fluidity of the DPPC domains. Interestingly, gel phase domains composed of sphingomyelin (SM) were not significantly affected by the two CPP (Chapter 4).

## 4. CELLULAR MODELS TO ASSESS CPP TRANSLOCATION

In addition to the above reviewed methodologies to probe the biophysical interactions of CPP with lipid membrane models, cellular models to assess the biological aspects of the translocation process play an equally important and complementary role. In the following sections, we review a series of cellular methodologies that are currently applied to elucidate the cellular translocation process, its mechanisms, and its toxicological implications. The critical use of such methodologies is of crucial importance as demonstrated by a number of unfortunate artefacts, misinterpretations and premature extrapolations that have lately compromised CPP research. To address this issue, we will critically evaluate the attributes of the different cellular approaches in CPP research and discuss both their assets and drawbacks.

### *4.1. Choice of cell culture models*

The so far most commonly used cell culture models are summarized in Table II. As yet a majority of related studies was performed in adherent or suspension type cell cultures of proliferating nature. Judging from literature the choice of these models seems to be determined often by chance rather than rationale. In

spite of their common use, however, such models may have distinct limitations as the level of their cellular complexity does not match that of organized biological tissues and barriers, which are predominantly composed of fully differentiated cells. For instance, to mimic epithelial translocation only few studies have so far used differentiated epithelial type cell cultures instead of adherent or suspended proliferating ones (22-25). It is well known, that through cellular differentiation, uptake capacities become markedly reduced, probably because of a generally lowered level of unspecific endocytic activity (130-134). Accordingly, the translocation phenomena of CPP observed in proliferating cell models may overestimate those in fully organized tissues. Below we review the most commonly used cell models.

*Proliferating cell models.* As long as in their proliferating state cells do not develop their specific phenotypes and therefore do not represent models for distinct tissues. Nevertheless, adherent or suspension type cell cultures of proliferating nature have been applied in the majority of cell biological studies in CPP research. Typical examples are the following: HeLa cells, derived from an epitheloid human cervix carcinoma, were successfully used in numerous CPP studies (2, 10, 16-18, 106, 135-140). Further, Cos-7, a monkey kidney cell line (5, 6, 141-144), or CHO K1 wild type cells, derived from a Chinese hamster ovary (17, 18, 136-138, 145-148), were also frequently applied. Efficient cellular uptake of CPP has been a common feature of proliferating cell models (10, 16, 140, 147). Remarkably enough, to our knowledge, no failures whatsoever were reported in literature for CPP to translocate the plasma membranes of these models. This may be explained by the fact that proliferating cells have a higher capacity for endocytic uptake of compounds of various chemical nature than confluent cell layers (130-134, 149). With respect to gene transfer mediated by cationic lipids, a significant drop in transfection was reported when polarized epithelial cells were applied instead of actively growing cells (133).

*Confluent cell models.* Unlike proliferating models, fully differentiated confluent cell models have only sporadically been used in CPP research. In most cases, epithelial characteristics were preferred, pointing towards an interest in epithelial uptake and permeation. In the following we give four examples for epithelial cell models that develop specific phenotypes when reaching confluence.

The first one, Madin-Darby canine kidney (MDCK) cell monolayers, derives from a distal renal epithelial cell line and forms confluent sheets of polarized cells joined by tight junctions. Confluent layers of this cell line represent a model for columnar-type absorptive epithelia, possessing transport and permeability qualities similar to those of absorptive epithelia *in vivo* (23, 150). Some of the findings on the translocation of CPP in confluent MDCK cell layers are contrasting. For example, in case of Tat, moderate translocation in MDCK monolayers has been described in one study (22-24), contrary to a complete lack of translocation in another, yet at a ten times lower CPP concentration (22).

Another confluent model of interest in CPP research is the Calu-3 model. It

---

**Table 2. Proliferation state, name, origin and representative publications of reviewed cell lines.**

Cell model	Name	Origin	Publication
proliferating, adherent	HeLa	human cervix carcinoma	[2, 10, 16-18, 106, 135-140]
	Cos-7	monkey kidney epithelium	[5, 6, 141-144]
	CHO K1	chinese hamster ovary	[17, 18, 136-138, 145-148]
	NIH-3T3	mouse fibroblasts	[5-7, 13, 173]
	HS 68	human fibroblasts	[5-7]
	HEK 293	human embryonic kidney tumour	[5, 144, 207]
	RAW264	mouse macrophages	[160]
proliferating, suspension	CEM-SS	human lymphoblasts	[6]
confluent	Caco-2	human colonic epithelial adenocarcinoma	[22, 23, 25, 182]
	Calu-3	human bronchial submucosal adenocarcinoma	[23]
	MDCK	canine distal renal epithelium	[22, 23, 106]
	TR146	neck node metastasis of a human buccal epithelium	[23]

derives from a human bronchial submucosal adenocarcinoma and forms confluent, polarized, and well differentiated monolayers with apical microvilli and cilia, as well as tight junctions (151). In addition, mimicking a typical feature of respiratory epithelia, confluent Calu-3 cells secrete apical mucus. Accordingly, Calu-3 layers represent a common model for the assessment of drug uptake and permeability in airway epithelia (152). Trehin et al. described an endocytic translocation of both Tat and penetratin. In contrast, hCT(9-32) showed only paracellular accumulation in the tight junctional complex without significant translocation of the cell membrane (23).

Correspondingly, CaCo-2 cells, a colonic carcinoma derived cell line, forms equally confluent, well differentiated and polarized monolayers with tight junctions. Through differentiation, CaCo-2 cells adopt morphological characteristics similar to the small intestinal epithelium. The CaCo-2 monolayer is an established standard for routine studies on intestinal drug transport and permeation (153). Remarkably, Tat showed neither translocation into nor permeation through CaCo-2 monolayers (22); Koch et al. found only a minor degree of permeation of Tat-modified nanoparticles through CaCo-2 monolayers (25). In conclusion, CaCo-2 monolayers represent a substantial barrier for translocation as well as permeation of Tat.

The TR146 cell line, finally, originates from a neck node metastasis of a human buccal carcinoma (154). Differentiated TR146 cell layers feature characteristics similar to the buccal epithelium and, therefore, have been used as an *in vitro* model for buccal absorption studies (155). Because of its stratified squamous phenotype, the TR146 model is a candidate to mimic other related epithelia as well, e.g. the rectal or the vaginal mucosa (23, 156). When incubated with the TR146 model, both hCT(9-32) and penetratin showed a sectoral punctuated cytoplasmic pattern indicating endocytic translocation, whereas the cellular interaction of Tat was restricted to paracellular staining, but showed no translocation (23). In conclusion, for yet unknown reasons, translocation in the TR146 model depends typically on the individual CPP.

Overall, differentiated cell culture models seem to have an intriguing potential for discrimination between different CPP. The implications of this aspect may be far reaching but have not yet been considered in great detail in CPP research. Moreover, the contrasts seen in the uptake patterns between the different models indicate a higher level of complexity for the underlying pathways and mechanisms of translocation than expected from studies using proliferating cell models only. Such work is yet ahead in CPP research.

Endothelial cell cultures were used by Koch for the translocation of nanoparticles whose surface has been modified by CPP of multiple cationic charge (157). No relevant rates of translocation were observed in this model.

#### *4.2. Spectroscopic methodologies to assess cellular translocation of CPP*

The majority of spectroscopic methodologies to assess the cellular translocation of CPP are based on the detection of fluorescence, such as by CLSM, FACS, and fluorescence based HPLC readings or multiwell readings on microtitre plates. In order to render CPP amenable for fluorescence detection they need to be labeled with suitable fluorescence markers (16, 66, 106, 143) or carry Trp residues. Alternatively, biotin may be coupled to CPP to allow for binding of fluorescently labeled streptavidin for fluorescence detection (137, 158). An alternative approach is the labeling of the cargoes. For instance, fluorescently labeled plasmid DNA (145), oligodeoxynucleotides (159) or proteins (5, 160) have been used to track their cellular translocation. Other methodologies to follow the translocation of CPP or their cargoes are the assessments by UV spectroscopy or radioactivity readings. Testing biological activities will be covered in another section. Here we review the most frequently used methodologies CLSM and FACS analysis.

*Confocal laser scanning microscopy (CLSM):* The key advantage of CLSM instead of classical fluorescence microscopy lies in its capacity to scan distinct

tissular or cellular sections and to generate high resolution 2D and 3D images of tissues or cells, respectively. This helped to precisely determine the localization of fluorescently labeled CPP or their cargoes, respectively, on a tissular or cellular level. Typically, CLSM is hoped to allow discrimination between surface bound and translocated fluorescence, and at the same time be useful to elucidate specific mechanisms of translocation. Yet, also limitations come along with the use of CLSM, which requires more expertise, and is more expensive and time consuming than simple fluorescence microscopy. First, CLSM is restricted to a qualitative, rather than quantitative analysis of translocation. Furthermore, an unbiased selection of representative sites for CLSM is difficult or impossible, and the statistical significance of the scanned micrographs is necessarily poor. In addition, even when generating 3D CLSM images, deposition of fluorescently labeled CPP in the cellular membrane could be mistaken for intracellular fluorescence. This may be a common cause of problems when evaluating CLSM micrographs, as previously observed in our own work (16) and by others (26, 27). Therefore, a number of protocols have been suggested in order to minimize the misinterpretation of surface bound for translocated CPP. These will be reviewed in another section.

In earlier CPP literature, CLSM studies on the translocation of CPP were frequently performed involving cell fixation, using methanol (26), acetone-methanol (161), formaldehyde (106, 137, 142, 159, 162), or formaldehyde containing ethanol or methanol (1, 14). However, based on conflicting evidence in literature, misinterpretations of CLSM studies owing to problematic fixation protocols have been recently suggested to pose a potential problem to CPP research (18). Evidence for both intracellular distribution and nuclear localization of CPP were found to eventually depend on the applied fixation protocol and not on real translocation. The mechanism of which may be explained as follows: Because of their multiple cationic charge CPP show strong and persistent binding to the negatively charged cell membrane of mammalian cells. Upon fixation with methanol, an agent that is known to cause permeabilization of cell membranes, such surface bound CPP were suggested to

form a reservoir from which CPP may be released and migrate into cytosolic compartments or the nucleus (163). In fact, translocation and nuclear localization of VP22 was not observed to occur in CHO cells unless prior fixation of the cells with methanol (163). Fixation using formaldehyde was reported as milder (164). But its effect on cellular translocation and distribution has been judged controversially: On the one hand, for the cellular translocation of oligonucleotides, Pichon et al. observed identical localization patterns with or without formaldehyde fixation. This would exclude artefacts. On the other hand, artefactual redistribution of surface bound CPP into the nucleus has been recently described even upon formaldehyde fixation (18, 66). In conclusion, because of the potential for post-fixation artefacts the respective protocols need to be judged carefully. As a consequence, more recent CPP translocation studies were increasingly performed without fixation (16, 23, 66, 106, 140, 165). Nevertheless, even some of the latest studies involved fixation, but included controls to rule out artefactual CPP migration phenomena (16, 137, 138).

*Fluorescence activated cell sorting (FACS).* In contrast to the more sporadic nature of CLSM observations, at best allowing a semi-quantitative analysis of CPP translocation, FACS analyses, counting up to about 10'000 cells per sample, are of more substantial statistical significance. However, like CLSM, FACS analysis cannot discriminate between surface bound and translocated fluorescence. Thus, sophisticated quenching protocols need to be employed to minimize or exclude the registration of surface bound CPP when analysing translocation rates (18, 166). This aspect is covered in detail below.

#### *4. 3 Distinction between translocation and surface binding*

In order to allow for fluorescence detection CPP are usually labeled with suitable fluorescence markers. However, the use of fluorescent labels is associated with a number of difficulties, such as limited sensitivity, photo

bleaching and pH dependency. Moreover, in some cases, detection is limited to concentrations which are close to levels causing membrane disturbance, e.g. with MAP and transportan (3). In this case the use of radioactively labeled CPP (167) may lower the detection limit and, therefore, allow the use of non-damaging CPP concentrations. Typically, spectroscopic methodologies as well as radioactivity readings are incapable to discriminate between translocated and surface bound CPP. Therefore, various protocols have been established to distinguish between surface binding and intracellular translocation. Below we describe a few important examples.

*Digestion of extracellular CPP.* An important approach to circumvent an overestimation of translocated CPP caused by surface bound CPP is the enzymatic digestion of surface bound CPP through trypsinization. Richard et al. showed that FACS analysis is incapable to exclusively monitor translocated CPP unless a trypsinization step to cleave surface bound CPP was included in the protocol (18). This is further supported by several examples of how trypsinization helped to discriminate between translocated and surface bound CPP (17, 135, 136, 145). Chico et al. showed that trypsinization could totally digest arginine rich peptides bound to cell surfaces and glass dishes (168). In addition, a combination of trypsinization and heparin treatment could completely displace Tat from the cell surface (143).

*Quenching of surface bound fluorescence.* In addition to enzymatic cleavage, fluorescence quenching is another established approach to discriminate between intracellular and surface bound CPP. For instance, in a CLSM study, Drin et al. and Christiaens et al. quenched the surface bound fluorescence of 7-nitro-2,1,3-benzoxadiazol-4-yl (NBD) labeled CPP by addition of sodium dithionite (26, 27, 167). Obviously, the function of dithionite to reduce the fluorescent NBD label to non-fluorescent derivatives is restricted to extracellular NBD (169). This concept was also applied for studies involving FACS analysis (26, 27, 66, 169). Another approach to exclude surface bound fluorescence is the addition of

Trypan blue, that is helpful with both CLSM (16, 25) or FACS (16, 25, 170-173). Since Trypan blue is excluded from translocating intact cell membranes, it can selectively quench surface bound fluorescence (170-173). Finally, washing with heparan sulphate, a soluble competitor of extracellular heparan sulphate proteoglycans (HPSG), removes surface bound Tat peptide (174).

*Resonance energy transfer (RET).* Another alternative to differentiate between translocated and surface bound fluorescence has been developed by Hallbrink et al., relying on the use of resonance energy transfer (RET) quenching. RET quenching is based on the principle that the absorbance of a quencher molecule overlaps with the emission wavelength of a fluorophore whose fluorescence is quenched as long as the two molecules are in close proximity (175). To apply this principle, it was suggested to covalently ligate a fluorophore labeled, cysteamine containing CPP, e.g. Tat, penetratin, Transportan, or MAP, via a disulfide bond to a small peptide cargo carrying a quencher group (3). Translocation into the reducing intracellular environment is a prerequisite of the disulfide bond to be cleaved, release the quencher and, thus, enhance the fluorescence signal. This reaction may be performed directly in multiwell plates, and is fast and convenient. Typically, the obtained fluorescence, hence CPP concentration, does not result from distinct cells, but represents an average value over the whole sample.

*Derivatization of surface bound CPP.* In case CPP translocation is quantified by means of high performance liquid chromatography (HPLC), which is of particular value to discriminate between translocated CPP and metabolites thereof, a special protocol may be applied to distinguish between intracellular and surface bound CPP. Prior to lysing the cells to prepare for subsequent HPLC analysis, cells may be treated with a membrane impermeable agent, diazotized 2-nitroaniline, resulting in a selective derivatization of accessible Lys side chains of either surface bound CPP, or CPP accumulated in dead cells with compromised membrane integrity. Derivatization results in a significant increase

in hydrophobicity of the construct and causes prolonged HPLC retention times for all surface bound CPP and, hence, discrimination from CPP truly translocated into intact cells (148, 165) and not accessible for derivatization.

#### *4.4 Biological methodologies to assess the cellular translocation of cargoes*

The most reliable method to circumvent an artefactual overestimation of CPP translocation is the measurement of biological effects through the translocated cargo. By this means undesired detection of surface bound CPP may be excluded. Suitable cargoes are (i) peptides or proteins, (ii) oligonucleotides, plasmid DNA or peptide nucleic acids (PNA), and (iii) small molecules or drugs (175-177).

Several fusion proteins ligated to Tat (160, 178) or VP22 (144) have been used for this approach. For example, Vocero-Akbani et al. synthesized Tat-Casp3, a fusion protein derived from the apoptosis-promoting caspase-3 protein. Tat-Casp3 exploits the HIV protease to kill HIV infected cells. However, because of the substitution of endogenous cleavage sites for HIV proteolytic cleavage sites, Tat-Casp3 is only activated by HIV protease in infected cells, resulting in apoptosis, whereas it remains inactive in non-infected cells (160).

In a further study, Wadia et al. demonstrated the successful delivery of a Tat fusion protein employing a test system, in which the cellular expression of a fluorescent protein, EGFP, depended on an efficient intracellular and nuclear delivery of a Tat fusion protein (178).

Alternatively, plasmid DNA, encoding for green fluorescent protein (GFP) (6, 146), luciferase (6, 141, 145), or  $\beta$ -galactosidase (73, 179) was non-covalently linked to CPP and the expression of the respective protein was quantified.

A disadvantage of some biological methodologies, however, is the use of highly specialized or modified cell culture systems whose relevance to represent meaningful drug delivery scenarios may be quite limited or doubtful.

#### *4.5. Assessments of cell viability and cell membrane integrity*

Another major criterion to be considered in the evaluation of CPP translocation is cellular viability. To examine the influence of CPP on cell viability and cell membrane integrity several methods have been applied. In the following we give an overview of the most frequently used methods.

*Cell viability.* The determination of cellular viability often relies on methodologies involving the intracellular cleavage of tetrazolium salts to form highly coloured formazan products. The reaction occurs only in the presence of active mitochondria but not in dead cells. The amount of formazan generated is directly proportional to the fraction of vital cells over a wide range of cell numbers. The most frequently used tetrazolium salts are 3-(4,5-dimethylthiazol-2-yl)-2,5-diphenyl tetrazolium bromide (MTT) (2, 5, 6, 27, 161, 180), sodium 3-[1-[(phenylamino)-carbonyl]-3,4-tetrazolium]-bis(4-methoxy-6-nitro)benzene-sulfonic acid hydrate (XTT) (16) and 3-(4,5-dimethylthiazol-2-yl)-5-(3-carboxymethoxyphenyl)-2-(4-sulfophenyl)-2H-tetra-zolium (MTS) (23). There are several drawbacks associated with the use of tetrazolium salts. First, they are generally cytotoxic; furthermore, the formazan crystals, particularly the reaction product of MTT, are insoluble in culture media and must be solubilized with an organic solvent prior to the readout on a scanning multiwell spectrophotometer. Hence, this protocol allows a single time point measurement only. XTT and MTS have the advantage over MTT that their products are water soluble and, therefore, suited for use with non-adherent as well as adherent cell lines. In addition, XTT or MTS assays can be continuously monitored. A disadvantage of XTT and MTS as compared to MTT is the fact that they may not be efficiently reduced in the cellular environment unless phenazine methosulfate (PMS) is present. The sensitivities of MTT, MTS and XTT are equivalent (181). Since these assays can be applied in multiwell plates, their readout is easy, fast and requires only small amounts of CPP.

*Determination of membrane integrity.* The assessment of the integrity of cellular membranes is generally based on the determination of their permeability for specific markers. Both the leakage of internalized compounds into the surrounding medium and the uptake of otherwise cell membrane impermeable agents into cells may be monitored.

One approach is based on the release of the intracellular enzyme lactate dehydrogenase (LDH) which is present in all mammalian cells. For analysis, the cell culture supernatant is mixed with nicotinamide adenine dinucleotide (NADH) and pyruvate. In the presence of LDH, pyruvate is converted to lactate concomitantly to the oxidation of NADH to NAD<sup>+</sup>. The loss of NADH can be monitored at 340 nm using a microplate reader (106, 148, 182). Alternatively, NAD<sup>+</sup> and lactate are added to the cell supernatant, and LDH activity is measured using an enzymatically coupled reaction (182).

Furthermore, the effect of CPP on the integrity of cellular membranes may be assessed using tritium labeled 2-deoxyglucose. Its cellular uptake across the membrane proceeds via glucose transporters. Once inside cells 2-deoxyglucose is phosphorylated by hexokinase (3, 162, 183). The product, 2-deoxy-D-[1-<sup>3</sup>H]-glucose-6-phosphate cannot leave the cell via the plasma membrane (183). Thus, the efflux of radioactivity from cells preloaded with tritium labeled 2-deoxyglucose may result from a CPP induced membrane disturbance and leakage (183-185). For instance, no membrane leakage was found for Tat and penetratin, whereas transportan and MAP induced membrane leakage at concentrations above 10 μM or 1 μM, respectively (3). For TP10, a transportan analogue, however, no change in membrane leakage was observed (185).

Alternatively, cells may be preincubated with the membrane permeable fluorescein diacetate. Its intracellular cleavage by non-specific esterases then leads to the membrane impermeable fluorescein. Leakage of fluorescein back into the supernatant is a measure for the degree of perturbation or damage to the cell membrane. For instance, following such a protocol, a 5 μM solution of an α-helical model peptide, KLA1, led to a 30% fluorescein leakage, pointing

towards considerably compromised cell membranes (165). The use of Calcein-acetoxy methyl ester (Calcein-AM) follows a similar approach. Readily passing the cell membrane, Calcein-AM will be cleaved by intracellular esterases of viable cells. The resulting metabolite becomes fluorescent and is retained in viable cells only. In case of a compromised cell membrane, the dye will leak out (66, 106, 186).

An alternative way to assess the integrity of the plasma membrane in the presence of CPP is the use of agents that are unable to cross intact plasma membranes but induce fluorescence when intercalating with the nucleic acids in the nucleus. Detection is by fluorescence microscopy, CLSM, or FACS, respectively. To this aim Kramer et al. used ethidium homodimer-1 (EthD-1) as intercalator (24, 106). The authors observed that cellular translocation of a Tat derivative in MDCK cells occurred only in parallel to a nuclear staining with EthD-1. This was taken as a strong indication that the cellular translocation of Tat was restricted to cells with compromised plasma membranes. Propidium iodide (PI) may be used analogously. Monitoring its binding to nucleic acids by FACS analysis is another measure to assess the perturbation or damage of plasma membranes when studying the cellular translocation of CPP (17, 25, 27, 143, 174).

#### *4.6. Methodologies to identify mechanisms of translocation*

Over the past years, the mechanisms by which CPP translocate across cellular membranes have been controversially discussed. Many early studies ascribe the cellular translocation of CPP to an energy independent mechanism, based on observations that translocation was neither significantly inhibited by low temperature nor depletion of the cellular ATP pool, nor by treatment with typical inhibitors of endocytosis, respectively (2). Moreover, a number of structure-activity studies with CPP indicated a minor significance of punctual amino acid modifications for translocation, seemingly implying independence of

receptor recognition and receptor mediated endocytosis (14, 18, 187). Richard et al. were the first to suggest that the strong postulates of passive and energy independent translocation mechanisms in prior studies might have been based on artefacts due to shortcomings in experimental protocols for fluorescence microscopy and FACS analysis (18). As explained above, a major source for misinterpretation may have been an overestimation of CPP translocation caused by non-validated fixation protocols. In addition, strong binding of CPP to the negatively charged cell membrane may have been difficult to distinguish from actual translocation when using fluorescence microscopy and FACS analysis (188). Accordingly, since 2003 more careful experimental precautions have been taken to exclude such artefacts. To date, there is increasing evidence that active translocation mechanisms are far more significant than previously postulated. In fact, endocytosis is the most likely mechanism of the cellular translocation of many major and minor CPP molecules (16, 18, 66, 135, 178). Nevertheless, evidence for passive translocation continues to be published (5, 44, 96, 189). Altogether, the exact mechanisms by which CPP translocate, are still incompletely understood and deserve further investigation. Clearly, diverse mechanisms may prevail depending on the CPP itself, their association with the cargo, the used cellular model and its cellular differentiation. But evidence for endocytic processes is definitely expanding in both numbers and significance. Below we review several approaches to elucidate the underlying mechanism of CPP translocation.

*Translocation at low temperature.* Active translocation mechanisms such as endocytosis are supposed to be retarded at low temperature (18). Yet, in the majority of early studies that demonstrated CPP to enter cells even when incubated at low temperature, the cell cultures were subject to fixation (1, 2, 14, 138, 161). As reviewed in a previous section, fixation protocols may be subject to redistribution and artefactual internalization of initially surface bound CPP. As a consequence, low temperature studies involving a fixation protocol and showing evidence for nuclear uptake of CPP or cargoes thereof need to be

handled with care. A representative example is the study of Morris et al. (7) on the CPP mediated nuclear transfer of fluorescently labeled oligonucleotides even at low temperature. Because of the involved fixation protocol, the unconditional exclusion of an endocytic mechanism in this study may deserve reconsideration. In the context of translocation at low temperature yet another aspect needs to be discussed. It has often been overseen in CPP literature that low temperatures may also slow down energy independent processes to a significant extent. This aspect was recently brought up by Letoha et al. (139) indicating that low temperatures may lead to a drop in cell membrane fluidity which may affect passive permeation of solutes. Overall, only by combination of a low temperature control with other controls (see below) reliable conclusions about the cellular entry mechanisms of CPP should be made (16-18, 66, 143, 178, 183).

*Identification of entry mechanisms using endocytosis inhibitors.* Another approach to explore active translocation mechanisms of CPP is by means of diverse endocytosis inhibitors which are known to block specific endocytic pathways. In the following we describe the most relevant inhibitors used in CPP research.

An unspecific suppression of all active mechanisms can be achieved by depletion of the intracellular ATP pool. This may be reached, e.g., by preincubation of the cell culture model with sodium azide ( $\text{NaN}_3$ ) together with 2-deoxy-D-glucose (DOG) (16-18, 66, 148).  $\text{NaN}_3$  inhibits the cytochrome oxidase in the mitochondrial membrane and thus blocks the oxidative phosphorylation resulting in a loss of the chemical energy of ATP. DOG, which acts as a competitive antagonist to glucose, can enter cells, but is no substrate to produce ATP (190, 191).

It is commonly known that actin and myosin, which polymerize to microfilaments, are involved in the formation of plasma membrane derived vesicles during endocytosis (192). Cytochalasin D induces depolymerization of the microfilaments of actin involved in macropinocytosis, without affecting

other endocytic processes (189, 193). In fact, translocation of Tat (135, 143) and a Tat fusion protein (147) was significantly impaired by cytochalasin D, whereas translocation of transferrin, a marker for clathrin mediated endocytosis, was not affected (135, 143). In agreement with these results, Elliot et al. found that the translocation of VP22 was sensitive to cytochalasin D treatment. Dowdy and co-workers recently showed that cellular uptake of Tat fusion protein was inhibited by treatment with amiloride, another inhibitor of macropinocytosis (178). Interestingly, internalization of the CPP SynB3 in K562 cells was not affected by the addition of cytochalasin D (66). This is in agreement with recent results, showing that the actin cytoskeleton has no major role in endocytic processes in K562 cells (66, 147).

For intracellular trafficking, in which the Golgi apparatus is involved, microtubules are essential. To investigate the role of the Golgi apparatus in CPP trafficking, Brefeldin A, which is known to disrupt the Golgi apparatus and thus impair Golgi trafficking, was used (135, 194, 195). As expected, Brefeldin A did not affect the entry of the Tat-fusion protein into cells, whereas it impaired its nuclear translocation (135) .

Two other drugs, vinblastin (66) and nocodazole (66, 147), inhibit microtubule polymerization. Nocodazol depolymerises cellular microtubules, thus leading to a breakdown of the Golgi apparatus (196). It has been shown that nocodazol did not have an effect on the translocation of a Tat-fusion protein (147), Tat (135), or transferrin (135). Elliot et al. described that VP22 accumulated in the nucleus in the absence as well as in the presence of nocodazole, indicating that intact microtubules were not required for cellular entry (194). For both SynB as well as penetratin, however, the cellular accumulation was reduced in the presence of nocodazole and peptides remained inside vesicles localized to the cell periphery rather than the perinuclear region (66). Finally, taxol, which is known to stabilize microtubules, influenced neither the cellular translocation of Tat nor of transferrin, whose uptake seems to be independent of microtubule polymerisation (135).

*Co-localization with endocytosis markers.* Endocytosis is a complex mechanism that involves different pathways. The best-characterized pathway so far is that of clathrin-dependent endocytosis, which sets in with the formation of clathrin-coated invaginations in the plasma membrane that pinch off to form clathrin-coated vesicles (135, 197). Less defined are non-classical, clathrin-independent pathways, such as caveolae-mediated endocytosis. Caveolae are flask-shaped, small (50-70 nm) invaginations in the plasma membrane that constitute a subclass of detergent-resistant membrane domains enriched in cholesterol and sphingolipids, called lipid rafts (198). Caveolae are characterized by the presence of the integral membrane protein caveolin-1 (147) and are involved in the intracellular transportation of lipid raft-associated molecules (199, 200). Several bacterial toxins, including cholera toxin (201), and some viruses, including SV40 (202), are known to make use of caveolae-mediated endocytosis to enter cells.

In CPP research, several markers have been suggested to elucidate the type of endocytosis involved in the translocation mechanism. For example, FM 4-64, a general marker for endocytosis (18, 178), and fluorescently labeled dextran, a marker for fluid phase endocytosis (203), have been used. Co-localization of Tat fusion protein (178), or Tat peptide (18) with FM 4-64 was found, and partially co-localization of CPP/protein complexes with dextran.

Transferrin, a marker for early endosomes, is known to be translocated via clathrin-dependent endocytosis (16, 18, 137, 197). For both Tat (135) and SAP (16) no co-localization with transferrin was found in HeLa cells. Therefore, at least in this model, the translocation pathway of Tat and SAP turned out to be different from endocytosis via clathrin-coated endosomes (16, 135). Remarkably and in large contrast to these findings, Richard et al. described Tat to predominantly co-localize with transferrin in HeLa and CHO cells (18).

Independently from clathrin mediated endocytosis, the active fraction of cholera toxin, similar to other microbial toxins, is translocated via caveolae mediated endocytosis using lipid rafts (204). In order to probe the potential of this pathway for CPP, we and others co-incubated the fluorescently labeled B-

subunit of cholera toxin and a Tat fusion protein (135), or SAP, hCT(9-32)-br and hCT(9-32) (16), respectively, with a cellular model. Subsequent CLSM based co-localization studies revealed that cholera toxin and the investigated CPP share a common internalization mechanism via lipid rafts. Furthermore, Tat was found to co-localize with caveolin-1, a membrane protein on caveolae, confirming that Tat translocates via this pathway (135).

After endocytic internalization, vesicles move to intracellular compartments within the cytosol where they often undergo complex trafficking and sorting events. In order to monitor the intracellular fate of the investigated CPP, we and others performed co-localization studies with early endosomal antigen 1 (EEA1), a protein associated with early endosomes. For Tat, no co-localization was observed (135), whereas SAP and hCT(9-32)-br, respectively, partially co-localized with EEA1. The latter results indicate the active involvement of endosomal compartments after translocation, and provide preliminary information on the pathways of intracellular trafficking (16).

Maturation and trafficking of most endosomes eventually lead to their fusion with lysosomes. To investigate the accumulation of CPP in lysosomes, co-localization of translocated CPP with Lysotracker red, a marker for acidic organelles such as lysosomes that emits light in a pH dependent manner (145), was investigated. Only a small fraction of penetratin was found to co-localize, indicating that only a fraction of this CPP accumulated in acidic organelles (27).

*Internalization mediated by lipid rafts.* Fittipaldi et al. (135) were the first to test the involvement of caveolae-mediated endocytosis as a potential pathway for CPP. Caveolae-mediated endocytosis is involved in the intracellular transportation of lipid raft-associated molecules. Lipid rafts are defined by their insolubility in non-ionic detergents (199). Fittipaldi et al. tested the effect of the non-ionic detergent Triton-X-100 on both Tat and transferrin. Triton X-100 completely solubilized endosomes containing transferrin, whereas those containing Tat remained unaffected (135). This is in agreement with the fact that

transferrin enters cells using clathrin-coated pits, whereas Tat relies on detergent resistant caveolae (135).

Another way to test the involvement of lipid rafts in the endocytosis of CPP is the pre-treatment with nystatin or methyl- $\beta$ -cyclodextrin (M $\beta$ CD). Nystatin elicits cholesterol sequestration (200) and, therefore, alters the structure and function of caveolae (66, 205). Similarly, treatment with M $\beta$ CD extracts cholesterol from cell membranes, impairing lipid raft mediated endocytosis, without influencing clathrin-dependent endocytosis (200). For the protegrin derived CPP SynB3, no effect was observed after incubation with nystatin, suggesting a caveolae-independent pathway (66). Interestingly, Tat internalization was only slightly affected by Nystatin (17), whereas the translocation of a Tat-fusion protein was strongly reduced, indicating that only the latter followed a lipid raft dependent pathway (178). Nevertheless, it was also described, that M $\beta$ CD treatments clearly impaired endocytosis of Tat fusion protein and Tat peptide (135, 143, 178), as well as SAP, hCT(9-32) and hCT(9-32)-br, respectively (16).

*Interactions of CPP with the extracellular matrix.* Interactions between CPP and proteoglycans (PG) of the extracellular matrix have been recently given wide attention in CPP research. PG encompass a heterogeneous group of proteins in the cellular membrane that are ligated to linear, polysulfated, and hence highly negatively charged glycosaminoglycan (GAG) polysaccharides, e.g. heparan sulphate (HS) or chondroitin sulfate (CS) (206). Most mammalian cells express heparan sulphate proteoglycans (HSPG), typically resulting in a negatively charged cell membrane (22, 138). It has been previously assumed that the translocation of distinct cationic CPP crucially depends on their prior binding to cell-surface HSPG, obviously promoted by the electrostatic interaction of cationic CPP and negatively charged sulphated glycosaminoglycans on the cell surface (137). In the following we will review three protocols described in literature to evaluate the internalization of CPP under the influence of HSPG:

Competition with exogenous HS chains. Coincubation with heparin, a close structural homologue of HS, was performed in order to evaluate its function as a soluble competitor to cell membrane associated HSPG (207). As expected, heparin impaired the internalization of Tat (147), a Tat fusion protein (178, 207) or other CPP (16). Surprisingly, co-incubation with other GAG, such as chondroitin sulphate A, B, C and hyaluronic acid, caused only little inhibition of Tat (136), Antp or Tat derivatized liposomes (137), and had no effect on the translocation of Tat or penetratin (137). The translocation of a Tat fusion protein, however, was strongly inhibited by coincubation with chondroitin sulphate B and C (178). These results indicate that the influence of HSPG is strongly dependent on the respective CPP or its cargo, respectively.

Pre-treatment with HS-degrading enzymes. In order to confirm the influence of cellular HS on the uptake of CPP, HeLa or CHO cells were treated with heparinase III, an enzyme digesting HS proteoglycan on the cell surface (17, 138). This treatment completely inhibited the uptake of Tat fusion protein but did not affect the uptake of a short Tat peptide (138). The participation of HS in translocation is also illustrated by a recent publication showing that pre-treatment with heparinase also inhibited Tat peptide uptake (17). Tyagi et al. described that the translocation of both full length Tat as well as Tat fusion proteins in CHO cells was abolished when the cells were treated with enzymes that specifically degraded HS chains (136). Furthermore, treatment of cells with enzymes like chondroitin ABC lyase or heparitinase to delete cell-associated GAG caused a significant drop in Tat/DNA complex translocation, indicating that both HSPG as well as CSPG were involved in the translocation process (145). Likewise, treatment of CHO cells with chlorate which inhibits GAG sulfation resulted in a dramatic decrease in the translocation rates of Tat/DNA complexes (145).

Use of mutant cell lines lacking GAG expression. An elegant alternative to the enzymatic digestion of HS is the study in cells, which are genetically deficient in the biosynthesis of fully sulphated HS. For Tat, internalization was only found in CHO cells but not in A-747 cells, a mutant of the former cell line, deficient in

proteoglycan biosynthesis (17, 137). In agreement, Tyagi et al. described, that the internalization of Tat fused to green fluorescent protein was selectively impaired in cells lacking the expression of proteoglycans (136). In some contrast to these results, Silhol et al. found no difference in the translocation of fluorescein labeled Tat in CHO cells as compared to HS-deficient cells, whereas translocation of Tat fusion protein could be observed in CHO wild type cells but not in HS deficient cells. However, in contrast to the former study, the latter involved cell fixation (138) casting the above mentioned doubts on its outcome. Nevertheless, as supported by several studies, a significant fraction of CPP was translocated even in the absence of HS, suggesting potential for the co-existence of a HS independent mechanism of entry (17, 137).

## 5. CONSISTENCY AND TRANSFERABILITY OF BIOPHYSICAL AND CELL BIOLOGICAL STUDIES

Despite numerous biophysical and cell biological studies in literature, systematic combinations of the two approaches have been sporadic. This is unfortunate because coupled studies could be particularly valuable in terms of understanding structure–activity relationships and in elucidating further mechanistic details in CPP translocation.

Earlier coupled biophysical and cell biological studies mainly addressed the question of structural requirements for cellular uptake. As described in previous sections many of the CPP adopt an  $\alpha$ -helical conformation, especially in an lipophilic environment. In this respect Derossi et al. (14) investigated the dependence between the cellular translocation of penetratin and derivatives thereof with their degree of  $\alpha$ -helicity. Interestingly, the introduction of one to three  $\alpha$ -helix-breaking Pro in the original penetratin sequence did not hamper cellular uptake. Similarly, Letoha et al. (139) discovered that not  $\alpha$ -helicity but amphiphilicity of penetratin derived CPP was necessary for efficient

translocation (139). In addition, as found with several synthetic peptides, the propensity to adopt an  $\alpha$ -helical conformation is crucial but not sufficient for cellular translocation. Further, Du et al. concluded peptide side-chain topology and/or peptide amide bond direction of the carrier sequence to represent prerequisites for successful CPP translocation (13).

Even more so, a study investigating several  $\alpha$ -helical derivatives of Tat(47-57) came up with a correlation between amphipathicity and translocation: As compared to Tat, the translocation of PTD-4, a derivative with optimized amphipathic properties, was more than thirty times higher in vitro, and five times in vivo. It is unfortunate, however, that in this FACS study no measure was taken to quench surface bound fluorescence, leaving final questions as to the robustness of the data. In conclusion, there is reasonable evidence that an  $\alpha$ -helical conformation may enhance translocation, but it is not firmly established whether  $\alpha$ -helicity represents a prerequisite for the translocation of CPP.

Other coupled studies focused on the correlation between the type and intensity of CPP interaction with lipid bilayer models on the one hand and translocation into cells on the other. Drin et al. (26) showed that the cellular uptake of penetratin derivatives required a minimal hydrophobicity and at the same time a certain positive net charge of the CPP, and correlated well with lipid binding to liposomal models. A similar correlation was observed by Christiaens et al. (27). Moreover, for hCT-derived CPP we came across a positive correlation of both liposome-buffer partitioning and extent of interfacial positioning of selected CPP with their uptake efficiency (Chapter 3). In fact, a Trp modified peptide sequence turned out to induce a stronger and more homogenously distributed interfacial positioning over most of the backbone. It is noteworthy that Trp also represents a crucial residue for penetratin. When replaced by Phe, the translocation efficiency of penetratin was essentially lost (102). Equal to our observations with hCT-derived CPP (Chapter 3), there is independent evidence that flat and  $\alpha$ -helical positioning of CPP on the lipid membrane appears to be a favorable feature for translocation, whereas positioning perpendicular to the

membrane surface may be associated with a membrane damage and an increase in toxicity (104).

## 6. CONCLUSION

Over the past decade, a variety of CPP have been developed and evaluated for their function as vectors for the cellular delivery of therapeutic agents that normally cannot cross the plasma membrane. In addition, by employing both cell biological and biophysical approaches, strong effort has been put into the elucidation of CPP translocation mechanisms. In the present work we reviewed the findings of numerous representative studies in this field with a particular focus on the thereby used methodologies and approaches. Through critical evaluation of the respective techniques we outlined both their potentials and limitations with the aim to provide useful information of how to select appropriate methodological approaches and avoid misinterpretations. Moreover, we indicated ways to correlate biophysical and cell biological studies. To avoid misinterpretation of data and for a better understanding of the mechanisms of translocation, we advocate strictly validated methodologies only and encourage a combination of both approaches.

## REFERENCES:

1. Derossi, D., A. H. Joliot, G. Chassaing, and A. Prochiantz, *The third helix of the Antennapedia homeodomain translocates through biological membranes*. J Biol Chem, (1994). **269**, 10444-50.
2. Vives, E., P. Brodin, and B. Lebleu, *A truncated HIV-1 Tat protein basic domain rapidly translocates through the plasma membrane and accumulates in the cell nucleus*. J Biol Chem, (1997). **272**, 16010-7.

3. Hallbrink, M., A. Floren, A. Elmquist, M. Pooga, T. Bartfai, and U. Langel, *Cargo delivery kinetics of cell-penetrating peptides*. *Biochim Biophys Acta*, (2001). **1515**, 101-109.
4. Pooga, M., M. Hallbrink, M. Zorko, and U. Langel, *Cell penetration by transportan*. *Faseb J*, (1998). **12**, 67-77.
5. Morris, M. C., J. Depollier, J. Mery, F. Heitz, and G. Divita, *A peptide carrier for the delivery of biologically active proteins into mammalian cells*. *Nat Biotechnol*, (2001). **19**, 1173-6.
6. Morris, M. C., L. Chaloin, J. Mery, F. Heitz, and G. Divita, *A novel potent strategy for gene delivery using a single peptide vector as a carrier*. *Nucleic Acids Res*, (1999). **27**, 3510-7.
7. Morris, M. C., P. Vidal, L. Chaloin, F. Heitz, and G. Divita, *A new peptide vector for efficient delivery of oligonucleotides into mammalian cells*. *Nucleic Acids Res*, (1997). **25**, 2730-6.
8. Koppelhus, U., S. K. Awasthi, V. Zachar, H. U. Holst, P. Ebbesen, and P. E. Nielsen, *Cell-dependent differential cellular uptake of PNA, peptides, and PNA-peptide conjugates*. *Antisense Nucleic Acid Drug Dev*, (2002). **12**, 51-63.
9. Eriksson, M., P. E. Nielsen, and L. Good, *Cell permeabilization and uptake of antisense peptide-peptide nucleic acid (PNA) into Escherichia coli*. *J Biol Chem*, (2002). **277**, 7144-7.
10. Koch, A. M., F. Reynolds, M. F. Kircher, H. P. Merkle, R. Weissleder, and L. Josephson, *Uptake and metabolism of a dual fluorochrome Tat-nanoparticle in HeLa cells*. *Bioconjug Chem*, (2003). **14**, 1115-21.
11. Tseng, Y. L., J. J. Liu, and R. L. Hong, *Translocation of liposomes into cancer cells by cell-penetrating peptides penetratin and tat: a kinetic and efficacy study*. *Mol Pharmacol*, (2002). **62**, 864-72.
12. Oehlke, J., A. Scheller, B. Wiesner, E. Krause, M. Beyermann, E. Klauschenz, M. Melzig, and M. Bienert, *Cellular uptake of an alpha-*

- helical amphipathic model peptide with the potential to deliver polar compounds into the cell interior non-endocytically.* Biochim Biophys Acta, (1998). **1414**, 127-39.
13. Du, C., S. Yao, M. Rojas, and Y. Z. Lin, *Conformational and topological requirements of cell-permeable peptide function.* J Pept Res, (1998). **51**, 235-243.
  14. Derossi, D., S. Calvet, A. Trembleau, A. Brunissen, G. Chassaing, and A. Prochiantz, *Cell internalization of the third helix of the Antennapedia homeodomain is receptor-independent.* J Biol Chem, (1996). **271**, 18188-18193.
  15. Vives, E., *Cellular uptake [correction of utake] of the Tat peptide: an endocytosis mechanism following ionic interactions.* J Mol Recognit, (2003). **16**, 265-71.
  16. Foerg, C., U. Ziegler, J. Fernandez-Carneado, E. Giralt, R. Rennert, A. G. Beck-Sickinger, and H. P. Merkle, *Decoding the Entry of Two Novel Cell-Penetrating Peptides in HeLa Cells: Lipid Raft-Mediated Endocytosis and Endosomal Escape.* Biochemistry, (2005). **44**, 72-81.
  17. Richard, J. P., K. Melikov, H. Brooks, P. Prevot, B. Lebleu, and L. V. Chernomordik, *Cellular uptake of unconjugated TAT peptide involves clathrin-dependent endocytosis and heparan sulfate receptors.* J Biol Chem, (2005).
  18. Richard, J. P., K. Melikov, E. Vives, C. Ramos, B. Verbeure, M. J. Gait, L. V. Chernomordik, and B. Lebleu, *Cell-penetrating peptides. A reevaluation of the mechanism of cellular uptake.* J Biol Chem, (2003). **278**, 585-90.
  19. Brockman, H., *Lipid monolayers: why use half a membrane to characterize protein-membrane interactions?* Curr Opin Struct Biol, (1999). **9**, 438-443.
  20. Seelig, J., *Titration calorimetry of lipid-peptide interactions.* Biochim Biophys Acta, (1997). **1331**, 103-16.

21. Rosengarth, A., A. Wintergalen, H. J. Galla, H. J. Hinz, and V. Gerke, *Ca<sup>2+</sup>-independent interaction of annexin I with phospholipid monolayers.* FEBS Lett, (1998). **438**, 279-84.
22. Violini, S., V. Sharma, J. L. Prior, M. Dyszlewski, and D. Piwnica-Worms, *Evidence for a plasma membrane-mediated permeability barrier to Tat basic domain in well-differentiated epithelial cells: lack of correlation with heparan sulfate.* Biochemistry, (2002). **41**, 12652-61.
23. Trehin, R., U. Krauss, A. G. Beck-Sickinger, H. P. Merkle, and H. M. Nielsen, *Cellular uptake but low permeation of human calcitonin-derived cell penetrating peptides and Tat(47-57) through well-differentiated epithelial models.* Pharm Res, (2004). **21**, 1248-56.
24. Kramer, S. D., and H. Wunderli-Allenspach, *No entry for TAT(44-57) into liposomes and intact MDCK cells: novel approach to study membrane permeation of cell-penetrating peptides.* Biochim Biophys Acta, (2003). **1609**, 161-169.
25. Koch, A. M., F. Reynolds, H. P. Merkle, R. Weissleder, and L. Josephson, *Transport Of Surface-Modified Nanoparticles Through Cell Monolayers.* Chembiochem, (2005). **6**, 337-345.
26. Drin, G., M. Mazel, P. Clair, D. Mathieu, M. Kaczorek, and J. Temsamani, *Physico-chemical requirements for cellular uptake of pAntp peptide. Role of lipid-binding affinity.* Eur J Biochem, (2001). **268**, 1304-1314.
27. Christiaens, B., J. Grootenhoeve, M. Reusens, A. Joliot, M. Goethals, J. Vandekerckhove, A. Prochiantz, and M. Rosseneu, *Membrane interaction and cellular internalization of penetratin peptides.* Eur J Biochem, (2004). **271**, 1187-1197.
28. Lasch, J., *Interaction of detergents with lipid vesicles.* Biochim Biophys Acta, (1995). **1241**, 269-292.
29. Seydel, J. K., and M. Wiese *Drug-Membrane Interactions,* (2002), Wiley-VCH, Weinheim.

30. Sitaram, N., and R. Nagaraj, *Interaction of antimicrobial peptides with biological and model membranes: structural and charge requirements for activity*. Biochim Biophys Acta, (1999). **1462**, 29-54.
31. van Balen, G. P., C. M. Martinet, G. Caron, G. Bouchard, M. Reist, P. A. Carrupt, R. Fruttero, A. Gasco, and B. Testa, *Liposome/water lipophilicity: methods, information content, and pharmaceutical applications*. Med Res Rev, (2004). **24**, 299-324.
32. Bonard, J., T. Stora, J. Salvetat, F. Maier, T. Stockli, C. Duschl, L. Forro, W. deHeer, and A. Chatelain, *Purification and size-selection of carbon nanotubes*. ADVANCED MATERIALS, (1997). **9**, 827-&.
33. Cushley, R., and M. Okon, *NMR studies of lipoprotein structure*. Annu Rev Biph Biom, (2002). **31**, 177-206.
34. Lewis, B. A., and D. M. Engelman, *Lipid bilayer thickness varies linearly with acyl chain length in fluid phosphatidylcholine vesicles*. J Mol Biol, (1983). **166**, 211-217.
35. Marsh, D. *Handbook of Lipid Bilayers*, (1990), CRC, Boca Raton, FL.
36. Nagle, J. F., and S. Tristram-Nagle, *Structure of lipid bilayers*. Biochim Biophys Acta, (2000). **1469**, 159-95.
37. Shenkarev, Z., T. Balashova, R. Efremov, Z. Yakimenko, T. Ovchinnikova, J. Raap, and A. Arseniev, *Spatial structure of zervamicin IIB bound to DPC micelles: Implications for voltage-gating*. BIOPHYSICAL JOURNAL, (2002). **82**, 762-771.
38. Seelig, A., *Interaction of a substance P agonist and of substance P antagonists with lipid membranes. A thermodynamic analysis*. Biochemistry, (1992). **31**, 2897-904.
39. Berlose, J. P., O. Convert, D. Derossi, A. Brunissen, and G. Chassaing, *Conformational and associative behaviours of the third helix of antennapedia homeodomain in membrane-mimetic environments*. Eur J Biochem, (1996). **242**, 372-386.

40. Lindberg, M., H. Biverstahl, A. Graslund, and L. Maler, *Structure and positioning comparison of two variants of penetratin in two different membrane mimicking systems by NMR*. Eur J Biochem, (2003). **270**, 3055-3063.
41. Lindberg, M., and A. Graslund, *The position of the cell penetrating peptide penetratin in SDS micelles determined by NMR*. FEBS Lett, (2001). **497**, 39-44.
42. Lindberg, M., J. Jarvet, U. Langel, and A. Graslund, *Secondary structure and position of the cell-penetrating peptide transportan in SDS micelles as determined by NMR*. Biochemistry, (2001). **40**, 3141-3149.
43. Biverstahl, H., A. Andersson, A. Graslund, and L. Maler, *NMR solution structure and membrane interaction of the N-terminal sequence (1-30) of the bovine prion protein*. Biochemistry, (2004). **43**, 14940-14947.
44. Deshayes, S., A. Heitz, M. C. Morris, P. Charnet, G. Divita, and F. Heitz, *Insight into the mechanism of internalization of the cell-penetrating carrier peptide Pep-1 through conformational analysis*. Biochemistry, (2004). **43**, 1449-1457.
45. Drin, G., H. Demene, J. Temsamani, and R. Brasseur, *Translocation of the pAntp peptide and its amphipathic analogue AP-2AL*. Biochemistry, (2001). **40**, 1824-1834.
46. Chaloin, L., P. Vidal, A. Heitz, N. Van Mau, J. Mery, G. Divita, and F. Heitz, *Conformations of primary amphipathic carrier peptides in membrane mimicking environments*. Biochemistry, (1997). **36**, 11179-11187.
47. Magzoub, M., K. Kilk, L. E. Eriksson, U. Langel, and A. Graslund, *Interaction and structure induction of cell-penetrating peptides in the presence of phospholipid vesicles*. Biochim Biophys Acta, (2001). **1512**, 77-89.

48. Vold, R. R., R. S. Prosser, and A. J. Deese, *Isotropic solutions of phospholipid bicelles: a new membrane mimetic for high-resolution NMR studies of polypeptides*. *J Biomol NMR*, (1997). **9**, 329-35.
49. Struppe, J., J. A. Whiles, and R. R. Vold, *Acidic phospholipid bicelles: a versatile model membrane system*. *Biophys J*, (2000). **78**, 281-9.
50. Bader, R., M. Lerch, and O. Zerbe. in *BioNMR in Drug Research* (Zerbe, O., Ed.) (2002) pp 95-120, Wiley-VCH, Weinheim.
51. Sanders, C. R., and R. S. Prosser, *Bicelles: a model membrane system for all seasons?* *Structure*, (1998). **6**, 1227-34.
52. New, R. B. C. in *Liposomes, A Practical Approach* (New, R. B. C., Ed.) (1990) pp 33-104, Oxford University Press, New York.
53. Maguire, L. A., H. Zhang, and P. A. Shamlou, *Preparation of small unilamellar vesicles (SUV) and biophysical characterization of their complexes with poly-L-lysine-condensed plasmid DNA*. *Biotechnology and Applied Biochemistry*, (2003). **37**, 73-81.
54. Schindler, H., *Formation of planar bilayers from artificial or native membrane vesicles*. *FEBS Lett*, (1980). **122**, 77-9.
55. Ladokhin, A. S., S. Jayasinghe, and S. H. White, *How to measure and analyze tryptophan fluorescence in membranes properly, and why bother?* *Anal Biochem*, (2000). **285**, 235-245.
56. Persson, D., P. E. Thoren, E. K. Esbjorner, M. Goksor, P. Lincoln, and B. Norden, *Vesicle size-dependent translocation of penetratin analogs across lipid membranes*. *Biochim Biophys Acta*, (2004). **1665**, 142-155.
57. Thoren, P. E., D. Persson, E. K. Esbjorner, M. Goksor, P. Lincoln, and B. Norden, *Membrane binding and translocation of cell-penetrating peptides*. *Biochemistry*, (2004). **43**, 3471-89.
58. Magzoub, M., L. E. Eriksson, and A. Graslund, *Conformational states of the cell-penetrating peptide penetratin when interacting with phospholipid*

- vesicles: effects of surface charge and peptide concentration.* Biochim Biophys Acta, (2002). **1563**, 53-63.
59. Lundberg, P., M. Magzoub, M. Lindberg, M. Hallbrink, J. Jarvet, L. E. Eriksson, U. Langel, and A. Graslund, *Cell membrane translocation of the N-terminal (1-28) part of the prion protein.* Biochem Biophys Res Commun, (2002). **299**, 85-90.
60. Mayer, L. D., M. J. Hope, and P. R. Cullis, *Vesicles of variable sizes produced by a rapid extrusion procedure.* Biochim Biophys Acta, (1986). **858**, 161-8.
61. Seelig, A., *Local anesthetics and pressure: a comparison of dibucaine binding to lipid monolayers and bilayers.* Biochim Biophys Acta, (1987). **899**, 196-204.
62. Rouyer, I., Y. Takahashi, and T. Ide, *Dietary phospholipid-dependent reductions in gene expression and activity of liver enzymes in fatty acid synthesis in fasted-refed rats.* JOURNAL OF NUTRITIONAL SCIENCE AND VITAMINOLOGY, (1999). **45**, 287-302.
63. van Meer, G., van Genderen, I.L. in *Subcellular Biochemistry: Physicochemical Methods in the Study of Biomembranes* (Hilderson, H. J., Ralston, G.B., Ed.) (1994) pp 1-24, Plenum Press, New York.
64. Binder, H., and G. Lindblom, *A molecular view on the interaction of the trojan peptide penetratin with the polar interface of lipid bilayers.* Biophys J, (2004). **87**, 332-343.
65. Deshayes, S., T. Plenat, G. Aldrian-Herrada, G. Divita, C. Le Grimellec, and F. Heitz, *Primary amphipathic cell-penetrating peptides: Structural requirements and interactions with model membranes.* Biochemistry, (2004). **43**, 7698-7706.
66. Drin, G., S. Cottin, E. Blanc, A. R. Rees, and J. Temsamani, *Studies on the internalisation mechanism of cationic cell-penetrating peptides.* J Biol Chem, (2003). **278**, 31192-31201.

67. Magzoub, M., L. E. Eriksson, and A. Graslund, *Comparison of the interaction, positioning, structure induction and membrane perturbation of cell-penetrating peptides and non-translocating variants with phospholipid vesicles*. Biophys Chem, (2003). **103**, 271-88.
68. Persson, D., P. E. Thoren, M. Herner, P. Lincoln, and B. Norden, *Application of a novel analysis to measure the binding of the membrane-translocating Peptide penetratin to negatively charged liposomes*. Biochemistry, (2003). **42**, 421-9.
69. Persson, D., P. E. Thoren, P. Lincoln, and B. Norden, *Vesicle membrane interactions of penetratin analogues*. Biochemistry, (2004). **43**, 11045-55.
70. Ziegler, A., X. L. Blatter, A. Seelig, and J. Seelig, *Protein transduction domains of HIV-1 and SIV TAT interact with charged lipid vesicles. Binding mechanism and thermodynamic analysis*. Biochemistry, (2003). **42**, 9185-94.
71. Persson, D., P. E. Thoren, and B. Norden, *Penetratin-induced aggregation and subsequent dissociation of negatively charged phospholipid vesicles*. FEBS Lett, (2001). **505**, 307-12.
72. Dom, G., C. Shaw-Jackson, C. Matis, O. Bouffoux, J. J. Picard, A. Prochiantz, M. P. Mingeot-Leclercq, R. Brasseur, and R. Rezsohazy, *Cellular uptake of Antennapedia Penetratin peptides is a two-step process in which phase transfer precedes a tryptophan-dependent translocation*. Nucleic Acids Res, (2003). **31**, 556-561.
73. Duguid, J. G., C. Li, M. Shi, M. J. Logan, H. Alila, A. Rolland, E. Tomlinson, J. T. Sparrow, and L. C. Smith, *A physicochemical approach for predicting the effectiveness of peptide-based gene delivery systems for use in plasmid-based gene therapy*. Biophys J, (1998). **74**, 2802-2814.
74. Koynova, R., and M. Caffrey, *An index of lipid phase diagrams*. Chem Phys Lipids, (2002). **115**, 107-219.

75. Castano, S., I. Cornut, K. Buttner, J. L. Dasseux, and J. Dufourcq, *The amphipathic helix concept: length effects on ideally amphipathic LiKj(i=2j) peptides to acquire optimal hemolytic activity.* Biochim Biophys Acta, (1999). **1416**, 161-175.
76. Castano, S., B. Desbat, and J. Dufourcq, *Ideally amphipathic beta-sheeted peptides at interfaces: structure, orientation, affinities for lipids and hemolytic activity of (KL)(m)K peptides.* Biochim Biophys Acta, (2000). **1463**, 65-80.
77. Christiaens, B., S. Symoens, S. Verheyden, Y. Engelborghs, A. Joliot, A. Prochiantz, J. Vandekerckhove, M. Rosseneu, B. Vanloo, and S. Vanderheyden, *Tryptophan fluorescence study of the interaction of penetratin peptides with model membranes.* Eur J Biochem, (2002). **269**, 2918-2926.
78. Kogan, M. J., O. Lopez, M. Cocera, C. Lopez-Iglesias, A. De La Maza, and E. Giralt, *Exploring the interaction of the surfactant N-terminal domain of gamma-Zein with soybean phosphatidylcholine liposomes.* Biopolymers, (2004). **73**, 258-268.
79. Thoren, P. E., D. Persson, M. Karlsson, and B. Norden, *The antennapedia peptide penetratin translocates across lipid bilayers - the first direct observation.* FEBS Lett, (2000). **482**, 265-8.
80. Bucher, P., A. Fischer, P. Luisi, T. Oberholzer, and P. Walde, *Giant vesicles as biochemical compartments: The use of microinjection techniques.* LANGMUIR, (1998). **14**, 2712-2721.
81. Karlsson, M., K. Nolkrantz, M. J. Davidson, A. Stromberg, F. Ryttsen, B. Akerman, and O. Orwar, *Electroinjection of colloid particles and biopolymers into single unilamellar liposomes and cells for bioanalytical applications.* Anal Chem, (2000). **72**, 5857-5862.

82. Fischer, A., T. Oberholzer, and P. L. Luisi, *Giant vesicles as models to study the interactions between membranes and proteins*. Biochim Biophys Acta, (2000). **1467**, 177-188.
83. Mathivet, L., S. Cribier, and P. F. Devaux, *Shape change and physical properties of giant phospholipid vesicles prepared in the presence of an AC electric field*. Biophys J, (1996). **70**, 1112-21.
84. Mou, J., J. Yang, and Z. Shao, *Tris(hydroxymethyl)aminomethane (C<sub>4</sub>H<sub>11</sub>NO<sub>3</sub>) induced a ripple phase in supported unilamellar phospholipid bilayers*. Biochemistry, (1994). **33**, 4439-43.
85. Mou, J., J. Yang, C. Huang, and Z. Shao, *Alcohol induces interdigitated domains in unilamellar phosphatidylcholine bilayers*. Biochemistry, (1994). **33**, 9981-5.
86. Tamm, L., and H. McConnell, *Supported Phospholipid-Bilayers*. BIOPHYSICAL JOURNAL, (1985). **47**, 105-113.
87. Berquand, A., M. P. Mingeot-Leclercq, and Y. F. Dufrene, *Real-time imaging of drug-membrane interactions by atomic force microscopy*. Biochimica Et Biophysica Acta-Biomembranes, (2004). **1664**, 198-205.
88. Boichot, S., U. Krauss, T. Plenat, R. Rennert, P. E. Milhiet, A. Beck-Sickinger, and C. Le Grimellec, *Calcitonin-derived carrier peptide plays a major role in the membrane localization of a peptide-cargo complex*. FEBS Lett, (2004). **569**, 346-350.
89. Herbig, M. E., U. Fromm, J. Leuenberger, U. Krauss, A. G. Beck-Sickinger, and H. P. Merkle, *Bilayer interaction and localization of cell penetrating peptides with model membranes: A comparative study of a human calcitonin (hCT)-derived peptide with pVEC and pAntp(43-58)*. Biochim Biophys Acta, (2005). **1712**, 197-211.
90. Engel, A., C. A. Schoenenberger, and D. J. Muller, *High resolution imaging of native biological sample surfaces using scanning probe microscopy*. Curr Opin Struct Biol, (1997). **7**, 279-284.

91. Welfe, H. in *Methoden in der Proteinanalytik* (Holtzhauer, M., Ed.) (1996) pp 103-122, Springer, Heidelberg.
92. Holzwarth, G., and P. Doty, *The Ultraviolet Circular Dichroism Of Polypeptides*. J Am Chem Soc, (1965). **87**, 218-228.
93. Provencher, S. W., and J. Glockner, *Estimation of globular protein secondary structure from circular dichroism*. Biochemistry, (1981). **20**, 33-7.
94. Chang, C. T., C. S. Wu, and J. T. Yang, *Circular dichroic analysis of protein conformation: inclusion of the beta-turns*. Anal Biochem, (1978). **91**, 13-31.
95. Barany-Wallje, E., A. Andersson, A. Graslund, and L. Maler, *NMR solution structure and position of transportan in neutral phospholipid bicelles*. FEBS Lett, (2004). **567**, 265-269.
96. Deshayes, S., S. Gerbal-Chaloin, M. C. Morris, G. Aldrian-Herrada, P. Charnet, G. Divita, and F. Heitz, *On the mechanism of non-endosomal peptide-mediated cellular delivery of nucleic acids*. Biochim Biophys Acta, (2004). **1667**, 141-147.
97. Brown, L. R., C. Bösch, and K. Wüthrich, *Location and orientation relative to the micelle surface for glucagon in mixed micelles with dodecylphosphocholine: EPR and NMR studies*. Biochim Biophys Acta, (1981). **642**, 296-312.
98. Chattopadhyay, A., and E. London, *Parallax method for direct measurement of membrane penetration depth utilizing fluorescence quenching by spin-labeled phospholipids*. Biochemistry, (1987). **26**, 39-45.
99. London, E., and G. W. Feigenson, *Fluorescence quenching in model membranes. 1. Characterization of quenching caused by a spin-labeled phospholipid*. Biochemistry, (1981). **20**, 1932-1938.

100. Jarvet, J., J. Zdunek, P. Damberg, and A. Graslund, *Three-dimensional structure and position of porcine motilin in sodium dodecyl sulfate micelles determined by <sup>1</sup>H NMR*. Biochemistry, (1997). **36**, 8153-8163.
101. Damberg, P., J. Jarvet, and A. Graslund, *Micellar systems as solvents in peptide and protein structure determination*. Methods Enzymol, (2001). **339**, 271-285.
102. Prochiantz, A., *Getting hydrophilic compounds into cells: lessons from homeopeptides*. Curr Opin Neurobiol, (1996). **6**, 629-34.
103. Andersson, A., J. Almqvist, F. Hagn, and L. Maler, *Diffusion and dynamics of penetratin in different membrane mimicking media*. Biochim Biophys Acta, (2004). **1661**, 18-25.
104. Whiles, J. A., R. Brasseur, K. J. Glover, G. Melacini, E. A. Komives, and R. R. Vold, *Orientation and effects of mastoparan X on phospholipid bicelles*. Biophys J, (2001). **80**, 280-93.
105. Schmidt, M. C., B. Rothen-Rutishauser, B. Rist, A. Beck-Sickinger, H. Wunderli-Allenspach, W. Rubas, W. Sadee, and H. P. Merkle, *Translocation of human calcitonin in respiratory nasal epithelium is associated with self-assembly in lipid membrane*. Biochemistry, (1998). **37**, 16582-90.
106. Trehin, R., U. Krauss, R. Muff, M. Meinecke, A. G. Beck-Sickinger, and H. P. Merkle, *Cellular internalization of human calcitonin derived peptides in MDCK monolayers: a comparative study with Tat(47-57) and penetratin(43-58)*. Pharm Res, (2004). **21**, 33-42.
107. Wagner, K., A. G. Beck-Sickinger, and D. Huster, *Structural investigations of a human calcitonin-derived carrier peptide in a membrane environment by solid-state NMR*. Biochemistry, (2004). **43**, 12459-68.
108. Abrams, F. S., and E. London, *Calibration of the parallax fluorescence quenching method for determination of membrane penetration depth*:

- refinement and comparison of quenching by spin-labeled and brominated lipids.* Biochemistry, (1992). **31**, 5312-5322.
109. Raghuraman, H., S. K. Pradhan, and A. Chattopadhyay, *Effect of urea on the organization and dynamics of triton X-100 micelles: A fluorescence approach.* J Phys Chem B, (2004). **108**, 2489-2496.
110. Abrams, F. S., and E. London, *Extension of the parallax analysis of membrane penetration depth to the polar region of model membranes: use of fluorescence quenching by a spin-label attached to the phospholipid polar headgroup.* Biochemistry, (1993). **32**, 10826-10831.
111. McIntosh, T. J., and P. W. Holloway, *Determination of the depth of bromine atoms in bilayers formed from bromolipid probes.* Biochemistry, (1987). **26**, 1783-8.
112. Bolen, E. J., and P. W. Holloway, *Quenching of tryptophan fluorescence by brominated phospholipid.* Biochemistry, (1990). **29**, 9638-9643.
113. Moro, F., F. M. Goni, and M. A. Urbaneja, *Fluorescence quenching at interfaces and the permeation of acrylamide and iodide across phospholipid bilayers.* FEBS Lett, (1993). **330**, 129-32.
114. Huang, Z. J., and R. P. Haugland, *Partition coefficients of fluorescent probes with phospholipid membranes.* Biochem Biophys Res Commun, (1991). **181**, 166-71.
115. Kaiser, R. D., and E. London, *Location of diphenylhexatriene (DPH) and its derivatives within membranes: comparison of different fluorescence quenching analyses of membrane depth.* Biochemistry, (1999). **38**, 2610.
116. Wang, S., J. M. Beechem, E. Gratton, and M. Glaser, *Orientational distribution of 1,6-diphenyl-1,3,5-hexatriene in phospholipid vesicles as determined by global analysis of frequency domain fluorimetry data.* Biochemistry, (1991). **30**, 5565-72.
117. Lakowicz, J. R. *Principles of Fluorescence Spectroscopy*, (1999), 2nd ed. ed., Kluwer Academic, New York.

118. Nagy, I. B., M. A. Alsina, I. Haro, F. Reig, and F. Hudecz, *Phospholipid-model membrane interactions with branched polypeptide conjugates of a hepatitis A virus peptide epitope*. Bioconjug Chem, (2000). **11**, 30-8.
119. Pauletti, G. M., and H. Wunderli Allenspach, *Partition-Coefficients in-Vitro - Artificial Membranes as a Standardized Distribution Model*. Eur. J. Pharm. Sci., (1994). **1**, 273-282.
120. Binnig, G., C. F. Quate, and C. Gerber, *Atomic Force Microscope*. Physical Review Letters, (1986). **56**, 930-933.
121. Dufrene, Y. F., and G. U. Lee, *Advances in the characterization of supported lipid films with the atomic force microscope*. Biochim Biophys Acta, (2000). **1509**, 14-41.
122. Milhiet, P. E., M. C. Giocondi, O. Baghdadi, F. Ronzon, B. Roux, and C. Le Grimellec, *Spontaneous insertion and partitioning of alkaline phosphatase into model lipid rafts*. EMBO Rep, (2002). **3**, 485-90.
123. Mou, J., D. M. Czajkowsky, and Z. Shao, *Gramicidin A aggregation in supported gel state phosphatidylcholine bilayers*. Biochemistry, (1996). **35**, 3222-6.
124. You, H. X., X. Qi, G. A. Grabowski, and L. Yu, *Phospholipid membrane interactions of saposin C: in situ atomic force microscopic study*. Biophys J, (2003). **84**, 2043-57.
125. Reviakine, I., W. Bergsma-Schutter, A. N. Morozov, and A. Brisson, *Two-dimensional crystallization of annexin A5 on phospholipid bilayers and monolayers: A solid-solid phase transition between crystal forms*. Langmuir, (2001). **17**, 1680-1686.
126. Milhiet, P. E., M. C. Giocondi, O. Baghdadi, F. Ronzon, C. Le Grimellec, and B. Roux, *AFM detection of GPI protein insertion into DOPC/DPPC model membranes*. Single Molecules, (2002). **3**, 135-140.
127. Rinia, H. A., R. A. Kik, R. A. Demel, M. M. Snel, J. A. Killian, J. P. van Der Eerden, and B. de Kruijff, *Visualization of highly ordered striated*

- domains induced by transmembrane peptides in supported phosphatidylcholine bilayers.* Biochemistry, (2000). **39**, 5852-8.
128. Rinia, H. A., J. W. Boots, D. T. Rijkers, R. A. Kik, M. M. Snel, R. A. Demel, J. A. Killian, J. P. van der Eerden, and B. de Kruijff, *Domain formation in phosphatidylcholine bilayers containing transmembrane peptides: specific effects of flanking residues.* Biochemistry, (2002). **41**, 2814-24.
129. Steinem, C., H. J. Galla, and A. Janshoff, *Interaction of melittin with solid supported membranes.* Physical Chemistry Chemical Physics, (2000). **2**, 4580-4585.
130. Shaw, A. J. *Epithelial Cell Culture*, (1996), Oxford University Press.
131. Matsui, H., L. G. Johnson, S. H. Randell, and R. C. Boucher, *Loss of binding and entry of liposome-DNA complexes decreases transfection efficiency in differentiated airway epithelial cells.* J Biol Chem, (1997). **272**, 1117-26.
132. Foster, K. A., M. L. Avery, M. Yazdanian, and K. L. Audus, *Characterization of the Calu-3 cell line as a tool to screen pulmonary drug delivery.* Int J Pharm, (2000). **208**, 1-11.
133. Duchler, M., M. Pengg, S. Brunner, M. Muller, G. Brem, and E. Wagner, *Transfection of epithelial cells is enhanced by combined treatment with mannitol and polyethyleneglycol.* J Gene Med, (2001). **3**, 115-24.
134. Kazmierczak, B. I., K. Mostov, and J. N. Engel, *Epithelial cell polarity alters Rho-GTPase responses to Pseudomonas aeruginosa.* Mol Biol Cell, (2004). **15**, 411-9.
135. Fittipaldi, A., A. Ferrari, M. Zoppe, C. Arcangeli, V. Pellegrini, F. Beltram, and M. Giacca, *Cell membrane lipid rafts mediate caveolar endocytosis of HIV-1 Tat fusion proteins.* J Biol Chem, (2003). **278**, 34141-9.

136. Tyagi, M., M. Rusnati, M. Presta, and M. Giacca, *Internalization of HIV-1 tat requires cell surface heparan sulfate proteoglycans*. J Biol Chem, (2001). **276**, 3254-61.
137. Console, S., C. Marty, C. Garcia-Echeverria, R. Schwendener, and K. Ballmer-Hofer, *Antennapedia and HIV TAT 'protein transduction domains' promote endocytosis of high Mr cargo upon binding to cell surface glycosaminoglycans*. J Biol Chem, (2003).
138. Silhol, M., M. Tyagi, M. Giacca, B. Lebleu, and E. Vives, *Different mechanisms for cellular internalization of the HIV-1 Tat-derived cell penetrating peptide and recombinant proteins fused to Tat*. Eur J Biochem, (2002). **269**, 494-501.
139. Letoha, T., S. Gaal, C. Somlai, A. Czajlik, A. Perczel, and B. Penke, *Membrane translocation of penetratin and its derivatives in different cell lines*. J Mol Recognit, (2003). **16**, 272-279.
140. Fischer, R., K. Kohler, M. Fotin-Mleczek, and R. Brock, *A stepwise dissection of the intracellular fate of cationic cell-penetrating peptides*. J Biol Chem, (2004). **279**, 12625-12635.
141. Niidome, T., N. Ohmori, A. Ichinose, A. Wada, H. Mihara, T. Hirayama, and H. Aoyagi, *Binding of cationic alpha-helical peptides to plasmid DNA and their gene transfer abilities into cells*. J Biol Chem, (1997). **272**, 15307-12.
142. Niidome, T., M. Wakamatsu, A. Wada, T. Hirayama, and H. Aoyagi, *Required structure of cationic peptide for oligonucleotide-binding and -delivering into cells*. J Pept Sci, (2000). **6**, 271-9.
143. Kaplan, I. M., J. S. Wadia, and S. F. Dowdy, *Cationic TAT peptide transduction domain enters cells by macropinocytosis*. J Control Release, (2005). **102**, 247-53.
144. Liu, C., B. Kong, H. H. Xia, K. A. O. Ellem, and M. Q. Wei, *VP22 enhanced intercellular trafficking of HSV thymidine kinase reduced the*

- level of ganciclovir needed to cause suicide cell death.* Journal of Gene Medicine, (2001). **3**, 145-152.
145. Sandgren, S., F. Cheng, and M. Belting, *Nuclear Targeting of Macromolecular Polyanions by an HIV-Tat Derived Peptide. ROLE FOR CELL-SURFACE PROTEOGLYCANS.* J Biol Chem, (2002). **277**, 38877-83.
146. Krauss, U., M. Muller, M. Stahl, and A. G. Beck-Sickinger, *In vitro gene delivery by a novel human calcitonin (hCT)-derived carrier peptide.* Bioorg Med Chem Lett, (2004). **14**, 51-4.
147. Ferrari, A., V. Pellegrini, C. Arcangeli, A. Fittipaldi, M. Giacca, and F. Beltram, *Caveolae-mediated internalization of extracellular HIV-1 tat fusion proteins visualized in real time.* Mol Ther, (2003). **8**, 284-94.
148. Hallbrink, M., J. Oehlke, G. Papsdorf, and M. Bienert, *Uptake of cell-penetrating peptides is dependent on peptide-to-cell ratio rather than on peptide concentration.* Biochim Biophys Acta, (2004). **1667**, 222-8.
149. Bacallao, R., C. Antony, C. Dotti, E. Karsenti, E. H. Stelzer, and K. Simons, *The subcellular organization of Madin-Darby canine kidney cells during the formation of a polarized epithelium.* J Cell Biol, (1989). **109**, 2817-32.
150. Cho, M. J., D. P. Thompson, C. T. Cramer, T. J. Vidmar, and J. F. Scieszka, *The Madin Darby canine kidney (MDCK) epithelial cell monolayer as a model cellular transport barrier.* Pharm Res, (1989). **6**, 71-7.
151. Shen, B. Q., W. E. Finkbeiner, J. J. Wine, R. J. Mrsny, and J. H. Widdicombe, *Calu-3: a human airway epithelial cell line that shows cAMP-dependent Cl<sup>-</sup> secretion.* Am J Physiol, (1994). **266**, L493-501.
152. Florea, B. I., M. L. Cassara, H. E. Junginger, and G. Borchard, *Drug transport and metabolism characteristics of the human airway epithelial cell line Calu-3.* J Control Release, (2003). **87**, 131-8.

153. Artursson, P., K. Palm, and K. Luthman, *Caco-2 monolayers in experimental and theoretical predictions of drug transport.* Adv Drug Deliv Rev, (2001). **46**, 27-43.
154. Rupniak, H. T., C. Rowlatt, E. B. Lane, J. G. Steele, L. K. Trejdosiewicz, B. Laskiewicz, S. Povey, and B. T. Hill, *Characteristics of four new human cell lines derived from squamous cell carcinomas of the head and neck.* J Natl Cancer Inst, (1985). **75**, 621-35.
155. Jacobsen, J., E. B. Nielsen, K. Brondum-Nielsen, M. E. Christensen, H. B. Olin, N. Tommerup, and M. R. Rassing, *Filter-grown TR146 cells as an in vitro model of human buccal epithelial permeability.* Eur J Oral Sci, (1999). **107**, 138-46.
156. Nielsen, H. M., J. C. Verhoef, M. Ponec, and M. R. Rassing, *TR146 cells grown on filters as a model of human buccal epithelium: permeability of fluorescein isothiocyanate-labelled dextrans in the presence of sodium glycocholate.* J Control Release, (1999). **60**, 223-33.
157. Koch, A. (2005) in *ETH Zurich*, Zurich.
158. Soomets, U., M. Lindgren, X. Gallet, M. Hallbrink, A. Elmquist, L. Balaspiri, M. Zorko, M. Pooga, R. Brasseur, and U. Langel, *Deletion analogues of transportan.* Biochim Biophys Acta, (2000). **1467**, 165-76.
159. Chaloin, L., P. Vidal, P. Lory, J. Mery, N. Lautredou, G. Divita, and F. Heitz, *Design of carrier peptide-oligonucleotide conjugates with rapid membrane translocation and nuclear localization properties.* Biochem Biophys Res Commun, (1998). **243**, 601-608.
160. Vocero-Akbani, A. M., N. V. Heyden, N. A. Lissy, L. Ratner, and S. F. Dowdy, *Killing HIV-infected cells by transduction with an HIV protease-activated caspase-3 protein.* Nat Med, (1999). **5**, 29-33.
161. Futaki, S., T. Suzuki, W. Ohashi, T. Yagami, S. Tanaka, K. Ueda, and Y. Sugiura, *Arginine-rich peptides. An abundant source of membrane-*

- permeable peptides having potential as carriers for intracellular protein delivery.* J Biol Chem, (2001). **276**, 5836-5840.
162. Elmquist, A., M. Lindgren, T. Bartfai, and U. Langel, *VE-cadherin-derived cell-penetrating peptide, pVEC, with carrier functions.* Exp Cell Res, (2001). **269**, 237-244.
163. Lundberg, M., and M. Johansson, *Is VP22 nuclear homing an artifact?* Nat Biotechnol, (2001). **19**, 713-4.
164. Pichon, C., M. Monsigny, and A. C. Roche, *Intracellular localization of oligonucleotides: influence of fixative protocols.* Antisense Nucleic Acid Drug Dev, (1999). **9**, 89-93.
165. Scheller, A., J. Oehlke, B. Wiesner, M. Dathe, E. Krause, M. Beyermann, M. Melzig, and M. Bienert, *Structural requirements for cellular uptake of alpha-helical amphipathic peptides.* J Pept Sci, (1999). **5**, 185-94.
166. Lundberg, M., and M. Johansson, *Positively charged DNA-binding proteins cause apparent cell membrane translocation.* Biochem Biophys Res Commun, (2002). **291**, 367-371.
167. Zorko, M., and U. Langel, *Cell-penetrating peptides: mechanism and kinetics of cargo delivery.* Adv Drug Deliv Rev, (2005). **57**, 529-45.
168. Chico, D. E., R. L. Given, and B. T. Miller, *Binding of cationic cell-permeable peptides to plastic and glass.* Peptides, (2003). **24**, 3-9.
169. McIntyre, J. C., and R. G. Sleight, *Fluorescence assay for phospholipid membrane asymmetry.* Biochemistry, (1991). **30**, 11819-27.
170. Sahlin, S., J. Hed, and I. Rundquist, *Differentiation between Attached and Ingested Immune-Complexes by a Fluorescence Quenching Cytofluorometric Assay.* J Immunol Methods, (1983). **60**, 115-124.
171. Wan, C. P., C. S. Park, and B. H. S. Lau, *A Rapid and Simple Microfluorometric Phagocytosis Assay.* J Immunol Methods, (1993). **162**, 1-7.

172. Ma, Z. S., and L. Y. Lim, *Uptake of chitosan and associated insulin in Caco-2 cell monolayers: A comparison between chitosan molecules and chitosan nanoparticles*. Pharm Res, (2003). **20**, 1812-1819.
173. Innes, N. P., and G. R. Ogden, *A technique for the study of endocytosis in human oral epithelial cells*. Arch Oral Biol, (1999). **44**, 519-23.
174. Ziegler, A., P. Nervi, M. Durrenberger, and J. Seelig, *The Cationic Cell-Penetrating Peptide CPP(TAT) Derived from the HIV-1 Protein TAT Is Rapidly Transported into Living Fibroblasts: Optical, Biophysical, and Metabolic Evidence*. Biochemistry, (2005). **44**, 138-48.
175. Langel, U. *Cell-Penetrating Peptides: processes and applications*, (2002), CRC Press.
176. Lindsay, M. A., *Peptide-mediated cell delivery: application in protein target validation*. Curr Opin Pharmacol, (2002). **2**, 587-594.
177. Zhao, M., and R. Weissleder, *Intracellular cargo delivery using tat peptide and derivatives*. Med Res Rev, (2004). **24**, 1-12.
178. Wadia, J. S., R. V. Stan, and S. F. Dowdy, *Transducible TAT-HA fusogenic peptide enhances escape of TAT-fusion proteins after lipid raft macropinocytosis*. Nat Med, (2004). **10**, 310-315.
179. Ignatovich, I. A., E. B. Dizhe, A. V. Pavlotskaya, B. N. Akifiev, S. V. Burov, S. V. Orlov, and A. P. Perevozchikov, *Complexes of plasmid DNA with basic domain 47-57 of the HIV-1 Tat protein are transferred to mammalian cells by endocytosis-mediated pathways*. J Biol Chem, (2003). **278**, 42625-36.
180. Mosmann, T., *Rapid colorimetric assay for cellular growth and survival: application to proliferation and cytotoxicity assays*. J Immunol Methods, (1983). **65**, 55-63.
181. Roehm, N. W., G. H. Rodgers, S. M. Hatfield, and A. L. Glasebrook, *An improved colorimetric assay for cell proliferation and viability utilizing the tetrazolium salt XTT*. J Immunol Methods, (1991). **142**, 257-65.

182. Decker, T., and M. L. Lohmann-Matthes, *A quick and simple method for the quantitation of lactate dehydrogenase release in measurements of cellular cytotoxicity and tumor necrosis factor (TNF) activity*. J Immunol Methods, (1988). **115**, 61-9.
183. Lindgren, M. E., M. M. Hallbrink, A. M. Elmquist, and U. Langel, *Passage of cell-penetrating peptides across a human epithelial cell layer in vitro*. Biochem J, (2003). **Pt.**
184. Walum, E., and A. Peterson, *Tritiated 2-deoxy-D-glucose as a probe for cell membrane permeability studies*. Anal Biochem, (1982). **120**, 8-11.
185. Kilk, K., S. El-Andaloussi, P. Jarver, A. Meikas, A. Valkna, T. Bartfai, P. Kogerman, M. Metsis, and U. Langel, *Evaluation of transportan 10 in PEI mediated plasmid delivery assay*. J Control Release, (2005). **103**, 511-523.
186. Ciapetti, G., D. Granchi, E. Verri, L. Savarino, D. Cavedagna, and A. Pizzoferrato, *Application of a combination of neutral red and amido black staining for rapid, reliable cytotoxicity testing of biomaterials*. Biomaterials, (1996). **17**, 1259-64.
187. Wender, P. A., D. J. Mitchell, K. Pattabiraman, E. T. Pelkey, L. Steinman, and J. B. Rothbard, *The design, synthesis, and evaluation of molecules that enable or enhance cellular uptake: peptoid molecular transporters*. Proc Natl Acad Sci U S A, (2000). **97**, 13003-8.
188. Nakase, I., M. Niwa, T. Takeuchi, K. Sonomura, N. Kawabata, Y. Koike, M. Takehashi, S. Tanaka, K. Ueda, J. C. Simpson, A. T. Jones, Y. Sugiura, and S. Futaki, *Cellular uptake of arginine-rich peptides: roles for macropinocytosis and actin rearrangement*. Mol Ther, (2004). **10**, 1011-22.
189. Simeoni, F., M. C. Morris, F. Heitz, and G. Divita, *Insight into the mechanism of the peptide-based gene delivery system MPG: implications for delivery of siRNA into mammalian cells*. Nucleic Acids Res, (2003). **31**, 2717-24.

190. Sandvig, K., and S. Olsnes, *Entry of the Toxic Proteins Abrin, Modeccin, Ricin, and Diphtheria-Toxin into Cells.2. Effect of Ph, Metabolic-Inhibitors, and Ionophores and Evidence for Toxin Penetration from Endocytotic Vesicles*. Journal of Biological Chemistry, (1982). **257**, 7504-7513.
191. Al-Arifi, A. (2003) in *Mathematisch-Naturwissenschaftlich-Technische Fakultät*, Martin-Luther-Universität Halle-Wittenberg, Halle.
192. Stryer, L. *Biochemie*, (1996), Spektrum, Akad. Verl.
193. Silverstein, S. C., R. M. Steinman, and Z. A. Cohn, *Endocytosis*. Annu Rev Biochem, (1977). **46**, 669-722.
194. Elliott, G., and P. O'Hare, *Intercellular trafficking and protein delivery by a herpesvirus structural protein*. Cell, (1997). **88**, 223-33.
195. Lippincott-Schwartz, J., J. G. Donaldson, A. Schweizer, E. G. Berger, H. P. Hauri, L. C. Yuan, and R. D. Klausner, *Microtubule-Dependent Retrograde Transport of Proteins into the Er in the Presence of Brefeldin-a Suggests an Er Recycling Pathway*. Cell, (1990). **60**, 821-836.
196. Dinter, A., and E. G. Berger, *Golgi-disturbing agents*. Histochem Cell Biol, (1998). **109**, 571-90.
197. Schmid, S. L., *Clathrin-coated vesicle formation and protein sorting: an integrated process*. Annu Rev Biochem, (1997). **66**, 511-48.
198. Anderson, R. G., *The caveolae membrane system*. Annu Rev Biochem, (1998). **67**, 199-225.
199. Simons, K., and E. Ikonen, *Functional rafts in cell membranes*. Nature, (1997). **387**, 569-72.
200. Simons, K., and D. Toomre, *Lipid rafts and signal transduction*. Nat Rev Mol Cell Biol, (2000). **1**, 31-9.
201. Nichols, B. J., A. K. Kenworthy, R. S. Polishchuk, R. Lodge, T. H. Roberts, K. Hirschberg, R. D. Phair, and J. Lippincott-Schwartz, *Rapid cycling of*

- lipid raft markers between the cell surface and Golgi complex.* J Cell Biol, (2001). **153**, 529-41.
202. Pelkmans, L., J. Kartenbeck, and A. Helenius, *Caveolar endocytosis of simian virus 40 reveals a new two-step vesicular-transport pathway to the ER.* Nat Cell Biol, (2001). **3**, 473-83.
203. Console, S., C. Marty, C. Garcia-Echeverria, R. Schwendener, and K. Ballmer-Hofer, *Antennapedia and HIV transactivator of transcription (TAT) "protein transduction domains" promote endocytosis of high molecular weight cargo upon binding to cell surface glycosaminoglycans.* J Biol Chem, (2003). **278**, 35109-35114.
204. Montesano, R., J. Roth, A. Robert, and L. Orci, *Non-coated membrane invaginations are involved in binding and internalization of cholera and tetanus toxins.* Nature, (1982). **296**, 651-3.
205. Anderson, R. G., B. A. Kamen, K. G. Rothberg, and S. W. Lacey, *Potocytosis: sequestration and transport of small molecules by caveolae.* Science, (1992). **255**, 410-1.
206. Belting, M., *Heparan sulfate proteoglycan as a plasma membrane carrier.* Trends Biochem Sci, (2003). **28**, 145-151.
207. Rusnati, M., G. Tulipano, D. Spillmann, E. Tanghetti, P. Oreste, G. Zoppetti, M. Giacca, and M. Presta, *Multiple interactions of HIV-I Tat protein with size-defined heparin oligosaccharides.* J Biol Chem, (1999). **274**, 28198-205.



## CHAPTER II

### **Bilayer interaction and localization of cell penetrating peptides with model membranes: a comparative study of a human calcitonin (hCT) derived peptide with pVEC and pAntp(43-58)**

*Michael E. Herbig<sup>1</sup>, Ursina Fromm<sup>1</sup>, Jeannine Leuenberger<sup>1</sup>, Ulrike Krauss<sup>2</sup>,  
Annette G. Beck-Sickinger<sup>2</sup>, and Hans P. Merkle<sup>1</sup>*

<sup>1</sup>Drug Formulation & Delivery Group, Department of Chemistry and Applied BioSciences, Swiss Federal Institute of Technology Zurich (ETH Zurich), Wolfgang-Pauli-Strasse 10, CH-8093 Zurich, Switzerland

<sup>2</sup>Institute of Biochemistry, University of Leipzig, Bruderstrasse 34, D-04103 Leipzig, Germany

## ABSTRACT

Cell penetrating peptides (CPPs) are able to translocate problematic therapeutic cargoes across cellular membranes. The exact mechanisms of translocation are still under investigation. However, evidence for endocytic uptake is increasing. We investigated the interactions of CPPs with phospholipid bilayers as first step of translocation. To this purpose, we employed four independent techniques, comprising (i) liposome buffer equilibrium dialysis, (ii) Trp fluorescence quenching, (iii) fluorescence polarization, and (iv) determination of  $\zeta$ -potentials. Using unilamellar vesicles (LUVs) of different phospholipid composition, we compared weakly cationic human calcitonin (hCT) derived peptides with the oligocationic CPPs pVEC and penetratin (pAntp). Apparent partition coefficients of hCT derived peptides in neutral POPC LUVs were dependent on amino acid composition and secondary structure; partitioning in negatively charged POPC/POPG (80:20) LUVs was increased and mainly governed by electrostatic interactions. For hCT(9-32) and its derivatives D values raised from about 100-200 in POPC to about 1000 to 1500 when negatively charged lipids were present. Localisation profiles of CPPs obtained by Trp fluorescence quenching were dependent on the charge density of LUVs. In POPC/POPG hCT derived CPPs were located on the bilayer surface, whereas pVEC and pAntp resided deeper in the membrane. In POPG LUVs an increase of fluorescence polarization was observed for pVEC and pAntp but not for hCT derived peptides. Generally, we found strong peptide-phospholipid interactions, especially when negatively charged lipids were present.

## INTRODUCTION

Over the past decade, several classes and/or prototypes of cell-penetrating peptides (CPPs) have been characterized in several aspects. Initially, their entry mechanisms were postulated not to be mediated by receptors or transporters (1, 2), suggesting a passive, non-endocytic transfer. More recently, however, increasing evidence has been brought up suggesting the involvement of active, endocytic processes (3-7). The ability of the CPPs to translocate when covalently or physically linked with a cargo, including polypeptides and nucleic acids, renders them of broad interest in cell biology, biotechnology and drug delivery. In fact, CPPs have been used as vectors for the cytoplasmic and nuclear delivery of hydrophilic biomolecules and drugs, both *in vivo* and *in vitro* (1, 2, 8). The exact mechanisms underlying the translocation across membranes are still under investigation. As a consequence of artefactual uptake phenomena due to cell fixation, the hypothesis of an energy independent, direct transport of CPPs through biomembranes, postulated in earlier CPP studies (9-11), had to give way to concepts involving endocytosis (3-6, 12). Increasing attention is concentrated on the first step of CPP uptake: an initial adherence on the membrane surface leading to an enrichment in the phospholipid bilayer, which may subsequently trigger endocytic uptake (3, 5, 12-15). In fact, in the few studies combining cell biological and biophysical approaches, good correlations between membrane affinity and uptake efficiency could be observed (16, 17). This underlines that both, the cell biology of the uptake and the biophysical analysis of the interactions between the CPPs and the bilayer membrane are legitimate approaches necessary for a better understanding of CPP translocation mechanisms.

In the present study, we investigate in detail the interactions of two classes of CPPs with several bilayer models with the aim to contribute to the mechanistic understanding of such interactions as a step towards cellular translocation. Four independent methodological approaches were employed, comprising liposome

buffer equilibrium dialysis, Trp fluorescence quenching, fluorescence polarization, and determination of  $\zeta$ -potentials. In particular, we compared weakly cationic C-terminal fragments of human calcitonin, hCT(9-32) and modifications thereof with two oligocationic CPPs, the vascular endothelial (VE)-cadherin-derived CPP, pVEC, and the *Antennapedia* homeodomain protein derived penetratin, denoted pAntp (Table 1).

Human calcitonin (hCT) is a peptide hormone that is approved for the treatment of established osteoporosis (18). N-terminally truncated derivatives of hCT, which lack hormonal activity, represent a novel class of weakly cationic CPPs and have been systematically investigated by Tréhin et al. It has been shown that sequences from hCT(9-32) to hCT(18-32) penetrated the plasma membrane of a fully organized epithelial model, differentiated MDCK monolayers, and resulted in a sectoral, vesicular cytoplasmic distribution. The uptake process was temperature-, time- and concentration-dependent, indicating that translocation may follow an endocytic pathway; among the investigated derivatives hCT(9-32) was the most efficient one, and its single, positively charged lysine in position 18 turned out to be essential for uptake (19). Furthermore, uptake was found to be cell-line specific with a punctuated, cytoplasmic pattern in MDCK cells and paracellular accumulation in Calu-3 cell monolayers. Remarkably, hCT derived peptides did not show significant permeation across the epithelial

**Table 1: Abbreviations, Amino Acid Sequences and Molecular Weight of the Peptides Studied in this Work. Amino acid substitutions are underlined.**

Abbreviation	MW (Da)	Sequence
hCT	3417.8	CGNLS TCMLG TYTQD FNKFH TFPQT AIGVG AP-NH <sub>2</sub>
hCT(9-32)	2609.9	LG <u>TYTQD</u> FNKFH TFPQT AIGVG AP-NH <sub>2</sub>
W10-hCT(9-32)	2739.0	L <u>W</u> TYTQD FNKFH TFPQT AIGVG AP-NH <sub>2</sub>
A23-hCT(9-32)	2583.8	LG TYTQD FNKFH <u>TFAQT</u> AIGVG AP-NH <sub>2</sub>
W30-hCT(9-32)	2739.0	LG TYTQD FNKFH TFPQT AIGV <u>W</u> AP-NH <sub>2</sub>
hCT(18-32)	1698.9	KFH TFPQT AIGVG AP-NH <sub>2</sub>
hCT(21-32)	1286.4	TFPQT AIGVG AP-NH <sub>2</sub>
hCT-random	2609.9	FL TAGQN TIQTP VKTGG HFPFA DY-NH <sub>2</sub>
pVEC	2208.7	LLIIL RRRIR KQAH <sub>2</sub> HSK-NH <sub>2</sub>
W2-pVEC	2281.7	<u>L</u> WIIL RRRIR KQAH <sub>2</sub> HSK-NH <sub>2</sub>
pAntp	2246.7	RQIKI WFQNR RMWKW K

models (20). This owes to their efficient metabolic cleavage when in contact with the epithelial cells (21).

Cadherins are single transmembrane-spanning glycoproteins of about 700 amino acids. pVEC, a peptide derived from the murine VE-cadherin, contains 18 amino acids (residues 615-632), with 13 cytosolic amino acids outside and 5 amino acids in the transmembrane region. It has been shown to translocate efficiently into various cell lines by a receptor-independent mechanism, and to carry macromolecular cargoes through plasma membranes (22, 23). The sequence of pAntp corresponds to the 16 amino acid sequence of the third  $\alpha$ -helix (residues 43–58) of the Antennapedia homeodomain protein of *Drosophila* (24, 25). Residues 48 and 56 are tryptophans (Trp) being useful fluorescent probes for biophysical analysis. The third helix was found to be responsible for interaction with DNA by binding specifically to cognate sites in the genome and also for the translocation of the entire protein across cell membranes (24, 25). The fragment pAntp retains the membrane translocation properties of the homeodomain and has, therefore, been proposed as a universal vector for cellular delivery (2). In fact, there are numerous studies proving the translocation of pAntp into different cell lines (26, 27). More recent studies propose an endocytic uptake (15, 16). Its exact translocation mechanism is still controversially discussed as reviewed by Trehin and Merkle (3).

To our knowledge, the present study provides the first investigation of a direct interaction of hCT derived peptides and pVEC with bilayer models. Indirectly, interactions of hCT derived CPPs have been suggested by atomic force microscopy on phase separated supported bilayers (28). The interaction of pAntp with model membranes, on the other hand, has been investigated in numerous studies (10, 17, 29-31). Its inclusion in this study was in order to allow comparison with previous data. In addition to that, we also provide new data to this peptide. Furthermore we like to draw attention to methods that are suited to detect comparably weak associations of peptides with the outer surface of the bilayer. So far, biophysical analysis of CPP was largely focused on insertions into the hydrophobic core of the bilayer, and mere association with

the surface of membranes was mostly neglected. Nevertheless, even weak forms of association may be the first step to trigger cellular uptake. Another focus of this work is a comprehensive Trp fluorescence quenching study on the localisation and insertion of the investigated CPPs in phospholipid bilayers of various compositions. A total of four quenchers were looked at in order to monitor (i) interaction with the water phase, (ii) with the surface of the bilayer, (iii) the interface, and (iv) the hydrophobic core of the bilayer. Although all investigated CPPs showed marked affinities towards phospholipid bilayers, especially for negatively charged lipids, distinct differences in the type and extent of interaction between weakly cationic hCT-derived and oligocationic CPPs could be revealed.

## MATERIALS AND METHODS

### *Materials*

The VE-cadherin-derived peptides were synthesized by NMI Peptides, Reutlingen, Germany; hCT was kindly provided by Novartis Pharma AG, Basle, Switzerland. All peptides were amidated in the N-terminus. Identity and purity (> 95%) were controlled by mass spectral and HPLC analysis. 1-palmitoyl-2-oleyl-phosphatidylcholine (POPC), 1-palmitoyl-2-oleyl-phosphatidylglycerol (POPG), dodecyl phosphocholine (DPC), and 1-palmitoyl-2-stearoyl-(11,12-dibromo)-*sn*-glycero-3-phosphocholine (Br-PC) were purchased from Avanti Polar Lipids (Alabaster, Alabama, USA), of the best quality available, and used without further purification. Trifluoroacetic acid (TFA), acrylamide, and 5-doxy stearic acid (5-DSA) were from Fluka, Buchs, Switzerland. N-(7-nitrobenzofuran-4-yl)-1,2-dipalmitoyl-*sn*-glycero-3-phosphoethanolamine (NBD-PE). 1,6-diphenyl-1,3,5-hexatriene (DPH) was purchased from Molecular Probes, Leiden, the Netherlands. Acetic acid (reagent grade) and phosphate

buffered saline (PBS) for buffer preparation were purchased from Fluka, Buchs, Switzerland.

### *Synthesis and purification of hCT derived peptides*

The sequences of the investigated hCT derived peptides are given in Table I. The peptides were synthesized by automated multiple solid phase peptide synthesis using a robot system (Syro, MultiSynTech, Bochum, Germany) and Fmoc/tert. butyl strategy as described previously (32). Peptides were then purified by preparative reversed phase high performance liquid chromatography (RP-HPLC, Merck KGaA, Darmstadt, Germany) and their purity was confirmed by analytical RP-HPLC using a LiChrospher 100 RP-18 column (125 mm x 4 mm, 5 µM) from Merck (Merck KGaA, Darmstadt, Germany) with a linear gradient mobile phase starting at 90% solvent A (water:TFA, 99.9:0.1) (v/v) and 10% solvent B (acetonitrile:TFA, 99.92:0.08) (v/v) to 60% solvent B over 30 min at a flow rate of 1mL/min. UV detection was monitored at 220 nm. The expected molecular weight was verified by MALDI-mass spectrometry (Voyager Perseptive, Weiterstadt, Germany). The analytical data for the not yet described derivatives were as follows: W10-hCT(9-32): mass<sub>calc.</sub> 2739.0 Da, mass<sub>exp.</sub> 2740.83 Da, HPLC retention time 19.95 min; A23-hCT(9-32): mass<sub>calc.</sub> 2583.8 Da, mass<sub>exp.</sub> 2584.90 Da, 19.41 min; W30-hCT(9-32): mass<sub>calc.</sub> 2739.0 Da, mass<sub>exp.</sub> 2740.72 Da, 20.75 min.

### *Preparation of unilamellar vesicles and micelles*

Large unilamellar vesicles (LUVs) were prepared by dissolving the phospholipids, either pure, or in the desired molar ratio, in chloroform to ensure complete solution and mixing of the components. The lipids were dried at 37°C in a rotary evaporator to yield a thin film and then kept under high vacuum over night. The dry film was then redispersed in the respective buffer (PBS, pH 7.4,

10 mM phosphate or acetic acid buffer, pH 3.5, 100 mM acetate) and the resulting multilamellar vesicle (MLV) dispersion was treated by five freeze-thaw cycles in liquid nitrogen and water at 37°C. LUVs were obtained by extruding the MLVs four times through 0.4 µm and eight times through 0.1 µm Nuclepore polycarbonate membranes (Sterico, Wangen, Switzerland) by means of the Lipex extruder (Vancouver, Canada). Lipid concentration was determined by an enzymatic colorimetric test for phospholipids (MPR 2) obtained from Roche Diagnostics, Mannheim, Germany. To assure the quality of the liposomes, the LUV size was checked by photon correlation spectroscopy on a Zetasizer 3000 HSA (Malvern, Malvern, UK).

To obtain small unilamellar vesicles (SUVs), MLVs were prepared as described for LUVs. After five freeze-thaw cycles, in addition, the ice-cooled dispersion was sonicated under nitrogen, using a Digitana UP 200H tip sonicator (Digitana, Horgen, Switzerland). The sonification was performed in 15 cycles of one minute each at 60% amplitude and 100% duty cycle, followed by a one minute pause to allow the dispersion to cool down. Titanium debris and lipid particles were removed by centrifugation at 10 000 g during 25 minutes using a Beckman L-60 ultracentrifuge (Beckman-Coulter, Palo Alto, USA). The size of the resulting SUVs obtained by DLS analysis was  $33.5 \pm 1.32$  nm (volume distribution).

Micelles of approximately 4 nm in diameter were obtained by dissolving DPC in PBS buffer.

#### *Liposome-buffer partitioning experiments*

Liposome-buffer partitioning experiments were performed by equilibrium dialysis at 37°C during 7 h; 1 mL Teflon dialysis cells (Dianorm, Munich, Germany) separated by a cellulose dialysis membrane, molecular weight-cutoff 10000 by Dianorm were mounted within the Dianorm-4 drive cell carrier and gently shaken during dialysis. Chambers were filled with a liposome suspension at a total lipid concentration of 4 mM in a 10 mM acetic acid buffer, pH 3.5,

containing peptides at a concentration of 20 µM on the one and acetate buffer on the other side (33). An acidic pH was chosen, as hCT derived peptides occasionally aggregated at pH 7.4 under the conditions used for partitioning studies. For VE-cadherin derived peptides PBS buffer of pH 7.4 was used. Schmidt et al. (34) could previously show that equilibrium was reached after 7 h. Over this time range good stability of the posphatidylcholine liposomes at 37°C has been reported by Ottiger et al. (35). For HPLC analysis, liposomes were dissolved in methanol (1:3, v/v). The HPLC method described by Buck and Maxl (36) was applied with some modifications. Mobile phases consisted of water:acetonitrile:TFA, 899:100:1 (v/v) for A and 199:800:1 (v/v) for B. A linear gradient from 100% A to 100% B within 35 minutes was applied. A RP-18 capillary column (LiChroCART® 250-4, LiChrophor® 100, RP-18 (5µm), Merck, Darmstadt, Germany) was used. UV detection was set at 214 nm; for Trp containing peptides an additional fluorescence detector was employed (excitation 280 nm, emission 320 nm). Injection volume was 100 µL. Throughout values at 7 h were used for calculation of apparent partition coefficients ( $D$ ) which were calculated according to:

$$D = \frac{C_{P(b)}}{C_{P(f)} \cdot C_L} \quad (1)$$

where  $C_{P(b)}$  is the concentration of peptide bound to liposomes,  $C_{P(f)}$  the concentration of free peptide, and  $C_L$  is the concentration of lipid molecules.  $C_{P(b)}$  was calculated by subtracting the peptide concentration in the buffer compartment from the peptide concentration in the liposome compartment.

### *Zeta-potential measurements*

The zeta potential ( $\zeta$ ) of the liposomes was determined by laser Doppler electrophoresis using a Malvern ZetaSizer 3000HS (Malvern Instruments Ltd, Malvern, UK) equipped with a He–Ne ion laser (633 nm). From the obtained

electrophoretic mobility, the zeta potential was calculated using the Smoluchowski equation as follows:

$$\zeta = \frac{4\pi \eta u}{\epsilon} \quad (2)$$

where  $u$  is the electrophoretic mobility,  $\eta$  the viscosity of the solvent and  $\epsilon$  the dielectric constant of the solvent. The reported results are expressed as mean values ( $\pm$  S.D.) of three experiments. The instrument was calibrated with a -50 mV standard (DTS1050; Malvern Instruments Ltd.). Measurements were performed at 20°C with an electrical field strength of 150 V/cm. Samples at a fixed lipid concentration of 50 μM and peptide/lipid-ratios ranging from 1:1000 to 1:10 were incubated for 1 h at room temperature.

### *Dynamic light scattering (DLS)*

The size distribution of a 50 μM LUV alone or after 60 min incubation at 22 °C at variable concentrations of peptide was determined by dynamic light scattering (DLS) at a scattering angle of 90° on a Malvern ZetaSizer 3000HS (Malvern Instruments Ltd, Malvern, UK) equipped with a He–Ne ion laser (633 nm). Hydrodynamic diameters ( $d_H$ , nm) were calculated from the diffusion coefficient (D) using the Stokes-Einstein equation:

$$d_H = \frac{k T}{3\pi \eta D} \quad (3)$$

where  $k$  is the Boltzmann constant;  $T$  the absolute temperature (K) and  $\eta$  the viscosity (mPa·s<sup>-1</sup>) of the solvent. The correlation function was analysed by the CONTIN method and the intensity distribution was chosen for evaluation of the data.

*Fluorescence spectroscopy*

Fluorescence was measured on a Varian Cary Eclipse spectrofluorometer (Mulgrave, Australia). All measurements were made in 10 mm wide 40 µL micro-cuvettes at an ambient temperature of approximately 20 °C. To guarantee exclusive Trp excitation when measuring Trp fluorescence, the excitation wavelength was set to 295 nm and the emission scanned from 300 to 500 nm. For quenching experiments the excitation wavelength was set to 375 nm. Scans were recorded with 5 nm excitation and emission bandwidths and a scan speed of 600 nm min<sup>-1</sup>. Three scans were recorded and averaged for each sample. For DPH analyses, fluorescence was excited at 340 nm and the emission was determined at 452 nm; five measurements were performed and averaged for each sample.

*Acrylamide and spin-probe quenching.* Trp fluorescence quenching experiments were performed at a fixed lipid/peptide-ratio (L/P) of 100 with peptide concentrations of 10 µM in presence of LUVs at a total phospholipid concentration of 1 mM. Acrylamide, a quenching molecule for Trp residues exposed to the water phase, was added from an aqueous 1 M stock solution, resulting in concentrations between 10 and 100 mM. For all samples containing vesicles, background intensity was subtracted. Quenching efficiency ( $F_0/F$ ) was calculated by dividing the Trp fluorescence intensity of the peptide/LUV solution alone ( $F_0$ ) by the fluorescence intensity of the peptide/LUV solution in presence of different concentrations of quenching probes (F). Quenching constants  $K_{SV}$  were determined by linear regression using the Stern–Volmer equation for a dynamic process:

$$\frac{F_0}{F} = 1 + K_{SV} [Q] \quad (4)$$

where  $F$  and  $F_0$  are the fluorescence intensities in presence and absence of acrylamide, respectively, and  $[Q]$  is the total molar concentration of the quencher in the sample.

To gain information on the accessibility of the tryptophans in the lipid bilayer, we employed three different membrane-anchored quenching probes: NBD-PE as a probe for the bilayer surface (37), 5-doxyl stearic acid for the deeper interface region (38), and Br-PC for the lipophilic core of the bilayer (37, 39). Again, peptide solutions for a final concentration of 10  $\mu\text{M}$  were added to vesicles composed of 1 mM phospholipid mixture of various POPG/POPC contents. The respective quenching probe was added from a 2 mM ethanolic stock solution, resulting in concentrations between 48 and 200  $\mu\text{M}$ . After allowing the system to equilibrate, the intrinsic Trp fluorescence of the peptide was measured. The quenching constants  $K_{\text{SV}}$  were again determined by linear regression using the Stern–Volmer equation according to Eq. 5. Information about the localization of the peptides in phospholipid bilayers was derived by comparison of the  $F_0/F$  values for all four quenching probes.

*Fluorescence polarization.* To monitor the membrane perturbation upon addition of the peptides, we labeled the vesicles with the membrane-bound probes DPH or TMA-DPH, respectively. Both probes are nonfluorescent in aqueous media but partition readily into membranes and other lipid assemblies, accompanied by strong fluorescence enhancement. DPH is located in the membrane interior, whereas TMA-DPH is anchored to the surface by the trimethylammonium substituent. To prepare the samples, 2  $\mu\text{M}$  DPH (from a 1 mM stock solution in acetonitrile) was added to LUVs composed of 1 mM phospholipid mixtures of various POPG/POPC contents. The samples were allowed to stand for 10 min before measurement. Increasing concentrations of peptides, from a 1 mM stock solution, were added to the samples. A polarization attachment (Varian, Mulgrave, Australia) was adapted to the Varian Cary

Eclipse spectrofluorometer. Steady-state polarization  $P$  was determined according to the following equation (40):

$$P = \frac{I_{VV} - G I_{VH}}{I_{VV} + G I_{VH}} \quad (5)$$

where  $I_{VV}$  is the emission intensity of vertically polarized light parallel to the plane of excitation and  $I_{VH}$  is the emission intensity of horizontally polarized light perpendicular to the plane of excitation. The instrumental factor  $G$  ( $G = I_{HV}/I_{HH}$ ) was determined by measuring the polarized components of the probe's fluorescence with horizontally polarized excitation.

## RESULTS

### *Peptide design*

An overview over all investigated peptides is given in Table 1. A systematic investigation of the internalisation efficiency of N-terminally truncated hCT derivatives in a MDCK cell model (19) revealed that hCT(18-32) is the shortest sequence that was internalised while hCT(9-32) turned out to be the most efficient derivative. In a  $^1\text{H}$  NMR study we found that hCT(9-32) contains two short  $\alpha$ -helices interrupted by the central Pro (M. Herbig, unpublished data); A23-hCT(9-32) was synthesized to investigate the influence of a continuous  $\alpha$ -helix on the properties of the peptide. W10-hCT(9-32) and W30-hCT(9-32) were synthesized with the intention to enhance membrane affinity of the peptides by means of replacing terminal Gly-residues by Trp showing enhanced affinity to phospholipid bilayers. Furthermore, the insertion of Trp allowed us to perform Trp quenching studies. This was also the intention for synthesizing W2-pVEC; we replaced a lipophilic Leu close to the N-terminus in order to change the peptide's physicochemical properties as little as possible.

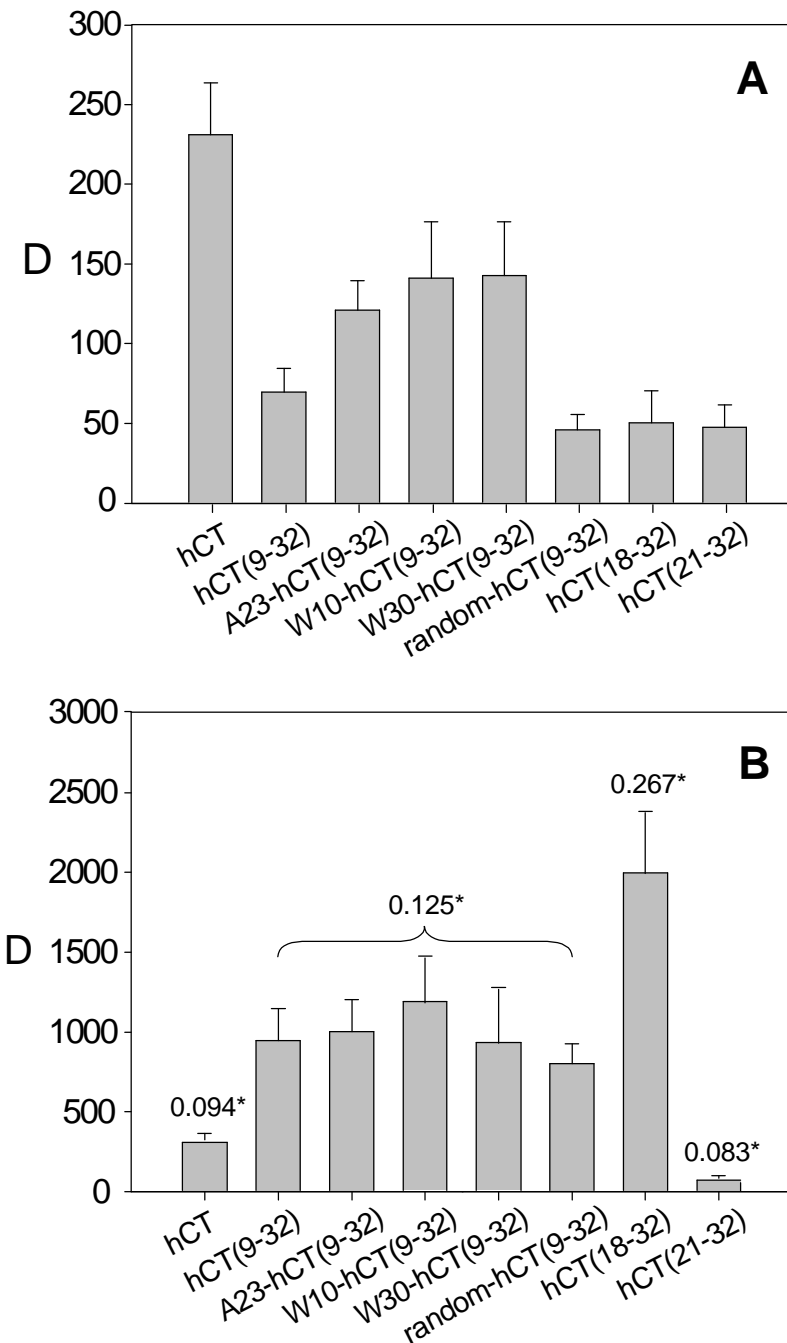


**Fig. 1. Non-logarithmic representation of apparent liposome-buffer partition coefficients (D) between extruded LUVs and acidic acid/acetate buffer pH = 3.5 at a total lipid concentration of 4 mM and a peptide concentration of 20  $\mu$ M. (A) Pure POPC liposomes and (B) liposomes composed of POPC/POPG 80:20.** The numbers labelled with an asterisk in (B) indicate the net positive charge per amino acid at pH 3.5.

*Liposome-buffer partitioning experiments.*

To test the propensity of hCT to interact with cell membranes, partition coefficients were determined in a liposome-buffer equilibrium system (33). In contrast to partitioning studies in isotropic media, e.g. water/octanol, the choice of anisotropic media like liposomes also includes ionic interactions and, therefore, represents a more realistic model. The concept of anisotropic lipophilicity can be regarded as being an intermediate case between partitioning and binding (41). LUVs were prepared by extrusion and their size distribution determined by dynamic light scattering (intensity distribution). All liposomes showed monomodal distributions, and their mean diameters were  $103.4 \pm 1.9$  nm for POPC LUVs and  $83.8 \pm 0.3$  nm for POPC/POPG (80:20) LUVs. A high excess of lipids (lipid/peptide molar ratio of 200) was chosen to avoid significant influence of membrane bound peptides on the typical bilayer structure.

For the hCT derivatives a pH of 3.5 was chosen to avoid potential aggregation of some of the peptides during the duration of the experiments. Apparent partition coefficients D were determined after 7 hours. Fig. 1A demonstrates the resulting partition coefficients of various hCT derived CPPs in neutral POPC LUVs. Owing to its hydrophobic C-terminal part, the untruncated hCT showed a D value of about 220, which was higher than the D values of the truncated derivatives. The partition coefficient of hCT(9-32) increased by a factor of 2 when replacing the Gly in position 10 or 30 by a Trp. Trp is known to have the strongest membrane anchoring properties of all amino acids (42). We were able to demonstrate by NMR experiments in DPC micelles at pH 5.5 that the replacement of the Pro in position 23 by an Ala led to the formation of a continuous  $\alpha$ -helix (M. Herbig, unpublished data) and a 1.7 fold increase in D. The hCT(9-32) derivative with randomised amino acid composition (hCT-random) and more truncated derivatives had moderately reduced D values as compared to hCT(9-32).

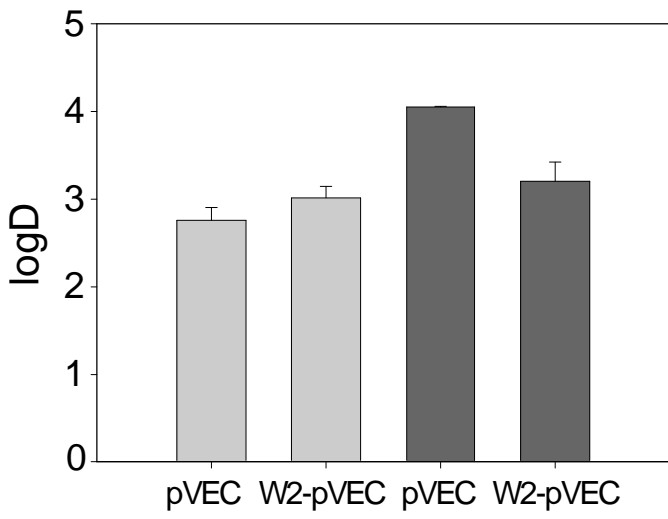


*Fig. 2. Apparent liposome-buffer partition coefficients ( $\log D$ ) between extruded LUVs and PBS pH = 7.4. The total lipid concentration was 4 mM and peptide concentration 20  $\mu M$ . Columns for pure POPC liposomes are represented in light grey and those for liposomes composed of POPC/POPG 80:20 in dark grey.*

Partition coefficients  $D$  of up to 2006 ( $\log D$  3.30) were found in experiments with negatively charged POPC/POPG (80:20) LUVs (Fig. 1B). Unlike the experiments with neutral POPC, the extent of interaction was mainly governed by the density of positive charges in the peptide sequences. For hCT(18-32) with an average positive net charge per amino acid (c/AA) of 0.267 a  $D$  of 2006 was obtained, whereas hCT(21-32) with a c/AA ratio of 0.083 had a  $D$  of only 70. For hCT(9-32) and all of its modifications, irrespective of their sequence,  $D$  values in the range of between 799 (random hCT(9-32)) and 1193 (W10-hCT(9-32)) were obtained. Whereas the  $D$  value of hCT remained almost unchanged,  $D$  values of hCT(9-32) and its modifications were increased up to 8- to 10-fold upon addition of 20% POPG; an even 40-fold increase was found with hCT(18-32). The obvious reason for the enhanced interaction of positively charged peptides is its electrostatic binding to the negatively charged lipid. Partitioning experiments with pVEC and W2-pVEC were performed at a pH of 7.4 (Fig. 2). As compared to the hCT derivatives,  $D$  values were clearly higher in POPC LUVs, but only moderately higher with POPC/POPG (80:20). Typically, the enhancement of interaction due to negatively charged lipids was less pronounced as compared to hCT derivatives.

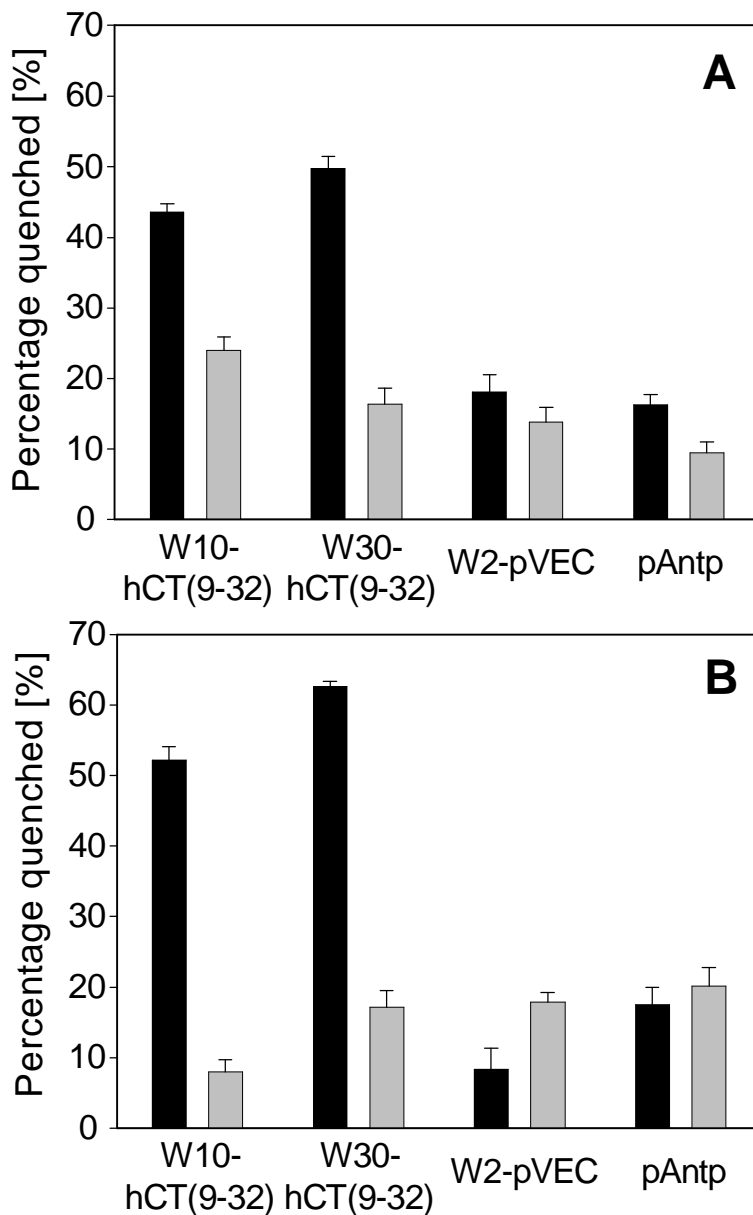


*Fig. 3. Percentage of quenched intrinsic Trp fluorescence of various CPPs in LUVs at an acrylamide concentration of 100 mM. Filled columns represent LUVs composed of POPC/POPG (80:20) and grey columns LUVs of pure POPG. Experiments were performed in PBS buffer of pH 7.4 (A), or acetate buffer of pH 3.5 (B). Spectra were recorded at ambient temperature (approx. 22°C). Results are represented as mean and standard deviation of three independent experiments.*

#### *Fluorescence spectroscopy*

*Acrylamide quenching.* To determine the exposure of the Trp containing CPPs in LUV dispersions to the aqueous phase we used the neutral hydrophilic quencher

acrylamide to quench intrinsic Trp fluorescence. Acrylamide is unable to penetrate the hydrophobic membrane core and, therefore, non-polar fluorophores embedded in the bilayer cannot be quenched (43). The studies were performed at pH 7.4 and 3.5 in LUVs composed of POPC, POPG, or a mixture (80:20) of both. As shown in Table 1, pAntp has two Trp residues (position 6 and 14), whereas W10-hCT(9-32), W30-hCT(9-32), and W2-pVEC have only one. The Trp fluorescence of all four CPPs followed the linear Stern-Volmer equation (Eq. 5) for the quencher acrylamide. Table 2 shows the Stern-Volmer quenching constants  $K_{SV}[\text{M}^{-1}]$  for W10-hCT(9-32), W30-hCT(9-32), W2-pVEC, and pAntp in POPC/POPG (80:20) and POPG LUVs in buffers of pH 7.4 and 3.5. In POPC/POPG high  $K_{SV}$  of 9 to 21  $\text{M}^{-1}$  were found for the hCT derivatives, suggesting strong exposure to the water phase and, therefore, a more superficial localisation. In both types of LUVs quenching was somewhat more pronounced at pH 3.5 than pH 7.4, and quenching of W30-hCT(9-32) stronger than W10-hCT(9-32), suggesting a slightly weaker interaction. In POPG LUVs  $K_{SV}$  values were largely decreased, indicating a much deeper insertion of the peptides. The cationic peptides W2-pVEC and pAntp showed low  $K_{SV}$  values, ranging from 0.7 to 3.1  $\text{M}^{-1}$ , for all media, indicating that the peptides were buried to a large extent inside the bilayer. Fig. 3 depicts the percentage of the original fluorescence quenched after addition of 100 mM acrylamide; in this

---

**Table 2. Stern-Volmer constants  $K_{SV}$  for acrylamide quenching of tryptophan fluorescence.** Increasing concentrations (10 mM to 100 mM) of acrylamide were added to LUVs incubated with different peptides, and  $K_{SV}$  were calculated according to Eq. 5. The lipid/peptide ratio was 100. Relative standard deviations were in the range of 1-5%.

---

		$K_{SV} [\text{M}^{-1}]$				
		lipid	W10-hCT(9-32)	W30-hCT(9-32)	W2-pVEC	pAntp
<b>pH 7.4</b>	POPC/POPG		9.83	15.17	2.94	1.81
	POPG		2.05	1.38	2.05	1.89
<b>pH 3.5</b>	POPC/POPG		15.69	20.63	0.72	3.13
	POPG		3.38	3.77	2.07	2.31

---

representation – especially for week and moderate quenching – differences in the effects became more apparent, which simplified the comparison of the extents of quenching. Interestingly, at pH 7.4, for both of these peptides, the quenching effects were slightly more pronounced in POPC/POPG (80:20) as compared to POPG, whereas the opposite was the case at pH 3.5.

*Trp quenching with membrane-anchored quenchers.* To obtain more precise information about the localisation of the CPPs within the lipid bilayers, membrane anchored probes were used to quench the intrinsic Trp fluorescence of the peptides inside the bilayer. In NBD-PE, the NBD group is covalently attached to the head group of a phosphatidylethanolamine molecule. Therefore, it acts as a probe for the polar head groups on the level of the phosphate groups in lipid bilayers (37, 44, 45). 5-doxyl stearic acid is a probe for the deeper interface region (38), and 11,12-Br-PC for the lipophilic core of the bilayer (37, 39). The radius of quenching for brominated probes is 8 - 9 Å (46), whereas spin-labelled probes quench over a range of 11 - 12 Å (47, 48). Therefore, it was necessary to employ several quenchers located at different positions in the bilayer in order to convincingly predict the localisation of the peptides. A summary of all  $K_{SV}$  values is given in Table III.

In POPC/POPG (80:20) LUVs at pH 7.4 (Fig. 4A), NBD-PE - the quencher for the bilayer surface - led to a total extinction of the fluorescence signal for all four peptides, whereas the more deeply inserted quenchers 5-DSA and Br-PC exhibited only moderate effects for W10-hCT(9-32), W30-hCT(9-32), but strong effects for W2-pVEC and pAntp. This observation, in very good agreement with the acrylamide quenching data, led to the conclusion that the hCT derived peptides were localised at the surface of the bilayer, while the cationic peptides remained in the upper region of the acyl chains of the phospholipids. At pH 3.5, the positive net charge – especially for hCT derived CPPs – was elevated. As a consequence, NBD-PE effects at pH 3.5 were partially reduced but remained high (Fig 4B), while 5-DSA and Br-PC effects

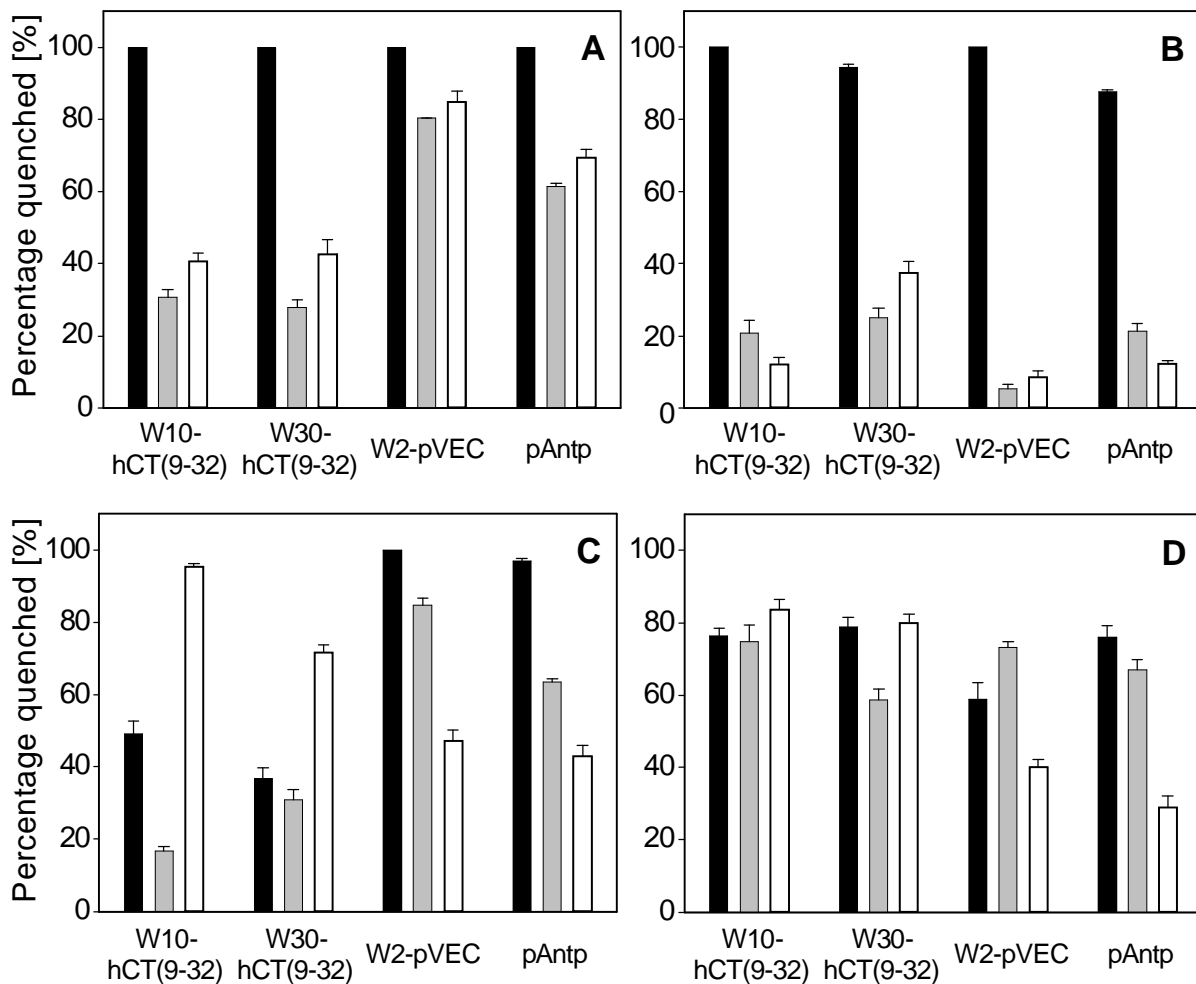


*Fig. 4. Percentages of quenched intrinsic Trp fluorescence (100 %: complete quenching; 0%: no effect) of various CPPs in LUVs. The quenching probes NBD-PE, 5-DSA, and Br-PC are represented in filled, grey, or open columns, respectively. The concentration of all quenchers was 100  $\mu$ M, corresponding to a lipid/quencher ratio of 10. (A) LUVs composed of POPC/POPG (80:20) in PBS buffer of pH 7.4, (B) LUVs composed of POPC/POPG (80:20) in acetate buffer of pH 3.5, (C) LUVs composed of pure POPG in PBS buffer of pH 7.4, (D) LUVs composed of pure POPG in acetate buffer of pH 3.5. Spectra were recorded at ambient temperature (approx. 22°C). Results are represented as mean and standard deviation of three independent experiments.*

were clearly decreased, indicating a shallower localisation of all investigated CPPs.

In highly negatively charged POPG LUVs (Fig. 4C and D), the Br-PC effects were high for the hCT derivatives at pH 7.4, whereas effects of NDB-PE, but also of the interface probe 5-DSA, were comparably low. These findings, along

*Table 3. Stern-Volmer constants  $K_{SV}$  for tryptophan fluorescence quenching of various membrane anchored quenching molecules. Increasing concentrations (50  $\mu M$  to 200  $\mu M$ ) of quenchers were added to LUVs incubated with different CPPs, and  $K_{SV}$  were calculated according to equation (5)<sup>a</sup>. The lipid/peptide ratio was 100. Relative standard deviations were in the range of 1-6%.*

<b>POPG/POPC (80:20)</b>					
$K_{SV} [M^{-1}]$					
		<b>W10-hCT(9-32)</b>	<b>W30-hCT(9-32)</b>	<b>W2-pVEC</b>	<b>pAntp</b>
<b>pH 7.4</b>	NBD-PE	26467.0	33107.5	69413.6	41793.9
	5-DSA	2874.9	3646.7	31672.4	7723.6
	Br-PC	4359.8	7943.5	14113.7	17528.5
<b>pH 3.5</b>	NBD-PE	64761.0	83727.2	47165.9	19119.9
	5-DSA	1406.5	2166.7	516.3	903.3
	Br-PC	613.9	3802.9	505.9	1203.3

<b>POPG</b>					
$K_{SV} [M^{-1}]$					
		<b>W10-hCT(9-32)</b>	<b>W30-hCT(9-32)</b>	<b>W2-pVEC</b>	<b>pAntp</b>
<b>pH 7.4</b>	NBD-PE	4398.2	2889.3	295473.0	181815.0
	5-DSA	1341.4	679.3	18193.3	7838.1
	Br-PC	432627.0	19710.0	5267.2	2093.1
<b>pH 3.5</b>	NBD-PE	14420.6	17704.3	7841.6	11422.7
	5-DSA	13553.6	7373.5	11518.4	9493.7
	Br-PC	30361.7	19556.0	3100.3	1313.4

<sup>a</sup>In cases of very efficient quenching ( $K_{SV} > 10000$ ), occasionally a plateau in the Stern-Volmer plot was obtained below the final quencher concentration of 200  $\mu M$ . In that case, only the linear part of the curve was used to calculate the constants.

with poor acrylamide quenching, lead to the conclusion that these two peptides were more intensely buried in the hydrophobic region of the membrane, albeit

not in the core of the bilayer. In this case differences to pH 3.5 were less pronounced than in the POPC/POPG (80:20) system. Again, Br-PC showed very efficient quenching, but also NBD-PE and 5-DSA quenched between 60% and 80% of Trp fluorescence, suggesting insertion close to the 5-DSA spin label position in the upper region of the acyl chains. Also W2-pVEC and pAntp show no pronounced differences between pH 7.4 and 3.5. Thus, both peptides resided in the upper acyl chain region. Data of the membrane-anchored quenchers allow no clear decision, at which pH the peptides reside closer to the interface region, but the acrylamide results suggested that at a pH of 3.5, there was a somewhat higher exposure to the water phase and, therefore, the localization of the peptides was more closely to the interface.

In neutral LUVs composed of pure POPC, hCT derivatives were only moderately quenched by NPD-PE, while 5-DSA and Br-PC exhibited weak effects only (Fig. 5). W2-pVEC and pAntp showed higher NBD-PE effects, whereas the deeper quenchers also caused only minimal effects (data not shown).

In general, this study demonstrates that both, the two hCT derived peptides on the one hand, and the two oligocationic peptides on the other, showed surprisingly similar behaviour. W10-hCT(9-32) and W30-hCT(9-32) demonstrated a conspicuous difference between POPG/POPC (80:2) LUVs, where they were located close to the bilayer surface, and those with POPG, with a deeper insertion towards the range of the hydrophobic acyl chains. Furthermore, there was an expected trend towards a slightly more superficial localization at pH 3.5 as compared to pH 7.4.

*Comparison of quenching effects in LUVs, SUVs, and micelles.* In literature there is a large variety of different membrane mimicking models to study peptide-bilayer membrane interactions, using LUVs (17, 49-51), SUVs (29-31), and micelles (26, 52-55). However, as these models feature different physical-

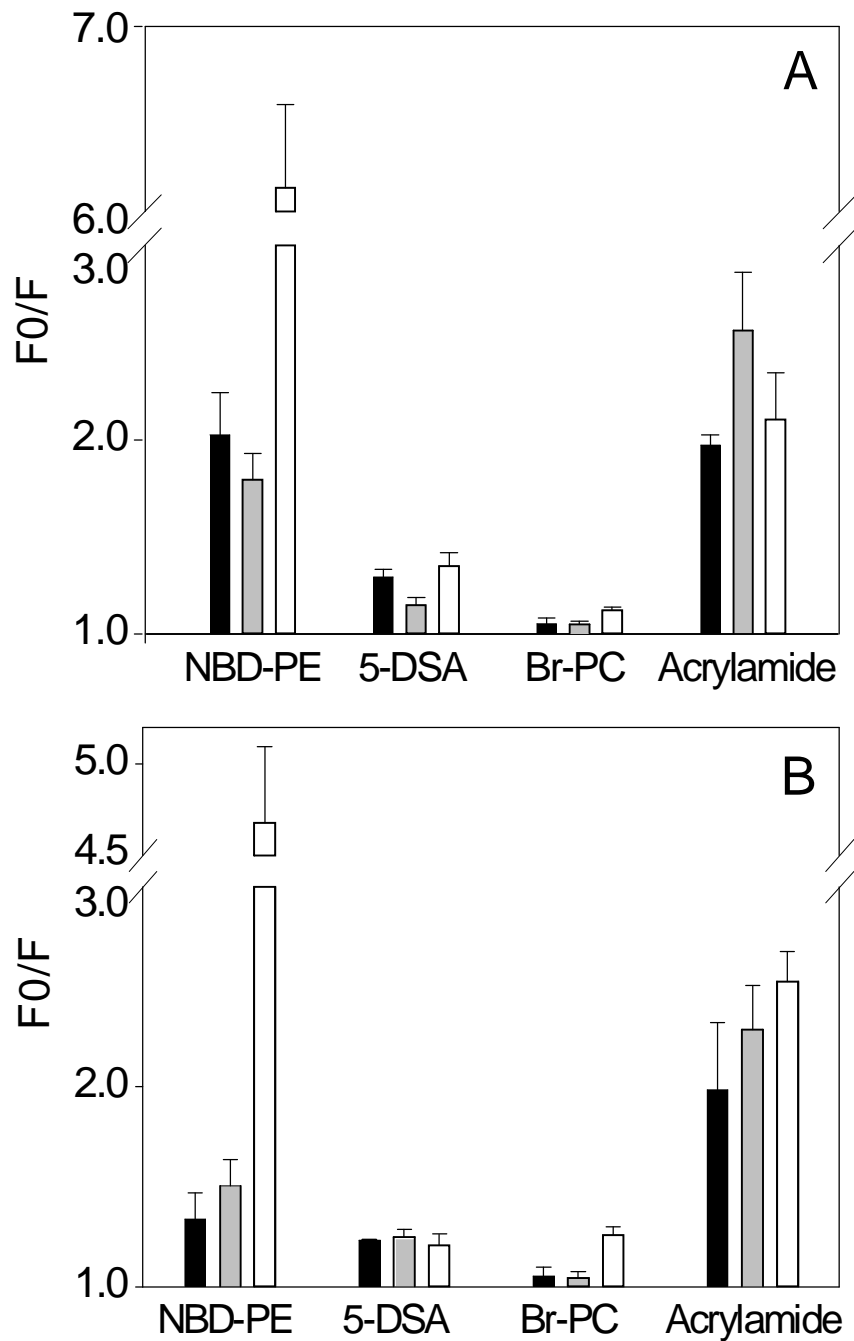


**Fig. 5. Comparison of quenching effects in different uncharged membrane mimicking media.** POPC LUVs are represented in filled columns, POPC SUVs in grey, and DPC micelles in open columns. The extent of Trp fluorescence quenching is shown by dividing the fluorescence without quencher ( $F_0$ ) through the fluorescence after addition of 200  $\mu\text{M}$  of membrane anchored quenchers, or 100 mM acrylamide, respectively. (A) effects of W10-hCT(9-32), and (B) effects of W30-hCT(9-32), both in PBS buffer, pH 7.4. Spectra were recorded at ambient temperature (approx. 22°C). Results are represented as mean and standard deviation of three independent experiments.

chemical properties, their results may depend on the chosen model. In particular, SUVs and especially DPC micelles are characterized by lower surface pressures due to their higher surface curvature. With respect to W10-hCT(9-32) and W30-hCT(9-32) we compared quenching effects of acrylamide and the membrane anchored quenchers NBD-PE, 5-DSA, and Br-PC in POPC LUVs, POPC SUVs, and DPC micelles. We found no clear differences between LUVs and SUVs. In DPC micelles, effects of the surface-bound quencher NBD-PE were strongly increased, whereas only slight differences were determined for Br-PC, and no differences for acrylamide and 5-DSA. Expectedly, these findings indicate that peptide solutes integrated more likely into the less tightly packed surface of DPC micelles than into the bilayers of liposomes.

*Fluorescence polarization.* The polarization of the membrane-bound fluorophores DPH was used to estimate the internal microviscosity of bilayer membranes. By this means effects of CPPs on membrane order and fluidity can be detected. DPH is non-fluorescent in aqueous dispersion but partitions readily into lipid membranes with lipid–water partition coefficients  $K_p$  of  $1.3 \times 10^6$ , accompanied by strong fluorescence enhancement (56). Previously, the localization of DPH was found to be close to the centre of a lipid bilayer (57, 58). The polarization of the DPH probe was measured after the addition of increasing concentrations of CPP solutions in LUVs with varying negative charge density in PBS buffer at pH 7.4.

Fig. 6 shows DPH fluorescence polarization dependent on peptide concentration in POPG LUVs. The highly cationic CPPs pVEC, W2pVEC, and pAntp showed an increase in fluorescence polarization  $P$  from 0.13 for blank liposomes to approximately 0.19 at a concentration of 0.1 mM, i.e. a peptide/lipid ratio of 0.1. For all hCT-derived peptides no significant effects could be found. In POPC as well as in POPC/POPG (80:20) liposomes none of the investigated peptides caused significant effects. These findings led us to the conclusion that strong

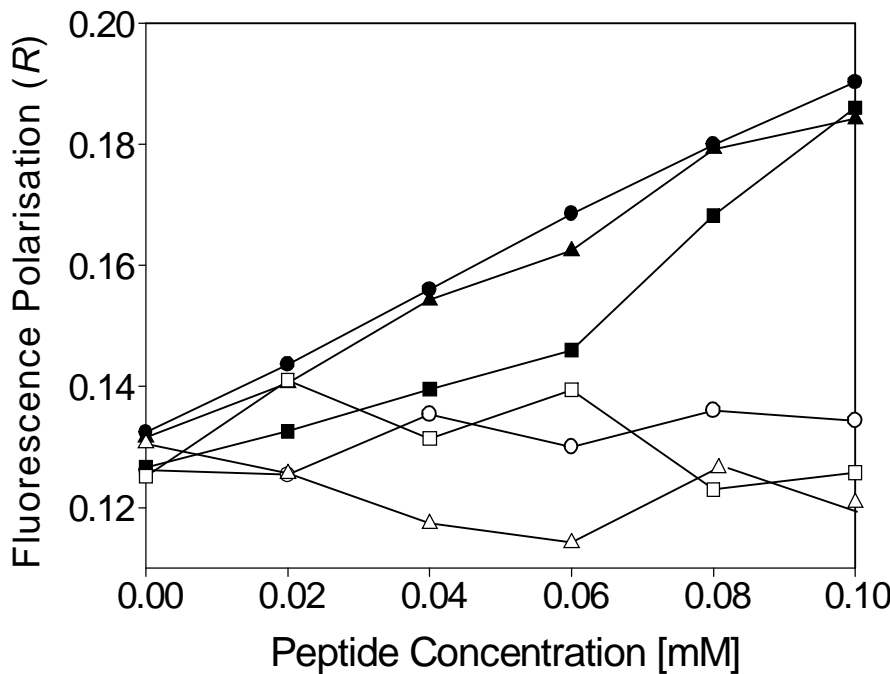


*Fig. 6. Fluorescence polarization of DPH labelled POPG LUVs as a function of concentrations of different CPPs. The peptides pVEC (▲), W2-pVEC (●), pAntp (■), hCT(9-32) (△), W10-hCT(9-32) (□), and W30-hCT(9-32) (○) were added to LUV dispersion in PBS (pH 7.4) containing 2 mM DPH. Spectra were recorded at ambient temperature (approx. 22°C).*

electrostatic interactions are required to cause a distinctive increase in DPH polarization.

#### $\zeta$ -potential measurements

The  $\zeta$ -potential describes the electric potential of particles in aqueous solution at the shear plane close to their surface. Neutral LUVs have a  $\zeta$ -potential slightly below zero and POPC/POPG LUVs at about -50 mV in very diluted buffers. If charged solutes bind to the surface of liposomes, a shift in  $\zeta$ -potential can be expected. Because buffers of high ionic strength lead to a reduction of the  $\zeta$ -potential, a very dilute phosphate buffer (1 mM, pH 7.4) was used. Fig. 7 shows an increase in  $\zeta$ -potential with POPC and POPG/POPC (80:20) liposomes

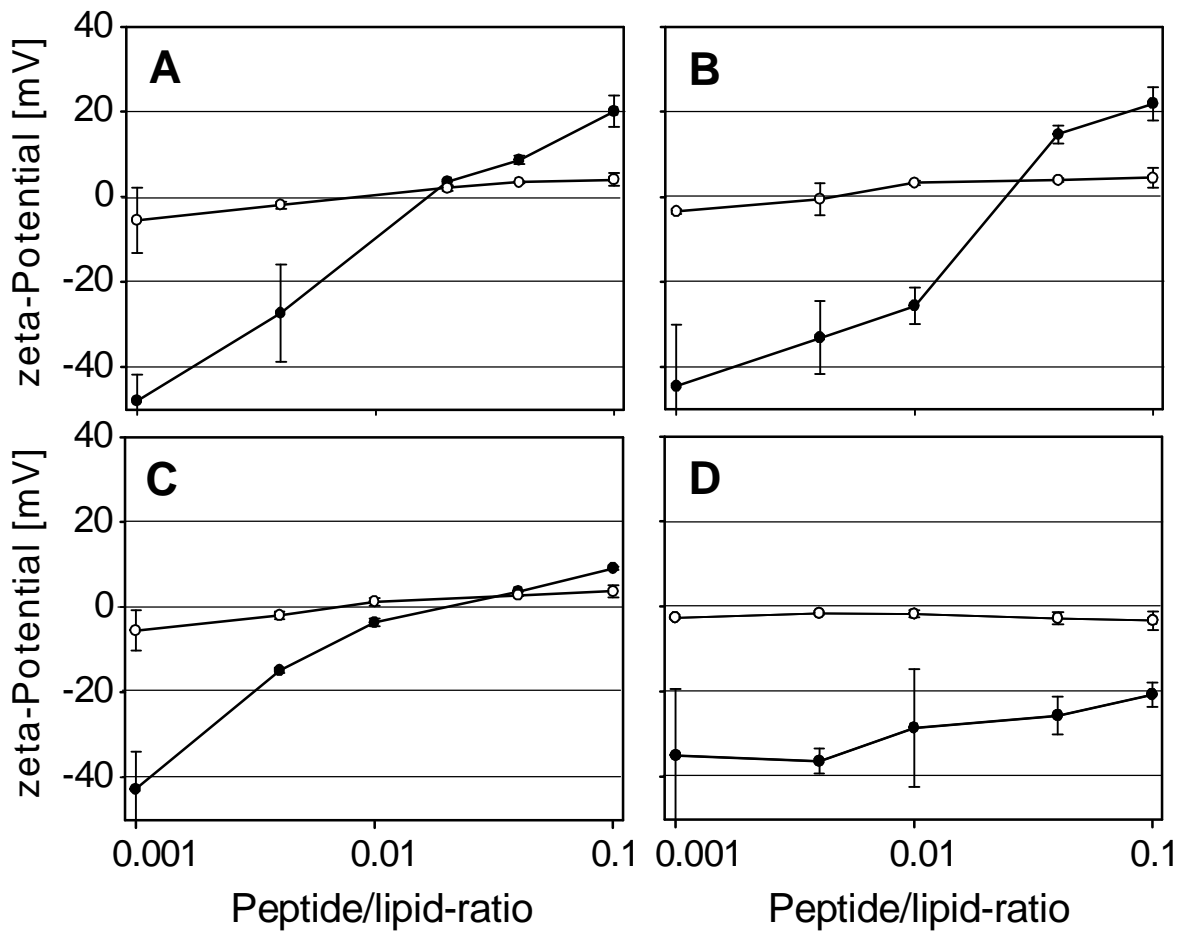


*Fig. 7. Effects of different CPPs on the  $\zeta$ -potential of POPC/POPG (80:20) LUVs. Different concentrations of (A) pVEC, (B) W2-pVEC, (C) pAntp, and (D) hCT(9-32) were added to a 50 mM solution of LUV in a 1 mM PBS buffer, pH 7.4. Measurements were performed at ambient temperature (approx. 22°C). Results are represented as mean and standard deviation of three independent experiments.*

when adding increasing concentrations of various CPPs. As expected, pVEC (Fig. 7A) and W2-pVEC (Fig. 7B) caused very similar effects; in both cases the  $\zeta$ -potential of POPC/POPG (80:20) LUVs was increased from about -45 mV to 20 mV at a peptide/lipid ratio of 0.1. For neutral POPC liposomes only a slight rise from about -5 mV to 5 mV was observed. Also pAntp (Fig. 7C) caused comparable effects, except for a flatter curve for POPC/POPG (80:20). As expected, hCT(9-32) with a net charge of +1 at pH 7.4, gave rise to a  $\zeta$ -potential increase to -20 mV only in POPG/POPC (80:20) LUVs, whereas a slight but insignificant increase could be observed in POPG LUVs. Obviously the small

net charge of hCT(9-32) is incapable to compensate the large charge density of POPG LUVs. The modifications W10-hCT(9-32) and W30-hCT(9-32) showed no significant differences as compared to hCT(9-32) (data not shown).

## DISCUSSION

Over the past years, the field of CPP research experienced a shift of its major paradigm: The intriguing idea of an energy independent, passive pathway of CPPs through biomembranes, playing a predominant role in earlier CPP studies (9-11), has been increasingly abolished in favour of the involvement of endocytosis (3-6, 12). In several studies a two-step process was suggested, involving initial adherence and enrichment at or in the phospholipid bilayer, which may subsequently trigger endocytosis (3, 5, 12-14).

Whereas sufficient proof for an endocytic uptake of hCT derived peptides (19, 20, 34) as well as for pVEC (22, 23) has been demonstrated in a variety of cellular models, as yet only limited information is accessible about their interaction with the lipid membrane, leaving the biophysical background to their cellular internalization largely elusive. Biophysical studies on the interaction of CPPs with biomembranes are expected to deepen the mechanistic understanding of the first step in CPP internalisation. Here we focus on interactions with established bilayer models employing four independent methodologies, namely liposome-buffer partitioning,  $\zeta$ -potential measurements, tryptophane fluorescence quenching, and fluorescence polarization.

We compared hCT(9-32) and a series of derivatives thereof, representing a class of weakly cationic peptides equipped with a hydrophobic C-terminal domain on the one hand, with two oligocationic CPPs, pVEC and pAntp (penetratin), on the other hand. In contrast to the endocytic uptake of hCT derived peptides (19, 20, 34), Elmqvist *et al.* proposed a non-endocytic, passive mechanism for pVEC (5, 22, 23). The authors draw their hypothesis from (i) reduced uptake at 4°C, in

combination with (ii) positive uptake of an all-D analogue of pVEC. Numerous uptake studies have been performed to elucidate the cellular uptake of pAntp. Early publications proposed passive uptake via inverted micelles (2, 24) (and references therein), but more recent ones suggest endocytic uptake (15, 16, 59). Even consecutive contributions of the two mechanisms have been proposed (27, 60). Passive pAntp permeation through lipid bilayers was demonstrated for giant unilamellar vesicles (GUVs) only (10, 31), but not for LUVs (10, 31). GUVs show undulated membrane structures differing considerably from LUVs (31, 61).

Our liposome-buffer partition experiments demonstrated marked to high affinities of hCT derived peptides to both negatively charged and even neutral bilayers. Expectedly, the affinities to POPC LUVs decreased with increasing molecular size of the derivatives, and increased when Gly was replaced by the more lipophilic Trp. The lower partition coefficient of the random sequence as compared to the hCT derived peptides demonstrated that, additional to amino acid sequence, secondary structure may play an equally significant role for their affinity to phospholipid membranes. In contrast, the interaction of the hCT derived CPPs with negatively charged POPC/POPG LUVs was governed by the ratio of positive charges per amino acid. Generally, the affinity to negatively charged lipid membranes was particularly enhanced. Remarkably, partition coefficients of pVEC in both POPC and POPC/POPG liposomes were about tenfold higher than with hCT(9-32).

To our knowledge, liposome-buffer equilibrium dialysis was not yet considered for studying CPPs. In contrast to binding studies utilizing the blue shift in Trp fluorescence emission (49, 62) caused by the interaction of Trp with a hydrophobic environment, liposome-buffer equilibrium dialysis offers a more general tool to monitor various types of peptide-bilayer interactions, even mere association on or with the outer bilayer surface. Nevertheless, because of its unspecific nature, the data need to be interpreted in concert with more specific assays. Our assumption of a superficial localization of hCT derived CPPs on neutral bilayers is supported by the low Trp fluorescence quenching in pure

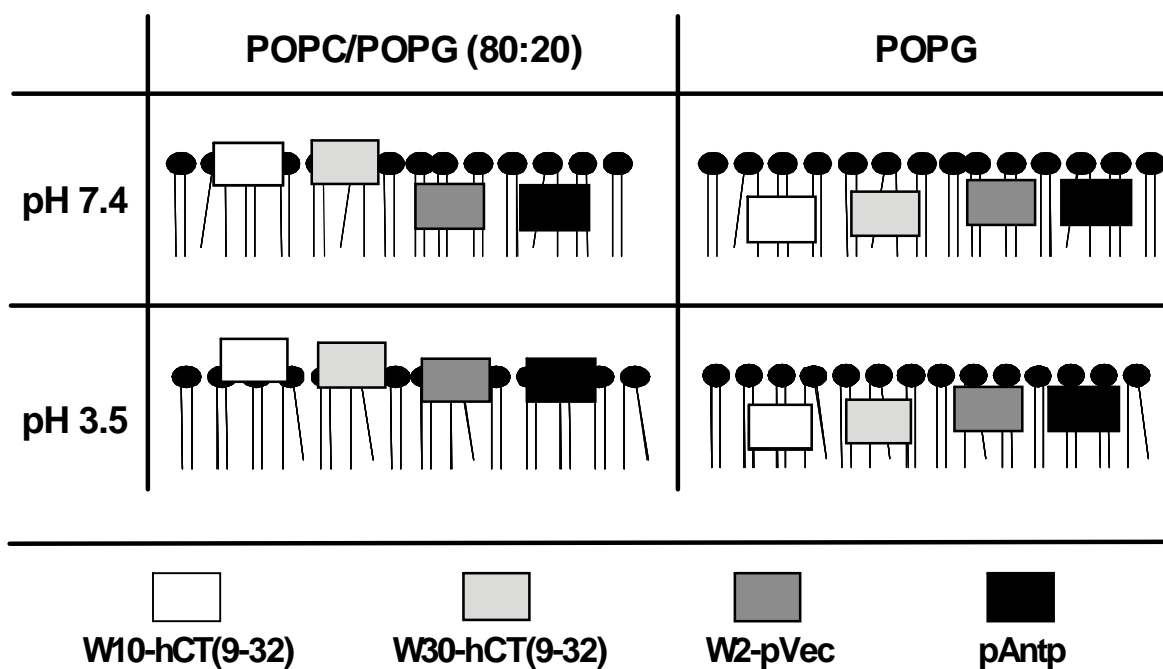


*Fig. 8. Schematic representation for insertion of CPPs in POPC/POPG (80:20) and POPG LUVs at pH 7.4 or 3.5, respectively. The respective positions were estimated based on Trp fluorescence quenching data from Tables 2 and 3 and Figures 3 and 4.*

POPC (Fig. 5), in combination with moderate effects of the interface quenchers and strong quenching of acrylamide. Concomitantly, effects on the deep quencher were negligible.

A schematic summary of the Trp quenching studies in terms of the CPP's localization in bilayers is given in Fig. 8. Interestingly, not only the two hCT derived peptides on the one hand, but also the two oligocationic peptides, pVEC and pAntp, on the other hand, show similar localization in the respective buffers and phospholipid compositions. W10-hCT(9-32) and W30-hCT(9-32) stay at the interface of POPC/POPG (80:20) bilayers with partial exposure to the surrounding aqueous phase, but penetrate more deeply into the hydrophobic region of pure POPG bilayers. The deep penetration into highly negatively charged bilayers may be explained by the low positive net charge and relative hydrophobicity of hCT derived peptides causing anchorage in the hydrophobic core of the membrane, whereas the high redundancy in positively charged amino acids of the two oligocationic CPPs is likely to restrict insertion into the deeper

interface/upper acyl chain region. However, at no instance were the peptides found to be localized in the innermost core of the bilayer.

Electrostatic attraction to negatively charged phospholipids prior to insertion into the lipid membrane seems to be a prerequisite for all investigated CPPs, irrespective of charge density. This may be concluded from the generally somewhat shallower localization at pH 3.5 as compared to 7.4. Nevertheless, the pH effect is most pronounced with the oligocationic pVEC and pAntp in POPC/POPG and explained by an increased positive net charge at the lower pH. Our findings with pAnpt are in agreement with corresponding data in literature (17, 30, 31): Likewise to the findings of Magzoub *et al.* (30) we found a slight reduction in the quenching constants of the deeper quenchers at high charge densities (pure POPG) as compared to lower charge densities (20% POPG in our study, 30% in the cited work). As compared to Christiaens *et al.* (17), however, we found distinctly higher quenching effects with the core quencher 11,12-Br-PC, which may be explained by the use of POPC/POPG (80:20) LUVs instead of PC/PS (70:30) SUVs in the work of Christiaens et al.

The LUV model system was chosen because of its superior resemblance to biological membranes. Cell membranes are characterized by a lipid packing density of 35 mN/m or slightly higher (63). Whereas LUVs of 100 nm have lipid packing density of about 32 mN/m (64, 65), SUVs of 30 nm have only about 23 mN/m (64), obviously because of their higher bilayer curvature. At reduced surface pressure, insertion of solutes is more likely. In fact, anomalous peptide binding to SUVs has been reported in literature (66). Despite, we found no significant differences between SUVs and LUVs concerning the membrane-anchored quenchers, except for slightly higher acrylamide quenching observed with SUVs. Accordingly, we observed dramatically increased NBD-PE quenching and a significantly higher Br-PC quenching rate when using lipid micelles, which are characterized by lipid packing densities of about 10 mN/m (67), instead of LUVs. Although easier to prepare and in spite of their excellent physical stability, head group structure and packing of lipid micelles deviate markedly from those of biological membranes. The minor differences in the

interaction of hCT derived CPPs with the deep quenchers are the result of their superficial localisation and cannot be extrapolated to deeply inserted CPP.

In the DPH polarization studies, again a profound difference between the weakly cationic hCT derived peptides and the two oligocationic peptides pVEC and pAntp was observed. Whereas distinct polarization effects of the oligocationic CPPs were demonstrated in POPG LUVs, no significant effect for any of the hCT derived peptides could be observed. Interestingly, in POPC/POPG (80:20), where the Trp fluorescence studies showed insertion towards the hydrophobic core, no change in polarization could be detected. Obviously, deep insertion alone is not sufficient to cause changes in the microviscosity of the bilayer and hence polarization. Our observation that polarization effects cannot be predicted by the depths of insertion, is also supported by the work of Magzoub et al. who also found similar effects for pAntp (30). Similarly, none of the investigated peptides showed any effects in POPC LUVs. So far, polarization effects in neutral liposomes could only be shown for transportan, owing to the fact that its C-terminal domain consists of the pore-forming wasp venom peptide mastoparan (30). Several pore forming peptides like bak, the C-terminal sequence of the pro-apoptotic protein (68), and melittin (M. Herbig, unpublished data) have been found to disturb neutral lipid membranes and increase DPH polarization. Usually, pore forming peptide agents elicit marked cellular toxicity (69, 70). Analysis of the  $\zeta$ -potential provides further evidence for preferential interaction with (partially) negatively charged lipids as compared to neutral bilayers. Though, even with neutral lipids the cationic peptides show a moderate, but significant interaction. Previous studies observed significant interactions of pAntp (17, 30) and Tat derived CPP (53) only with negatively charged vesicles. Our findings confirm that deeper penetration of pAntp (and possibly oligocationic CPPs in general) occurs only when the bilayers contains negatively charged lipids. Nevertheless, in addition to that, we also observed interactions with neutral POPC LUVs. Obviously, these interactions are of weaker nature and restricted to the outermost surface of the bilayer so that several methods commonly used in CPP research failed to detect them. This

superficial association on the bilayer surface may be in line with the observation of Wagner et al. (71) who found no relevant insertion of hCT(9-32) into monolayers composed of neutral phospholipids.

Nevertheless, by combination of liposome-buffer equilibrium dialysis,  $\zeta$ -potential measurements and Trp fluorescence quenching with the surface-anchored probe NBD-PE, demonstration of these interactions was successful. The fact that positively charged CPPs show an affinity even towards neutral phosphatidyl choline is not surprising because binding of positively charged solutes may lead to repellence of the positively charged end group of the choline towards the water phase (72). This has been hypothesized by van Balen et al. to open the polar surface and allow the charged solute to interact with the interface region (41). This would explain our findings.

All the investigated peptides' affinities were significantly higher when negatively charged lipids were present in the bilayer as compared to neutral lipids. Unlike the oligocationic CPPs, the hCT derived peptides remained on the bilayer surface even in the presence of 20% POPG. However, as supported by strong evidence for endocytic uptake of hCT(9-32) in various cell models with predominantly neutral lipids (19, 20), interfacial localization may be sufficient to trigger endocytosis.

Recently, Lundberg et al. concluded that the main feature of CPPs is to mediate the cell surface adherence. This was thought to occur after a first step of electrostatic interaction and is then followed by an uptake into endosomes (5). Also a correlation of cell surface association or membrane affinity and uptake efficiency could be observed (16, chapter III). The manner and intensity of interaction, especially the pronounced interfacial localization, of all studied CPPs with lipid bilayers are better compatible with the idea of an endocytic uptake rather than the assumption of passive transport. This includes also pVEC, having pronounced similarities to pAntp. Elmquist et al. (22, 23) proposed a non-endocytic uptake of pVEC, just based on uptake at 4°C after fixation and the successful uptake of an all-D analogue of pVEC. Nevertheless, on this evidence alone, an endocytic contribution at 37°C cannot be excluded. Even

more so, in a subsequent study, Richard et al. (4) demonstrated that cell fixation, even under mild conditions, may lead to artifactual uptake of CPP. In fact, in a recent study, more specific investigations of the uptake of pVEC, namely ATP depletion experiments and intracellular localization studies, brought up strong evidence for endocytic uptake (73).

Pore formation as a possible mechanism of passive translocation could be excluded for pAntp (74) as well as for hCT derivatives and pVEC (M. Herbig, unpublished data). The higher affinity towards the interface as compared to the hydrophobic core and the strong enrichment in the interface of phospholipid bilayers made passive uptake unlikely. On the other hand, enrichment of CPPs at the interface, possibly followed by aggregation, may have triggered endocytic uptake. Especially for hCT derived CPPs there is now strong evidence for endocytic uptake since several *in vitro* uptake studies (6, 19, 20, 34) suggest this uptake mechanism. The previously published monolayer study (71) and the present bilayer study provide detailed insight into their interactions with the lipid membrane that are well consistent with this uptake mechanism.

#### ACKNOWLEDGEMENTS:

This work was supported by the Commission of the European Union (EU project on Quality of Life and Management of Living Resources, Project No. QLK2-CT-2001-01451). The excellent support in mass spectrometry of R. Reppich, University of Leipzig, is kindly acknowledged. We thank Dr. Anna Seelig, Biozentrum Basel, for carefully reviewing the manuscript.

**REFERENCES:**

1. Lindgren, M., M. Hallbrink, A. Prochiantz, and U. Langel, *Cell-penetrating peptides*. Trends Pharmacol Sci, (2000). **21**(3): p. 99-103.
2. Derossi, D., G. Chassaing, and A. Prochiantz, *Trojan peptides: the penetratin system for intracellular delivery*. Trends Cell Biol, (1998). **8**(2): p. 84-87.
3. Trehin, R. and H.P. Merkle, *Chances and pitfalls of cell penetrating peptides for cellular drug delivery*. Eur J Pharm Biopharm, (2004). **58**(2): p. 209-223.
4. Richard, J.P., K. Melikov, E. Vives, C. Ramos, B. Verbeure, M.J. Gait, L.V. Chernomordik, and B. Lebleu, *Cell-penetrating peptides. A reevaluation of the mechanism of cellular uptake*. J Biol Chem, (2003). **278**(1): p. 585-590.
5. Lundberg, M., S. Wikstrom, and M. Johansson, *Cell surface adherence and endocytosis of protein transduction domains*. Mol Ther, (2003). **8**(1): p. 143-150.
6. Vives, E., J.P. Richard, C. Rispal, and B. Lebleu, *TAT peptide internalization: seeking the mechanism of entry*. Curr Protein Pept Sci, (2003). **4**(2): p. 125-132.
7. Foerg, C., U. Ziegler, J. Fernandez-Carneado, E. Giralt, R. Rennert, A.G. Beck-Sickinger, and H.P. Merkle, *Decoding the Entry of Two Novel Cell-Penetrating Peptides in HeLa Cells: Lipid Raft-Mediated Endocytosis and Endosomal Escape*. Biochemistry, (2005). **44**(1): p. 72-81.
8. Snyder, E.L. and S.F. Dowdy, *Cell penetrating peptides in drug delivery*. Pharm Res, (2004). **21**(3): p. 389-393.
9. Schwarze, S.R., K.A. Hruska, and S.F. Dowdy, *Protein transduction: unrestricted delivery into all cells?* Trends Cell Biol, (2000). **10**(7): p. 290-295.
10. Thoren, P.E., D. Persson, M. Karlsson, and B. Norden, *The antennapedia peptide penetratin translocates across lipid bilayers - the first direct observation*. FEBS Lett, (2000). **482**(3): p. 265-268.

11. Prochiantz, A., *Getting hydrophilic compounds into cells: lessons from homeopeptides*. Curr Opin Neurobiol, (1996). **6**(5): p. 629-634.
12. Wadia, J.S., R.V. Stan, and S.F. Dowdy, *Transducible TAT-HA fusogenic peptide enhances escape of TAT-fusion proteins after lipid raft macropinocytosis*. Nat Med, (2004). **10**(3): p. 310-315.
13. Scheller, A., J. Oehlke, B. Wiesner, M. Dathe, E. Krause, M. Beyermann, M. Melzig, and M. Bienert, *Structural requirements for cellular uptake of alpha-helical amphipathic peptides*. J Pept Sci, (1999). **5**(4): p. 185-194.
14. Oehlke, J., A. Scheller, B. Wiesner, E. Krause, M. Beyermann, E. Klauschenz, M. Melzig, and M. Bienert, *Cellular uptake of an alpha-helical amphipathic model peptide with the potential to deliver polar compounds into the cell interior non-endocytically*. Biochim Biophys Acta, (1998). **1414**(1-2): p. 127-139.
15. Drin, G., S. Cottin, E. Blanc, A.R. Rees, and J. Temsamani, *Studies on the internalisation mechanism of cationic cell-penetrating peptides*. J Biol Chem, (2003). **278**: p. 31192-31201.
16. Drin, G., M. Mazel, P. Clair, D. Mathieu, M. Kaczorek, and J. Temsamani, *Physico-chemical requirements for cellular uptake of pAntp peptide. Role of lipid-binding affinity*. Eur J Biochem, (2001). **268**(5): p. 1304-1314.
17. Christiaens, B., J. Grootenhoven, M. Reusens, A. Joliot, M. Goethals, J. Vandekerckhove, A. Prochiantz, and M. Rosseneu, *Membrane interaction and cellular internalization of penetratin peptides*. Eur J Biochem, (2004). **271**(6): p. 1187-1197.
18. Silverman, S.L., *Calcitonin*. Endocrinol Metab Clin North Am, (2003). **32**(1): p. 273-284.
19. Trehin, R., U. Krauss, R. Muff, M. Meinecke, A.G. Beck-Sickinger, and H.P. Merkle, *Cellular internalization of human calcitonin derived peptides in MDCK monolayers: a comparative study with Tat(47-57) and penetratin(43-58)*. Pharm Res, (2004). **21**(1): p. 33-42.
20. Trehin, R., U. Krauss, A.G. Beck-Sickinger, H.P. Merkle, and H.M. Nielsen, *Cellular uptake but low permeation of human calcitonin-derived cell*

- penetrating peptides and Tat(47-57) through well-differentiated epithelial models.* Pharm Res, (2004). **21**(7): p. 1248-1256.
21. Trehin, R., H.M. Nielsen, H.G. Jahnke, U. Krauss, A.G. Beck-Sickinger, and H.P. Merkle, *Metabolic Cleavage of Cell Penetrating Peptides in Contact with Epithelial Models: Human Calcitonin (hCT) Derived Peptides, Tat(47-57) and Penetratin(43-58)*. Biochem J, (2004). **382**: p. 945-956.
  22. Elmquist, A. and U. Langel, *In vitro uptake and stability study of pVEC and its All-D analog*. Biol Chem, (2003). **384**(3): p. 387-393.
  23. Elmquist, A., M. Lindgren, T. Bartfai, and U. Langel, *VE-cadherin-derived cell-penetrating peptide, pVEC, with carrier functions*. Exp Cell Res, (2001). **269**(2): p. 237-244.
  24. Prochiantz, A., *Homeodomain-derived peptides. In and out of the cells*. Ann N Y Acad Sci, (1999). **886**: p. 172-179.
  25. Derossi, D., S. Calvet, A. Trembleau, A. Brunissen, G. Chassaing, and A. Prochiantz, *Cell internalization of the third helix of the Antennapedia homeodomain is receptor-independent*. J Biol Chem, (1996). **271**(30): p. 18188-18193.
  26. Kilk, K., M. Magzoub, M. Pooga, L.E. Eriksson, U. Langel, and A. Graslund, *Cellular internalization of a cargo complex with a novel peptide derived from the third helix of the islet-1 homeodomain. Comparison with the penetratin peptide*. Bioconjug Chem, (2001). **12**(6): p. 911-916.
  27. Dom, G., C. Shaw-Jackson, C. Matis, O. Bouffoux, J.J. Picard, A. Prochiantz, M.P. Mingeot-Leclercq, R. Brasseur, and R. Rezsohazy, *Cellular uptake of Antennapedia Penetratin peptides is a two-step process in which phase transfer precedes a tryptophan-dependent translocation*. Nucleic Acids Res, (2003). **31**(2): p. 556-561.
  28. Boichot, S., U. Krauss, T. Plenat, R. Rennert, P.E. Milhiet, A. Beck-Sickinger, and C. Le Grimellec, *Calcitonin-derived carrier peptide plays a major role in the membrane localization of a peptide-cargo complex*. FEBS Lett, (2004). **569**(1-3): p. 346-350.

29. Magzoub, M., L.E. Eriksson, and A. Graslund, *Conformational states of the cell-penetrating peptide penetratin when interacting with phospholipid vesicles: effects of surface charge and peptide concentration*. *Biochim Biophys Acta*, (2002). **1563**(1-2): p. 53-63.
30. Magzoub, M., L.E. Eriksson, and A. Graslund, *Comparison of the interaction, positioning, structure induction and membrane perturbation of cell-penetrating peptides and non-translocating variants with phospholipid vesicles*. *Biophys Chem*, (2003). **103**(3): p. 271-288.
31. Christiaens, B., S. Symoens, S. Verheyden, Y. Engelborghs, A. Joliot, A. Prochiantz, J. Vandekerckhove, M. Rosseneu, B. Vanloo, and S. Vanderheyden, *Tryptophan fluorescence study of the interaction of penetratin peptides with model membranes*. *Eur J Biochem*, (2002). **269**(12): p. 2918-2926.
32. Krauss, U., F. Kratz, and A.G. Beck-Sickinger, *Novel daunorubicin-carrier peptide conjugates derived from human calcitonin segments*. *J Mol Recognit*, (2003). **16**(5): p. 280-287.
33. Pauletti, G.M. and H. Wunderli Allenspach, *Partition-Coefficients in-Vitro - Artificial Membranes as a Standardized Distribution Model*. *Eur. J. Pharm. Sci.*, (1994). **1**(5): p. 273-282.
34. Schmidt, M.C., B. Rothen-Rutishauser, B. Rist, A. Beck-Sickinger, H. Wunderli-Allenspach, W. Rubas, W. Sadee, and H.P. Merkle, *Translocation of human calcitonin in respiratory nasal epithelium is associated with self-assembly in lipid membrane*. *Biochemistry*, (1998). **37**(47): p. 16582-16590.
35. Ottiger, C. and H. Wunderli-Allenspach, *Partition behaviour of acids and bases in a phosphatidylcholine liposome-buffer equilibrium dialysis system*. *Eur. J. Pharm. Sci.*, (1997). **5**(4): p. 223-231.
36. Buck, R.H. and F. Maxl, *A validated HPLC assay for salmon calcitonin analysis. Comparison of HPLC and biological assay*. *J Pharm Biomed Anal*, (1990). **8**(8-12): p. 761-769.
37. Abrams, F.S. and E. London, *Calibration of the parallax fluorescence quenching method for determination of membrane penetration depth*:

- refinement and comparison of quenching by spin-labeled and brominated lipids.* Biochemistry, (1992). **31**(23): p. 5312-5322.
38. Damberg, P., J. Jarvet, and A. Graslund, *Micellar systems as solvents in peptide and protein structure determination.* Methods Enzymol, (2001). **339**: p. 271-285.
39. McIntosh, T.J. and P.W. Holloway, *Determination of the depth of bromine atoms in bilayers formed from bromolipid probes.* Biochemistry, (1987). **26**(6): p. 1783-1788.
40. Lakowicz, J.R., *Principles of Fluorescence Spectroscopy.* 2nd ed. ed. (1999), New York: Kluwer Academic. 291-303.
41. van Balen, G.P., C.M. Martinet, G. Caron, G. Bouchard, M. Reist, P.A. Carrupt, R. Fruttero, A. Gasco, and B. Testa, *Liposome/water lipophilicity: methods, information content, and pharmaceutical applications.* Med Res Rev, (2004). **24**(3): p. 299-324.
42. White, S.H. and W.C. Wimley, *Hydrophobic interactions of peptides with membrane interfaces.* Biochim Biophys Acta, (1998). **1376**(3): p. 339-352.
43. Moro, F., F.M. Goni, and M.A. Urbaneja, *Fluorescence quenching at interfaces and the permeation of acrylamide and iodide across phospholipid bilayers.* FEBS Lett, (1993). **330**(2): p. 129-132.
44. Raghuraman, H., S.K. Pradhan, and A. Chattopadhyay, *Effect of urea on the organization and dynamics of triton X-100 micelles: A fluorescence approach.* J Phys Chem B, (2004). **108**(7): p. 2489-2496.
45. Abrams, F.S. and E. London, *Extension of the parallax analysis of membrane penetration depth to the polar region of model membranes: use of fluorescence quenching by a spin-label attached to the phospholipid polar headgroup.* Biochemistry, (1993). **32**(40): p. 10826-10831.
46. Bolen, E.J. and P.W. Holloway, *Quenching of tryptophan fluorescence by brominated phospholipid.* Biochemistry, (1990). **29**(41): p. 9638-9643.
47. Chattopadhyay, A. and E. London, *Parallax method for direct measurement of membrane penetration depth utilizing fluorescence quenching by spin-labeled phospholipids.* Biochemistry, (1987). **26**(1): p. 39-45.

48. London, E. and G.W. Feigenson, *Fluorescence quenching in model membranes. 1. Characterization of quenching caused by a spin-labeled phospholipid*. Biochemistry, (1981). **20**(7): p. 1932-1938.
49. Persson, D., P.E. Thoren, M. Herner, P. Lincoln, and B. Norden, *Application of a novel analysis to measure the binding of the membrane-translocating Peptide penetratin to negatively charged liposomes*. Biochemistry, (2003). **42**(2): p. 421-429.
50. Persson, D., P.E. Thoren, and B. Norden, *Penetratin-induced aggregation and subsequent dissociation of negatively charged phospholipid vesicles*. FEBS Lett, (2001). **505**(2): p. 307-312.
51. Agirre, A., C. Flach, F.M. Goni, R. Mendelsohn, J.M. Valpuesta, F. Wu, and J.L. Nieva, *Interactions of the HIV-1 fusion peptide with large unilamellar vesicles and monolayers. A cryo-TEM and spectroscopic study*. Biochim Biophys Acta, (2000). **1467**(1): p. 153-64.
52. Lindberg, M., J. Jarvet, U. Langel, and A. Graslund, *Secondary structure and position of the cell-penetrating peptide transportan in SDS micelles as determined by NMR*. Biochemistry, (2001). **40**(10): p. 3141-3149.
53. Ziegler, A., X.L. Blatter, A. Seelig, and J. Seelig, *Protein transduction domains of HIV-1 and SIV TAT interact with charged lipid vesicles. Binding mechanism and thermodynamic analysis*. Biochemistry, (2003). **42**(30): p. 9185-9194.
54. Lindberg, M., H. Biverstahl, A. Graslund, and L. Maler, *Structure and positioning comparison of two variants of penetratin in two different membrane mimicking systems by NMR*. Eur J Biochem, (2003). **270**(14): p. 3055-3063.
55. Chaloin, L., P. Vidal, A. Heitz, N. Van Mau, J. Mery, G. Divita, and F. Heitz, *Conformations of primary amphipathic carrier peptides in membrane mimicking environments*. Biochemistry, (1997). **36**(37): p. 11179-11187.
56. Huang, Z.J. and R.P. Haugland, *Partition coefficients of fluorescent probes with phospholipid membranes*. Biochem Biophys Res Commun, (1991). **181**(1): p. 166-71.

57. Kaiser, R.D. and E. London, *Location of diphenylhexatriene (DPH) and its derivatives within membranes: comparison of different fluorescence quenching analyses of membrane depth.* Biochemistry, (1999). **38**(8): p. 2610.
58. Wang, S., J.M. Beechem, E. Gratton, and M. Glaser, *Orientational distribution of 1,6-diphenyl-1,3,5-hexatriene in phospholipid vesicles as determined by global analysis of frequency domain fluorimetry data.* Biochemistry, (1991). **30**(22): p. 5565-5572.
59. Console, S., C. Marty, C. Garcia-Echeverria, R. Schwendener, and K. Ballmer-Hofer, *Antennapedia and HIV transactivator of transcription (TAT) "protein transduction domains" promote endocytosis of high molecular weight cargo upon binding to cell surface glycosaminoglycans.* J Biol Chem, (2003). **278**(37): p. 35109-35114.
60. Hallbrink, M., A. Floren, A. Elmquist, M. Pooga, T. Bartfai, and U. Langel, *Cargo delivery kinetics of cell-penetrating peptides.* Biochim Biophys Acta, (2001). **1515**(2): p. 101-109.
61. Fischer, A., T. Oberholzer, and P.L. Luisi, *Giant vesicles as models to study the interactions between membranes and proteins.* Biochim Biophys Acta, (2000). **1467**(1): p. 177-188.
62. Thoren, P.E., D. Persson, E.K. Esbjorner, M. Goksor, P. Lincoln, and B. Norden, *Membrane binding and translocation of cell-penetrating peptides.* Biochemistry, (2004). **43**(12): p. 3471-3489.
63. Brockman, H., *Lipid monolayers: why use half a membrane to characterize protein-membrane interactions?* Curr Opin Struct Biol, (1999). **9**(4): p. 438-443.
64. Schindler, H., *Formation of planar bilayers from artificial or native membrane vesicles.* FEBS Lett, (1980). **122**(1): p. 77-79.
65. Seelig, A., *Local anesthetics and pressure: a comparison of dibucaine binding to lipid monolayers and bilayers.* Biochim Biophys Acta, (1987). **899**(2): p. 196-204.

66. Ladokhin, A.S., S. Jayasinghe, and S.H. White, *How to measure and analyze tryptophan fluorescence in membranes properly, and why bother?* Anal Biochem, (2000). **285**(2): p. 235-245.
67. Seelig, A., *Interaction of a substance P agonist and of substance P antagonists with lipid membranes. A thermodynamic analysis.* Biochemistry, (1992). **31**(11): p. 2897-2904.
68. Martinez-Senac Mdel, M., S. Corbalan-Garcia, and J.C. Gomez-Fernandez, *The structure of the C-terminal domain of the pro-apoptotic protein Bak and its interaction with model membranes.* Biophys J, (2002). **82**(1 Pt 1): p. 233-243.
69. Matsuzaki, K., *Magainins as paradigm for the mode of action of pore forming polypeptides.* Biochim Biophys Acta, (1998). **1376**(3): p. 391-400.
70. Matsuzaki, K., S. Yoneyama, and K. Miyajima, *Pore formation and translocation of melittin.* Biophys J, (1997). **73**(2): p. 831-838.
71. Wagner, K., N. Van Mau, S. Boichot, A.V. Kajava, U. Krauss, C. Le Grimellec, A. Beck-Sickinger, and F. Heitz, *Interactions of the human calcitonin fragment 9-32 with phospholipids: a monolayer study.* Biophys J, (2004). **87**(1): p. 386-395.
72. Bauerle, H.D. and J. Seelig, *Interaction of charged and uncharged calcium channel antagonists with phospholipid membranes. Binding equilibrium, binding enthalpy, and membrane location.* Biochemistry, (1991). **30**(29): p. 7203-7211.
73. Saalik, P., A. Elmquist, M. Hansen, K. Padari, K. Saar, K. Viht, U. Langel, and M. Pooga, *Protein cargo delivery properties of cell-penetrating peptides. A comparative study.* Bioconjug Chem, (2004). **15**(6): p. 1246-1253.
74. Drin, G., H. Demene, J. Temsamani, and R. Brasseur, *Translocation of the pAntp peptide and its amphipathic analogue AP-2AL.* Biochemistry, (2001). **40**(6): p. 1824-1834.



## CHAPTER III

# Membrane surface associated helices promote lipid interactions and cellular uptake of human calcitonin-derived cell penetrating peptides

*Michael E. Herbig<sup>1</sup>, Kathrin Weller<sup>1</sup>, Ulrike Krauss<sup>2</sup>,  
Annette G. Beck-Sickinger<sup>2</sup>, Hans P. Merkle<sup>1</sup>, and Oliver Zerbe<sup>3</sup>*

<sup>1</sup>Drug Formulation & Delivery Group, Department of Chemistry and Applied BioSciences, Swiss Federal Institute of Technology Zurich (ETH Zurich), Wolfgang-Pauli-Strasse 10, CH-8093 Zurich, Switzerland

<sup>2</sup>Institute of Biochemistry, University of Leipzig, Bruderstrasse 34, D-04103 Leipzig, Germany

<sup>3</sup>Institute of Organic Chemistry, University of Zurich, Winterthurerstrasse 190, CH-8057 Zürich, Switzerland

*Revised version accepted by Biophys. J.*

## ABSTRACT

hCT(9-32) is a human calcitonin (hCT) derived cell penetrating peptide (CPP) that has been shown to translocate the plasma membrane of mammalian cells. It has been suggested as a cellular carrier for drugs, green fluorescent protein, and plasmid DNA. Because of its temperature dependent cellular translocation resulting in punctuated cytoplasmatic distribution, its uptake is likely to follow an endocytic pathway. To gain insight into the molecular orientation of hCT(9-32) when interacting with lipid models, and to learn more about its mode of action, various biophysical techniques from liposome partitioning to high-resolution NMR spectroscopy were utilized. Moreover, to establish the role of individual residues for the topology of its association with the lipid membrane, two mutants of hCT(9-32), i.e. W30-hCT(9-32) and A23-hCT(9-32), were also investigated. Whereas unstructured in aqueous solution, hCT(9-32) adopted two short helical stretches when bound to dodecylphosphocholine (DPC) micelles, extending from Thr10 to Asn17 and from Gln24 to Val29. A23-hCT(9-32), in which the helix-breaking Pro23 was replaced by Ala, displayed a continuous  $\alpha$ -helix extending from residue 12 to 26. Probing with the spin-label 5-doxylstearate revealed that association with DPC micelles was such that the helix engaged in *parallel* orientation to the micelle surface. Moreover, the Gly to Trp exchange in W30-hCT(9-32) resulted in a more stable anchoring of the C-terminal segment close to the interface, as reflected by a twofold increase in the partition coefficient in liposomes. Interestingly, tighter binding to model membranes was associated with an increase in the *in vitro* uptake in HeLa cells. Liposome leakage studies excluded pore formation, and the punctuated fluorescence pattern of internalized peptide indicated vesicular localization and, in conclusion, strongly suggested an endocytic pathway of translocation.

## INTRODUCTION

Appropriate delivery of drugs to their sites of action is complicated by a number of factors. A prominent one is poor translocation through the cellular membrane that represents a major barrier for peptide, protein and nucleic acid biopharmaceuticals. To aid in this process, several classes and/or prototypes of cell penetrating peptides (CPPs) have been introduced during the past decade. Most of them consist of short, often oligocationic peptide sequences, which may be covalently linked to the compound of interest.

Recently, also peptides capable of forming non-covalent complexes with the cargo have been developed (1-3).

The ability of CPPs to translocate the membrane when covalently linked or non-covalently complexed with a cargo renders them of broad interest in cell biology, biotechnology and drug delivery. In fact, CPPs have been suggested as vectors for the cytoplasmic and nuclear delivery of hydrophilic biomolecules and drugs, both *in vivo* and *in vitro* (4-6). Initially, the mechanism of entry was firmly believed not to be mediated by receptors or transporters (4, 5), suggesting a passive, non-endocytic transfer. However, it was soon recognized that cell fixation could cause artefactual uptake phenomena. Hence, the hypothesis of an energy-independent, direct transport of CPPs through biomembranes, as postulated in earlier CPP studies (7-9), had to give way to concepts involving endocytosis (10-14).

Much attention has been concentrated on the first step of CPP uptake, i.e. the interaction with the surface of the membrane leading to an enrichment and/or perturbation of the phospholipid bilayer, which may subsequently trigger endocytic uptake (14, 15). In fact, in the few studies available in literature that combine cell biological and biophysical approaches, good correlations between membrane affinity and uptake efficiency have been observed (16, 17).

In the present study we determined the secondary structure and micellar localization of a human calcitonin derived CPP, hCT (9-32), in contact with a membrane-mimicking environment, namely dodecylphosphocholine (DPC)

micelles. Based on these results we identified amino acids critical for membrane binding. Amino acids were replaced in order to enhance the affinity of the modified peptides towards biomembranes. The propensity of the modified peptides to bind to phospholipid bilayers was first assessed in liposome/buffer equilibrium dialysis experiments and compared to data for the wild-type peptide. A more detailed investigation of the positioning of the CPPs in DPC micelles was then performed in a NMR study utilizing a paramagnetic spin label. Finally the membrane translocating potential was investigated in a cell culture model.

Human calcitonin (hCT) is a peptide hormone that is approved for the treatment of established osteoporosis (18). N-terminally truncated derivatives of hCT, lacking hormonal activity, represent a novel class of weakly cationic CPPs, and have been systematically investigated by Tréhin *et al* (19). It has been shown that sequences from hCT(9-32) to hCT(18-32) could – at least to some extent - translocate the plasma membrane of a fully organized epithelial model, fully differentiated MDCK monolayers, resulting in a sectoral, vesicular cytoplasmic distribution of the peptide. The uptake process was temperature-, time-, and concentration dependent, indicating that translocation may follow an endocytic pathway. Among the investigated derivatives hCT(9-32) was the most efficient one in this respect, and its single, positively charged lysine in position 18 turned out to be essential for uptake (19). Furthermore, uptake was found to be cell-line specific with a punctuated, cytoplasmic pattern in MDCK cells and paracellular accumulation in Calu-3 cell monolayers. Remarkably, hCT derived peptides did not show significant permeation across epithelial models (20). This owes to their efficient metabolic cleavage when in contact with epithelial cells (21).

In a previous <sup>1</sup>H NMR study full-length hCT was structurally characterized in SDS micelles and found to form an amphipathic  $\alpha$ -helix encompassing residues 9 to 16 (22). A recent solid-state NMR study showed that hCT (9-32) interacts preferably with the head groups of a bilayer formed by a mixture of POPC, POPE, and POPG (in a 5:3:2 molar ratio) rather than with the hydrophobic core of the phospholipids (23). The present work represents the

first solution state NMR study to determine the secondary structure of hCT(9-32) and its orientation relative to the surface of the lipid micelle. As a result we observed formation of two short  $\alpha$ -helical stretches in DPC micelles, which were interrupted by the Pro in position 23 for hCT(9-32). The wild-type sequence only moderately interacted with the interface of the micelles, whereas A23-hCT(9-32) revealed higher affinity for membrane binding due to its extended  $\alpha$ -helix. Moreover, insertion of an additional, hydrophobic membrane anchor in W30-hCT(9-32) caused an even increased interaction with the micelle along the entire sequence. The enhanced affinity for membrane binding was reflected by a significantly higher uptake of W30-hCT(9-32) in HeLa cells when compared to hCT(9-32).

## MATERIALS AND METHODS

### *Materials*

Deuterated docecyolphosphatidylcholine (DPC-d<sub>38</sub>, 99%-d) and dideuterium oxide (D<sub>2</sub>O) were ordered from Cambridge Isotope Laboratories (Andover, Massachusetts, USA). 1-palmitoyl-2-oleoyl-phosphatidylcholine (POPC) of the best quality available was purchased from Avanti Polar Lipids (Alabaster, Alabama, USA) and used without further purification. Melittin (purity > 93%), 5-doxylstearic acid was bought from Aldrich, Buchs, Switzerland. The peptides used for uptake studies were N-terminally labelled with 5-carboxyfluorescein and synthesized by NMI Peptides, Reutlingen, Germany; their identity and purity (> 95%) were controlled by mass spectral and HPLC analysis. Trifluoroacetic acid (TFA), manganese chloride (both analytical grade), Calcein, acetic acid (reagent grade), phosphate buffered saline (PBS) for buffer preparation, and Trypan blue solution in 0.81% sodium chloride and 0.06% potassium phosphate were purchased from Fluka, Buchs, Switzerland. hCT was kindly provided by Novartis Pharma AG, Basle, Switzerland.

*Synthesis and purification of hCT derived peptides*

The sequences of the investigated hCT derived peptides are given in Table I. The peptides were synthesized by automated multiple solid phase peptide synthesis employing Fmoc/tert. butyl strategy (24). After cleavage from the resin with TFA the lyophilized peptides were purified by preparative reversed phase (RP) HPLC. The expected molecular weight was verified by MALDI-TOF mass spectrometry (Voyager Perseptive II, Weiterstadt, Germany), and retention times were determined using a LiChrospher 100 RP-18 column with a linear gradient mobile phase starting at 90% solvent A (water:TFA, 99.9:0.1) (v/v) and 10% solvent B (acetonitrile:TFA, 99.92:0.08) (v/v) to 60% solvent B over 30 min at a flow rate of 1mL/min: A23-hCT(9-32): mass<sub>calc.</sub> 2583.8 Da, mass<sub>exp.</sub> 2584.90 Da, RP-HPLC retention time 19.41 min; W30-hCT(9-32): mass<sub>calc.</sub> 2739.0 Da, mass<sub>exp.</sub> 2740.72 Da, HPLC retention time 20.75 min.

*Preparation of large unilamellar vesicles*

Large unilamellar vesicles (LUVs) were prepared by dissolving the phospholipids in chloroform to ensure complete solution and mixing of the components. The lipids were dried at 37°C in a rotary evaporator to yield a thin film and then kept under high vacuum over night. The dry film then was redispersed in the buffer and the resulting multilamellar vesicle (MLV) dispersion was subjected to five freeze-thaw cycles. Large unilamellar vesicles (LUVs) were obtained by extruding four times through 0.4 µm and eight times through 0.1 µm Nuclepore polycarbonate membranes. Lipid concentration was determined by an enzymatic colorimetric test for phospholipids (MPR 2) obtained from Roche Diagnostics, and the LUV size was checked by photon correlation spectroscopy on a Zetasizer 3000 HSA (Malvern, Malvern, UK).

**Table 1:** Abbreviations, amino acid sequences and molecular weights of the peptides studied in this work. Amino acid substitutions are underlined.

Abbreviation	MW (Da)	Sequence
hCT	3417.8	CGNLS TCMLG TYTQD FNKFH TFPQT AIGVG AP-NH <sub>2</sub>
hCT(9-32)	2609.9	LG TYTQD FNKFH TFPQT AIGVG AP-NH <sub>2</sub>
A23-hCT(9-32)	2583.8	LG TYTQD FNKFH <u>TFA</u> QT AIGVG AP-NH <sub>2</sub>
W30-hCT(9-32)	2739.0	LG TYTQD FNKFH TFPQT AIGV <u>W</u> AP-NH <sub>2</sub>
hCT-random	2609.9	FL TAGQN TIQTP VKTGG HFPFA DY-NH <sub>2</sub>

### Liposome-buffer partitioning experiments

Liposome-buffer partitioning experiments were performed by equilibrium dialysis through a cellulose dialysis membrane, molecular weight-cutoff 10000 Da, at 37°C during 7 h using a protocol described by Pauletti *et al.* in more detail (25). Lipid concentrations of 4 mM and peptide concentrations of 20 μM were used. For HPLC analysis, liposomes were dissolved in a threefold excess of methanol and analyzed according to the method described by Buck and Maxl (26). In all measurements values at 7 h were used for calculation of apparent partition coefficients (*D*) according to Schurtenberger *et al.* (27):

$$D = \frac{C_{P(b)}}{C_{P(f)} \cdot C_L} \quad (1)$$

where  $C_{P(b)}$  is the concentration of peptide bound to liposomes,  $C_{P(f)}$  the concentration of free peptide, and  $C_L$  is the concentration of lipid molecules.  $C_{P(b)}$  was calculated by subtracting the peptide concentration in the buffer compartment from the peptide concentration in the liposome compartment.

### Preparation of Calcein containing large unilamellar vesicles

LUVs were prepared by dissolving the phospholipids in chloroform as described above. The lipids were dried at 37°C in a rotary evaporator to yield a thin film and then kept under high vacuum over night. The dry film then was

redispersed in buffer (20 mM Calcein, in PBS pH 7.4, containing 1 mM EDTA for complexing of  $\text{Ca}^{2+}/\text{Mg}^{2+}$ , which could affect Calcein fluorescence) and the resulting multilamellar vesicle (MLV) solution was treated by five freeze-thaw cycles. LUVs were then obtained by extruding four times through 0.4  $\mu\text{m}$  and eight times through 0.1  $\mu\text{m}$  Nuclepore polycarbonate membranes (28). A plastic syringe mounted in a centrifugation tube was filled with hydrated Sephadex G-50 gel. After spinning at 200 g for 3 min the gel column had dried and parted from the sides of the syringe. Untrapped dye was removed by the minicolumn centrifugation method (29).

#### *Dye efflux measurements*

50  $\mu\text{L}$  of a 400  $\mu\text{M}$  LUV suspension was injected into 96-well plates (Nunc, Wiesbaden, Germany) containing 50  $\mu\text{L}$  of peptide solutions of different concentration. Calcein leakage from vesicles was monitored fluorimetrically by measuring the decrease in self-quenching (excitation at 462 nm, emission at 525 nm) after 60 min at room temperature on a Varian Cary Eclipse spectrofluorometer (Mulgrave, Australia). The buffer blank was subtracted form all values and the fluorescence intensity corresponding to 100% leakage was determined after the addition of Triton X-100 (30). Results were displayed as percentage of maximum leakage.

#### *NMR spectroscopy*

All NMR experiments utilized 2 mM solutions of peptides at pH 5.6 in the presence of 300 mM d<sub>38</sub>-dodecylphosphocholine (resulting in approx. one peptide associated to every third micelle (31)) in 90% H<sub>2</sub>O/D<sub>2</sub>O. Spectra were recorded at 310K on a Bruker DRX-500 spectrometer. Sequence-specific resonance assignments were performed based on 2D data from a 12ms and 40ms clean

TOCSY experiments (32) and from a 120 ms NOESY experiment (33). Otherwise, we largely followed protocols developed by Wüthrich and coworkers for assignment purposes (34). Upper limits derived from the NOESY data were used as restraints for torsion angle molecular dynamics runs performed within the program DYANA (35), using its standard simulated annealing protocol.

In order to determine the micelle-binding interface we measured the decrease in peak intensity in the 12 ms TOCSY spectra following addition of the micelle-integrating spin-label 5-doxylstearate, which could previously shown to be positioned in vicinity to the phospholipids head groups (36, 37). We computed two subsets of values corresponding to integrals from only the HN,H $\alpha$  cross peaks in the fingerprint region and from the average from all peaks corresponding to one amino acid, and analyzed their intensity ratio in the presence and absence of the spin labels as determined in the program XEASY (38). Otherwise we used methodology described by us in more detail in Bader et al. (39, 40).

### *Cell Culture.*

HeLa cells, a human cervix epithelial adenocarcinoma derived cell line, used throughout this study, were obtained from American Type Culture Collection ATCC (Rockville, MD, USA). Cells were used within 5 passages. Cell culture was maintained under standard cell culture conditions in humidified 5% CO<sub>2</sub>. For cultivation we used trypsin-EDTA 0.25% and phosphate buffered saline, pH 7.4 (PBS). Cells were cultured as exponentially growing subconfluent monolayers and maintained in Dulbecco's modified Eagles medium with GlutaMAX, sodium pyruvate, 4500 mg/L glucose (DMEM), supplemented with 10% heat-inactivated fetal calf serum and penicillin/streptomycin (100 units/mL and 100 µg/mL, respectively).

*Confocal laser scanning microscopy - Uptake studies in living cells.*

In order to assess the cellular localization of the investigated fluorescent labeled CPPs we performed confocal laser scanning microscopy. Exponentially growing HeLa cells were seeded onto 8 well Lab-Tek chambered coverglass at a density of 35'000 cells/cm<sup>2</sup>. Cells were used one day after seeding. For uptake experiments, cells were incubated for 2 hours in serum-free medium containing fluorescence labeled CPP or unconjugated 5-carboxyfluorescein (Fluka, Buchs, Switzerland) as a control at a concentration of 40 µM. This concentration was chosen in agreement with previous studies (19, 20), as the uptake mechanism of hCT derived peptides may involve enrichment (41) and self-assembly (42) of peptide in the membrane interface. 4 mM stock solutions of the CPP or of unconjugated carboxyfluorescein were prepared in DMSO in order to increase the solubility and subsequently diluted (1:100) with serum-free medium to a final concentration of 40 µM. The concentration of DMSO was 1%. Simultaneously, nuclei were stained with 1 µg/ml Hoechst 33342 (Molecular Probes, Leiden, Netherlands) for 30 min. Subsequently, cells were rinsed 3 times with Hank's balanced salt solution buffer (HBSS) and overlaid with HBSS buffer for observation using CLSM. To avoid misinterpretation due to unspecifically bound extracellular fluorescence, half of the volume was replaced with an aqueous 0.4% Trypan blue solution in order to quench extracellular fluorescence (43-45). Cells were then scanned using a Zeiss CLSM 410 inverted microscope. Image processing was performed using Imaris (Bitplane, Zurich, Switzerland).

*Fluorescence-activated cell sorting – Quantification of internalized CPP.*

To quantify internalized fluorescence-labeled CPP we performed fluorescence-activated cell sorting analysis (FACS). Again, exponentially growing HeLa cells were seeded onto 24 well plates at a density of 35'000

cells/cm<sup>2</sup> and were used one day after seeding. For uptake experiments, cells were incubated for 2 hours in serum-free medium containing fluorescence-labeled CPPs or unconjugated 5-carboxyfluorescein as a control at a concentration of 40 µM. 40 µM solutions of the CPPs or of unconjugated dye were prepared analogously to the procedure used in the CLSM. After incubation, all cells were extensively washed with PBS buffer and cells were treated with trypsin for 7 min to detach cells from the surface and to digest membrane bound peptide as adopted from the literature (13, 46), and washed once more with PBS before measurement. After addition of Trypan blue as a quencher for extracellularly bound fluorescence (47, 48) FACS was performed on a FacScan (BectonDickinson, Franklin Lakes, NJ) within one hour after trypsinization. A total of 8'000 gated cells per sample were analyzed using Cytomation Summit software (Cytomation Inc., Fort Collins, USA). The 5-carboxyfluorescein control value was subtracted and results were normalized to the unmodified hCT(9-32). Statistical comparisons for significance were made with Student's t-test;  $p \leq 0.02$  was considered statistically significant. All experiments were performed in triplicate.

To check for cell proliferation and viability of HeLa cells after two hours of incubation with the so far not tested CPP A23-hCT(9-32) and W30-hCT(9-32), we measured the overall activity of mitochondrial dehydrogenase (MTT assay) according to the instructions of ATCC (ATCC, MTT Cell Proliferation Assay Instructions) (49). Briefly, HeLa cells were incubated in 96 well plates (Nunc, Roskilde, Denmark) until 70-80% confluence and then incubated as described above. As controls we used untreated cells and cells treated with methanol for 7 min, respectively. After discarding the CPP solutions, MTT (Sigma, St. Louis, MO, USA) was added for 4 h at 37°C. After removing the MTT solution, the purple precipitate was dissolved for 12 h by addition of detergent (81 ml isopropanol, 15 ml SDS 20%, 4 ml 1 M HCl). Overall activity of mitochondrial dehydrogenase in each well was measured spectrophotometrically at 570 nm using a ThermoMax microplate reader (Molecular Device, Sunnyvale, CA, USA).

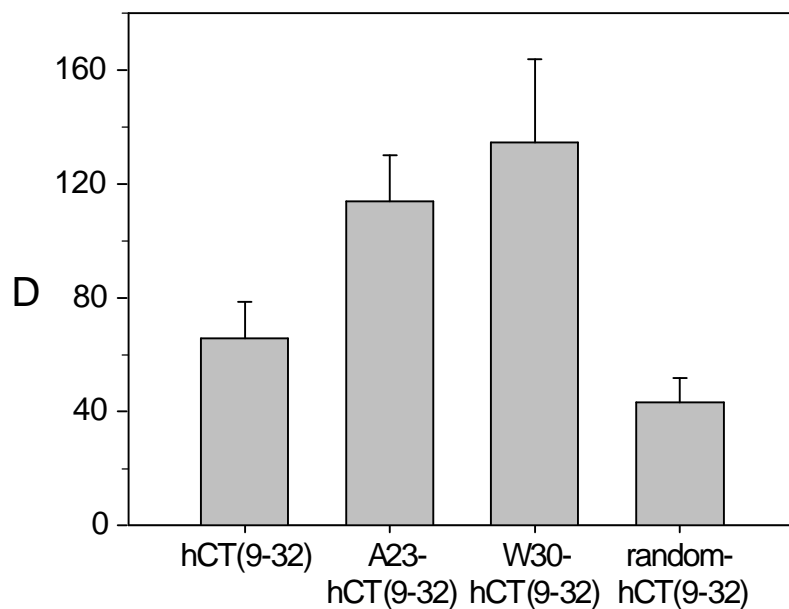


*Fig. 1. Apparent liposome-buffer partition coefficients (D) between extruded POPC LUVs and acidic acid/acetate buffer pH = 3.5.* D values were determined at a total lipid concentration of 4 mM and a peptide concentration of 20  $\mu$ M. Dialysis was performed for 7 h at 37°C. Results are represented as means  $\pm$  SD of three independent experiments.

## RESULTS

### Liposome-buffer partitioning experiments

To test the propensity of hCT to interact with cell membranes, partition coefficients were determined in a liposome-buffer equilibrium system (25). In contrast to partitioning studies in isotropic media, e.g. water/octanol, anisotropic media like liposomes also include ionic interactions and, therefore, represent a more realistic model. All LUV liposomes prepared displayed unimodal size distributions with mean diameters of  $103.4 \pm 1.9$  nm for POPC. A large molar ratio of lipid to peptide (approx. 200) was chosen in order to exclude disturbance of bilayer structure by the lipids.

For the hCT derivatives a pH of 3.5 was chosen to avoid potential aggregation of some of the peptides. The apparent partition coefficients D at that

pH were determined after 7 hours. Fig. 1 demonstrates the resulting partition coefficients of various hCT derived CPPs in neutral POPC LUVs. For hCT(9-32) a D of 66 was determined; it increased by a factor of 2 when replacing Gly2 or Gly30 by Trp. Among all amino acids Trp is known to partition most into the water-membrane interface (50). Also the replacement of the helix-breaking Pro23 by Ala, bridging the two short  $\alpha$ -helical segments, caused a 1.7 fold increase in D. The hCT(9-32) derivative with a randomized amino acid sequence showed a largely reduced D value as compared to hCT(9-32), indicating that not only the amino acid composition, but also the secondary structure and possibly the amphipathicity played a significant role for the affinity towards membranes.

#### *Peptide effects on bilayer integrity - Calcein leakage experiments*

An advantage of hCT-derived CPPs is their low toxicity: hCT is a human hormone and an approved drug for the treatment of postmenopausal osteoporosis (18). Furthermore, Tréhin et al. (20), using several cell lines, demonstrated the absence of cytotoxic effects of hCT(9-32), even when incubated for periods as long as 24 hours. To investigate whether the amino acid substitutions in A23-hCT(9-32) and W30-hCT(9-32) increased their potential to affect the integrity of phospholipid membranes, we performed a dye leakage assay with Calcein loaded POPC LUVs. As shown in Fig. 2 we compared membrane-permeabilizing effects at increasing concentrations of the hCT-derived CPPs and melittin as control in a 200  $\mu$ M solution of neutral POPC LUVs at pH 7.4. Melittin is a basic, amphipathic 26-amino acid peptide, for which pore formation in lipid bilayers has been previously demonstrated to lead to complete Calcein leakage at peptide concentrations as low as 1  $\mu$ M (51). In contrast, hCT caused a leakage of only about 8% at a peptide concentration of 40  $\mu$ M, which corresponds to a peptide/lipid ratio of 0.2. None of its derivatives exhibited any significant leakage. At the highest concentration of 200  $\mu$ M, corresponding to a peptide/lipid ratio of 1.0, hCT caused a leakage of about

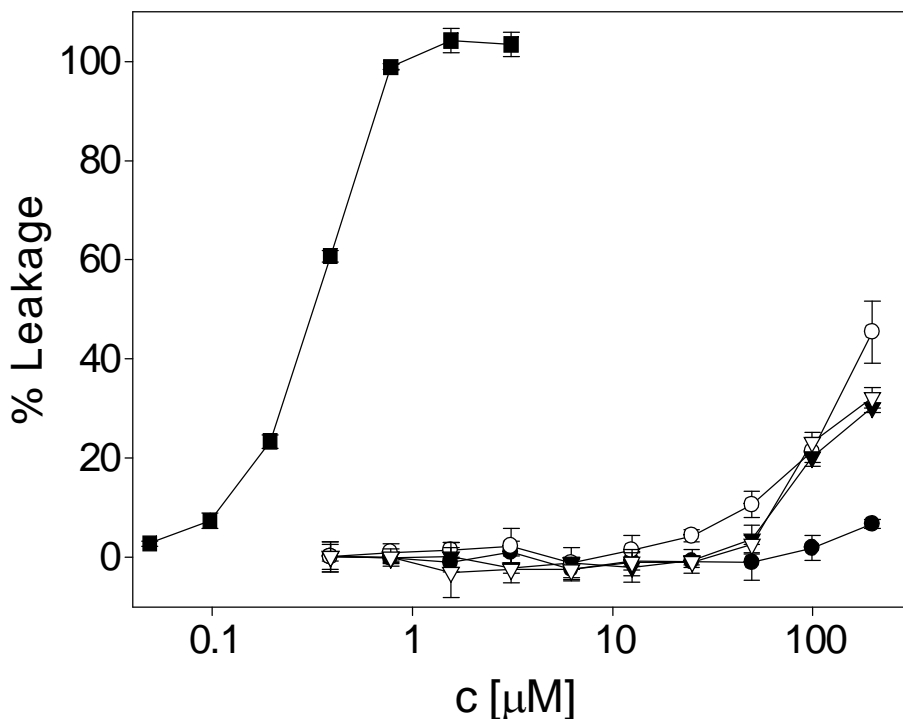


**Fig. 2. Percent leakage of the LUV entrapped fluorescent dye Calcein as a function of peptide concentration.** Peptide solutions up to a final concentration of 200 μM were added to a 400 μM POPC LUV solution in PBS buffer, pH 7.4. From the increase of Calcein fluorescence the peptide induced leakage in percent was calculated for melittin (■), hCT (○), hCT(9-32) (●), A23-hCT(9-32) (△), and W30-hCT(9-32) (▲). Data were recorded after 60 min of incubation at ambient temperature (approx. 22°C) and are represented as mean ± SD ( $n = 3$ ).

40%. The values for A23-hCT(9-32) and W30-hCT(9-32) were markedly lower, and hCT(9-32) caused a leakage of about 10% only.

#### *Structural data from NMR experiments:*

200ms NOESY data of hCT(9-32) in pure aqueous solution at pH 4.1 indicate that the peptide is unstructured in solution. The NOESY spectra are devoid of medium range contacts and only display intra-residual and sequential NOEs. This observation is supported by scalar coupling constants close to rotationally averaged values of about 7 Hz.

We also recorded a 120ms NOESY on hCT(9-32) in the presence of DPC micelles. Continuous stretches of sequential NOEs of amide protons ( $H^N(i),H^N(i+1)$ ) were observed between Thr10-Ans17 and Gln24-Val29. In addition, a few  $H^\alpha,H^N(i,i+2)$  and  $H^\alpha,H^\beta(i,i+3)$  restraints were also observed in these stretches. Structure calculations within the program DYANA confirmed helical folds in these segments. However, the polypeptide conformation was not sufficiently well-defined to assign the conformation to a specific helix type, and the data clearly indicated that residual flexibility was contained in the structures (e.g. scalar couplings  $^3J(H^N,H^\alpha)$  adopted values between 6 and 7 Hz). As derived from the structure calculations, hCT(9-32) forms two amphipathic helices connected via a flexible linker, which is terminated by Pro23.

We used the micelle-integrating spin-labels 5- and 16-doxylstearate to probe the orientation of the peptide on the micelle. Whereas the former spin-label probes vicinity to phospholipid head groups, the latter should affect protons more deeply inserted into the micelles. We also added  $Mn^{2+}$  to the micellar solution, a spin-label that mostly affects solvent-exposed protons. The relative signal attenuation due to the presence of 5-doxyl stearate was plotted against the sequence of each of the three peptides hCT(9-32), A23-hCT(9-32) and W30-hCT(9-32). Signal attenuations for all three peptides largely followed periodic patterns. Interestingly, the amount of signal reductions generally followed the order of hCT(9-32) < A23-hCT(9-32) < W30-hCT(9-32) indicating that the micellar association of the Trp30 analogue was tighter than for the other two peptides. Moreover, introduction of Trp at position 30 induced membrane association of the C-terminal tetrapeptide. Helical periodicity was most clearly observed for A23-hCT(9-32). Prominent signal reductions were mainly observed for the aromatic amino acids Tyr12, Phe16, 18 and 22 as well as for His20, and for Ala23 and Gly28. Our observations are fully compatible with thermodynamic data of partitioning whole amino acids into water-membrane interfaces as measured by White and Wimley (50). We noticed that only weak signal reductions were observed in the C-terminal half of hCT(9-32). In order to investigate whether the C-terminus integrated into the micelle interior or was

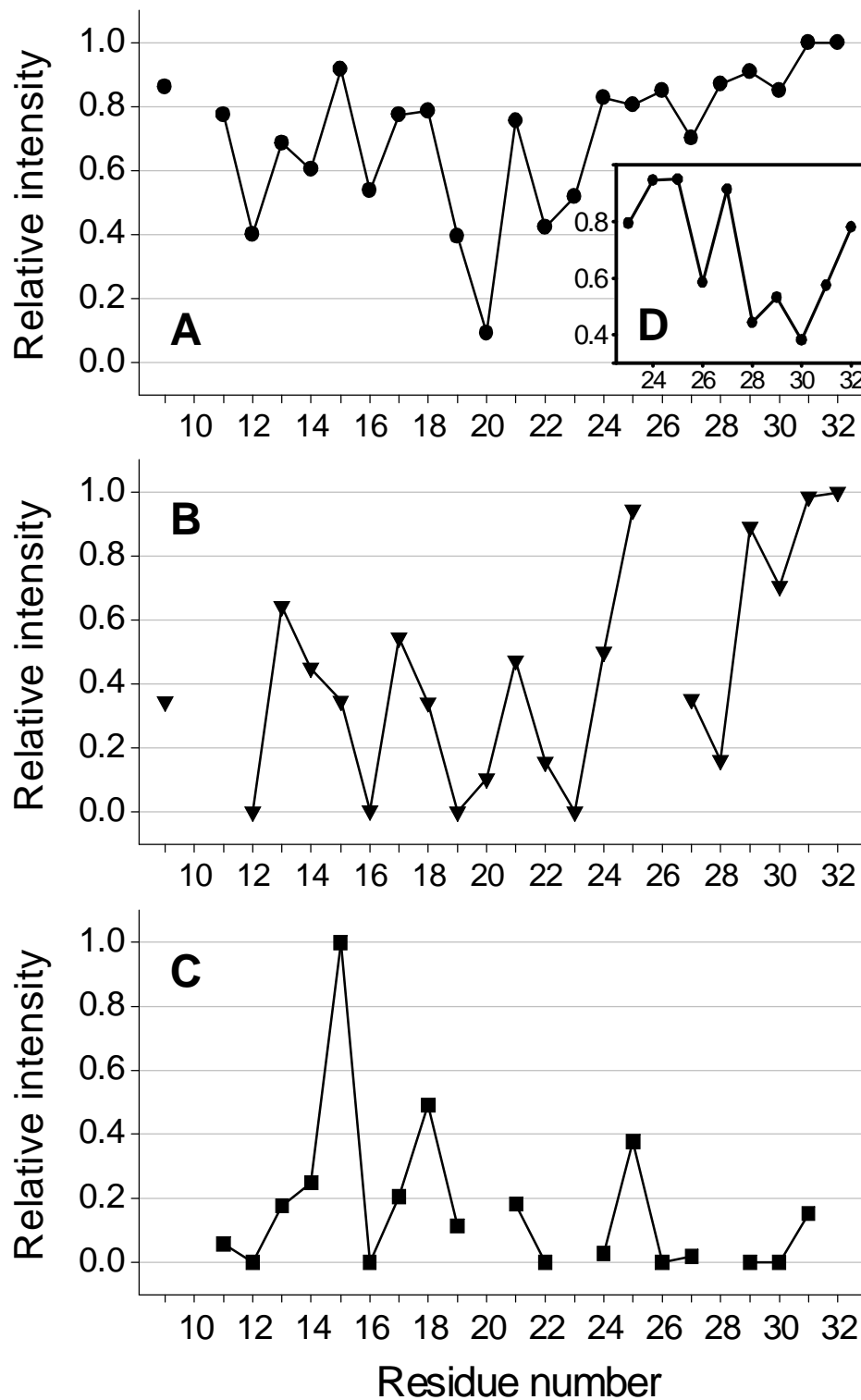


**Fig. 3. Relative signal intensities in  $^1\text{H}$ -TOCSY spectra of hCT derived peptides in DPC micelles in presence of the spin-label 5-doxylstearic acid with respect to a reference spectrum without spin-label.** 2 mM solutions of hCT(9-32) (A), A23- hCT(9-32) (B), and W30- hCT(9-32) (C) were measured in 300 mM  $d_{38}$ -DPC micelles at pH 5.6. The inset in A depicts the reduction for hCT(9-32) in presence of the spin-label manganese chloride with respect to a reference spectrum without spin-label (D).

freely diffusing in solution we conducted experiments with the spin-label Mn<sup>2+</sup>. As a result we observed significant signal reductions for the C-terminal segment of hCT(9-32) (see Fig. 3D) proving that this part protruded into the aqueous phase. However, we also observed signal reductions in the region around residue 15 (data not shown) indicating that Mn<sup>2+</sup> also coordinated to the side-chain carboxy group of Asp15. The replacement of Pro23 by Ala resulted in the extension of the amphipathic helix, but whether this structural effect or the more favorable partitioning properties of Ala when compared to Pro led to higher uptake is presently unclear. Nevertheless, Trp30 introduced a new membrane anchor in the C-terminal tetrapeptide domain, resulting in stronger and more homogenous signal reductions along the sequence. As derived from these spin-label studies, the membrane-binding affinities followed the order of hCT(9-32) < A23-hCT(9-32) < W30-hCT(9-32). This result owed most likely to the extent by which the C-terminal part of the peptides associated with the micelle.

#### *Confocal laser scanning microscopy (CLSM) - Uptake studies in living cells.*

Recently, an intense debate occurred in literature whether artifacts in the mechanistic interpretation of CPP studies were caused through cell fixation. Even mild fixation protocols have been described to give rise to misleading interpretations about peptide internalization. Therefore, throughout we conducted our cellular uptake study in living, non-fixed HeLa cells. In addition, we were aware that routine washings with buffer did not reliably remove all membrane bound CPP as already found in previous studies (13). For both CLSM and FACS we quenched extracellular fluorescence using Trypan blue. Cells were exposed to either one of the three CPP or the unconjugated dye. After incubation at 37°C for 2 hours, cells showed cellular uptake of all investigated peptides. Cell nuclei were stained with Hoechst 33342. hCT(9-32) (Fig. 5A) and W30-hCT(9-32) (Fig. 5B) exhibited punctuated fluorescence patterns indicating that the translocated fluorescence was localized in discrete vesicular

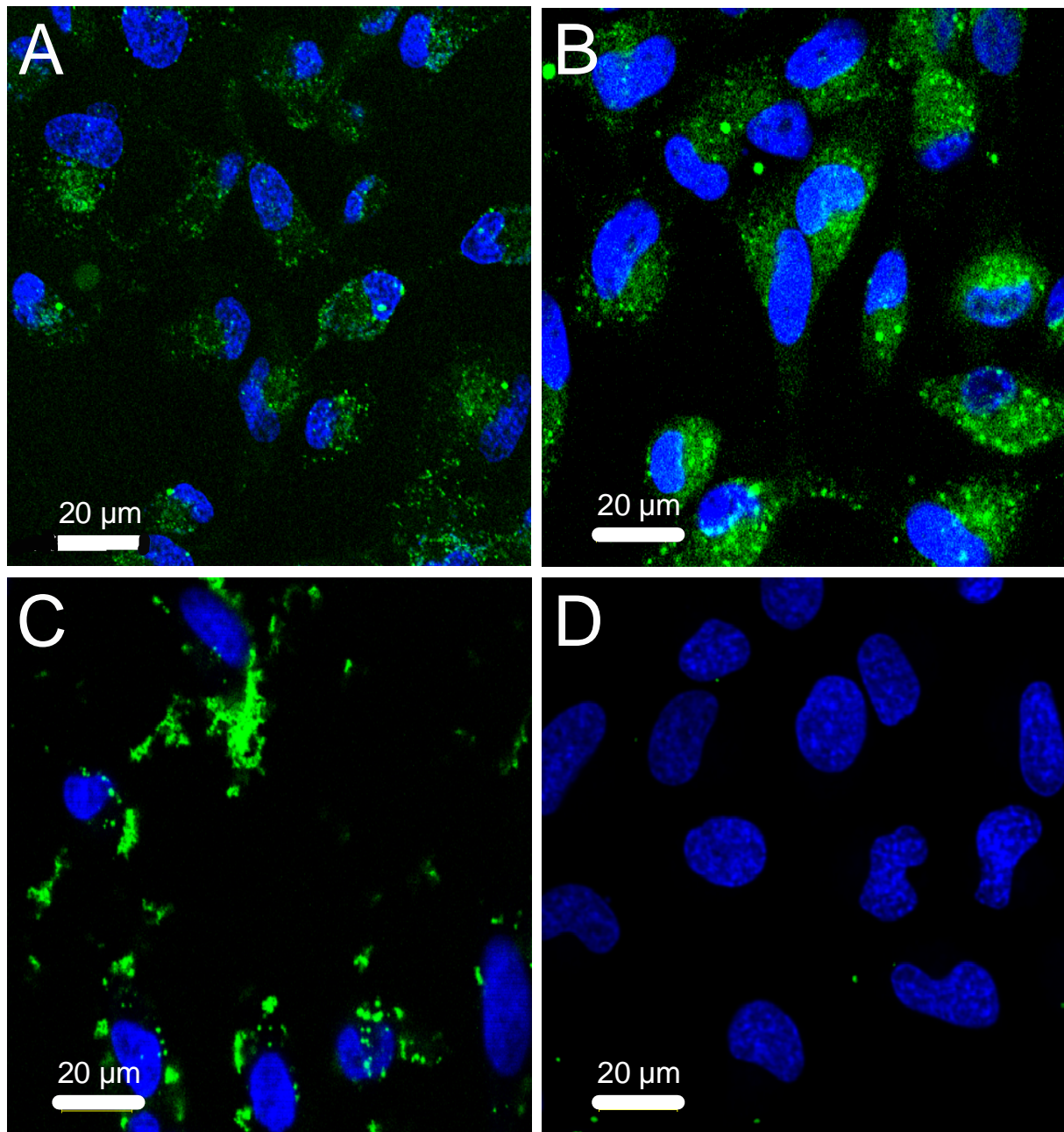


*Fig. 4: Confocal microscopy of translocation of hCT(9-32) and its modifications in HeLa cells.* HeLa cells were incubated for 2 hours with 40  $\mu\text{M}$  peptide solution in serum free medium of (A) hCT(9-32), (B) W30-hCT(9-32), (C) A23-hCT(9-32) or (D) 5-carboxyfluorescein. Cell nuclei (in blue) were stained for 30 minutes with Hoechst 33342 at a concentration of 1  $\mu\text{g/ml}$ . For extracellular fluorescence quenching CLSM pictures were taken after addition of Trypan blue.

compartments in the cytoplasm, suggestive of an endocytic pathway of internalization.

The cytosolic fluorescence of W30-hCT(9-32) was higher as compared to the unmodified hCT(9-32), indicating a more efficient uptake. The coarse fluorescence pattern for A23-hCT(9-32) (Fig. 5C) suggests that, owing to its limited solubility in serum-free medium, the peptide may have aggregated in larger clusters on the cell membrane, which cannot be completely quenched by Trypan blue. No intracellular fluorescence was observed in control cells incubated with the fluorescence marker 5-carboxyfluorescein alone.

#### *Quantitative assessment of peptide internalization by FACS analysis.*

In addition to the general trends in translocation as observed by CLSM, cellular uptake of the CPPs was also monitored through FACS analysis. HeLa cells were incubated for 2 hours with either the respective CPP or 5-carboxyfluorescein as control at concentrations of 40  $\mu$ M. The relative median fluorescence of the cells after internalization is demonstrated in Fig. 6. Again, Trypan blue was added as a quencher for extracellularly bound fluorescence. For A23-hCT(9-32) a more extensive membrane binding was observed as compared to the other two CPP as shown by a more pronounced reduction in fluorescence after incubation with the quencher (data not shown). The relative median fluorescence of HeLa cells after uptake of W30-hCT(9-32) was about 1.4 times higher ( $p < 0.02$ ) than that of unmodified hCT(9-32). However, we attribute the increase in fluorescence upon A23-hCT(9-32) partially to a contribution of incompletely quenched membrane bound fluorescence. FACS and CLSM data were in good agreement.

Cellular viability of HeLa cells after incubation with the investigated peptides was monitored by a MTT assay. None of the investigated peptides

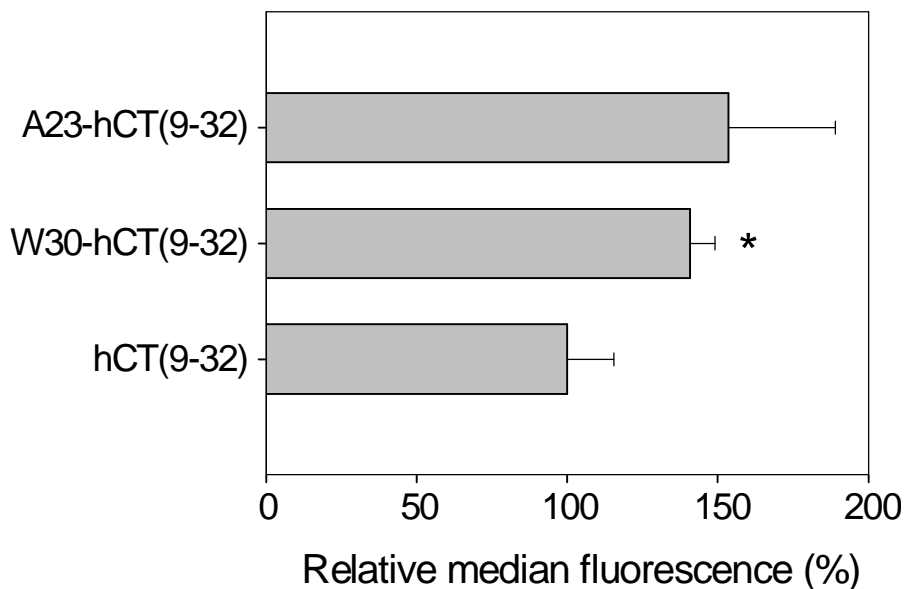


*Fig. 5: Quantification of cellular internalisation of hCT(9-32) and its modifications in HeLa cells.* HeLa cells were incubated with 40  $\mu$ M peptide solutions in serum free medium for 2 hours. FACS analysis was performed after the addition of Trypan blue to quench extracellular fluorescence. The internalisation of the unmodified hCT(9-32) was set to 100 %, the modifications' internalisation efficiency are expressed as relative percentages. The results are represented as mean values  $\pm$  SD ( $n=3$ ). Asterisks (\*) indicate a statistically significant difference ( $p < 0.02$ ).

exerted a relevant impact on cellular viability at concentrations ranging from 5  $\mu$ M to 100  $\mu$ M (data not shown).

## DISCUSSION

The objective of this study was to understand the molecular mechanism of hCT derived cell penetrating peptides as related to their association with membrane lipids and the translocation of the plasma membrane. In order to establish the role of individual residues we investigated hCT(9-32) (19, 20) and two mutants thereof. Exchange of residues was in order to enhance the peptides' affinity towards membrane lipids in order to promote their cellular uptake. For this aim we utilized various experimental techniques from

partitioning and leakage experiments to high-resolution NMR spectroscopy to probe peptide-lipid interactions. Biological membranes were mimicked by phospholipid liposomes for partitioning studies, and micelles for NMR analysis, respectively. Moreover, we studied the peptides' uptake in HeLa cells.

The mode of interaction of CPPs with the lipid membrane has been vividly discussed. For a short review on this topic see Lundberg *et al.* (52). To summarize, three different models have been developed: In the case of the inverted micelle model, CPPs associate with the bilayer surface, mainly through electrostatic interactions (53) (Fig. 6A) resulting in a concave curvature of the membrane, containment in an inverted micelle and leakage of its contents into the cytosole. The carpet model (Fig. 6B), on the other hand, which has been previously suggested for the cellular translocation of antimicrobial peptides, assumes an initial association of the peptides with the surface of the membrane. Interactions with basic residues then result in the reorganization of the lipids and cause disruption of lipid packing (54, 55). Finally, in the barrel-stave model (Fig. 6C), rearrangements of lipid-associated peptides lead to pore formation. Pores are created by circular assembly of amphipathic peptides in transmembrane fashion in such a way that their hydrophobic domains point to the lipid chains of the membrane and the hydrophilic side chains to the interior of the pore (56). In contrast, in the toroidal model (57) pores are also formed, but head groups form contacts to transmembrane-inserted peptides throughout (see Fig. 6B), similar to the situation in the carpet model. It is believed that the mode of action for CPPs in general may follow different mechanisms.

Which mechanism would apply to a particular CPP will depend on molecular features. In all models described above an initial association of the peptide with the surface of the bilayer constitutes the first step. Although this step is generally assumed to be governed by electrostatic interactions with negatively charged membrane lipids, hydrophobic partitioning cannot be excluded. The thermodynamics of peptide-lipid interactions has been recently reviewed and the interested reader is referred to the excellent review by Seelig (58). To which

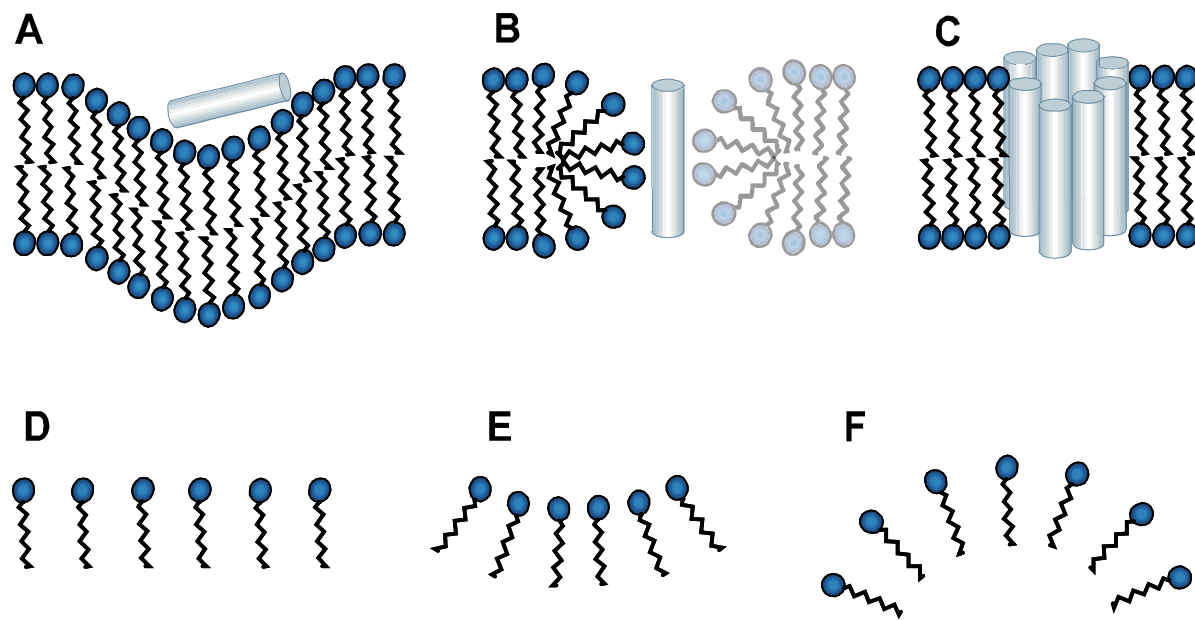


*Fig. 6: Scheme presenting the peptide-phospholipid arrangements in the inverted micelle (A), the carpet or toroidal pore (B) and the barrel-stave (C) mechanism. The membrane curvature induced by decreased (E) or increased (F) headgroup-headgroup distances are compared to a planar arrangement (D). Note that for clarity only the outer leaflet has been depicted for D, E and F.*

extent electrostatic interactions dominate the first step depends on the presence of basic and acidic amino acids, pH and salt concentration. Since electrostatic interactions are long-ranged, *intrinsic* structuring of the peptide is less important for electrostatic association with the membrane as compared to a situation where hydrophobic interactions would dominate. In fact, many membrane-active peptides are unstructured in solution but readily fold in vicinity to the membrane by a coupled partitioning-folding mechanism (59).

Whereas the first step is similar in the three models described above, the following events are different. In the inverted micelle model, a peptide is surface-bound throughout the complete translocation process, and never penetrates deeply into the hydrophobic interior. In contrast, in both the carpet and the barrel-stave model the peptide inserts into the membrane in a transmembrane fashion. Whereas no major membrane reorganization occurs in the barrel-stave model, the carpet model implies a rearrangement of phospholipid

head groups such that they interact with the hydrophobic side of the peptide and thereby become transferred into the interior of the membrane. Clearly, pore formation requires an additional interaction interface for homo-oligomerization of the CPPs in order to assemble to the barrel. It is presently not clear which molecular features favor one mechanism over the other. However, it can be expected that *balancing and positioning* of hydrophobic and hydrophilic residues influence the mechanism. Both properties will have an influence on membrane binding and membrane insertion.

In the barrel-stave-model interactions with the phospholipid head groups are made by both C- and N-terminal residues. In particular Tyr and Trp residues possess a high tendency to partition into the interface. In the trans-membrane segments of helical peptides that favor the barrel-stave mechanism, hydrophobic residues need to be directed towards the outside of the barrel, whereas the inside of the barrel is likely to accommodate hydrophilic residues. Otherwise no pores but helical bundles would be formed.

Therefore, the successful assembly of such barrels depends critically on how likely oligomerization is, and is also strongly favored in the *absence* of residues like Tyr and Trp in the central segment of the peptide. In contrast, in the carpet model reorganization of the phospholipids occurs such that interactions with phospholipid head groups take place *throughout* the helix. Therefore, we expect this mode to be favored when aromatic residues are placed in the central segment. The requirements for an inverted-micelle type mechanism seem to be different in that a few residues that anchor the peptide on the membrane are sufficient, but their position is probably not critical. In contrast to the barrel-stave mechanism there is no need for oligomerization. Moreover, the membrane surface in the inverted-micelle mechanism is concave whereas it is convex in the carpet mechanism (60). A concave membrane surface is formed when the head groups move together more closely, whereas the convex surface is characterized by increased distances between them (see Fig.6E and F, respectively). It has been argued that the distance between the head groups is promoted by electrostatic repulsion. Thus cationic residues may act by partially compensating

the negative charges, thereby allowing the head groups to move more closely together (61). In contrast, intercalation of side chains into the hydrophobic interior may increase distances between head groups thereby promoting concave surfaces.

The overall hydrophobicity of the peptides and their affinity towards membranes was probed by liposome-buffer partitioning experiments and demonstrated marked to high affinities of hCT-derived peptides to neutral POPC bilayers. In particular, we observed close agreement of partitioning with published thermodynamic data. Wimley and White have experimentally determined free energies of transferring whole amino acids from bulk solution into the membrane-water interface or into the hydrophobic interior (50). The corresponding values for Gly and Trp residues are 0.01 and  $-1.85\text{ kcal/mol}$  for the transfer into the interface ( $\Delta G_{\text{wif}}$ ) and  $1.15$  and  $-2.09\text{ kcal/mol}$  into the hydrophobic interior ( $\Delta G_{\text{oct}}$ ), respectively. Accordingly, we observed a substantial increase in affinity to POPC LUVs in our partitioning experiments when Gly was replaced by Trp. A similar increase in affinity was observed by replacing Pro23 ( $\Delta G_{\text{wif}} = 0.45\text{ kcal/mol}$ ,  $\Delta G_{\text{oct}} = 0.14\text{ kcal/mol}$ ) in the middle of the peptide sequence by an Ala ( $\Delta G_{\text{wif}} = 0.17\text{ kcal/mol}$ ,  $\Delta G_{\text{oct}} = 0.50\text{ kcal/mol}$ ).

After initial membrane-association of the peptides, which is most probably governed by the net charge of the peptide in vicinity to the membrane (note that this may substantially differ from that in bulk solution), any further steps, in particular those requiring interactions with the hydrophobic side-chains, will certainly depend on the *structure* of the peptides when bound to the membrane. This view is supported by our observation that the partition coefficient of the random sequence is much lower when compared to the values from the hCT-derived peptides demonstrating that, additional to amino acid sequence, secondary structure also plays a significant role for their affinity to phospholipid membranes. We would like to add that, due to the coupled partitioning-folding mechanism, residues such as Trp are likely to increase membrane-binding affinity, and exert a stabilizing effect on secondary structure.

Previously, structures and positioning of the CPPs penetratin and transportan have been determined by NMR in different membrane model systems. Penetratin was found to adopt an  $\alpha$ -helical conformation in SDS micelles as well as in partially negatively charged bicelles (62-64), with the helix being parallel aligned to the bicelle surface. Berlose et al. similarly proposed a parallel adoption to the surface also for SDS micelles (62), whereas others could not unambiguously position the peptide on SDS micelles (63). Transportan, a chimeric peptide constructed from galanin and mastoparan, was found to be  $\alpha$ -helical in the mastoparan part and mainly unstructured in the galanin part in SDS. Based on spin-label experiments the mastoparan segment inserts into the micelle whereas the galanin part resides in the interface (65). In a recent study in neutral bicelles the mastoparan part was observed to adopt a well-defined  $\alpha$ -helix, and the galanin part displayed a weaker tendency to form an  $\alpha$ -helix. The whole peptide was found to be oriented in parallel with the membrane-water interface (66). Interestingly, like the hCT derived CPPs investigated in the present study, these two peptides were also mainly located at the interface, indicating that an initial strong interaction of the CPPs with membranes is an important prerequisite for translocation.

Structures of the hCT(9-32) peptides in their micelle-bound form are predominantly helical in contrast to the unligated peptides in solution that are unstructured. hCT(9-32) is characterized by two short helical stretches, extending from Thr10 to Asn17 and from Gln24 to Val29, which, however, possess some additional flexibility. To gain further insight into the importance of secondary structure for translocation we replaced Pro23, the strongest  $\alpha$ -helix breaker, by Ala, which is known to be one of the most efficient  $\alpha$ -helix promoters (67). In fact, A23-hCT(9-32) adopted a continuous  $\alpha$ -helical structure from residue 12 to 26. Our spin-label studies with 5-doxylstearate demonstrated that the more hydrophobic residues Tyr12, Phe16, 18 and 22, and His20, Ala23 and Gly28 are integrated into the micelle, leaving the hydrophilic residues Gln14 and 24, Asp15, Asn17, and Lys18 exposed to the aqueous phase. Thereby

A23-hCT(9-32) forms a continuous amphipathic helix. The spin-label data for A23-hCT(9-32) nicely reflect periodicity of the helix, also indicating that the peptide was well anchored on the micelle surface. The prolonged helix should result in a larger membrane-binding interface, and this expectation was well met by both the increased partition coefficient as well as the increased propensity for aggregation of fluorescein labeled A23-hCT(9-32). Unfortunately, the increase in fluorescence intensity as detected by FACS analysis may also be due to formation of aggregates on the cells surface, which would present a drawback for the applicability of A23-hCT(9-32) as a CPP.

In addition, we introduced a Trp residue into the C-terminal segment by replacing Gly30, which in wild-type hCT(9-32) was not associated to the membrane. The Gly30Trp exchange resulted in stable anchoring of the C-terminal segment on the phospholipid micelles, clearly evident from the large attenuations observed in the spin-label experiments. The additional membrane-anchor resulted in a twofold increase of the partition coefficient. Interestingly, tighter binding to model membranes *in vitro* was accompanied by higher uptake into HeLa cells *in vitro*. The regular, punctuated fluorescence pattern indicated vesicular localization of W30-hCT(9-32) and therefore an endocytic pathway of internalization. The brighter fluorescence of W30-hCT(9-32) as compared to hCT(9-32) observed in the CLSM was confirmed by significantly higher fluorescence detected by FACS analysis. Together with the apparent lack of toxicity, this makes W30-hCT(9-32) a promising CPP candidate for further exploration.

Any mechanism for translocation resulting in membrane permeabilization would be unacceptable from a pharmaceutical point of view when associated with increased cytotoxicity. This study was also to reveal whether the CPPs confer cytotoxic effects that would prevent their use in drug delivery. Dye leakage experiments were performed to assure that the sequence modifications do not increase the potential for membrane permeabilization. In fact, no leakage was found to occur for any of the modifications up to a concentration of 50 µM, which was above the concentration used in cell culture experiments (40 µM). At

concentrations higher than 50  $\mu\text{M}$  the modified peptides, A23-hCT(9-32) and W30-hCT(9-32), display slightly increased propensity for leakage relative to hCT(9-32), but remain significantly below the values measured for full-length hCT. Accordingly, *in vitro* experiments with 5  $\mu\text{M}$  to 100  $\mu\text{M}$  peptide solution revealed no effects on cellular viability on HeLa cells, neither for hCT(9-32), nor the modified peptides A23-hCT(9-32) and W30-hCT(9-32). This in agreement with a previous study where 40 mM hCT(9-32) on MDCK monolayers revealed no significant toxicity after 120 min (19). In a study, in which fluorescein-labeled hCT(9-32) was tested on three different cell lines, no indications for toxicity was observed for any of the cell lines even at 100  $\mu\text{M}$ , the highest tested concentration (20). As shown by Christiaens et al. (17), peptides are generally more likely to induce leakage of dye-loaded LUVs than exhibit toxic effects on cell cultures. Nevertheless, in black lipid membranes composed of POPC/DOPG (85:15), untruncated hCT was shown to induce a slight formation of voltage-dependent channels that allow permeation of calcium ions (68) after 200 min of incubation. At the conditions of our study, pore formation as a possible mechanism of translocation can be ruled out. Hence we exclude the cellular translocation of the investigated CPP to follow the barrel-stave model.

Instead, both the spectroscopic part of our work as well as the *in vitro* studies indicate an endocytic mechanism. The liposome-leakage study disfavors any model that requires permeabilization such as the barrel-stave or, to a lesser extent, the carpet model. The structures of hCT(9-32) displayed two rather short helical segments disrupted by Pro23. Replacement of the latter by Ala resulted in a continuous helix. However, spin-label data indicated that membrane binding in the central segment was not particularly pronounced as supported by the absence of residues like Trp or Tyr in that segment which would strongly partition into the interface. Rather, the amino acid composition of the peptides implies a moderate association of the peptides with the membrane, and the spin-label data indicate that the peptides remain surface associated. The initial steps of the inverted micelle model require invaginations of the membrane, and are

highly similar to early events in endocytosis. Indeed, the punctuated fluorescence pattern indicating vesicular localization of fluorescein-labelled W30-hCT(9-32) suggests that endocytosis takes place, certainly to considerable extent.

## ACKNOWLEDGEMENTS

This work was supported by the Commission of the European Union (EU project on Quality of Life and Management of Living Resources, Project No. QLK2-CT-2001-01451)

## REFERENCES:

1. Simeoni, F., M.C. Morris, F. Heitz, and G. Divita, *Insight into the mechanism of the peptide-based gene delivery system MPG: implications for delivery of siRNA into mammalian cells*. Nucleic Acids Res, (2003) **31**: 2717-2724.
2. Morris, M.C., P. Vidal, L. Chaloin, F. Heitz, and G. Divita, *A new peptide vector for efficient delivery of oligonucleotides into mammalian cells*. Nucleic Acids Res, (1997) **25**: 2730-2736.
3. Morris, M.C., J. Depollier, J. Mery, F. Heitz, and G. Divita, *A peptide carrier for the delivery of biologically active proteins into mammalian cells*. Nat Biotechnol, (2001) **19**: 1173-1176.
4. Lindgren, M., M. Hallbrink, A. Prochiantz, and U. Langel, *Cell-penetrating peptides*. Trends Pharmacol Sci, (2000) **21**: 99-103.
5. Derossi, D., G. Chassaing, and A. Prochiantz, *Trojan peptides: the penetratin system for intracellular delivery*. Trends Cell Biol, (1998) **8**: 84-87.

6. Snyder, E.L. and S.F. Dowdy, *Cell penetrating peptides in drug delivery*. Pharm Res, (2004) **21**: 389-393.
7. Schwarze, S.R., K.A. Hruska, and S.F. Dowdy, *Protein transduction: unrestricted delivery into all cells?* Trends Cell Biol, (2000) **10**: 290-295.
8. Thoren, P.E., D. Persson, M. Karlsson, and B. Norden, *The antennapedia peptide penetratin translocates across lipid bilayers - the first direct observation*. FEBS Lett, (2000) **482**: 265-268.
9. Prochiantz, A., *Getting hydrophilic compounds into cells: lessons from homeopeptides*. Curr Opin Neurobiol, (1996) **6**: 629-634.
10. Lundberg, M., S. Wikstrom, and M. Johansson, *Cell surface adherence and endocytosis of protein transduction domains*. Mol Ther, (2003) **8**: 143-150.
11. Wadia, J.S., R.V. Stan, and S.F. Dowdy, *Transducible TAT-HA fusogenic peptide enhances escape of TAT-fusion proteins after lipid raft macropinocytosis*. Nat Med, (2004) **10**: 310-315.
12. Vives, E., J.P. Richard, C. Rispal, and B. Lebleu, *TAT peptide internalization: seeking the mechanism of entry*. Curr Protein Pept Sci, (2003) **4**: 125-132.
13. Richard, J.P., K. Melikov, E. Vives, C. Ramos, B. Verbeure, M.J. Gait, L.V. Chernomordik, and B. Lebleu, *Cell-penetrating peptides. A reevaluation of the mechanism of cellular uptake*. J Biol Chem, (2003) **278**: 585-590.
14. Trehin, R. and H.P. Merkle, *Chances and pitfalls of cell penetrating peptides for cellular drug delivery*. Eur J Pharm Biopharm, (2004) **58**: 209-223.
15. Scheller, A., J. Oehlke, B. Wiesner, M. Dathe, E. Krause, M. Beyermann, M. Melzig, and M. Bienert, *Structural requirements for cellular uptake of alpha-helical amphipathic peptides*. J Pept Sci, (1999) **5**: 185-194.

16. Drin, G., M. Mazel, P. Clair, D. Mathieu, M. Kaczorek, and J. Temsamani, *Physico-chemical requirements for cellular uptake of pAntp peptide. Role of lipid-binding affinity.* Eur J Biochem, (2001) **268**: 1304-1314.
17. Christiaens, B., J. Grooten, M. Reusens, A. Joliot, M. Goethals, J. Vandekerckhove, A. Prochiantz, and M. Rosseneu, *Membrane interaction and cellular internalization of penetratin peptides.* Eur J Biochem, (2004) **271**: 1187-1197.
18. Silverman, S.L., *Calcitonin.* Endocrinol Metab Clin North Am, (2003) **32**: 273-284.
19. Trehin, R., U. Krauss, R. Muff, M. Meinecke, A.G. Beck-Sickinger, and H.P. Merkle, *Cellular internalization of human calcitonin derived peptides in MDCK monolayers: a comparative study with Tat(47-57) and penetratin(43-58).* Pharm Res, (2004) **21**: 33-42.
20. Trehin, R., U. Krauss, A.G. Beck-Sickinger, H.P. Merkle, and H.M. Nielsen, *Cellular uptake but low permeation of human calcitonin-derived cell penetrating peptides and Tat(47-57) through well-differentiated epithelial models.* Pharm Res, (2004) **21**: 1248-1256.
21. Trehin, R., H.M. Nielsen, H.G. Jahnke, U. Krauss, A.G. Beck-Sickinger, and H.P. Merkle, *Metabolic Cleavage of Cell Penetrating Peptides in Contact with Epithelial Models: Human Calcitonin (hCT) Derived Peptides, Tat(47-57) and Penetratin(43-58).* Biochem J, (2004) **382**: 945-956.
22. Motta, A., G. Andreotti, P. Amodeo, G. Strazzullo, and M.A. Castiglione Morelli, *Solution structure of human calcitonin in membrane-mimetic environment: the role of the amphipathic helix.* Proteins, (1998) **32**: 314-323.
23. Wagner, K., A.G. Beck-Sickinger, and D. Huster, *Structural investigations of a human calcitonin-derived carrier peptide in a membrane environment by solid-state NMR.* Biochemistry, (2004) **43**: 12459-12468.

24. Krauss, U., F. Kratz, and A.G. Beck-Sickinger, *Novel daunorubicin-carrier peptide conjugates derived from human calcitonin segments.* J Mol Recognit, (2003) **16**: 280-287.
25. Pauletti, G.M. and H. Wunderli Allenspach, *Partition-Coefficients in-Vitro - Artificial Membranes as a Standardized Distribution Model.* Eur. J. Pharm. Sci., (1994) **1**: 273-282.
26. Buck, R.H. and F. Maxl, *A validated HPLC assay for salmon calcitonin analysis. Comparison of HPLC and biological assay.* J Pharm Biomed Anal, (1990) **8**: 761-769.
27. Schurtenberger, P., N. Mazer, and W. Kanzig, *Micelle to vesicle transition in aqueous-solutions of bile-salt and lecithin.* J Phys Chem-US, (1985) **89**: 1042-1049.
28. Mayer, L.D., M.J. Hope, and P.R. Cullis, *Vesicles of variable sizes produced by a rapid extrusion procedure.* Biochim Biophys Acta, (1986) **858**: 161-168.
29. New, R.B.C., *Characterization of liposomes*, in *Liposomes, A Practical Approach*, R.B.C. New, Editor. (1990), Oxford University Press: New York. p. 125-127.
30. Dathe, M., M. Schumann, T. Wieprecht, A. Winkler, M. Beyermann, E. Krause, K. Matsuzaki, O. Murase, and M. Bienert, *Peptide helicity and membrane surface charge modulate the balance of electrostatic and hydrophobic interactions with lipid bilayers and biological membranes.* Biochemistry, (1996) **35**: 12612-12622.
31. Brown, L.R., C. Bösch, and K. Wüthrich, *Location and orientation relative to the micelle surface for glucagon in mixed micelles with dodecylphosphocholine: EPR and NMR studies.* Biochim Biophys Acta, (1981) **642**: 296-312.

32. Griesinger, C., G. Otting, K. Wüthrich, and R.R. Ernst, *Clean TOCSY for <sup>1</sup>H Spin System Identification in Macromolecules*. J. Am. Chem. Soc., (1988) **110**: 7870-7872.
33. Kumar, A., R.R. Ernst, and K. Wüthrich, *A Two-Dimensional Nuclear Overhauser Enhancement (2D NOE) Experiment for the Elucidation of Complete Proton,Proton Cross-Relaxation Networks in Biological Macromolecules*. Biochem. Biophys. Res. Com., (1980) **95**: 1-6.
34. Wüthrich, K., *NMR of Proteins and Nucleic Acids*. (1986), New York: Wiley.
35. Güntert, P., C. Mumenthaler, and K. Wüthrich, *Torsion Angle Dynamics For Nmr Structure Calculation With the New Program Dyana*. J Mol Biol, (1997) **273**: 283-298.
36. Jarvet, J., J. Zdunek, P. Damberg, and A. Graslund, *Three-dimensional structure and position of porcine motilin in sodium dodecyl sulfate micelles determined by <sup>1</sup>H NMR*. Biochemistry, (1997) **36**: 8153-8163.
37. Papavoine, C.H., R.N. Konings, C.W. Hilbers, and F.J. Van de Veen, *Location of the M13 major coat protein in sodium dodecylsulfate micelles as determined by NMR*. Biochemistry, (1994) **33**: 12990-12997.
38. Bartels, C., T.-h. Xia, M. Billeter, P. Güntert, and K. Wüthrich, *The program XEASY for computer-supported spectral analysis of biological macromolecules*. J. Biomol. NMR, (1995) **6**: 1-10.
39. Bader, R., M. Lerch, and O. Zerbe, *NMR of membrane-associated peptides and proteins*, in *BioNMR in Drug Research*, O. Zerbe, Editor. (2002), Wiley-VCH: Weinheim. p. 95-120.
40. Bader, R., A. Bettio, A.G. Beck-Sickinger, and O. Zerbe, *Structure and dynamics of micelle-bound neuropeptide Y: comparison with unligated NPY and implications for receptor selection*. J Mol Biol, (2001) **305**: 307-329.

41. Herbig, M.E., U. Fromm, J. Leuenberger, U. Krauss, A.G. Beck-Sickinger, and H.P. Merkle, *Bilayer interaction and localization of cell penetrating peptides with model membranes: a comparative study of a human calcitonin (hCT) derived peptide with pVEC and pAntp(43-58)*. BBA Biomembranes, (2005) **(in press)**.
42. Schmidt, M.C., B. Rothen-Rutishauser, B. Rist, A. Beck-Sickinger, H. Wunderli-Allenspach, W. Rubas, W. Sadee, and H.P. Merkle, *Translocation of human calcitonin in respiratory nasal epithelium is associated with self-assembly in lipid membrane*. Biochemistry, (1998) **37**: 16582-16590.
43. Wan, C.P., C.S. Park, and B.H.S. Lau, *A Rapid and Simple Microfluorometric Phagocytosis Assay*. J Immunol Methods, (1993) **162**: 1-7.
44. Sahlin, S., J. Hed, and I. Rundquist, *Differentiation between Attached and Ingested Immune-Complexes by a Fluorescence Quenching Cytofluorometric Assay*. J Immunol Methods, (1983) **60**: 115-124.
45. Ma, Z.S. and L.Y. Lim, *Uptake of chitosan and associated insulin in Caco-2 cell monolayers: A comparison between chitosan molecules and chitosan nanoparticles*. Pharm Res, (2003) **20**: 1812-1819.
46. Tseng, W.C., N.B. Purvis, F.R. Haselton, and T.D. Giorgio, *Cationic liposomal delivery of plasmid to endothelial cells measured by quantitative flow cytometry*. Biotechnol Bioeng, (1996) **50**: 548-554.
47. Hed, J., G. Hallden, S.G. Johansson, and P. Larsson, *The use of fluorescence quenching in flow cytofluorometry to measure the attachment and ingestion phases in phagocytosis in peripheral blood without prior cell separation*. J Immunol Methods, (1987) **101**: 119-125.
48. Innes, N.P. and G.R. Ogden, *A technique for the study of endocytosis in human oral epithelial cells*. Arch Oral Biol, (1999) **44**: 519-23.

49. Lobner, D., *Comparison of the LDH and MTT assays for quantifying cell death: validity for neuronal apoptosis?* J Neurosci Methods, (2000) **96**: 147-52.
50. White, S.H. and W.C. Wimley, *Hydrophobic interactions of peptides with membrane interfaces.* Biochim Biophys Acta, (1998) **1376**: 339-352.
51. Matsuzaki, K., S. Yoneyama, and K. Miyajima, *Pore formation and translocation of melittin.* Biophys J, (1997) **73**: 831-838.
52. Lundberg, P. and U. Langel, *A brief introduction to cell-penetrating peptides.* J Mol Recognit, (2003) **16**: 227-33.
53. Derossi, D., S. Calvet, A. Trembleau, A. Brunissen, G. Chassaing, and A. Prochiantz, *Cell internalization of the third helix of the Antennapedia homeodomain is receptor-independent.* J Biol Chem, (1996) **271**: 18188-18193.
54. Pouny, Y., D. Rapaport, A. Mor, P. Nicolas, and Y. Shai, *Interaction of antimicrobial dermaseptin and its fluorescently labeled analogues with phospholipid membranes.* Biochemistry, (1992) **31**: 12416-23.
55. Matsuzaki, K., K. Sugishita, and K. Miyajima, *Interactions of an antimicrobial peptide, magainin 2, with lipopolysaccharide-containing liposomes as a model for outer membranes of gram-negative bacteria.* FEBS Lett, (1999) **449**: 221-4.
56. Gazit, E., W.J. Lee, P.T. Brey, and Y. Shai, *Mode of action of the antibacterial cecropin B2: a spectrofluorometric study.* Biochemistry, (1994) **33**: 10681-92.
57. Matsuzaki, K., O. Murase, N. Fujii, and K. Miyajima, *An antimicrobial peptide, magainin 2, induced rapid flip-flop of phospholipids coupled with pore formation and peptide translocation.* Biochemistry, (1996) **35**: 11361-11368.
58. Seelig, J., *Thermodynamics of lipid-peptide interactions.* Biochim Biophys Acta, (2004) **1666**: 40-50.

59. Popot, J.L. and D.M. Engelman, *Helical membrane protein folding, stability, and evolution.* Annu Rev Biochem, (2000) **69**: 881-922.
60. Lundberg, P. and U. Langel, *A brief introduction to cell-penetrating peptides.* J Mol Recognit, (2003) **16**: 227-233.
61. Kirk, G.L., S.M. Gruner, and D.L. Stein, *A thermodynamic model of the lamellar to inverse hexagonal phase transition of lipid-membrane water systems.* Biochemistry, (1984) **23**: 1093-1102.
62. Berlose, J.P., O. Convert, D. Derossi, A. Brunissen, and G. Chassaing, *Conformational and associative behaviours of the third helix of antennapedia homeodomain in membrane-mimetic environments.* Eur J Biochem, (1996) **242**: 372-386.
63. Lindberg, M., H. Biverstahl, A. Graslund, and L. Mäler, *Structure and positioning comparison of two variants of penetratin in two different membrane mimicking systems by NMR.* Eur J Biochem, (2003) **270**: 3055-3063.
64. Lindberg, M. and A. Graslund, *The position of the cell penetrating peptide penetratin in SDS micelles determined by NMR.* FEBS Lett, (2001) **497**: 39-44.
65. Lindberg, M., J. Jarvet, U. Langel, and A. Graslund, *Secondary structure and position of the cell-penetrating peptide transportan in SDS micelles as determined by NMR.* Biochemistry, (2001) **40**: 3141-3149.
66. Barany-Wallje, E., A. Andersson, A. Graslund, and L. Mäler, *NMR solution structure and position of transportan in neutral phospholipid bicelles.* FEBS Lett, (2004) **567**: 265-269.
67. Chou, P.Y. and G.D. Fasman, *Secondary Structural Prediction of Proteins from Their Amino-Acid Sequence.* Trends Biochem Sci, (1977) **2**: 128-131.
68. Stipani, V., E. Gallucci, S. Micelli, V. Picciarelli, and R. Benz, *Channel formation by salmon and human calcitonin in black lipid membranes.* Biophys J, (2001) **81**: 3332-3338.



## CHAPTER IV

The cell penetrating peptides pVEC and W2-pVEC induce transformation of gel phase domains in phospholipid bilayers without affecting their integrity

*Michael E. Herbig<sup>1</sup>, Fabiano Assi<sup>2</sup>, Marcus Textor<sup>2</sup>, and Hans P. Merkle<sup>1</sup>*

<sup>1</sup>Drug Formulation & Delivery Group, Department of Chemistry and Applied BioSciences, Swiss Federal Institute of Technology Zurich (ETH Zurich), Wolfgang-Pauli-Strasse 10, CH-8093 Zurich, Switzerland

<sup>2</sup>Laboratory for Surface Science and Technology, Department of Materials, Swiss Federal Institute of Technology (ETH), Wolfgang-Pauli-Strasse 10, CH-8093 Zürich, Switzerland

## ABSTRACT

The cell penetrating peptide (CPP) pVEC has been shown to translocate efficiently the plasma membrane of different mammalian cell lines by a receptor-independent mechanism without exhibiting cellular toxicity. This ability renders CPP of broad interest in cell biology, biotechnology and drug delivery. To gain insight into the interaction of CPP with biomembranes, we studied the interaction of pVEC and W2-pVEC, an Ile → Trp modification of the former, on phase separated supported phospholipid bilayers (SPB) by atomic force microscopy (AFM). W2-pVEC induced a transformation of dipalmitoyl phosphatidylcholine (DPPC) domains from a gel phase state via an intermediate state with fractal-like structures into essentially flat bilayers. With pVEC the transformation followed a similar pathway but was slower. Employing fluorescence polarisation, we revealed the capability of the investigated peptides to increase the fluidity of DPPC domains as the underlying mechanism of transformation. Due to their tighter packing sphingomyelin (SM) domains were not transformed. By combination, AFM observations, dynamic light scattering studies, and liposome leakage experiments indicated that bilayer integrity was not compromised by the peptides. Transformation of gel phase domains in SPB by CPP represents a novel aspect in the discussion on uptake mechanisms of CPP.

## INTRODUCTION

Difficult transportation through the cell membrane is a notorious hallmark for the cellular delivery of many large and hydrophilic therapeutics. To aid in this process, several classes and/or prototypes of cell-penetrating peptides (CPP) have been proposed during the past decade (1-3). Mostly, CPP are short peptides of about 10 to 30 amino acids, many of them of strongly cationic nature, which may be covalently conjugated to the cargo of interest. Moreover, many CPP form non-covalent electrostatic complexes with nucleic acid cargoes like DNA or oligonucleotides (4, 5). By hydrophobic interactions, CPP even have the capacity to form non-covalent complexes with large proteins carrying hydrophobic binding sites (6). The ability of the CPP to translocate a therapeutic cargo, particularly peptide, protein and nucleic acid biopharmaceuticals, across cellular membranes renders them of broad interest in cell biology, biotechnology and drug delivery. In fact, CPP have been used as vectors for the cytoplasmic and nuclear delivery of hydrophilic biomolecules and drugs (1, 7, 8).

There are currently two principal avenues to analyse the principles of CPP action. Cellular studies come first, using proliferating or confluent cell models with the aim, e.g., to identify the capacities of distinct CPP for translocation, their pertinent pathways and routes for cellular traffic, and the thereby involved mechanisms. A second branch in current CPP research is the study of the interactions of CPP with lipid bilayer and monolayer models of various lipid compositions. To this end, a large body of different methodologies is available, including liposome leakage, liposome partitioning, the study of microviscosity, electrical resistance, interaction with giant vesicles, and NMR, CD, or IR based spectroscopy on the interactions of CPP with lipid mono- and bilayers. Although rather distant from the actual cell biology of CPP translocation, the flavor of such methodologies lies in the clear definition of the experimental setup, sometimes at the expense of biological relevance. Nevertheless, when considered in conjunction with the cell biology of translocation, the physicochemical analysis of CPP/lipid membrane interactions remains an

indispensable tool. For the CPP investigated in this study translocation studies in cell culture models have been previously reported (9-11). Independently of their function as CPP, we propose them to induce a yet unknown transformation mechanism in phospholipid bilayers.

An initial event in CPP translocation is believed to be the interaction of a CPP, its covalent conjugate or complex thereof, with the cell membrane, possibly leading to an enrichment in or perturbation of the phospholipid bilayer, which may subsequently trigger endocytic uptake (2, 12-16). During the last decade, atomic force microscopy (AFM) of supported phospholipid bilayers (SPB) has become a tool in the analysis of membrane models, particularly for the study of the interactions of drugs, peptides and proteins with phospholipid bilayers (17). The major assets of AFM are (i) the capacity to probe the surface structure of SPB in real time and under conditions close to physiological, (ii) the flexibility to modify SPB composition and structure, and (iii) the opportunity to measure physical properties directly and at very high spatial resolution. In aqueous buffers structure topologies may be acquired with a lateral resolution of 0.5 – 1 nm and a vertical resolution of 0.1 – 0.2 nm (18).

So far, mainly distribution and aggregation phenomena, and effects of physiological proteins on SPB membrane restructuring have been characterized by AFM (19-23). Further, successful visualizations were reported for the formation of striated domains in DPPC bilayers induced by transmembrane peptides (24, 25), and the dissolution process of DOPC bilayers induced by the pore-forming peptide melittin (26). Despite the great potential of AFM to contribute to a better understanding of CPP action on lipid membranes, so far only a single AFM study featuring CPP effects on SPB has been published. In that study, a human calcitonin derived CPP, hCT(9-32), alone or coupled to a protein cargo, has been studied to aggregate in the DOPC fluid phase of DOPC/DPPC phase separated SPB in the absence of cholesterol, and in DPPC liquid ordered phase, when cholesterol was present (27). Aggregation was previously considered to trigger the endocytosis of human calcitonin and a CPP derivative thereof (28).

In the present study, we investigated the effects of two CPP, pVEC and W2-pVEC, a single point modification, replacing Leu in position 2 by Trp, on DOPC/DPPC phase separated SPB. pVEC, a peptide derived from the murine vascular endothelium cadherin (VE-cadherin), contains 18-amino acids (residues 615-632), 13 cytosolic amino acids closest to the membrane, and 5 amino acids from the transmembrane region. Cadherins are single transmembrane-spanning glycoproteins of about 700 amino acids. pVEC has been shown to translocate efficiently into cells of different cell lines by a receptor-independent mechanism and to be able to carry macromolecular cargoes across plasma membranes (9, 10). Whereas pVEC exhibits no toxicity on mammalian cells, it has been shown to possess potent antimicrobial properties (29). While an earlier study suggested an energy independent transport through the cell-membranes (9), recently strong evidence for an endocytic uptake mechanism of pVEC has been brought up (11). The paradigm shift from an energy independent, direct transport of CPP through biomembranes, as postulated in earlier studies to concepts involving endocytosis (2, 14, 15, 30-32), reflects a general trend in the CPP area.

W2-pVec was initially designed to allow Trp-fluorescence studies, without largely changing the properties of pVEC . In fact, we demonstrated in a previous study that both peptides possess very similar physico-chemical properties, despite of the desired fact of an increased affinity of W2-pVEC towards membrane interfaces (33).

In a time-lapse AFM study under conditions close to physiological, we were able to demonstrate for the first time a CPP-induced time- and concentration-dependent transformation process of DPPC domains without compromising the bilayer integrity. Both, pVEC and W2-pVEC, were able to transform the DPPC gel phase domains, which initially protruded by 1 nm from the DOPC phase, via an intermediate state of fractal appearance into a physical state that was indiscernible from the DOPC liquid-crystalline phase. Fluorescence polarization experiments revealed that these effects may be caused by the peptides' capabilities to increase the fluidity of the DPPC domains.

Interestingly, gel phase domains composed of sphingomyelin (SM) were not significantly affected by these peptides.

## MATERIALS AND METHODS

### *Materials*

The VE-cadherin-derived peptides were synthesized by NMI Peptides, Reutlingen, Germany. The peptides were N-terminally amidated and their identity and purity (> 98%) were controlled by mass spectral and HPLC analysis. The analytical data were as follows: pVEC (LLIILRRRIRKQAHAAHSK-NH<sub>2</sub>), mass<sub>calc.</sub> 2207.4 Da, mass<sub>exp.</sub> 2207.0 Da; W2-pVEC (LWIILRRRIRKQAHAAHSK-NH<sub>2</sub>), mass<sub>calc.</sub> 2280.4 Da, mass<sub>exp.</sub> 2280.2 Da. 1-palmitoyl-2-oleoyl-phosphatidylcholine (POPC), 1,2-Dipalmitoyl-phosphatidylglycerol (DPPC), 1,2-Dioleoyl-phosphatidylglycerol (DOPC), and Sphingomyelin (egg, chicken) were purchased from Avanti Polar Lipids (Alabaster, Alabama, USA), of the best quality available, and used without further purification. Analytical grade CaCl<sub>2</sub> x 2H<sub>2</sub>O, methanol and chloroform were purchased from Merck (Darmstadt, Germany); calcein, NaCl, EDTA, phosphate buffered saline (PBS), and HEPES were from FLUKA (Buchs, Switzerland). 1,6-diphenyl-1,3,5-hexatriene (DPH) was purchased from Molecular Probes (Leiden, The Netherlands).

### *Preparation of calcein containing large unilamellar vesicles*

For the Calcein leakage studies, large unilamellar vesicles (LUV) were prepared by dissolving the phospholipids, either pure, or in the desired molar ratio, in chloroform to ensure complete dissolution and mixing of the components. The lipid solution was dried at 37°C in a rotary evaporator to yield a thin film of the lipids, and then kept under high vacuum over night. The dry

film was then redispersed in buffer (20 mM calcein, in PBS pH 7.4, containing 1 mM EDTA for complexation of  $\text{Ca}^{2+}/\text{Mg}^{2+}$  to avoid interference with Calcein fluorescence) and the resulting multilamellar vesicle (MLV) solution was treated by five freeze-thaw cycles in liquid nitrogen and water at 37°C. LUV were then obtained by extruding four times through 0.4  $\mu\text{m}$  and eight times through 0.1  $\mu\text{m}$  Nuclepore polycarbonate membranes (Sterico, Wangen, Switzerland) by means of a Lipex extruder (Vancouver, Canada) (34). A plastic syringe (5 ml volume, plugged with a filter pad) mounted in a centrifugation tube was filled with hydrated Sephadex G-50 gel. After spinning at 2000 rpm for 3 min the gel column had dried and separated from the sides of the syringe. To remove untrapped dye 1 mL of the LUV dispersion was dropped onto the dry gel bed, and the liposomes were eluted by centrifugation at 200 g for 3 min (35). To assure the quality of the liposomes, the particle size distribution of the LUV was checked by photon correlation spectroscopy on a Zetasizer 3000 HSA (Malvern, Malvern, UK). Lipid concentration was determined by an enzymatic colorimetric test for phospholipids as obtained from Roche Diagnostics (Mannheim, Germany).

### *Calcein leakage tests*

Using 96-well plates (Nunc, Wiesbaden, Germany) 50  $\mu\text{L}$  of a 400  $\mu\text{M}$  LUV dispersion was mixed with 50  $\mu\text{L}$  of peptide solutions of different concentrations. Calcein leakage from vesicles was monitored fluorimetrically by measuring the decrease in self-quenching (excitation at 462 nm, emission at 525 nm) after 60 min at room temperature on a Varian Cary Eclipse spectrofluorometer (Mulgrave, Australia). The buffer blank was subtracted from all values and the fluorescence intensity corresponding to 100% leakage was determined after addition of Triton X-100 (36). Results were displayed as percentage of maximum leakage.

*Preparation of phase-separated supported phospholipid bilayers*

We made phase-separated supported phospholipid bilayers (SPB) by direct fusion of vesicles onto a mica surface (37). Mixtures of DOPC with DPPC (1:1) or SM (3:2) from 10 mM stock solutions in chloroform/methanol (2:1) were fed into a thoroughly rinsed glass tube, and the solvents evaporated under nitrogen at 37°C. Redispersion of the lipid film in 65°C HEPES buffer (pH 7.4 containing 2 mM Ca<sup>2+</sup>) resulted in MLVs. LUV were then obtained by extruding ten times through 0.1 µm Nuclepore polycarbonate membranes (Sterico, Wangen, Switzerland) by means of the Lipex extruder (Vancouver, Canada). During the whole process temperature was kept at 65°C. LUV were deposited on a freshly cleaved mica disk, which was glued on a magnetic disk with epoxy adhesive, then inserted into a 13 mm Swinney filter chasing (Millipure, Bedford, MA), and incubated in a water bath at 65°C. The phase-separated SPBs were left at room temperature for at least 12 h, but not more than 24 h, before being rinsed 15 times with sterile filtrated HEPES buffer to remove unfused LUV. The bilayers were carefully protected from desiccation and kept in a moist chamber at room temperature prior to AFM imaging.

*AFM imaging*

The AFM studies were performed on a Nanoscope IIIa MultiMode AFM (Digital Instruments, San Diego, CA) equipped with an “E” (16 µM) or a “J” (120 µM) scanner. The bilayers on mica disks were installed into a contact mode fluid cell (Digital instruments) and recorded in the contact mode using oxide-sharpened silicon nitrate tips mounted on triangular cantilevers with a nominal spring constant of 0.06 N/m at scanning rates of 1.5 to 3 Hz. The scan angle was 90° and the force used was maintained at the lowest possible value by continuously adjusting the set point during imaging. After having imaged the blank bilayers the HEPES buffer was replaced by a 5 µM or 10 µM solution of

the respective peptide. All experiments were performed at room temperature (22°C). Data processing was restricted to flattening (first or second order, Nanoscope Reference Manual, 1998). For every experiment at least three different parts of at least two independent samples were inspected.

### *Fluorescence polarization*

Large unilamellar vesicles (LUV) were prepared by dissolving DPPC in chloroform/methanol (2:1). After evaporation of the solvent, the dry film was redispersed in HEPES buffer pH 7.4, and the resulting multilamellar vesicle (MLV) dispersion was treated by five freeze-thaw cycles in liquid nitrogen and water at 37°C. LUV were obtained by extrusion through 0.1 µm Nuclepore polycarbonate membranes (Sterico, Wangen, Switzerland) by means of the Lipex extruder (Vancouver, Canada). Lipid concentration was determined by an enzymatic colorimetric test for phospholipids (MPR 2) obtained from Roche Diagnostics (Mannheim, Germany), and adjusted to 50 µM. DPH was added from a 1 mM stock solution in tetrahydrofuran to LUV composed of 50 µM DPPC to give a final concentration of 100 nM (probe/lipid molar ratio 1:500). Liposomes were used between 30 min and 8 h after addition of DPH. Prior to the measurement 300 µM peptide from a 1 mM stock solution was added and allowed to equilibrate for 15 min. Fluorescence polarization was measured on a Varian Cary Eclipse spectrofluorometer (Mulgrave, Australia). All measurements were made in 10 mm wide 40 µL micro-cuvettes using a multicell Peltier device connected to a temperature controller. Measurements started at 55 °C, and temperature was gradually lowered to 15 °C. After a desired temperature was reached, the sample was allowed to equilibrate for 5 minutes. Fluorescence was excited at 340 nm and the emission was determined at 452 nm; for each sample five measurements were performed and averaged. A polarization attachment (Varian, Mulgrave, Australia) was adapted to the Varian

Cary Eclipse spectrofluorometer. Steady-state fluorescence polarization  $P$  was determined according to the following equation (38):

$$P = \frac{I_{VV} - G I_{VH}}{I_{VV} + G I_{VH}} \quad (1)$$

where  $I_{VV}$  is the emission intensity of vertically polarized light parallel to the plane of excitation, and  $I_{VH}$  is the emission intensity of horizontally polarized light perpendicular to the plane of excitation. The instrumental factor  $G$  ( $G = I_{HV}/I_{HH}$ ) was determined by measuring the polarized components of the probe's fluorescence at horizontally polarized excitation.

### *Dynamic light scattering (DLS)*

Size and polydispersity of a 50  $\mu\text{M}$  LUV dispersion alone or after addition of 300  $\mu\text{M}$  peptide were monitored at 25 °C and 50 °C over a period of 30 minutes by dynamic light scattering (DLS) at a scattering angle of 90° on a Malvern ZetaSizer 3000HS (Malvern Instruments Ltd, Malvern, UK) which was equipped with a He–Ne ion laser (633 nm). Hydrodynamic diameters ( $d_H$ , nm) were calculated from the diffusion coefficient  $D$  using the Stokes-Einstein equation:

$$d_H = \frac{k T}{3\pi \eta D} \quad (2)$$

where  $k$  is the Boltzmann constant,  $T$  the absolute temperature (K), and  $\eta$  the viscosity ( $\text{mPa}\cdot\text{s}^{-1}$ ) of the solvent. The correlation function was analysed by the CONTIN method and the intensity distribution was chosen for evaluation of the data.

*Circular dichroism (CD) measurements*

Circular dichroism was measured on a Jasco J720 spectropolarimeter (Jasco, Tokyo, Japan) at 25°C using a 0.2 mm quartz cell. All spectra were recorded between 190 and 250 nm and corrected for background contributions. The peptide concentration was 20  $\mu\text{M}$  in a 5 mM PBS buffer, pH 7.4. For micelle formation DPC in a concentration of 2.5 mM was used. The results were expressed as mean residue ellipticities,  $[\theta]_{\text{MR}}$  (deg cm<sup>2</sup>/dmol).

## RESULTS

*AFM imaging*

**Effects of pVEC and W2pVEC on DOPC/DPPC bilayers.** Fusion of unilamellar vesicles on freshly cleaved mica resulted in phase separated SPB. After careful and extensive rinsing with sterile filtrated HEPES buffer, clean bilayers were obtained (Fig. 2A). Occurrence of unfused liposomes was sporadic. The round-shaped DPPC domains with diameters ranging from 0.3 to 3  $\mu\text{m}$  protruded by approximately 0.8 to 1.0 nm out of the DOPC fluid phase. When we replaced the HEPES buffer covering the bilayer with an aqueous 10  $\mu\text{M}$ , pH 7.4 W2-pVEC solution in HEPES buffer an efficient transformation process of the DPPC gel phase was observed (Fig. 1). The first scans of good quality could be recorded already 9 minutes after addition of W2-pVEC. Due to technical reasons, namely thermal drift after the replacement of the buffer, earlier observations are impossible or suffer from low resolution. We observed a time-dependent transformation of the 2 to 3  $\mu\text{m}$  large gel domains. The process set on at the edges of the domains, which were increasingly pervaded by branched channels (Fig. 1A) leading to structures of fractal appearance (Fig 1A and 1B). Especially between 12 and 26 minutes (Fig. 1B – 1F) three levels differing in height by about 0.5 nm became visible. The lowest, and therefore

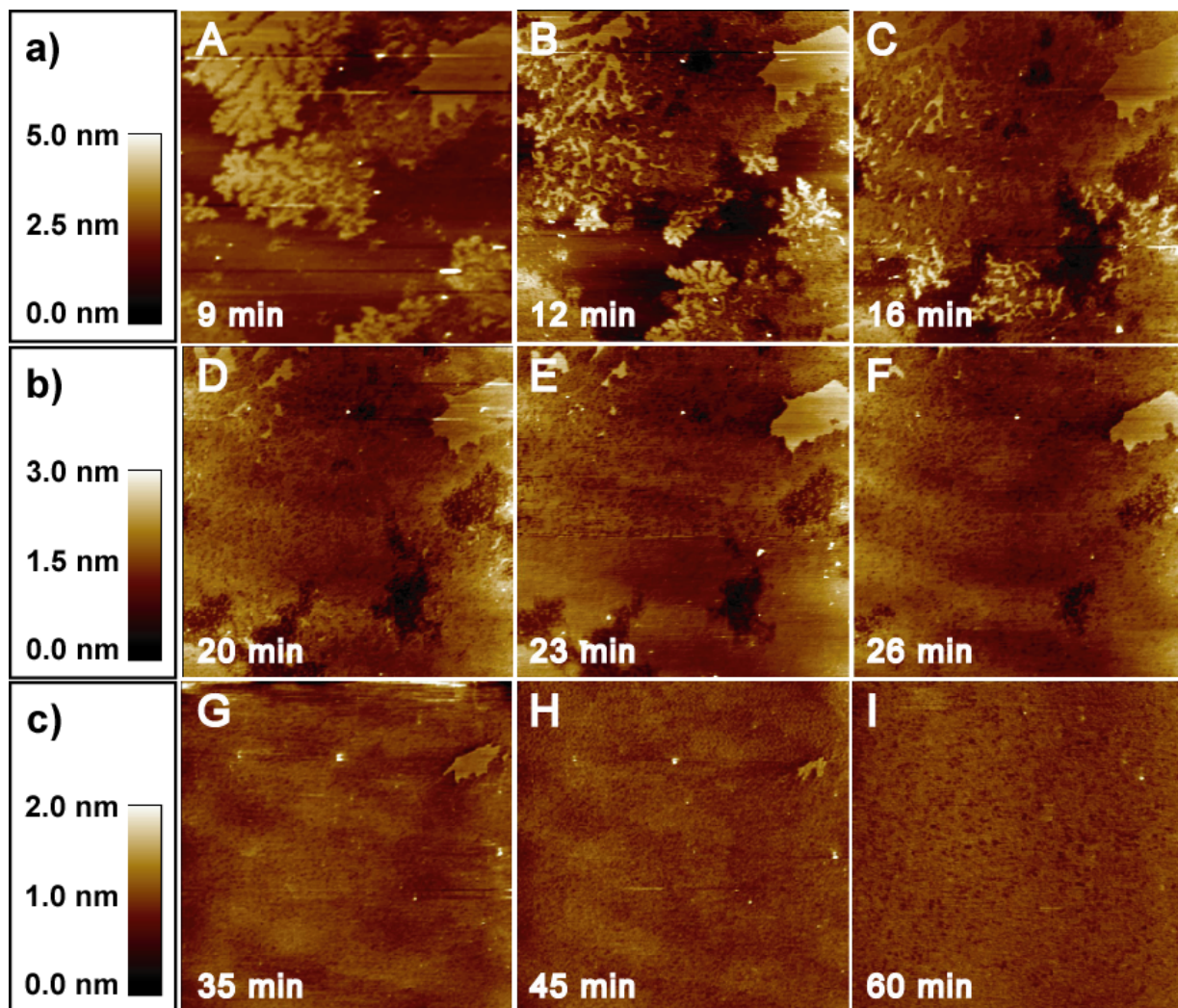
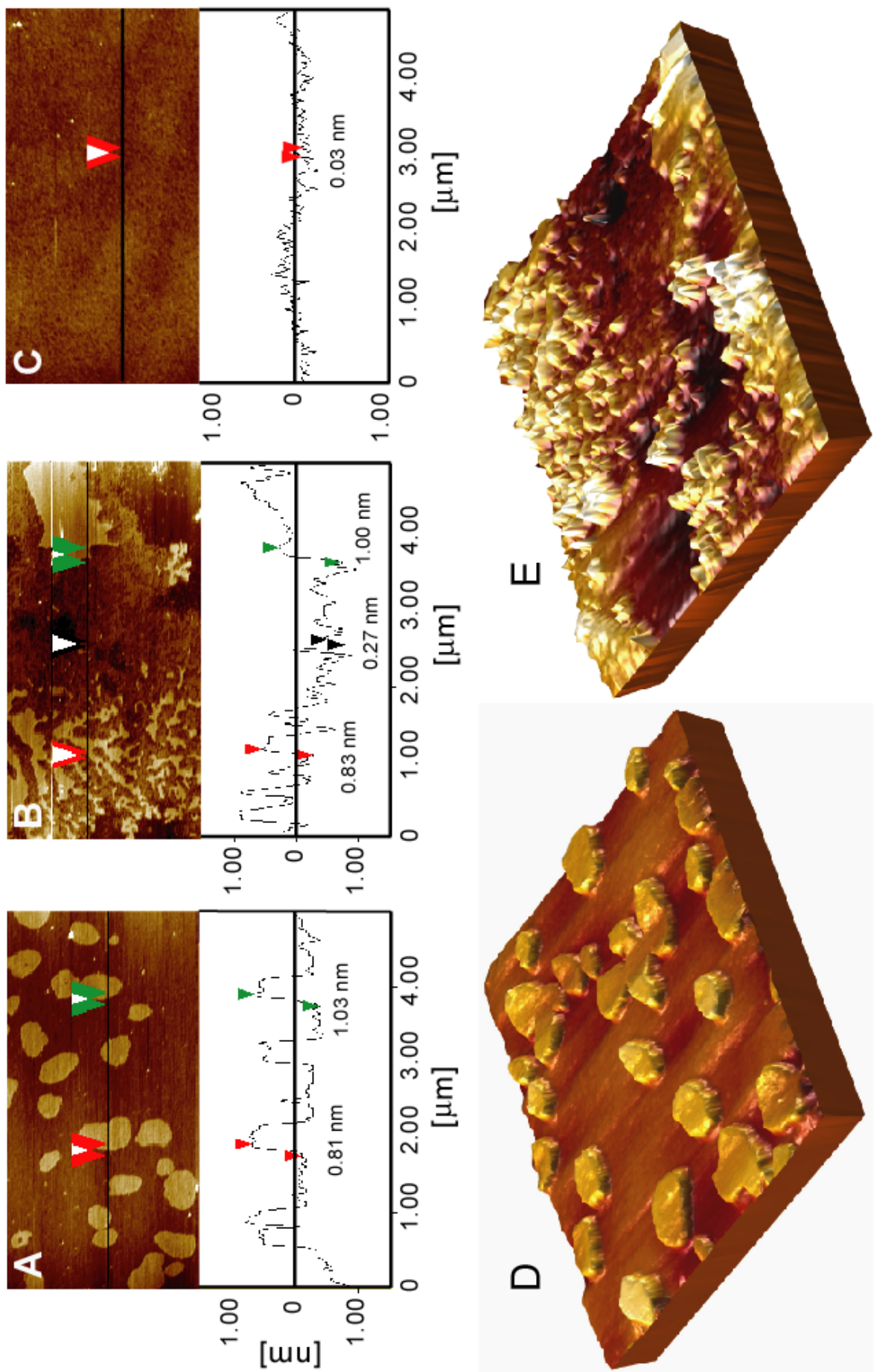


*Fig. 1. (above) AFM scans of the time dependent transformation of DPPC gel phase domains upon addition of W2-pVEC. A 10  $\mu\text{M}$  solution of W2-pVEC in HEPES pH 7.4 was added to a phase separated SPB composed of DOPC and DPPC (1:1). The defined part was observed for 60 min. The scale for the A - H scans is 5  $\mu\text{m} \times 5 \mu\text{m}$ , scan I is shown in higher magnification (2  $\mu\text{m} \times 2 \mu\text{m}$ ). The height scale a) applies to scan A, the scale b) to scans B to F, and scale c) to scans G to I.*

*Fig. 2. (right) AFM scans, section analysis and 3D representation of phase separated SPB composed of DOPC/DPPC (1:1). A blank bilayer and its height profile obtained by a section along the indicated line (A) and bilayers 12 min (B) and 60 min (C) after addition of a 10  $\mu\text{M}$  solution of W2-pVEC. The heights of the structures were estimated from AFM scans using the section analysis software provided by Digital Instruments. (D) 3D representation of Fig. 2A and (E) of Fig. 2B.*



darkest level was understood to correspond to lipid domains in the liquid crystalline state (DOPC), whereas the uppermost and brightest level represented the domains of gel phase lipid (DPPC), which was largely unaffected by peptide induced transformation. The intermediate level consisted of those parts of the bilayer, where transformation was in process. Upon addition of W2-pVEC, only a small part of an initially large DPPC gel phase domain with a sharp borderline to the liquid crystalline phase was left after 35 – 45 min (Fig. 1G and H). After 60 min the initially phase-separated bilayer was completely flattened (Fig. 1I; compare to Fig. 1A-H).

To analyze the peptide induced transformation process further and exclude the peptide to cause erosional damage of the bilayer we performed a section analysis. Fig. 2A shows a typical blank bilayer with DPPC gel phase domains protruding by 0.8 nm to 1.1 nm from the surface of the DOPC fluid phase. 12 minutes after the addition of W2-pVEC those parts of the DPPC gel phase that were not yet transformed still protruded by the typical value of 0.8 to 1.1 nm from the surface, whereas in the region where the turnover took place predominantly differences of about 0.3 nm in height were found (Fig. 2B). 60 minutes after addition of W2-pVEC (Fig 2C) the bilayer was almost completely flat with some minor unevenness below 0.1 nm height. The typical height of phase-separated SPB (including a thin layer of water between the mica surface and the lower leaflet of the bilayer) was previously found to be  $5.6 \pm 0.3$  nm to  $6.0 \pm 0.2$  nm in height (20, 39, 40), therefore approximately 6 nm deep defects would be observable in case of bilayer damage by erosion. In fact, we found no such defects in any of the scans. Fig. 2 represents three-dimensional representations of a blank DPPC/DOPC phase-separated SPB (Fig. 2D) and of a phase-separated SPB of the same composition but 12 minutes after addition of 10  $\mu\text{M}$  W2-pVEC (Fig. 2E).

When a 5  $\mu\text{M}$  instead of 10  $\mu\text{M}$  W2-pVEC solution was added to the phase-separated SPBs the same phenomena could be observed but the turnover process occurred markedly slower (data not shown).

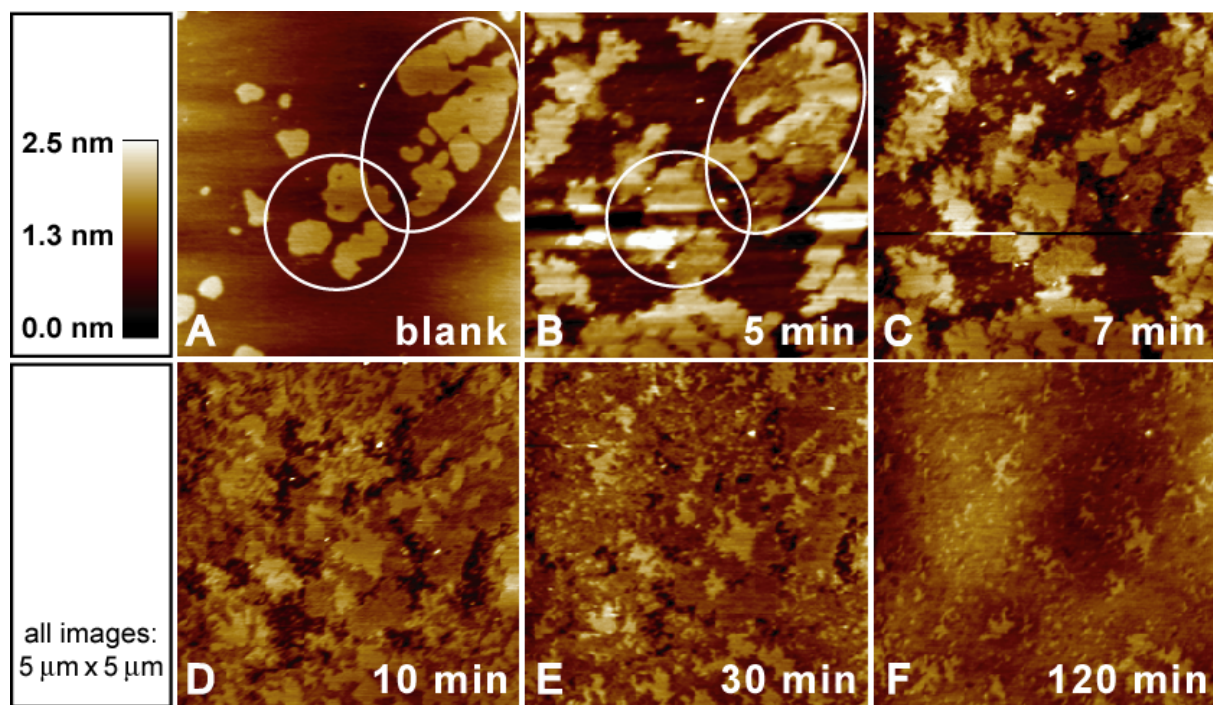


**Fig. 3. AFM scans of the time dependent transformation of DPPC gel phase domains upon addition of pVEC.** A 10  $\mu\text{M}$  solution of pVEC in HEPES pH 7.4 was added to a phase separated SPB composed of DOPC and DPPC (1:1). The defined part was observed for 120 min. The scale for all scans is 5  $\mu\text{m} \times 5 \mu\text{m}$ . The height scale given in the insert applies to all scans.

Fig. 3 shows the effects of a 10  $\mu\text{M}$  pVEC solution on a DPPC/DOPC SPB. After addition of the peptide, the previously distinct DPPC domains of the blank bilayer (Fig. 3A) expanded and spread into the fluid DOPC phase (Fig 3B). At the borders between gel and fluid phase again structures of fractal appearance could be observed (Fig. 3C – 3E), although this phenomenon was less pronounced as compared to W2-pVEC solutions. Again, in particular between 7 and 30 minutes (Fig. 3C – 3E), three distinct levels were visible. After 120 minutes (Fig. 3F) a flat bilayer with regularly distributed, small domains remained. The section analysis of the bilayer revealed that, as compared to the blank bilayer (Fig. 4A), the differences in height of the domains increased shortly after addition of pVEC (Fig. 4B and 4C). After 45 minutes (Fig. 4D), the differences flattened out, and after 120 minutes (Fig. 4E), a more regular surface structure with only small differences in height was observed to

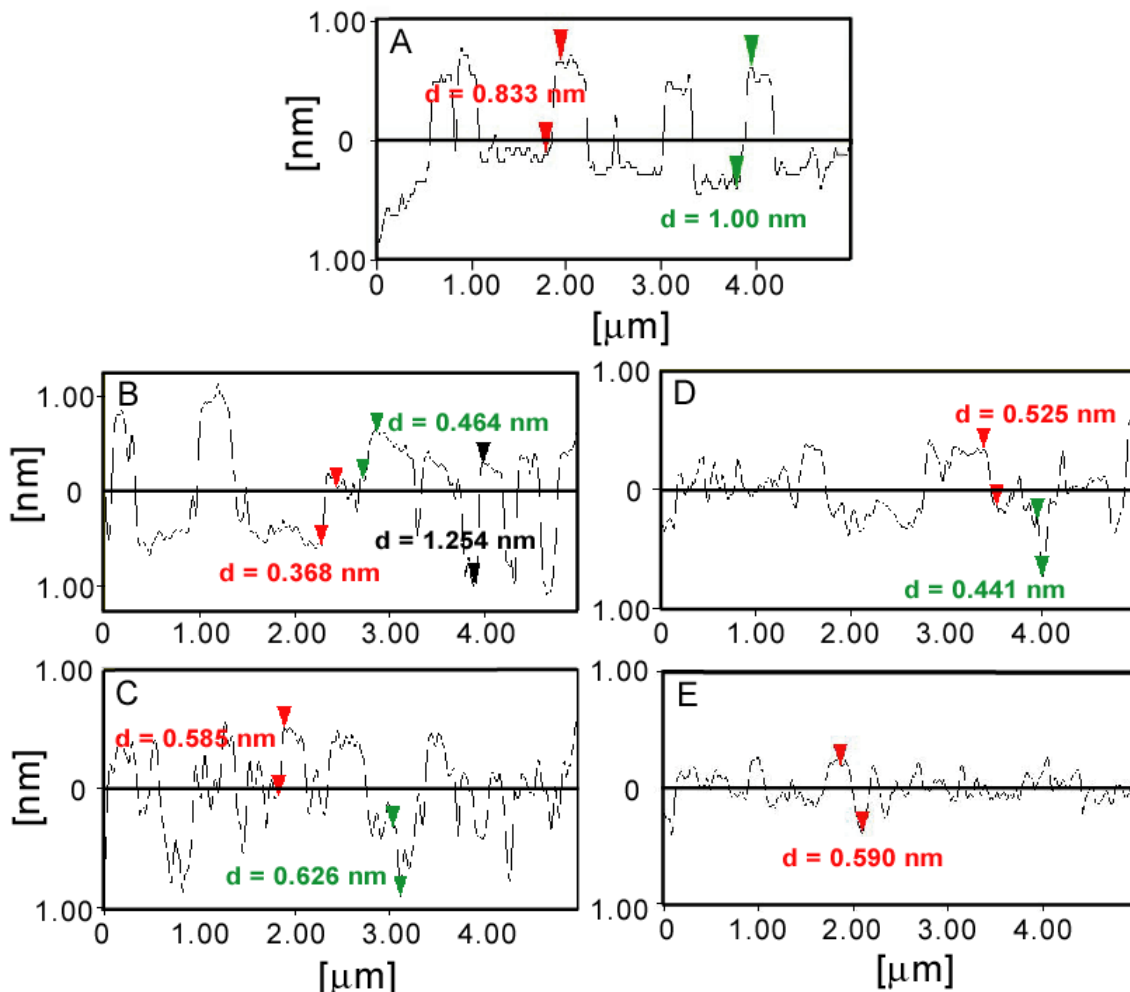


**Fig. 4. AFM section analysis of phase separated SPB composed of DOPC/DPPC (1:1) upon pVEC treatment.** Height profiles obtained by cross sections of a blank bilayer (A), 5 min (B), 10 min (C), 45 min (D), and 120 min (E) after addition of a 10  $\mu\text{M}$  pVEC solution. The heights of the structures were estimated from AFM scans using the section analysis software provided by Digital Instruments.

develop. Generally, the effects induced by pVEC were similar to those of W2-pVEC but the process was slower and somewhat less efficient. Similar to W2-pVEC, lowering the concentration of the pVEC solution to 5  $\mu\text{M}$  resulted in a slower transformation of the bilayer (data not shown).

**Effects of pVEC and W2pVEC on DOPC/SM bilayers.** To investigate whether the peptide-induced transformation processes were specific for glycerophospholipids, we also studied phase-separated SPB where DPPC was

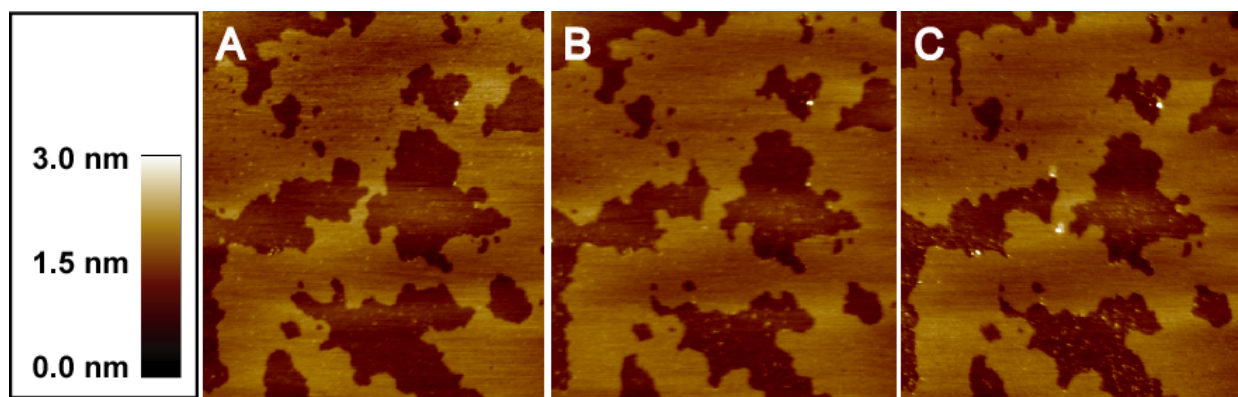


*Fig. 5. AFM scans of a POPC/SM bilayer before (A), 15 min (B), or 90 min after addition of 10  $\mu\text{M}$  solution of pVEC. The scale for all scans is 5  $\mu\text{m} \times 5 \mu\text{m}$ . The height scale given in the insert applies to all scans.*

replaced by egg SM, having a similar phase transition temperature ( $T_m$ ) as DPPC. Egg SM consists of fully saturated fatty acids only, namely 84 % palmitic acid and small amounts of longer chain saturated fatty acids (41). For palmitoyl SM a  $T_m$  of 37.5 °C has been determined (42), and for the complete egg SM a  $T_m$  of 38 °C (43). As compared to DPPC gel phase domains, SM domains were generally somewhat less regular and showed mostly diameters above 1  $\mu\text{m}$  (Fig. 5A). As shown in Fig. 5B and C, neither 15 minutes nor 90 minutes after addition of 10  $\mu\text{M}$  W2-pVEC significant changes in the domain structure could be observed. After 90 minutes we observed sporadic small dots on the SPB surface, which may represent aggregated peptide (Fig. 5C). Also 10  $\mu\text{M}$  pVEC exhibited no significant effects on DOPC/SM SPBs over a period of 120 min (data not shown).

#### *Peptide effects on bilayer integrity. Calcein leakage experiments*

Previous *in vitro* studies showed that pVEC concentrations up to 20  $\mu\text{M}$  did not (Bowes cells) or only very slightly (bEnd and AEC cells) increase membrane permeability (9). Furthermore, it has been demonstrated that pVEC permeabilize microbial cells at concentrations that can not cause damage to

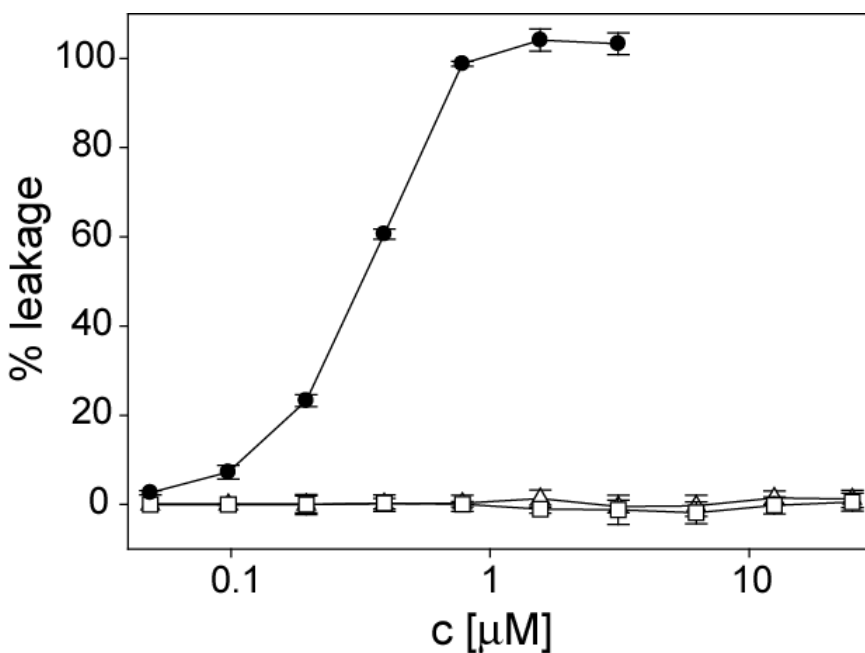


**Fig. 6. Percent leakage of LUV entrapped fluorescent Calcein as a function of peptide concentration.** Peptide solutions up to a final concentration of 25  $\mu\text{M}$  were added to a 400  $\mu\text{M}$  POPC LUV solution in PBS buffer, pH 7.4. From the increase in Calcein fluorescence the peptide induced leakage in percent was calculated for melittin (●), pVEC ( $\triangle$ ), and W2-pVEC ( $\square$ ). Data were recorded after 120 min incubation at ambient temperature (approx. 22°C) and are represented as mean  $\pm$  SD ( $n = 3$ ).

mammalian cells (29). In order to test whether pVEC could permeabilize pure phospholipid membranes, and whether the modification in W2-pVEC may affect lipid membrane integrity, we performed a dye leakage assay with Calcein loaded POPC LUV. In Fig. 6 we compare membrane permeabilizing effects of increasing concentrations of pVEC, W2-pVEC, and melittin as control in a 200  $\mu\text{M}$  solution of neutral POPC LUV at pH 7.4. Melittin, a basic, amphipathic 26-amino acid peptide, which has the propensity to form pores in lipid bilayers (44), led to a complete leakage at a concentration as low as 1  $\mu\text{M}$ . Up to peptide concentrations of 25  $\mu\text{M}$  neither pVEC, nor W2-pVEC caused any significant leakage. These concentrations were largely above those used in the AFM experiments, which were 5  $\mu\text{M}$  and 10  $\mu\text{M}$ .

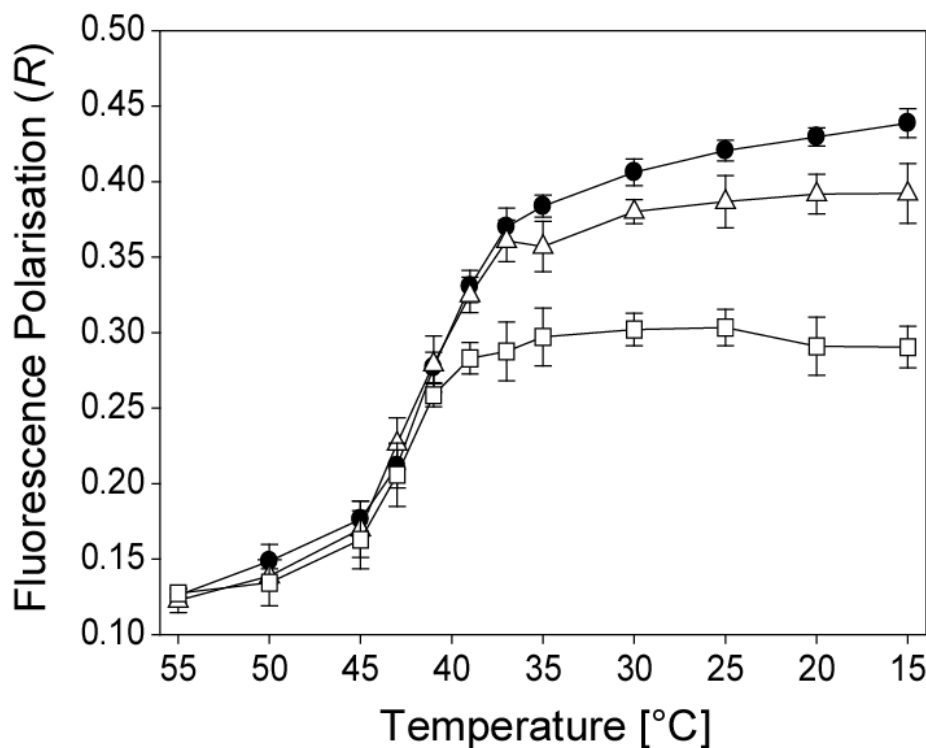


**Fig. 7. Fluorescence polarisation of 100 nM DPH incorporated in 50  $\mu$ M DPPC LUVs as a function of the temperature.** A blank dispersion of DPPC LUVs (●) was compared with LUVs containing 300  $\mu$ M solutions of the peptides pVEC (△) and W2-pVEC (□). Results are represented as means  $\pm$  SD ( $n = 3$ )

### Fluorescence polarization

To scrutinize whether the effects of the investigated peptides on the DPPC gel phase domains can in fact be explained by a shift in the phase transition temperature ( $T_m$ ) and/or the viscosity of the gel phase, we performed a fluorescence polarization study. For this purpose the polarization of the membrane-bound fluorophore DPH was used to monitor the internal microviscosity of DPPC bilayers as a function of the temperature. DPH is non-fluorescent in aqueous dispersion but partitions readily into the hydrophobic core of lipid membranes owing to its high lipid–water partition coefficient  $K_p$  of  $1.3 \times 10^6$ , associated with a strong increase in fluorescence intensity (45). A

temperature scan of blank DPPC LUV showed an increase in fluorescence polarization from 0.13 at 55 °C to 0.44 at 15 °C with a phase transition temperature of about 40 °C (Fig. 7). This is in good agreement with a previous differential scanning calorimetry study of DPPC that found a phase transition temperature at 41 °C (46). In the presence of 300 μM pVEC the profile of the curve was identical with that of blank LUV up to the region where phase transition occurs, whereas the microviscosity of the gel phase was reduced, as shown by the maximum polarization degree of 0.39 as compared to 0.44 at 15 °C. W2-pVEC caused an even stronger reduction in gel phase microviscosity with a maximum polarization of only 0.29. Again, at higher temperatures, where DPPC is in the liquid crystalline state, no differences were observed. When the peptide concentration was reduced to one half, the effect of W2-pVEC was also cut down to one half; pVEC had no significant effect. Generally, the peptides caused no significant changes in phase transition temperature but led to a pronounced decrease in gel phase viscosity at higher concentrations.

### *Dynamic light scattering (DLS)*

Although no indications for peptide-induced damage on the bilayers could be found by AFM analysis, we performed a DLS analysis to investigate whether the integrity of LUV could be compromised at high concentrations of the investigated peptides. At 25 °C (Fig. 8A) the diameters of blank LUV increased minimally over time from 99.4 nm ± 1.2 to 100.6 nm ± 0.8 at 30 min. With mean diameters of 120 nm immediately after addition of the peptides, LUV increased in size to 131 nm for pVEC and 179 nm for W2-pVEC. To decide, whether the increase in mean diameter was due to (i) insertion and/or association of the peptide into or onto the LUV bilayers, or (ii) owed to a peptide induced turnover and damage of the vesicles, we also monitored the polydispersity index of the size distribution. In case of insertion or association, an increase in the LUV mean diameter would be expected, whereas polydispersity should be

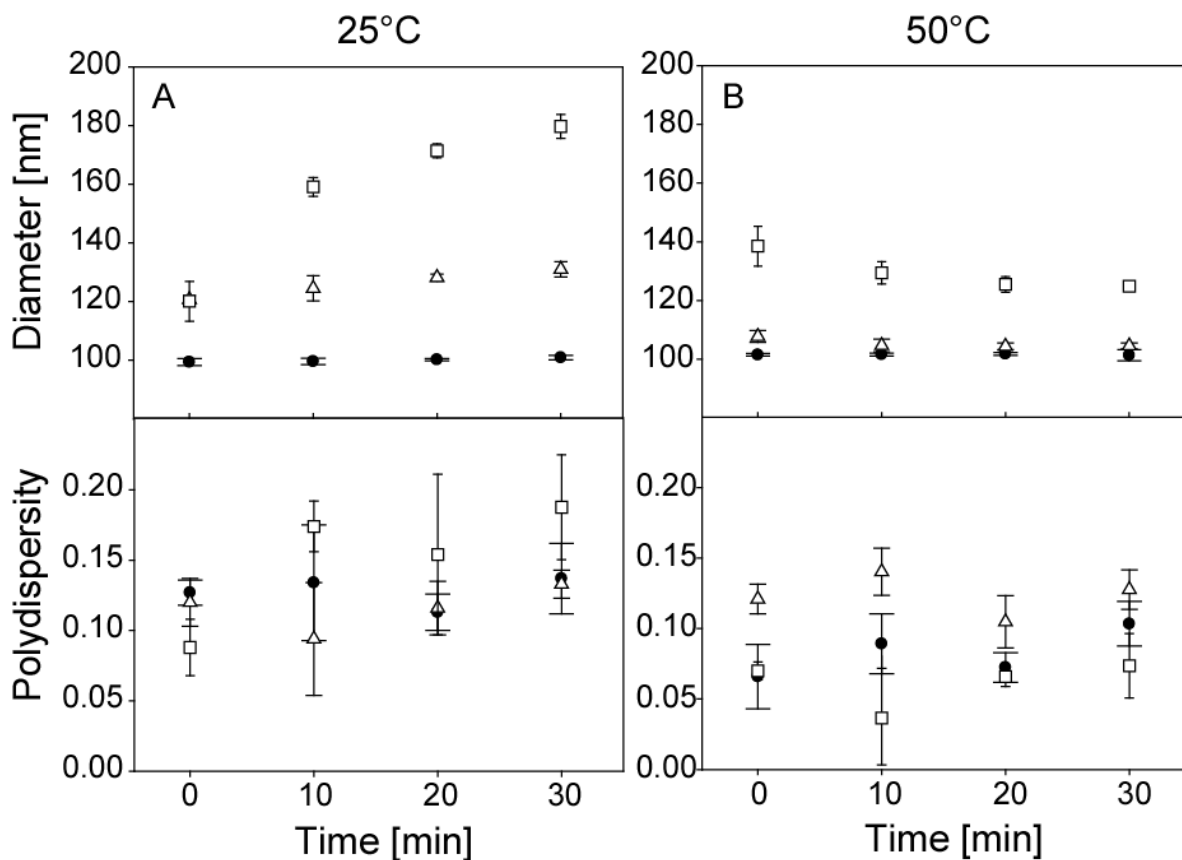


*Fig. 8. Diameters and polydispersity indices of size distributions of 50  $\mu$ M DPPC LUVs without and with peptide monitored over 30 minutes. A blank dispersion of DPPC LUVs (●) was compared with LUVs containing 300  $\mu$ M solutions of the peptides pVEC ( $\triangle$ ) and W2-pVEC ( $\square$ ). Experiments were performed in triplicate. SD error bars of DPPC blanks are shown with long, of pVEC with medium, and of W2-pVEC with short caps.*

largely unchanged. In the case of compromised LUV integrity a formation of larger and/or smaller liposomes and, hence, a broader distribution and higher polydispersity could be envisaged. Also aggregation could lead to increased polydispersity. As shown in the lower panel of Fig. 8A, there is only a slight tendency towards higher polydispersity after addition of W2-pVEC, but none of the peptides caused significant changes ( $p > 0.1$  throughout).

As shown in Fig 8B, LUV had diameters of  $107.8 \pm 2.1$  nm immediately after addition of pVEC which then stabilized at about 104 nm. For W2-pVEC LUV, diameters were highest immediately after addition ( $138.5 \pm 6.8$  nm) and then dropped to  $124.9 \pm 1.3$  nm. Polydispersity indices ranged from 0.037 to

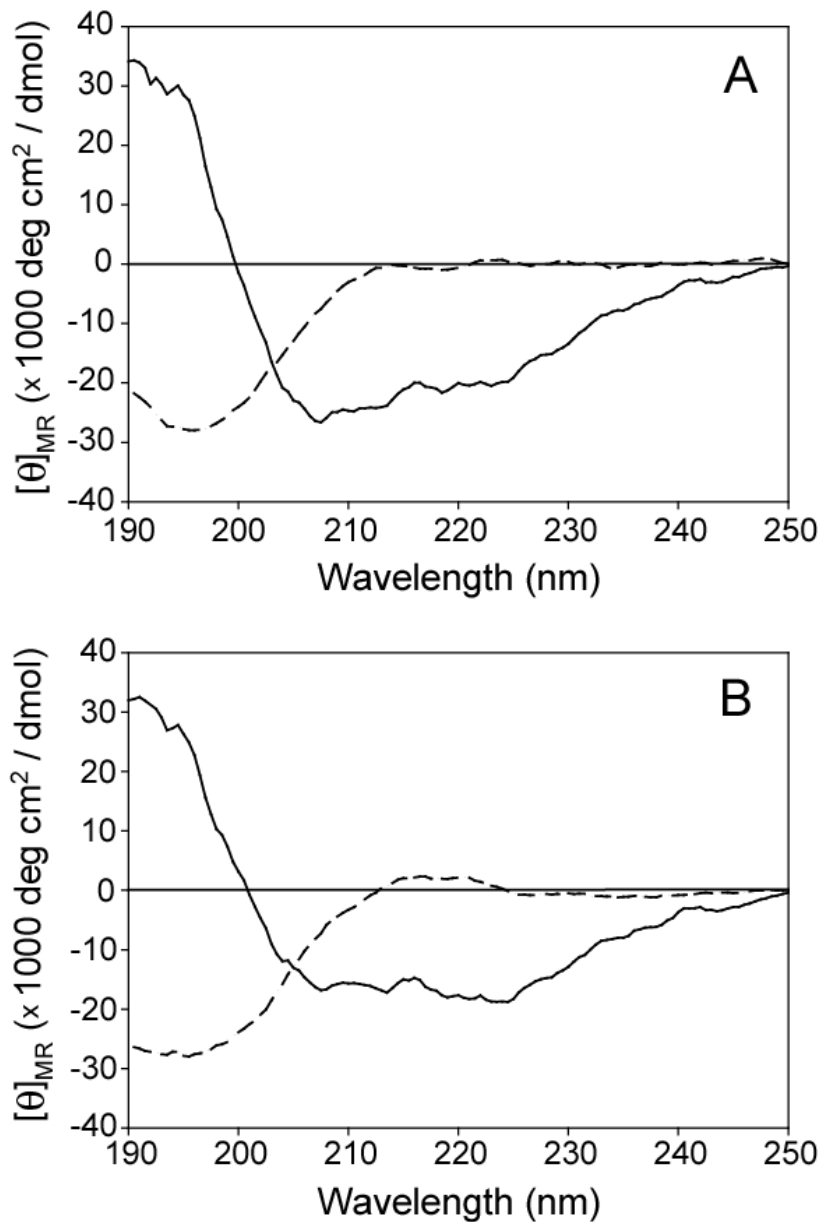


*Fig. 9. CD spectra of 20  $\mu\text{M}$  solutions of pVEC and W2-pVEC in different media. pVEC (A) and W2-pVEC (B) in buffer (dashed line) and in presence of DPC micelles (2.5 mM, peptide/lipid ratio = 0.008) (solid line). The spectra were recorded at 25°C and the buffer was 5 mM PBS pH 7.4 in all cases.*

0.140. At  $t = 0$  there was a significant difference in polydispersity between untreated and pVEC treated LUV ( $p < 0.02$ ), which disappeared over time. LUV treated with W2-pVEC were never significantly different from the untreated ones ( $p > 0.1$  in all cases). This provides evidence for association or integration in the bilayer rather than for any form of turnover or damage to the membrane.

*Circular dichroism (CD) measurements*

In aqueous buffer solution (PBS, 5 mM, pH 7.4) pVEC as well as W2-pVEC show CD spectra with a single minimum at about 198 nm, characteristic for a non-ordered structure (dashed lines in Fig. 9). However, in the presence of an excess of DPC micelles, a marked induction of secondary structure was observed for both peptides (solid lines in Fig. 9). The spectra with maxima at 190 – 195 nm and minima at 205 nm associated with a shoulder around 220 nm indicate a tendency to adopt, at least in part, an  $\alpha$ -helical conformation (47). For pVEC (Fig. 9A) the evidence for  $\alpha$ -helicity was slightly better than for W2-pVEC (Fig. 9B).

## DISCUSSION

In this study we show for the first time that CPP, namely pVEC and W2-pVEC, are capable of transforming DPPC gel phase domains of phase separated SPB into a less ordered and more fluid state. Importantly, the peptides did not affect the bilayer integrity, neither of SPBs nor of unilamellar liposomes. Right after the peptides were added to the supported bilayers, the transformation process set in, starting at the edges of the DPPC gel phase domains. From here, kind of an erosion process began, with branched channels of already transformed lipids penetrating into the centre of the gel phase domains. The larger the DPPC domains, the more time was required for their complete transformation. Speculatively, this suggests an initial, spontaneous interaction of the peptides with the DOPC liquid phase from where the two CPP may enter the DPPC gel phase domains. In fact, in a previous study we observed a high affinity of pVEC and W2-pVEC towards fluid phase POPC LUV (logD about 3) (33). Similarly, other  $\alpha$ -helical peptides (48, 49) and a membrane-inserted hydrophobic polypeptide (50) have been found to be located preferably in the

liquid phase. Like several other CPP (51-53), pVEC and W2-pVEC are unstructured in buffer and become  $\alpha$ -helical in a lipidic environment.

Derived from such observations we propose the following model for the molecular reorganization induced by the investigated peptides (Fig. 10): Before addition of peptide, the DPPC gel phase appears to protrude - due to its extended acyl chains – by about 1.0 nm from the DOPC fluid phase (A). Over time, with increasing penetration of peptide into the DPPC phase, the lipids of the gel phase transform into a less ordered state of higher fluidity. Often, an intermediate phase, approximately 0.5 nm above the DOPC phase, but about 0.5 nm below the original DPPC domains (B) appears to occur. This may be caused by the fact, that at first the upper lipid leaflet only is affected by the peptides, before the entire bilayer can be transformed; in this final state the former DPPC domains are indiscernible from the DOPC phase (C). This hypothesis is strongly supported by (i) the fact that DPPC bilayers in the fluid state were 3.7 nm in height (54) and, therefore, exactly 1 nm less than in the gel state (4.7 nm) (55), (ii) the peptides' capability to increase the fluidity of DPPC bilayers, as demonstrated by fluorescence polarisation, and (iii) the fact the peptides induce neither visible damage on SPBs nor Calcein leakage of LUV.

In general, pVEC and its modification W2-pVEC showed very similar effects. However, the transformation induced by W2-pVEC was faster and more efficient: At a concentration of 10  $\mu$ M the bilayer was completely transformed within 60 min, whereas transformation caused by 10  $\mu$ M pVEC was indeed extensive, but could not lead to an entirely completed transformation after two hours. This is consistent with the higher potential of W2-pVEC to increase the fluidity of DPPC bilayers above the phase transition temperature, which was determined by fluorescence polarisation. The observed increase in affinity towards phospholipid bilayers corresponds well with experimentally determined free energies of transferring whole amino acids from bulk solution into the membrane-water interface or into the hydrophobic interior, which are -0.31 and -1.85 kcal/mol for the transfer into the interface ( $\Delta G_{wif}$ ) and -1.12 and -2.09

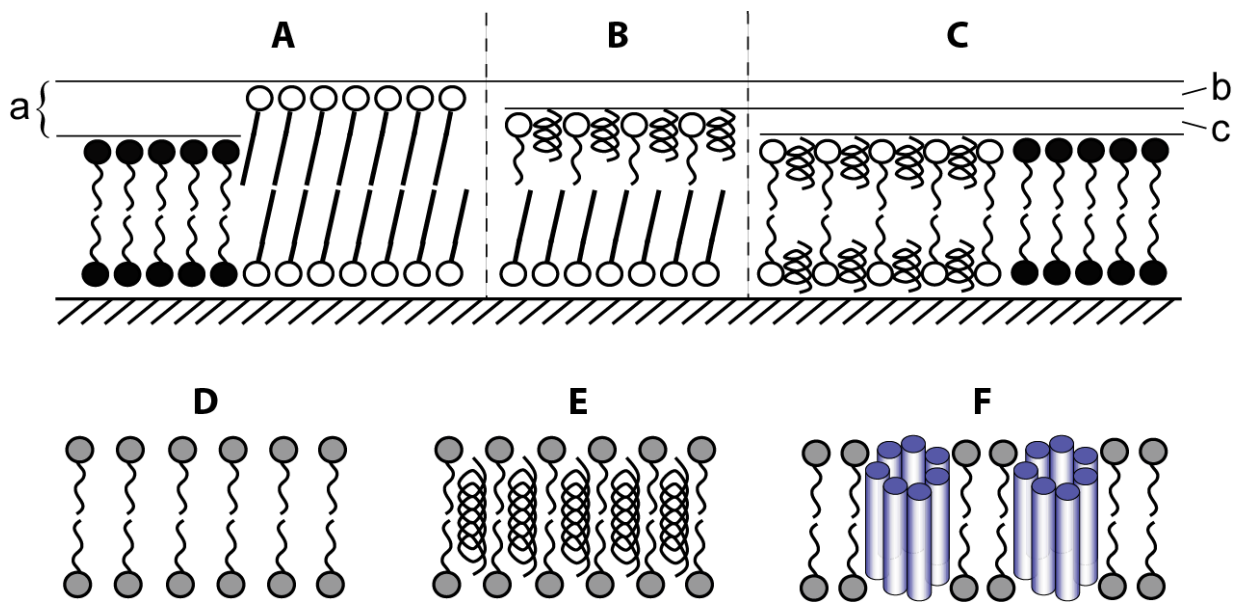


**Fig. 10. Proposed model for the molecular organization of DOPC/DPPC bilayer with and without pVEC/W2-pVEC incorporated.** Blank DOPC/DPPC SPB (A) are characterised by DPPC lipids (open head groups) with tilted, extended acyl chains, whereas acyl chains of DOPC lipids (filled head groups) are less ordered. This results in a height difference of about 1 nm (a). After addition of the peptides, in an intermediate state, first the upper lipid leaflet is transformed to a less ordered state by interaction with the peptides (B). In this state the bilayer is about 0.5 nm lower (b) than the unaffected DPPC and 0.5 nm higher (c) than DOPC. Finally, the whole DPPC bilayer is transformed to a less ordered and more fluid state (C) of the same height as DOPC. In contrast, when inserting in a bilayer in the fluid state (D), membrane-spanning peptides and proteins lead to a restriction of acyl chain mobility and therefore an increase in fluorescence polarisation. This insertion may occur in the form of single molecules (E) or oligomeric pores (F) formed by barrel-stave type peptide association.

kcal/mol into the hydrophobic interior ( $\Delta G_{\text{oct}}$ ), for Ile (unmodified pVEC) and Trp (W2-pVEC) residues, respectively (56).

The effects on the microviscosity of phospholipid bilayers as induced by pVEC and W2-pVEC were distinctly different from effects observed for cationic amphiphilic drugs or peptides and proteins, which insert into the hydrophobic core of membranes. These  $\alpha$ -helical membrane-spanning proteins like the C-terminal domain of the pro-apoptotic protein Bak (57), the Pf1 coat protein (58) and the C-terminal domain of the antiapoptotic protein Bcl-2 (59) increase the

viscosity and hence the fluorescence polarisation of phospholipid bilayers. The pVEC-derived peptides on the other hand, *decrease* the viscosity of lipid bilayers below the phase transition temperature. This reflects two different modes of interaction with phospholipid bilayers: In a previous study we demonstrated that pVEC and W2-pVEC were preferably localized in the interface of phospholipid bilayers (33). As suggested in Fig. 10 C, interfacial insertion may lead to an increased flexibility of the acyl chains and, therefore, to a decreased microviscosity and fluorescence polarisation. As also illustrated in Fig. 10, membrane-spanning proteins, independently of insertion as single molecules (Fig. 10 E) or as oligomeric pores according to a barrel-stave model (3) (Fig. 10 F), restrict the motion of lipid molecules, decrease their flexibility and hence increase the viscosity as compared to a blank bilayer (Fig. 10 D). Several of these membrane-spanning peptides have also shown to destabilize unilamellar vesicles inducing leakage of an encapsulated dye (57, 59), whereas neither pVEC nor W2-pVEC induced any kind of membrane damage, indicating a mild form of membrane perturbation. Whether this may result in lower toxicity when used in living systems has yet to be demonstrated.

Several amphiphilic cationic drugs have been shown to be able to lower the phase transition temperature of DPPA (60) and DPPC (61) lipids. Although in that case the mode of interaction was different from pVEC and W2-pVEC, where not the phase transition temperature, but the viscosity of the gel phase was decreased, a similar effect on phase separated supported bilayers was observed for the antibiotic azithromycin. Berquand et al. (62) showed that 1 mM of the amphiphilic and cationic azithromycin induces progressive erosion of DPPC domains of DOPC/DPPC SPB resulting in a flat bilayer after 60 minutes. Unlike pVEC, no intermediate fractal-like structures were observed. Instead, the borders of the domains remained smooth during the entire transformation process. Another major difference was that a 100 times higher concentration than in our study was required to induce DPPC transformation. Interestingly, similar to our observation that SM domains were unaffected by the peptides, Berquand et al. found that, in contrast to DPPC domains, azithromycin could not

significantly transform SM domains. Although this difference may surprise at first sight, since both lipids have the same polar head group, there are specific features in the molecular structure of SM which may account for its particular stability against physical transformation: The amide and hydroxyl groups in the interface of SM can act as both hydrogen bond donors and acceptors, whereas the amide carbonyl provides an additional hydrogen acceptor. These interfacial particularity gives SM the unique ability to form both strong intra- and intermolecular hydrogen bonds (63). In contrast, phosphatidyl cholines with two ester carbonyls in this region have only hydrogen bond accepting features. The stronger interactions in the interface of SM result in closer lipid packing, better chain stacking, membrane stabilization and lower membrane permeability (64). Therefore, we conclude that the resistance of SM domains against transformation by the peptides as demonstrated in our studies reflects tighter lipid packing owing to stronger intermolecular interactions between SM lipids as compared to DPPC lipids.

Relative to our work we would now like to briefly discuss both similarities and distinct differences in two other phenomena of reorganisation of phospholipid bilayers: namely the formation of highly ordered, striated domains in SPB induced by transmembrane peptides and the induction of interdigitated domains in gel phase bilayers, which can be caused by different solvents, chemicals, and also by physical pressure or heat.

The formation of striated domains in gel phase lipids of SPB was first reported by Rinia et al. (24); they were induced by hydrophobic,  $\alpha$ -helical transmembrane peptides – so called WALP peptides – preferably at peptide concentrations between 2 and 10 mol %. These striated domains were characterized by line-type depressions consisting of peptide arrays, which appeared about 0.3 nm below the surface of unaffected bilayer areas. The depressions were flanked by elevated areas 0.1 nm to 0.3 nm higher than the bilayer, which are probably the result of packing constraints caused by the included peptide and lead to less tilt in the lipids' acyl chains. At high peptide concentrations (10 mol %), large parts of the bilayer were covered by striated

domains with a repeat distance of 7.6 nm, forming an extremely ordered, mainly hexagonal pattern characterized by angles of 120°. Although also the WALP peptides caused transformation of DPPC SPB, four characteristic differences to our findings could be identified: (i) the depressions consisted of pure WALP peptides, instead of peptide inserted into the bilayer in our study, (ii) the difference in height was 0.3 nm as compared to 0.8 to 1.0 nm in our study, (iii) also areas higher than a blank bilayer appeared, and (iv) the transformation process led to extremely ordered, hexagonal structures, whereas rather irregular, fractal-like structures were observed in our study. In an ensuing study, Rinia et al. (25) found that replacement of the Trp residues in the flanking area of WALP peptides by other uncharged amino acids caused only minimal differences in the formation of striated domains, whereas replacement by positively charged residues gave rise to completely different morphologies.

The formation of interdigitated domains represents a less specific response of phospholipid bilayers to various surface active molecules (alcohols, anaesthetics, certain proteins), which are able to replace water from the phospholipid head groups without penetrating deep into the bilayer (65, 66). Whereas in a normal bilayer the tails of the lipid chains border on each other in the centre of the bilayer, interdigitated bilayers are characterized by fully intercalated lipid chains. Therefore their thickness was estimated to be 1.6 nm (65) to 1.9 nm (39) less than that of normal DPPC bilayers. Two major discrepancies to our observation led us to exclude interdigitation as a possible mechanism of the peptides investigated in our study: (i) as a consequence of interdigitation, the bilayer is rigidified, and the lateral mobility within the bilayer decreased (65, 67), whereas we demonstrated an increased mobility of the lipids after incubation with the peptides. Furthermore, (ii) interdigitated domains differed by 1.6 nm to 1.9 nm from blank DPPC bilayers, whereas the depressions in our study differed only by 0.8 nm to 1.0 nm.

Any mechanism of translocation resulting in significant permabilization of the membrane would be unacceptable from a pharmaceutical or toxicological point of view. The dye leakage experiments were, therefore, performed to check

whether the peptide caused damage of pure phospholipid bilayers and to assure that the insertion of a Trp in W2-pVEC would not increase the membrane permeabilization potential of the peptides. In fact, no calcein leakage was found for any of the modifications up to a concentration of 50 µM, which is well above the concentrations used in the AFM studies (5 - 10 µM) and the cell culture experiments, i.e. 0.5 µM (11) or 10 µM (9). Accordingly, *in vitro* studies showed that pVEC concentrations up to 20 µM did not (Bowes cells) or only very slightly (bEnd and AEC cells) increase membrane permeability (9). Interestingly, pVEC permeabilized bacterial cells at concentrations as low as 2 µM, which can not cause damage to mammalian cells (29). This may be explained by the abundance of negative charges in bacterial membranes (68) together with the fact that for many cationic antimicrobial peptides an increased affinity for negative lipids has been demonstrated (69-71). The combination of efficient uptake, cellular compatibility in mammalian cells and its antimicrobial activity renders pVEC and modifications thereof of potential interest for the treatment of intracellular infections.

### *Conclusions*

In this study we present time-lapse AFM observations on the effects of two CPP, pVEC and its modification W2-pVEC, on phase separated SPB. Both peptides induce a transformation process in the DPPC domains of the gel phase, which led via an intermediate state with fractal-like structures to entirely or almost entirely flat bilayers. By fluorescence polarisation experiments we revealed the capability of the investigated peptides to increase the fluidity of DPPC domains as the underlying mechanism of this transformation. Owing to the particular molecular structure of their interfacial region, which allows strong hydrogen bonds and hence tighter packing, SM domains could not be affected by the peptides. In contrast to membrane-spanning peptides, which decrease the fluidity of bilayers, and in agreement with a previous study, we propose that the

investigated peptides mainly interact with the bilayer interface and, therefore, lessen the packing density of acyl chains of the lipid. Evidence from AFM observations, dynamic light scattering studies and liposome dye leakage experiments indicated that bilayer integrity was not compromised by the peptides. Our work represents the first observation of a CPP induced transformation process of phase separated phospholipid bilayers and reveals a novel aspect to be considered for the cellular uptake of CPP.

## ACKNOWLEDGEMENTS

The authors thank Fernanda Rossetti and Marc Dusseiller (ETH Zurich) for valuable advices concerning the AFM, Dr. Markus Birringer (ETH Zurich) for introduction into CD, and Carmen Herbig for 3D renderings. This work was supported by the Commission of the European Union (EU project on Quality of Life and Management of Living Resources, Project No. QLK2-CT-2001-01451).

## REFERENCES:

1. Snyder, E.L. and S.F. Dowdy, *Cell penetrating peptides in drug delivery*. Pharm Res, (2004). **21**(3): p. 389-393.
2. Trehin, R. and H.P. Merkle, *Chances and pitfalls of cell penetrating peptides for cellular drug delivery*. Eur J Pharm Biopharm, (2004). **58**(2): p. 209-223.
3. Lundberg, P. and U. Langel, *A brief introduction to cell-penetrating peptides*. J Mol Recognit, (2003). **16**(5): p. 227-233.

4. Morris, M.C., P. Vidal, L. Chaloin, F. Heitz, and G. Divita, *A new peptide vector for efficient delivery of oligonucleotides into mammalian cells.* Nucleic Acids Res, (1997). **25**(14): p. 2730-2736.
5. Simeoni, F., M.C. Morris, F. Heitz, and G. Divita, *Insight into the mechanism of the peptide-based gene delivery system MPG: implications for delivery of siRNA into mammalian cells.* Nucleic Acids Res, (2003). **31**(11): p. 2717-2724.
6. Morris, M.C., J. Depollier, J. Mery, F. Heitz, and G. Divita, *A peptide carrier for the delivery of biologically active proteins into mammalian cells.* Nat Biotechnol, (2001). **19**(12): p. 1173-1176.
7. Lindgren, M., M. Hallbrink, A. Prochiantz, and U. Langel, *Cell-penetrating peptides.* Trends Pharmacol Sci, (2000). **21**(3): p. 99-103.
8. Derossi, D., G. Chassaing, and A. Prochiantz, *Trojan peptides: the penetratin system for intracellular delivery.* Trends Cell Biol, (1998). **8**(2): p. 84-87.
9. Elmquist, A., M. Lindgren, T. Bartfai, and U. Langel, *VE-cadherin-derived cell-penetrating peptide, pVEC, with carrier functions.* Exp Cell Res, (2001). **269**(2): p. 237-244.
10. Elmquist, A. and U. Langel, *In vitro uptake and stability study of pVEC and its All-D analog.* Biol Chem, (2003). **384**(3): p. 387-393.
11. Saalik, P., A. Elmquist, M. Hansen, K. Padari, K. Saar, K. Viht, U. Langel, and M. Pooga, *Protein cargo delivery properties of cell-penetrating peptides. A comparative study.* Bioconjug Chem, (2004). **15**(6): p. 1246-1253.
12. Scheller, A., J. Oehlke, B. Wiesner, M. Dathe, E. Krause, M. Beyermann, M. Melzig, and M. Bienert, *Structural requirements for cellular uptake of alpha-helical amphipathic peptides.* J Pept Sci, (1999). **5**(4): p. 185-194.
13. Oehlke, J., A. Scheller, B. Wiesner, E. Krause, M. Beyermann, E. Klauschenz, M. Melzig, and M. Bienert, *Cellular uptake of an alpha-helical amphipathic model peptide with the potential to deliver polar*

- compounds into the cell interior non-endocytically.* Biochim Biophys Acta, (1998). **1414**(1-2): p. 127-139.
14. Lundberg, M., S. Wikstrom, and M. Johansson, *Cell surface adherence and endocytosis of protein transduction domains.* Mol Ther, (2003). **8**(1): p. 143-150.
  15. Wadia, J.S., R.V. Stan, and S.F. Dowdy, *Transducible TAT-HA fusogenic peptide enhances escape of TAT-fusion proteins after lipid raft macropinocytosis.* Nat Med, (2004). **10**(3): p. 310-315.
  16. Drin, G., S. Cottin, E. Blanc, A.R. Rees, and J. Temsamani, *Studies on the internalisation mechanism of cationic cell-penetrating peptides.* J Biol Chem, (2003). **278**: p. 31192-31201.
  17. Dufrene, Y.F. and G.U. Lee, *Advances in the characterization of supported lipid films with the atomic force microscope.* Biochim Biophys Acta, (2000). **1509**(1-2): p. 14-41.
  18. Engel, A., C.A. Schoenenberger, and D.J. Muller, *High resolution imaging of native biological sample surfaces using scanning probe microscopy.* Curr Opin Struct Biol, (1997). **7**(2): p. 279-284.
  19. Milhiet, P.E., M.C. Giocondi, O. Baghdadi, F. Ronzon, B. Roux, and C. Le Grimellec, *Spontaneous insertion and partitioning of alkaline phosphatase into model lipid rafts.* EMBO Rep, (2002). **3**(5): p. 485-490.
  20. Mou, J., D.M. Czajkowsky, and Z. Shao, *Gramicidin A aggregation in supported gel state phosphatidylcholine bilayers.* Biochemistry, (1996). **35**(10): p. 3222-3226.
  21. You, H.X., X. Qi, G.A. Grabowski, and L. Yu, *Phospholipid membrane interactions of saposin C: in situ atomic force microscopic study.* Biophys J, (2003). **84**(3): p. 2043-2057.
  22. Reviakine, I., W. Bergsma-Schutter, A.N. Morozov, and A. Brisson, *Two-dimensional crystallization of annexin A5 on phospholipid bilayers and monolayers: A solid-solid phase transition between crystal forms.* Langmuir, (2001). **17**(5): p. 1680-1686.

23. Milhiet, P.E., M.C. Giocondi, O. Baghdadi, F. Ronzon, C. Le Grimellec, and B. Roux, *AFM detection of GPI protein insertion into DOPC/DPPC model membranes*. Single Molecules, (2002). **3**(2-3): p. 135-140.
24. Rinia, H.A., R.A. Kik, R.A. Demel, M.M. Snel, J.A. Killian, J.P. van Der Eerden, and B. de Kruijff, *Visualization of highly ordered striated domains induced by transmembrane peptides in supported phosphatidylcholine bilayers*. Biochemistry, (2000). **39**(19): p. 5852-5858.
25. Rinia, H.A., J.W. Boots, D.T. Rijkers, R.A. Kik, M.M. Snel, R.A. Demel, J.A. Killian, J.P. van der Eerden, and B. de Kruijff, *Domain formation in phosphatidylcholine bilayers containing transmembrane peptides: specific effects of flanking residues*. Biochemistry, (2002). **41**(8): p. 2814-2824.
26. Steinem, C., H.J. Galla, and A. Janshoff, *Interaction of melittin with solid supported membranes*. Physical Chemistry Chemical Physics, (2000). **2**(20): p. 4580-4585.
27. Boichot, S., U. Krauss, T. Plenat, R. Rennert, P.E. Milhiet, A. Beck-Sickinger, and C. Le Grimellec, *Calcitonin-derived carrier peptide plays a major role in the membrane localization of a peptide-cargo complex*. FEBS Lett, (2004). **569**(1-3): p. 346-350.
28. Schmidt, M.C., B. Rothen-Rutishauser, B. Rist, A. Beck-Sickinger, H. Wunderli-Allenspach, W. Rubas, W. Sadee, and H.P. Merkle, *Translocation of human calcitonin in respiratory nasal epithelium is associated with self-assembly in lipid membrane*. Biochemistry, (1998). **37**(47): p. 16582-16590.
29. Nekhotiaeva, N., A. Elmquist, G.K. Rajarao, M. Hallbrink, U. Langel, and L. Good, *Cell entry and antimicrobial properties of eukaryotic cell-penetrating peptides*. Faseb J, (2004). **18**(2): p. 394-396.
30. Vives, E., J.P. Richard, C. Rispal, and B. Lebleu, *TAT peptide internalization: seeking the mechanism of entry*. Curr Protein Pept Sci, (2003). **4**(2): p. 125-132.
31. Richard, J.P., K. Melikov, E. Vives, C. Ramos, B. Verbeure, M.J. Gait, L.V. Chernomordik, and B. Lebleu, *Cell-penetrating peptides. A*

- reevaluation of the mechanism of cellular uptake.* J Biol Chem, (2003). **278**(1): p. 585-590.
32. Foerg, C., U. Ziegler, J. Fernandez-Carneado, E. Giralt, R. Rennert, A.G. Beck-Sickinger, and H.P. Merkle, *Decoding the Entry of Two Novel Cell-Penetrating Peptides in HeLa Cells: Lipid Raft-Mediated Endocytosis and Endosomal Escape.* Biochemistry, (2005). **44**(1): p. 72-81.
33. Herbig, M.E., U. Fromm, J. Leuenberger, U. Krauss, A.G. Beck-Sickinger, and H.P. Merkle, *Bilayer interaction and localization of cell penetrating peptides with model membranes: a comparative study of a human calcitonin (hCT) derived peptide with pVEC and pAntp(43-58).* BBA Biomembranes, (2005). **(in press)**.
34. Mayer, L.D., M.J. Hope, and P.R. Cullis, *Vesicles of variable sizes produced by a rapid extrusion procedure.* Biochim Biophys Acta, (1986). **858**(1): p. 161-168.
35. New, R.B.C., *Characterization of liposomes*, in *Liposomes, A Practical Approach*, R.B.C. New, Editor. (1990), Oxford University Press: New York. p. 125-127.
36. Dathe, M., M. Schumann, T. Wieprecht, A. Winkler, M. Beyermann, E. Krause, K. Matsuzaki, O. Murase, and M. Bienert, *Peptide helicity and membrane surface charge modulate the balance of electrostatic and hydrophobic interactions with lipid bilayers and biological membranes.* Biochemistry, (1996). **35**(38): p. 12612-12622.
37. Mou, J., J. Yang, and Z. Shao, *Tris(hydroxymethyl)aminomethane (C<sub>4</sub>H<sub>11</sub>NO<sub>3</sub>) induced a ripple phase in supported unilamellar phospholipid bilayers.* Biochemistry, (1994). **33**(15): p. 4439-4443.
38. Lakowicz, J.R., *Principles of Fluorescence Spectroscopy*. 2nd ed. ed. (1999), New York: Kluwer Academic. 291-303.
39. Mou, J., J. Yang, C. Huang, and Z. Shao, *Alcohol induces interdigitated domains in unilamellar phosphatidylcholine bilayers.* Biochemistry, (1994). **33**(33): p. 9981-9985.

40. Grandbois, M., H. Clausen-Schaumann, and H. Gaub, *Atomic force microscope imaging of phospholipid bilayer degradation by phospholipase A2*. Biophys J, (1998). **74**(5): p. 2398-2404.
41. Wood, P.D. and S. Holton, *Human Plasma Sphingomyelins*. Proc Soc Exp Biol Med, (1964). **115**: p. 990-992.
42. Cohen, R., Y. Barenholz, S. Gatt, and A. Dagan, *Preparation and characterization of well defined D-erythro sphingomyelins*. Chem Phys Lipids, (1984). **35**(4): p. 371-384.
43. Wu, W.G., L.M. Chi, T.S. Yang, and S.Y. Fang, *Freezing of phosphocholine headgroup in fully hydrated sphingomyelin bilayers and its effect on the dynamics of nonfreezable water at subzero temperatures*. J Biol Chem, (1991). **266**(21): p. 13602-13606.
44. Matsuzaki, K., S. Yoneyama, and K. Miyajima, *Pore formation and translocation of melittin*. Biophys J, (1997). **73**(2): p. 831-838.
45. Huang, Z.J. and R.P. Haugland, *Partition coefficients of fluorescent probes with phospholipid membranes*. Biochem Biophys Res Commun, (1991). **181**(1): p. 166-71.
46. Silvius, J.R., B.D. Read, and R.N. McElhaney, *Thermotropic phase transitions of phosphatidylcholines with odd-numbered n-acyl chains*. Biochim Biophys Acta, (1979). **555**(1): p. 175-178.
47. Greenfield, N. and G.D. Fasman, *Computed circular dichroism spectra for the evaluation of protein conformation*. Biochemistry, (1969). **8**(10): p. 4108-4016.
48. Fastenberg, M.E., H. Shogomori, X. Xu, D.A. Brown, and E. London, *Exclusion of a transmembrane-type peptide from ordered-lipid domains (rafts) detected by fluorescence quenching: extension of quenching analysis to account for the effects of domain size and domain boundaries*. Biochemistry, (2003). **42**(42): p. 12376-12390.
49. van Duyl, B.Y., D.T. Rijkers, B. de Kruijff, and J.A. Killian, *Influence of hydrophobic mismatch and palmitoylation on the association of*

- transmembrane alpha-helical peptides with detergent-resistant membranes.*  
FEBS Lett, (2002). **523**(1-3): p. 79-84.
50. Polozov, I.V., A.I. Polozova, J.G. Molotkovsky, and R.M. Epand, *Amphipathic peptide affects the lateral domain organization of lipid bilayers*. Biochim Biophys Acta, (1997). **1328**(2): p. 125-139.
51. Czajlik, A., E. Mesko, B. Penke, and A. Perczel, *Investigation of penetratin peptides. Part 1. The environment dependent conformational properties of penetratin and two of its derivatives*. J Pept Sci, (2002). **8**(4): p. 151-171.
52. Deshayes, S., T. Plenat, G. Aldrian-Herrada, G. Divita, C. Le Grimellec, and F. Heitz, *Primary amphipathic cell-penetrating peptides: Structural requirements and interactions with model membranes*. Biochemistry, (2004). **43**(24): p. 7698-7706.
53. Magzoub, M., K. Kilk, L.E. Eriksson, U. Langel, and A. Graslund, *Interaction and structure induction of cell-penetrating peptides in the presence of phospholipid vesicles*. Biochim Biophys Acta, (2001). **1512**(1): p. 77-89.
54. Lewis, B.A. and D.M. Engelman, *Lipid bilayer thickness varies linearly with acyl chain length in fluid phosphatidylcholine vesicles*. J Mol Biol, (1983). **166**(2): p. 211-217.
55. Marsh, D., *Handbook of Lipid Bilayers*. (1990), Boca Raton, FL: CRC.
56. White, S.H. and W.C. Wimley, *Hydrophobic interactions of peptides with membrane interfaces*. Biochim Biophys Acta, (1998). **1376**(3): p. 339-352.
57. Martinez-Senac Mdel, M., S. Corbalan-Garcia, and J.C. Gomez-Fernandez, *The structure of the C-terminal domain of the pro-apoptotic protein Bak and its interaction with model membranes*. Biophys J, (2002). **82**(1 Pt 1): p. 233-243.
58. Azpiazu, I., J.C. Gomez-Fernandez, and D. Chapman, *Biophysical studies of the Pfl coat protein in the filamentous phage, in detergent micelles, and in a membrane environment*. Biochemistry, (1993). **32**(40): p. 10720-10726.

59. Martinez-Senac, M.D., S. Corbalan-Garcia, and J.C. Gomez-Fernandez, *Study of the secondary structure of the C-terminal domain of the antiapoptotic protein Bcl-2 and its interaction with model membranes.* Biochemistry, (2000). **39**(26): p. 7744-7752.
60. Borchardt, K., D. Heber, M. Klingmuller, K. Mohr, and B. Muller, *The Ability of Cationic Amphiphilic Compounds to Depress the Transition-Temperature of Dipalmitoylphosphatidic Acid Liposomes Depends on the Spatial Arrangement of the Lipophilic Moiety.* Biochem Pharmacol, (1991). **42**: p. S61-S65.
61. Kursch, B., H. Lullmann, and K. Mohr, *Influence of various cationic amphiphilic drugs on the phase-transition temperature of phosphatidylcholine liposomes.* Biochem Pharmacol, (1983). **32**(17): p. 2589-2594.
62. Berquand, A., M.P. Mingeot-Leclercq, and Y.F. Dufrene, *Real-time imaging of drug-membrane interactions by atomic force microscopy.* Biochim Biophys Acta, (2004). **1664**(2): p. 198-205.
63. Ramstedt, B. and J.P. Slotte, *Membrane properties of sphingomyelins.* FEBS Lett, (2002). **531**(1): p. 33-37.
64. Barenholz, Y., Cevc, G., in *Physical Chemistry of Biological Interfaces*, A. Baskin, Norde, W. (Eds.), Editor. (2000): New York. p. 171-241.
65. Janshoff, A., D.T. Bong, C. Steinem, J.E. Johnson, and M.R. Ghadiri, *An animal virus-derived peptide switches membrane morphology: possible relevance to nodaviral transfection processes.* Biochemistry, (1999). **38**(17): p. 5328-5336.
66. Simon, S.A. and T.J. McIntosh, *Interdigitated hydrocarbon chain packing causes the biphasic transition behavior in lipid/alcohol suspensions.* Biochim Biophys Acta, (1984). **773**(1): p. 169-172.
67. Kinoshita, K. and M. Yamazaki, *Organic solvents induce interdigitated gel structures in multilamellar vesicles of dipalmitoylphosphatidylcholine.* Biochim Biophys Acta, (1996). **1284**(2): p. 233-239.

68. Seydel, J.K. and M. Wiese, *Drug-Membrane Interactions*, ed. J.K. Seydel and M. Wiese. (2002), Weinheim: Wiley-VCH.
69. Matsuzaki, K., M. Fukui, N. Fujii, and K. Miyajima, *Permeabilization and Morphological-Changes in Phosphatidylglycerol Bilayers Induced by an Antimicrobial Peptide, Tachyplesin-I*. Colloid and Polymer Science, (1993). **271**(9): p. 901-908.
70. Gidalevitz, D., Y. Ishitsuka, A.S. Muresan, O. Konovalov, A.J. Waring, R.I. Lehrer, and K.Y. Lee, *Interaction of antimicrobial peptide protegrin with biomembranes*. Proc Natl Acad Sci U S A, (2003). **100**(11): p. 6302-6307.
71. Schibli, D.J., R.F. Epand, H.J. Vogel, and R.M. Epand, *Tryptophan-rich antimicrobial peptides: comparative properties and membrane interactions*. Biochem Cell Biol, (2002). **80**(5): p. 667-677.

## GENERAL DISCUSSION AND CONCLUSION

After its pioneering phase in the late 1990ies the field of CPP has received broad and continuing interest in the scientific community. More recently, a rich discussion on conflicting evidence regarding the fundamental driving forces for CPP translocation has further stimulated the scientific community. In principle, there are presently two main avenues of research in this field. One is primarily concerned with biochemical aspects and the cell biology of the translocation process, the other one with the respective biophysical aspects of the interactions with the lipid membrane. This PhD thesis is focused on the fundamental principles of how CPP interact with the lipid membrane. We believe a detailed understanding of such interactions, which we consider to represent the first step in the translocation of CPP across the lipid bilayer of the cell membrane, to be crucial for the elucidation of their cellular uptake mechanisms that are still under vivid and partially controversial discussion in literature. To this end we followed three different experimental approaches.

In a first study we performed a comprehensive evaluation of the interactions of representative CPP from different families with several lipid bilayer models using liposome-buffer equilibrium dialysis, Trp fluorescence quenching, fluorescence polarization, and  $\zeta$ -potential analysis. As a result we found evidence for two distinct alternatives for interaction, i.e. interfacial versus superficial membrane localisation, respectively. None of the investigated CCP showed significant evidence for penetration into the lipid bilayer or pore formation. Similar to other CPP of multiple cationic charge (1-3), we observed pVEC and penetratin to preferentially localize in the interfacial region of the lipid bilayer. CPP of moderately cationic character, such as the hCT derived CPP investigated in our work, seem to constitute a CPP family of its own. Depending on factors like lipid composition and pH, they showed a distinctly different behaviour as compared to the strongly cationic CCP. Their higher affinity towards the interface as compared to the hydrophobic core and the

strong enrichment at the interface of phospholipid bilayers makes passive uptake rather unlikely. On the other hand, their enrichment at the interface, possibly followed by aggregation, has potential to trigger endocytic uptake. These findings are in line with a majority of CPP studies in recent years. For hCT derived CPP there is now strong evidence for endocytic uptake since several in vitro uptake studies (4-7) suggest this uptake mechanism. In fact, in contrast to earlier studies, recently published works demonstrated endocytic uptake also to occur with pVEC (8) and penetratin (9, 10). Occasionally, pore formation has been discussed as a possible mechanism of uptake or an unwanted detrimental effect on cellular integrity (11). By means of liposome leakage studies we were able to exclude any damage of bilayer integrity caused by pVEC, hCT(9-32), or their respective modifications.

In a next step, beyond the various methodologies covered above, we pursued a more molecular approach. We investigated the secondary structure and the topology of lipid membrane associated hCT(9-32) by means of NMR. This allowed us to gain insight into its molecular orientation and function when interacting with lipid micelles as a bilayer model. Whereas hCT(9-32) turned out to be largely unstructured in aqueous solution, it adopted two short helical stretches when bound to DPC micelles. While the mid part of the sequence was moderately integrated in the interface of the micelles, its hydrophobic C-terminal tail was found to extend into the water phase. Based on these results, we identified Pro23 and Gly30 as particularly crucial residues for the topology of the association with the lipid membrane. To gain further information we systematically replaced the respective amino acids leading to two mutants, W30-hCT(9-32) and A23-hCT(9-32). The latter one, with the helix-breaking Pro23 replaced by an Ala, displayed a continuous  $\alpha$ -helix extending from residue 12 through 26, and engaged in an orientation *parallel* to the surface of the micelle. Moreover, as expected, the Gly to Trp exchange in W30-hCT(9-32) resulted in a stable anchoring of the C-terminal segment in the interface of the micelle. This outcome was consistent with a twofold increase in the partition coefficients of the modified CPP in a liposomal LUV model. In harmony with the biophysical

data, tighter binding to the model membranes corresponded to an increased *in vitro* uptake in HeLa cells. Finally, liposome leakage studies excluded pore formation, and the punctuated fluorescence pattern of internalized peptide indicated vesicular localization. Altogether, association of the CPP with the lipid bilayer was concluded to represent the trigger for the endocytic pathway of translocation. Interestingly, our results were in line with other CPP showing flat and  $\alpha$ -helical localization of CPP on the lipid membrane (12, 13). Localization and penetration perpendicular to the membrane surface has been associated with an increase in toxicity (14).

As a final step, we employed AFM to visualize CPP-bilayer interactions. Phase separated SPB adsorbed on mica were the biophysical model used in this study. So far, despite its large potential in surface imaging, this methodology is quite scarce in CPP research. We performed time-lapse AFM studies on the effects of two CPP, pVEC and its derivative W2-pVEC, on phase separated SPB. Both peptides induced a transformation process in the DPPC gel phase domains, which led via an intermediate state with fractal-like structures to entirely or almost entirely flat bilayers. A related investigation of the molecular mechanisms of this transformation by fluorescence polarization revealed the capacity of the studied CPP to increase the fluidity of the DPPC domains. Owing to the distinct molecular structure of their interfacial region, allowing for intermolecular hydrogen bonding and, hence, tight packing densities, SM domains were not affected by the investigated CPP. In contrast to membrane-spanning peptides, which decrease the fluidity of bilayers, and in agreement with the results of our initial Trp fluorescence quenching study, we propose that the investigated CPP interact with the bilayer interface and, therefore, lessen the packing density of the acyl chains of the lipid. This contrasts to previous proposals for membrane spanning peptides (15, 16). The observed mechanism is more specific and distinct from the interfacial aggregation phenomenon proposed for hCT(9-32) that has been analyzed by AFM on SPB (17).

Importantly, by combination of experimental evidence from AFM, dynamic light scattering and dye leakage from liposomes, our data substantiate the view that the investigated CPP did not compromise bilayer integrity. Our study represents the first observation of a CPP induced transformation process of phase separated phospholipid bilayers and reveals a novel aspect to be considered to explain the cellular translocation of CPP.

In conclusion, this work contributes in several innovative aspects to the currently ongoing scientific discourse on the interactions of CPP with phospholipid bilayers and the basic biophysical principles involved in the mechanisms of translocation. We performed the first characterization of bilayer interactions of the moderately cationic hCT derived CPP, which represent a CPP family of its own, and demonstrated a superficial localization in neutral and slightly negatively charged bilayers with potential to trigger endocytic cellular uptake. Furthermore, the presented work demonstrates the value of coupled biophysical and cell biological studies, by showing that a punctual exchange of amino acids led to an enhanced interfacial anchoring over the entire CPP sequence and – at the same time – to an increased in vitro cellular uptake. Finally, the discovery of the capability of pVEC derived CPP to transform gel phase domains in SPB without affecting their integrity demonstrates the potential of AFM studies in CPP research and reveals a novel aspect to be considered for the cellular uptake of CPP. The exact role of the discovered CPP effect on the fluidity of bilayer in the course of cellular translocation can be an interesting subject for further investigations.

## REFERENCES

1. Christiaens, B., J. Grooten, M. Reusens, A. Joliot, M. Goethals, J. Vandekerckhove, A. Prochiantz, and M. Rosseneu, *Membrane interaction*

- and cellular internalization of penetratin peptides.* Eur J Biochem, (2004) **271**: 1187-1197.
2. Christiaens, B., S. Symoens, S. Verheyden, Y. Engelborghs, A. Joliot, A. Prochiantz, J. Vandekerckhove, M. Rosseneu, B. Vanloo, and S. Vanderheyden, *Tryptophan fluorescence study of the interaction of penetratin peptides with model membranes.* Eur J Biochem, (2002) **269**: 2918-2926.
  3. Magzoub, M., L.E. Eriksson, and A. Graslund, *Comparison of the interaction, positioning, structure induction and membrane perturbation of cell-penetrating peptides and non-translocating variants with phospholipid vesicles.* Biophys Chem, (2003) **103**: 271-288.
  4. Vives, E., J.P. Richard, C. Rispal, and B. Lebleu, *TAT peptide internalization: seeking the mechanism of entry.* Curr Protein Pept Sci, (2003) **4**: 125-132.
  5. Trehin, R., U. Krauss, R. Muff, M. Meinecke, A.G. Beck-Sickinger, and H.P. Merkle, *Cellular internalization of human calcitonin derived peptides in MDCK monolayers: a comparative study with Tat(47-57) and penetratin(43-58).* Pharm Res, (2004) **21**: 33-42.
  6. Trehin, R., U. Krauss, A.G. Beck-Sickinger, H.P. Merkle, and H.M. Nielsen, *Cellular uptake but low permeation of human calcitonin-derived cell penetrating peptides and Tat(47-57) through well-differentiated epithelial models.* Pharm Res, (2004) **21**: 1248-1256.
  7. Schmidt, M.C., B. Rothen-Rutishauser, B. Rist, A. Beck-Sickinger, H. Wunderli-Allenspach, W. Rubas, W. Sadee, and H.P. Merkle, *Translocation of human calcitonin in respiratory nasal epithelium is associated with self-assembly in lipid membrane.* Biochemistry, (1998) **37**: 16582-16590.
  8. Saalik, P., A. Elmquist, M. Hansen, K. Padari, K. Saar, K. Viht, U. Langel, and M. Pooga, *Protein cargo delivery properties of cell-penetrating peptides. A comparative study.* Bioconjug Chem, (2004) **15**: 1246-1253.

9. Drin, G., S. Cottin, E. Blanc, A.R. Rees, and J. Temsamani, *Studies on the internalisation mechanism of cationic cell-penetrating peptides.* J Biol Chem, (2003) **278**: 31192-31201.
10. Drin, G., M. Mazel, P. Clair, D. Mathieu, M. Kaczorek, and J. Temsamani, *Physico-chemical requirements for cellular uptake of pAntp peptide. Role of lipid-binding affinity.* Eur J Biochem, (2001) **268**: 1304-1314.
11. Lundberg, P. and U. Langel, *A brief introduction to cell-penetrating peptides.* J Mol Recognit, (2003) **16**: 227-233.
12. Berlose, J.P., O. Convert, D. Derossi, A. Brunissen, and G. Chassaing, *Conformational and associative behaviours of the third helix of antennapedia homeodomain in membrane-mimetic environments.* Eur J Biochem, (1996) **242**: 372-386.
13. Lindberg, M., H. Biverstahl, A. Graslund, and L. Maler, *Structure and positioning comparison of two variants of penetratin in two different membrane mimicking systems by NMR.* Eur J Biochem, (2003) **270**: 3055-3063.
14. Whiles, J.A., R. Brasseur, K.J. Glover, G. Melacini, E.A. Komives, and R.R. Vold, *Orientation and effects of mastoparan X on phospholipid bicelles.* Biophys J, (2001) **80**: 280-293.
15. Martinez-Senac, M.D., S. Corbalan-Garcia, and J.C. Gomez-Fernandez, *Study of the secondary structure of the C-terminal domain of the antiapoptotic protein Bcl-2 and its interaction with model membranes.* Biochemistry, (2000) **39**: 7744-7752.
16. Martinez-Senac Mdel, M., S. Corbalan-Garcia, and J.C. Gomez-Fernandez, *The structure of the C-terminal domain of the pro-apoptotic protein Bak and its interaction with model membranes.* Biophys J, (2002) **82**: 233-243.
17. Boichot, S., U. Krauss, T. Plenat, R. Rennert, P.E. Milhiet, A. Beck-Sickinger, and C. Le Grimellec, *Calcitonin-derived carrier peptide plays a major role in the membrane localization of a peptide-cargo complex.* FEBS Lett, (2004) **569**: 346-350.

**Michael Edgar Herbig**

born in Würzburg, Germany  
on November, 11th, 1975  
citizen of Germany

**Education and positions held**

---

since 2005	Junior Laboratory Head/Senior Scientist at Novartis Pharma AG, Basel, Switzerland
2001 - 2005	PhD studies and teaching assistant at the Institute of Pharmaceutical sciences, Drug Formulation & Delivery (Prof. H. P. Merkle), Swiss Federal Institute of Technology (ETH) Zurich, Switzerland
2002	Research stay (2 month) at the Centre de Biochimie Structurale, INSERM, Montpellier, France
2001	Approbation as pharmacist
2000	Intership (6 month) at the Apotheke am Ziegelhof (public pharmacy), Berlin, Germany
1999 - 2000	Intership (6 month) at Hoffmann-La Roche AG, Grenzach-Whylen, Germany
1995 – 1999	Undergraduate studies in pharmaceutical sciences at the University of Würzburg, Germany
	1997 First State Examination
	1999 Second State Examination
	2000 Third State Examination
1986 – 1995	Egbert-Gymnasium Münsterschwarzach, Germany (Abitur 1995)

## PUBLICATIONS AND PRESENTATIONS

### ARTICLES

Herbig M. E., Fromm U., Leuenberger J., Krauss U., Beck-Sickinger A. G., and Merkle H. P. *Bilayer interaction and localization of cell penetrating peptides with model membranes: a comparative study of a human calcitonin (hCT) derived peptide with pVEC and pAntp(43-58)*. *Biochim. Biophys. Acta*, 2005. **1712**: 197-211

Herbig M. E., Weller K., Krauss U., Beck-Sickinger A. G., Merkle H. P., and Zerbe O. *Membrane surface associated helices promote lipid interactions and cellular uptake of human calcitonin-derived cell penetrating peptides*. Accepted after minor revisions by *Biophys. J.*

Herbig M. E., Assi F., Textor M., and Merkle H.P. *The cell penetrating peptides pVEC and W2-pVEC induce transformation of gel phase domains in phospholipid bilayers without affecting their integrity*. Submitted to *Biochemistry*

### POSTER PRESENTATIONS

Herbig M. E., Zerbe O., and Merkle H. P. *Membrane interaction and structural characterization of human calcitonin derived carrier peptides*. Pharma-Day 02, Biozentrum Basel - ETH Zurich, Zurich, July 30, 2002

Herbig M. E., Fromm U., Zerbe O., and Merkle H. P. *Interactions of hCT derived cell-penetrating peptides with mono- and bilayer models*. 30<sup>th</sup> Int. Symp. Controlled Release Bioact. Mater., Glasgow, July 28-30 **2003**

Herbig M. E., Fromm U., Zerbe O., and Merkle H. P. *Interactions of human calcitonin (hCT) derived cell-penetrating peptides with mono- and bilayer models*. Pharma-Day 03, Biozentrum Basel - ETH Zurich, University of Basel, July 11, **2003**

Herbig M. E., Assi F., and Merkle H. P. *Interactions of human calcitonin and VE-cadherin derived cell penetrating peptides with phospholipid bilayers*. Pharma-Day 04, Biozentrum Basel - ETH Zurich, Zurich, May 2<sup>nd</sup> **2004**

Herbig M. E., Assi F., and Merkle H. P. *Interactions of human calcitonin and VE-cadherin derived cell penetrating peptides with model membranes*. Pharmaceutical Sciences World Congress (PSWC 2004), Kyoto, Japan, May 29 – June 03 **2004**

## ORAL PRESENTATIONS

Herbig, M. E. *Interaction with lipid bilayers and structure determination of human calcitonin derived peptides*. Zurich-Geneva Joint Seminar Series on Drug Formulation & Drug Delivery, Zurich, Switzerland, March **2002**

Herbig M. E. *Interactions of hCT derived peptides with mono- and bilayers: SUV partitioning, NMR analysis and AFM*. European Project Consortium Meeting, Dortmund, January 23-25, **2003**

Herbig M. E. *Human calcitonin (hCT) derived cell-penetrating peptides: Structure determination and interactions with mono- and bilayer models.*

Doktorandentag, ETH Zürich, April 02, **2003**

Herbig M. E. *Localization and interaction of human calcitonin derived CPP with phospholipid bilayers.* European Project Consortium Meeting, Leipzig, October 10-12, 2003

Herbig M. E. *Interactions of cell penetrating peptides (CPPs) with model membranes.* European Project Consortium Meeting, Zurich, Switzerland, April **2004**

Herbig M. E. *Interactions of cell penetrating peptides (CPPs) with model membranes.* Laboratory of surface science and technology, ETH Zürich, Schlieren, Switzerland, April 26, **2004**

Herbig M. E. *Interactions of human calcitonin and VE-cadherin derived cell penetrating peptides with model membranes.* Globalization in Pharmaceutics Education Network (GPEN) 2004, Kyoto, Japan, May 26 –28 **2004**

Herbig M. E. *Interactions of CPPs with model membranes: (i) distinct characteristics of different classes, (ii) optimization of sequences, and (iii) visualization of effects on bilayers.* Zurich-Geneva Joint Seminar Series on Drug Formulation & Drug Delivery, Zurich, Switzerland, October **2004**

Herbig M. E. *Updates on: (i) a NMR study with hCT modifications and (ii) AFM studies of pVEC/W2-pVEC – bilayer interactions.* European Project Consortium Meeting, Montpellier, France, November 30, **2004**

## ACKNOWLEDGEMENTS

My sincerest thanks go to Prof. Hans Peter Merkle, head of the Drug Formulation & Delivery group at the ETH Zurich, for giving me the opportunity to do my Ph.D. studies in this interesting field. I appreciated his constant support, his friendly personality, and the interesting discussions on my project and beyond.

I gratefully acknowledge the contribution of PD Dr. Oliver Zerbe, University of Zurich. I profited a lot by his expertise in NMR and his friendly support.

I thank Prof. Annette Beck-Sickinger, University of Leipzig, for the support with peptide design and synthesis.

I am grateful to Prof. Marcus Textor, head of the BioInterface group, ETH Zurich, for the opportunity to use the AFM microscope and to Dr. Fabiano Assi for advice and technical support.

During the years of Ph.D. studies I was fortunate to have met and worked with a lot of great people:

I thank Dr. Rachel Tréhin, Dr. Hanne Mørck Nielsen and Kathrin Weller for collaboration, input and interesting discussions on my Ph.D. project.

I want to express my sincere thanks to Dr. Sergio Freitas and Kathrin for the great atmosphere in our lab “K36” at the Irchel Campus and their continuous friendship. By fortunate coincidence we are now neighbors in Basel - together with Dr. Annette Koch, another dear colleague.

Likewise, I appreciated the always friendly and open atmosphere with my charming colleagues Christina Förg, Annina Hafner, Uta Wattendorf (who made

me enjoy various kinds of exotically flavored tea), and Kathrin in the Hönggerberg lab. I also thank all other members of the group, starting from Prof. Bruno Gander and Ruth Alder to Dr. Lorenz Meinel, Lukas Pfister, Sandra Hofmann, Esther Wenk, Vera Luginbühl, Henri Hagenmüller, and Lorenz Übersax. Beyond that, special thanks go to Stefan Fischer for spending many evenings with me at first-class jazz concerts at “our” Moods, for vivid interchange of musical discoveries and insightful discussions on sport injuries and to Dr. Lars Thiele, Michael Ulrich, Sergio, and Stefan for great Badminton sessions on Friday evenings.

I gratefully acknowledge the contributions of my diploma and semester students Ursina Fromm, Jeannine Leuenberger, Kati Buck, and Gisela Näf.

Ganz besonders dankbar bin ich meinen Eltern Agnes und Walter für ihre immerwährende Unterstützung und Zuneigung, meinen Schwestern Carmen und Simone für die lebendige, interessante, lustige Atmosphäre zu Hause, meinen Großmüttern für ihre großzügige Unterstützung und meinen verstorbenen Großvätern, die durch ihr praktisches Wissen viel dazu beigetragen haben, mein naturwissenschaftliches Interesse zu entwickeln.